Intelligent Voltage Dip Mitigation in Power Networks with Distributed Generation

Prepared by:

IPINNIMO, OLUWAFEMI

Department of Electrical Engineering

University of Cape Town

Supervisor:

Dr Sunetra Chowdhury

Department of Electrical Engineering

University of Cape Town

Thesis presented for the degree of

Doctor of Philosophy in Electrical Engineering

in the Department of Electrical Engineering

University of Cape Town

April 2014

Key Words: Artificial neural network, Eskom voltage dip windows, mean square error, power quality, renewable distributed generation, root mean square, voltage dip mitigation

As the candidate's supervisor, I have approved this dissertation for submission.

Name: Dr S. Chowdhury

Signed: _____ Date: April 2014

Declaration

I declare that this thesis is my own original and unaided work. Where collaborations with other researchers are involved, or materials generated by other researchers are included, the parties and/or materials are acknowledged or are explicitly referenced as appropriate.

This work is being submitted for the degree of Doctor of Philosophy in Electrical Engineering of the University of Cape Town, South Africa. It has not been submitted to any other university or institution for any other degree or examination.

Name: **IPINNIMO Oluwafemi**

Signature: _____ **Date:** 24 November 2014

Dedication

To God for His Great Mercies

Acknowledgements

My sincere gratitude goes first to God Almighty for divine help, inspiration and protection throughout the time of this research. He has always been my help whenever times were hard and my provider whenever I was in need.

I would like to express my sincere gratitude to my supervisor Dr Sunetra Chowdhury for her support, guidance and encouragement during my study as well as my daily life. Her gentle personality and rigorous attitude toward research have benefited my career as well as my whole personal life.

Special thanks go to Professor S.P. Chowdhury for his words of encouragement and inspiration.

I would like to express my appreciation to Prof Mitra and University of Michigan community for their love and words of encouragement.

I thank Eskom for providing me with the data and resource I used in this thesis.

I also thank the university of Lagos community, especially my HODs past and present, the Dean past and present and the VC for all their support. I owe a lot to my teachers, my colleagues, my friends and my students in the University of Lagos.

I am also greatly indebted to Mr. Ikena for his advice and encouragement during my research.

I am very grateful to all my colleagues in at the University of Cape Town for their friendship. I may not be able to list all the names.

To my in-laws, I thank you for your prayers and love. Iya Olu, I thank you for your care and prayers.

To you: Mom and Dad you are the best in the world. Thank you for the prayers, fasting and love you always show me. May God Bless you. My siblings: Dare, Funmi, Seyi and Tope. Nephews and nieces and the entire family, your love and the words of encouragement that you offered are kindly appreciated, and I am grateful for all your

support. I love you all.

Finally, to Funmi and Damilare thanks for staying with Mummy and not given her too much trouble and for been nice. Most importantly, I am hugely indebted to my wife. I can't thank you enough; you have shown me the love of a mother, not of lovers or a wife; the love of lovers can be unfaithful; a wife can be unfaithful to her man, but that of a mother to her child no matter the circumstance it will never be unfaithful. I love you Yemisi.

Summary

The need for ensuring good power quality (PQ) cannot be over-emphasized in electrical power system operation and management. PQ problem is associated with any electrical distribution and utilization system that experiences any voltage, current or frequency deviation from normal operation. In the current power and energy scenario, voltage-related PQ disturbances like voltage dips are a fact which cannot be eliminated from electrical power systems since electrical faults, and disturbances are stochastic in nature. Voltage dip tends to lead to malfunction or shut down of costly and mandatory equipment and appliances in consumers' systems causing significant financial losses for domestic, commercial and industrial consumers. It accounts for the disruption of both the performance and operation of sensitive electrical and electronic equipment, which reduces the efficiency and the productivity of power utilities and consumers across the globe. Voltage dips are usually experienced as a result of short duration reduction in the r.m.s. (r.m.s.-root mean square) value of the declared or nominal voltage at the power frequency and is usually followed by recovery of the voltage dip after few seconds. The IEEE recommended practice for monitoring electric power quality (IEEE Std. 1159-2009, revised version of June 2009), provides definitions to label an r.m.s. voltage disturbance based upon its duration and voltage magnitude. These disturbances can be classified into transient events such as voltage dips, swells and spikes. Other long duration r.m.s. voltage variations are mains failures, interruption, harmonic voltage distortion and steady-state overvoltages and undervoltages. This PhD research work deals with voltage dip phenomena only.

Initially, the present power network was not designed to accommodate renewable distributed generation (RDG) units. The advent and deployment of RDG over recent years and high penetration of RDG has made the power network more complex and vulnerable to PQ disturbances. It is a well-known fact that the degree of newly introduced RDG has increased rapidly and growing further because of several reasons, which include the need to reduce environmental pollution and global warming caused by emission of carbon particles and greenhouse gases, alleviating transmission congestion and loss reduction. RDG ancillary services support especially voltage and reactive power support in electricity networks are currently being recognized, researched and found to be quite useful in voltage dip mitigation.

In order to secure quality power supply various solutions have been proposed by several researchers to eliminate or mitigate the problem of voltage dip. Recent research shows that high

degree of penetration of RDG in the power system network might be effectively employed to deliver various benefits through ancillary services. Therefore, with more RDG penetration into the network, utilizing them for improving power quality through voltage dip mitigation has become an important area of research in itself. This has led to the development of various distributed generation schemes for the mitigation of voltage dips in electricity networks.

In this context, this thesis proposes a novel technique that uses an intelligent artificial neural network (ANN) approach to facilitate voltage dip mitigation in power networks, in order to eliminate power quality problems, through the ancillary service provided by grid-integrated RDG. The aim of the proposed intelligent system is to eliminate the power quality problems arising out of voltage dips in a power network, thereby affecting power quality sensitive loads. This scheme evaluates and compares the classified dip types after detection, provides distinctive characteristics of each class and guides the utility in selecting judiciously a RDG-based voltage dip mitigation scheme. In addition, a novel missing data restoration (MDR) algorithm is also developed for the ANN in case of faulty input data, error signals and loss of signal from the system.

The thesis proposes the application of ANN as compared to other available intelligent techniques is due to their learning ability from past experience. They can also handle noisy and incomplete data and are powerful for the problems characterized by small samples, nonlinear and high-dimensional pattern recognition. The scheme is developed and simulated in DIgSILENT Power Factory 14.0 and MATLAB software packages. IEEE test system and a typical South African electricity network model are used as bench mark test networks for testing and validating the proposed scheme. Data collected from the simulation in time and frequency domain are used to train the ANN network. The model is trained, tested and validated using simulated data in Matlab environment using the Neural Network Toolbox.

This corrective scheme investigates maximum level or range of RDG penetration that is good enough for voltage dip mitigation with modeling of different RDGs. Performance of this scheme in terms of voltage levels and effectiveness during and after the dip are investigated and its ability to facilitate mitigation of multiple voltage dips within a short duration and from different fault locations is analysed and reported in results. The thesis also investigates the effects and applicability of various RDG on voltage dip mitigation in electricity networks. In addition, the

thesis shows how the model was applied to South African context using voltage dip windows defined by the South African power utility.

The result obtained using the South African utility voltage dip windows reveals that when RDG units were connected into the system, the severity of voltage dip is definitely reduced compared to when they are disconnected. These findings evaluate and compare the classified dip types after detection and provide distinctive characteristics of each class and give the guidelines for the automatic processing of the dip types. It was also found out that the result can be used for improving the voltage quality, especially since a wrong mitigation solution can cause a severe power quality problem on the power network. The performances of the ANN detector and classifier are judged using the performance plot and the confusion matrix. Other results were presented in form of tables, matrix and graphs in r.m.s. value and in per unit.

Table of Contents

Chapter 1

Chapter 2

Chapter 3

Chapter 4

Chapter 5

Chapter 6

Chapter 7

Chapter 8

List of Figures

List of Tables

Acronyms

A/D	is the Analog to Digital
AC	is the Alternative Current
ANN	is the Artificial Neural Networks
CHP	is the Combined Heat and Power
CIGRE	is the International Council on Large Electricity Systems
CIRED	is the International Conference on Electricity Distribution
CNS	is the Central Nervous System
CVT	is the Constant Voltage Transformer
D/A	is the Digital to Analog
DC	is the Direct Current
DER	is the Distributed Energy Resources
DFIG	is the Doubly-Fed Induction Generator
DG	is the Distributed Generation
DSP	is the Digital signal Processor
DVR	is the Dynamic Voltage Restorer
EMF	is the Electromotive Force
EMTP	is the Electromagnetic Transients Program
FFNN	is the Feed-Forward Neural Network
FSWTs	is the Fixed Speed Wind Turbines
GRDG	is the Grid-Connected RDG GRDG
GRDG	is the Grid-Connected Renewable Distributed Generation
GRNN	is the Generalized Regression Neural Network
IEA	is the International Energy Agency
IEC	is the International Electrotechnical Commission
IEEE	Is the Institute of Electrical and Electronics
IEEE	is theEuropean (CENELEC), and North American

IET	is the Institution of Engineering and Technology
IET	is the institution of engineering and technology
LPF	is the Low Pass Filter
LVRT	is the Voltage Ride-Through
MLP	is the Multilayer Perceptron
MPPT	is the Maximum Power Point Tracker
MSE	is the Mean Square Error
NERSA	is the National Energy Regulator of South Africa
PCC	is the Point Of Common Connection Or Point Of Common Coupling
PCS	is the Power Conversion System
PI	is the Proportional Integrator
PMG	is the Permanent Magnet Generator
PMSG	is the Permanent Magnet Synchronous Generator
PMSG	is the Permanent Magnet Synchronous Generator
PNN	is the Probabilistic Neural Networks
PQ	is the Power Quality
PQ	is the Power Quality
PQM	is the Power Quality Monitors
PWM	is the Pulse Width Modulation
QOS	is the Quality Of Supply
RBF	is the Radial Base Function
RBF	is the Radial Basis Function
RDG	is the Renewable Distributed Generation
R.M.S	is the Root Mean Square
SARFI	is the System Average Rms (Variation) Frequency Index
SCIG	is the Squirrel-Cage Induction Generator
STATCOM	is the Static Synchronous Compensator
STFT	Is the Short-Time Fourier Transform
UNFCCC	is the United Nations Framework Convention on Climate Change

UPS	is the Uninterruptible Power Supply
VQ	is the Voltage Quality
VSC	is the Voltage Source Converter
VSI	is the Voltage Source Inverter
VSWTs	is the Variable Speed Wind Turbines
WES	is the Wind Energy System

Chapter 1

1.1 Introduction

The daily increase in demand for cheaper, cleaner and reliable electricity by both the power utilities and consumers has led to a significant amount of renewable-energy resources being installed on the distribution side of power network. Few decades ago, researchers and experts within the field of power and energy have forecasted that the installation of renewable distributed generation will be increased due to the need to provide more clean energy [1].

Global warming and climate changes have been a matter of concern and attention in the last decade to government and international organizations. The emissions of the greenhouse gases are also a major concern within the energy industry. Power utilitiePs and consumers are not left out of these phenomena. It is essential to reduce poisonous gases from the atmosphere in order to comply with the Kyoto protocol which was adopted in 1997 by parties to the UNFCCC. In 2007, as a result of this process, many parts around the world have developed and implemented a clean development mechanism (CDM) [2].

These factors have ultimately led to an increasing implementation of renewable energy sources which are usually connected and utilized at the distribution grid either at the low or medium voltage level close to the load being served. Furthermore, the recent improvement in distributed generation (DG) technology gave rise to production of cleaner energy from renewable resources [3]. Existing research literature indicates that renewable DGs are also able to provide voltage support to the grid during faults and participate in the mitigation of voltage dip [4].

Voltage dips are usually experienced as short-duration reduction in the r.m.s. value of the declared or nominal voltage at the power frequency; it is usually followed by recovery of the voltage after few seconds. Voltage dip is also known as voltage sag, the term sag is used by some power quality experts as a synonym to the International Electrotechnical Commission (IEC) term dip [5]. Voltage dips are not easy to eliminate fully from electrical power systems,

and they are an integral phenomenon of power system operation. The main concern about voltage dip is due to its impact on end-user equipment. A severe dip might lead to malfunction or shut down in the industries causing significant financial losses for domestic, industrial and commercial consumers.

Voltage dips are the most frequent power quality disturbance in an electrical network [6]. Most faults and short circuit events that lead to large current flow in the power system can cause voltage dips, which can adversely affect specifically the power quality sensitive loads, such as the computer and other modern electronic equipment. Thus, increased use of sophisticated electronics, high-efficiency variable-speed drive, and power electronic controller has become an increasing concern to utilities, customers and researchers within the field of electrical power systems and the need to provide a good power quality.

1.2 Power quality

The main objective of electric power utility is to produce electrical energy and deliver the energy at the end-user equipment at an acceptable voltage and frequency [7]. Demand for reliable electric power is growing faster than its supply and generation today as most human activity today depend on electricity. Electricity is thus one of the most important infrastructures in any country needed for its economic development. The provision of excellent AC power quality will always be the main emphasis of interest to electrical experts throughout the globe due to the perpetual advent of power quality sensitive equipment has made the provision of good power quality a real challenge across the world.

The term power quality (PQ) is described as deviation of all or any one of voltage, current or frequency from their normal operational values. Theoretically, it is believed that a supply with a good power quality must have perfectly sinusoidal voltage and current of constant magnitude and frequency. Hence, [8] defines power quality as the study on the quality of electric power signals. In [9] power quality is defined as a set of limits of electrical properties that allows electrical systems to function in their intended manner without significant loss of performance or life. It is seen as any power system problem manifested in voltage, current, or frequency

deviations that result in failure or mal-operation of customer equipment [10]. Power quality is also regarded as the combination of voltage quality and current quality [7].

In the advanced countries, the issue of PQ has been due to factors such as increasing use of nonlinear power electronic loads such as converter driven equipment, and also due to the power networks being exposed to natural environmental disturbances like lightning strikes. In addition, it is observed that continually interconnected power grids, which contain large numbers of power sources, transmission lines, transformers and loads can as well contribute to poor PQ [9]. These usually lead to negative impact on both the economic and technical operation on the electricity networks.

The importance of high quality and reliable power supply cannot be over emphasized. It ensures a healthy electric power supply to consumers who have to pay for electricity. In addition, sophisticated electrical and electronics equipment has become more sensitive to voltage disturbances and the need for standardization and performance criteria in an electricity network. Many of these PQ disturbances like voltage dip have serious negative impacts on the utilities and the consumers in terms of technical and economic losses and they need to be identified and mitigated [11].

In electric power systems, there are not too many sophisticated online systems to monitor any discrepancy of power disturbances and hence there is a necessity to have such systems in place for enhancing power system diagnostics. An aspect of power quality includes voltage stability, continuity of supplying power and voltage waveform as shown in Table 1.1 [12].

Table 1.1: Voltage and Power Aspects of Power Quality [12]

Voltage Stability	**Continuity of Power Supply**	**voltage waveform**
Under-voltage	Momentary interruption	Transient
Over-voltage	Temporary interruption	Three phase voltage unbalance
Voltage dip	Sustained interruption	Harmonic voltage , current

Voltage swell		Notch
Flicker		
Frequency		
Phase shift		

Table 1.2: Types of Disturbances based on the UNE standard in Spain [8]

Types of disturbance	**Disturbance subtypes**		**Time**	**Range**	
				Min. value	**Max. value**
Frequency	Slight deviation		10s	49.5Hz.	50.5Hz.
	Severe deviation			47 Hz.	52 Hz.
Voltage	Average		10 min	0.85 U	1.1 U
	Flicker		-	-	7%
	Dip	Short	10 ms-1s	O.I U	0.9 U
		Long	1s-1min		
		Long-time Disturbance	>1 min		
	Under-voltage	Short	<3 min	0.99 U	
		Long	>3 min		
	Swell	Temporary short	10 ms-1s	1.1U	1.5 KV
		Temporary long	1s-1min		
		Temporary long-time	>1 min		
		Over-voltage	< 10 ms		6 KV
Harmonics and other information signals	Harmonics		-	THD > 8%	
	Information signals		-	Included in other disturbances	

Where U is the value of the declared or nominal voltage and THD is the total harmonic distortion.

1.3 Electric power network

In traditional power networks, the flow of electrical power (energy) takes place from the generating station through transmission and distribution networks to the customers' loads. This conventional radial arrangement is shown in Figure 1.1. Power is normally generated in bulk in central utility power stations. During power generation, electro-mechanical conversion takes place in the turbine and alternators; the generation voltage is stepped up to a transmission level high voltage (HV) to reduce transmission losses during long distance transmission. Further in the sub- transmission distribution levels, voltage is further stepped down to medium voltage (MV) and low voltage (LV) and finally power is delivered to the loads connected to the customers' terminals [13]. This type of radial network has a unidirectional power flow from generation end to the load end. In some cases, the loads can also be connected at high or medium voltage for industrial customers such as refinery industries and rolling steel mail. Some generating stations that are associated with this structure are coal-fired power stations, nuclear power stations, the Hydro power station, the wind power station, Solar PV power station, nuclear power station, coal or gas power station.

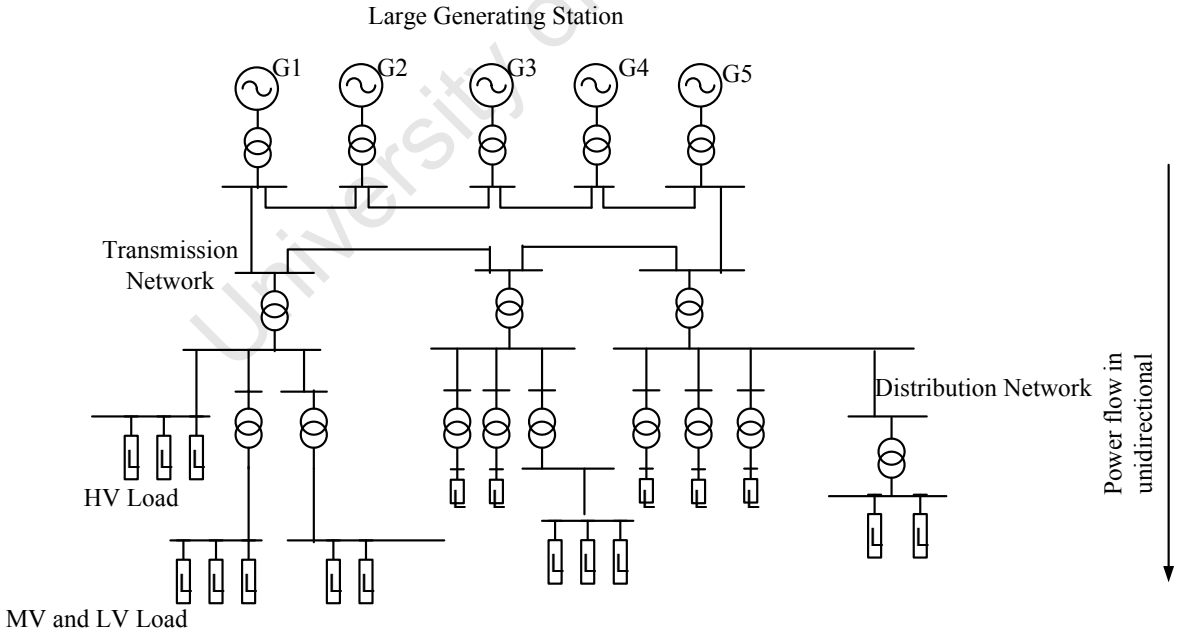

Figure 1.1: Centralized power network [14]

Nowadays, the introduction of distributed generation within the electrical power networks tends to make power flow from unidirectional to bidirectional. This arrangement has made the power system to be decentralized from the initial conventional arrangement. The decentralized power is characterized by generation of power nearer to the demand centers, focusing mainly on meeting local energy needs [15]. Figure 1.2 shows an example of decentralized power network.

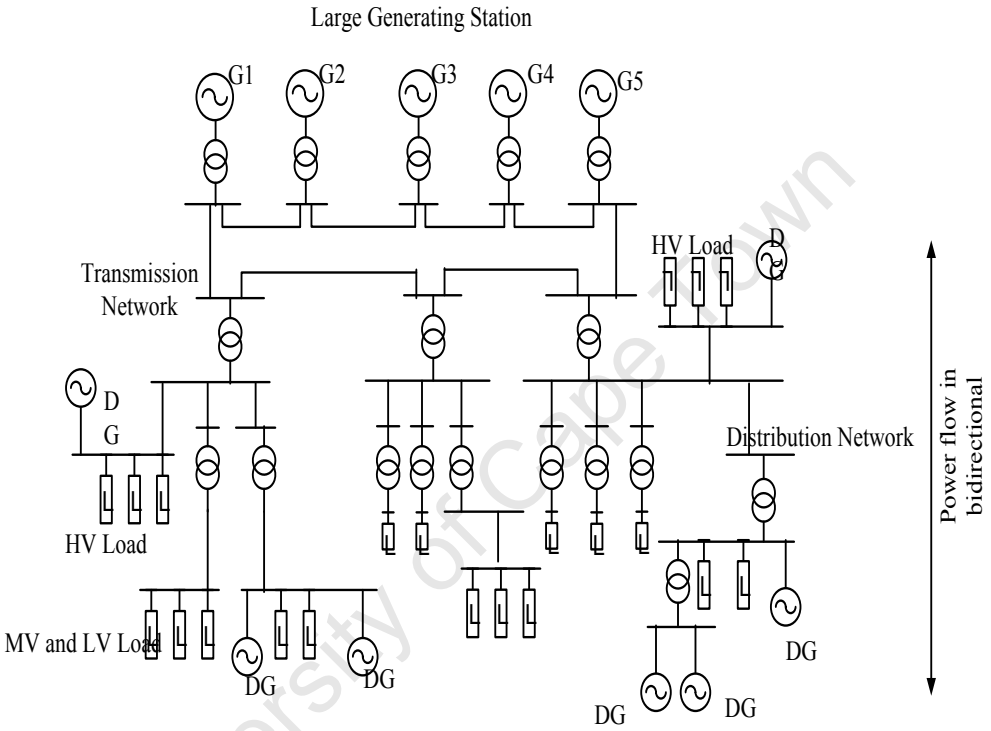

Figure 1.2: Decentralized power network with distributed generation [14]

1.4 Power Quality Disturbances

Power quality disturbances observed as a result of frequency deviation are harmonics, frequency variations and high-frequency noise. Voltage deviation disturbances exist in numerous forms, such as, transients, sags, swells, over voltages, under voltages, outages and voltage fluctuations, especially those causing flickers.

1.5 Examples of poor power quality problems

1.5.1 Flicker

Voltage Flicker is the disturbance in lighting induced by voltage fluctuations [16]. It is defined in as an impression of unsteadiness of visual sensation induced by a light stimulus whose luminance or spectral distribution fluctuates with time. It is different from other power distortions because it deals with the effect on the power quality on humans rather than on equipment. Flicker can be caused by variable industrial load or distributed generation such as the wind generator. Apart from its negative effects on human vision, it is also regarded as one of the power quality problems [17].

1.5.2 Voltage swell

This is defined as a temporary increase in the r.m.s. value of the voltage at the power frequency of a magnitude more than 10% of the nominal voltage for durations from 0.5 cycle to one minute. Its magnitude is also described by the remaining voltage and hence will always be greater than 1.0 p.u. (where p.u. means per unit) [5]. Typical magnitudes for remaining voltage for a voltage swell are between 1.1p.u. and 1.2p.u. Voltage swell can usually leads to overheating and destruction of industrial equipment such as motor drives and control relays [18].

1.5.3 Voltage dip or sag

At present, days, the economic losses caused by voltage dips may even be higher than the costs associated with interruptions for some industrial customers such as the textile and refinery industries. Voltage dip is cause by power system faults, switching operations, starting of big motors, etc. It is defined as sudden reduction in voltage to a value ranging between 10% and 90% of the nominal voltage or declared voltage, followed by the voltage recovery within a short period ranging between half a cycle and 1 minute [19]. The IEEE Std 1159-2009 IEEE Recommended Practice for Monitoring Electric Power Quality defines voltage dip as is "*a decrease in r.m.s. voltage at the power frequency for durations ranging from 0.5 cycles to 1 minute, reported as the remaining voltage. Typical values are between 0.1 p.u. and 0.9 p.u.*" [5].

1.5.4 Interruption

Interruption is defined as a 0.9 p.u. reduction in voltage magnitude for a period less than one minute. An interruption is characterized by the duration as the magnitude is more or less constant [20]. Both the electric utilities and the consumers are usually responsible for the economic impacts and negative effects of interruption, as a result of power service interruptions [21].

1.5.5 Over-voltage

An over-voltage differs from a voltage swell in terms of time duration. An over-voltage is an r.m.s. increase in ac voltage greater than 1.1 p.u. for a duration longer than 1 min. Typical values are 1.1 p.u. to 1.2 p.u. Over-voltages might be due to poor voltage regulation within the power network as a result of the regulator installed or set incorrectly, malfunction of capacitor-bank controller or malfunction of the voltage regulator [22]. All these processes have a negative effect, such as overheating and malfunction of control relays, which can cause damage on the customer's load [18].

1.5.6 Under-voltage

An under-voltage differs from a voltage dip or sag in terms of time duration. An under-voltage is a decrease in r.m.s. voltage magnitude to less than 0.9 p.u. for a duration longer than 1 min. Typical values are between 0.8 p.u. and 0.9 p.u. They are caused as a result of abrupt increase in loads or power system faults as a result leading to high impact on production cost [23].

1.6 Characteristics of Voltage Disturbances

Figure 1.3 shows the different types of voltage disturbances with their magnitude and duration in electrical power network.

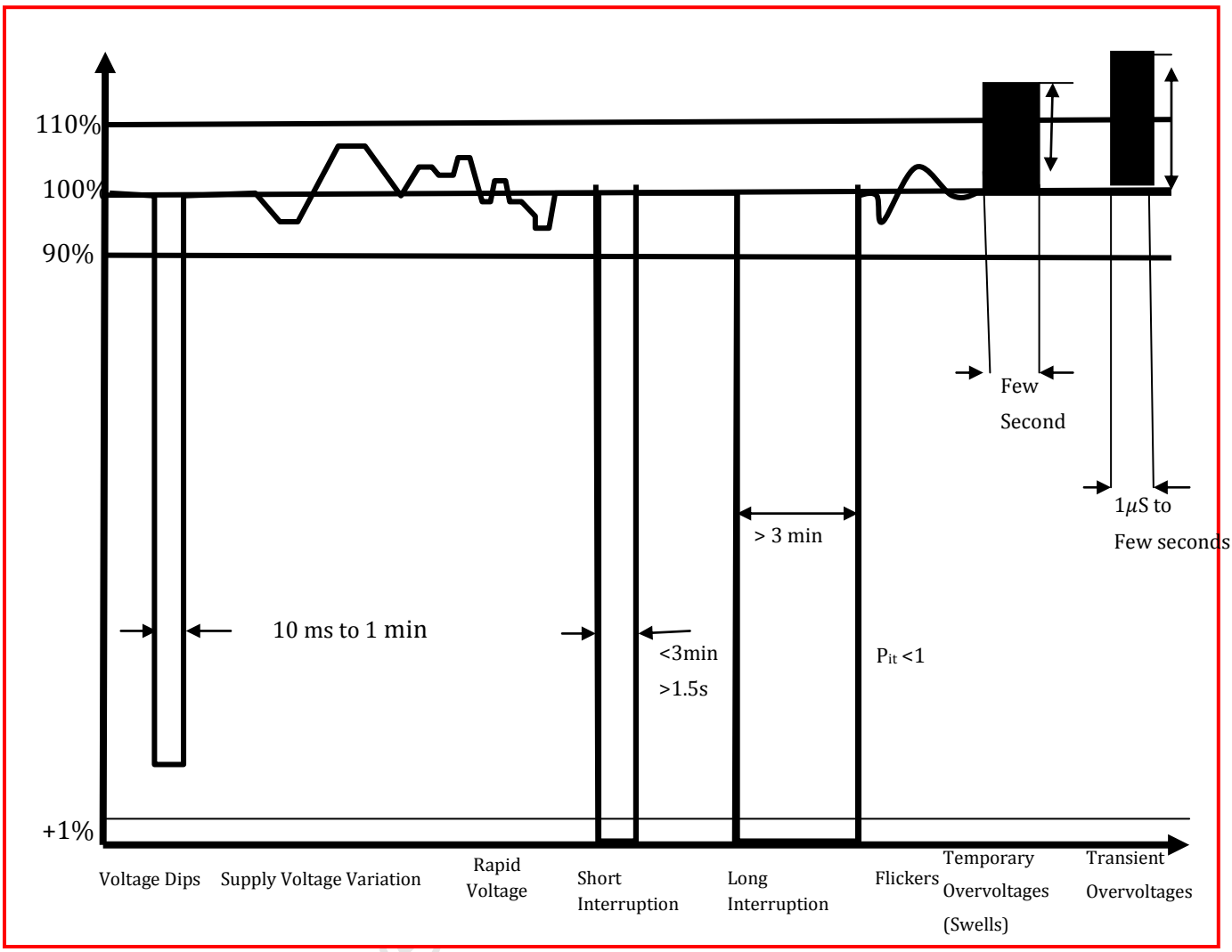

Figure 1.3: Nature of different types of voltage disturbances with magnitude and duration [24]

1.7 Application of intelligent systems in monitoring, operation and control of power networks

The increased awareness about the need for good power quality from both the utility's side and the consumers' side has led to the application of intelligent systems to monitor and enhance power quality in the recent times. Every day, power networks are becoming more efficient, smarter, intelligent and reliable due to the integration of intelligent systems in the electric power network management and control.

In electric power systems, intelligent techniques are efficiently used for monitoring and analysis of disturbances. It can also be used to detect, localize and estimate any variations in the electric power quality. Many times it is required for decision making and classification of parameters or events. Artificial intelligence (AI) simulates human thinking, decision making, problem solving, learning, perception and reasoning [9]. Several signal processing techniques have been used by researchers within the field of electrical engineering for PQ event classification and detection. Examples of such intelligent tools are expert systems, decision tree, fuzzy logic, artificial neural networks, adaptive fuzzy logic, etc. [25]. L.C. Saikia *et al* [26] presented a technique for detection and classification of PQ disturbances using wavelet transform, fuzzy logic and neural network and S. Mishra *et al* [27] used S-transform and probabilistic neural network for detection and classification of power quality disturbances.

Expert systems are expensive and are not suitable for real-time applications because of their slow execution times. Fuzzy-logic systems are unsuitable for PQ disturbance classification because the distinction between the various types of disturbances is discretely defined by standards or recommendations. Artificial Neural Network (ANN) has the advantage of being used for real-time due to their low computational time [8]. One of the major burdens of an ANN model is its greater computational resources and they are prone to overfitting [28].

1.8 Artificial Neural Networks (ANN)

Artificial neural networks are seen as a new generation of information processing system that resemble the human brain and are known for solving complex problems [25]. ANN is a promising solution for nonlinear system controls; it can learn, predict and provide short response time with a high-precision [29]. ANNs are massively parallel systems with large numbers of interconnected simple processors and are fault tolerant [30]. In an electric power system, there are now widespread applications of ANN in power system fault classification, load forecasting, system planning, voltage stability, economic dispatch and design of voltage stabilizers [31], [32].

The categorization of ANN is shown in Figure 1.4. Its architecture indicates the number of layers present. The topology gives the connectivity pattern, for example, feedforward or recurrent, etc., and the learning regime. Its characteristics include the number of layers, number of nodes per layer, activation function (linear, binary), error function (mean squared error (MSE), cross entropy) and the type of learning algorithms (gradient descent, perceptron, delta rule) [33], [30].

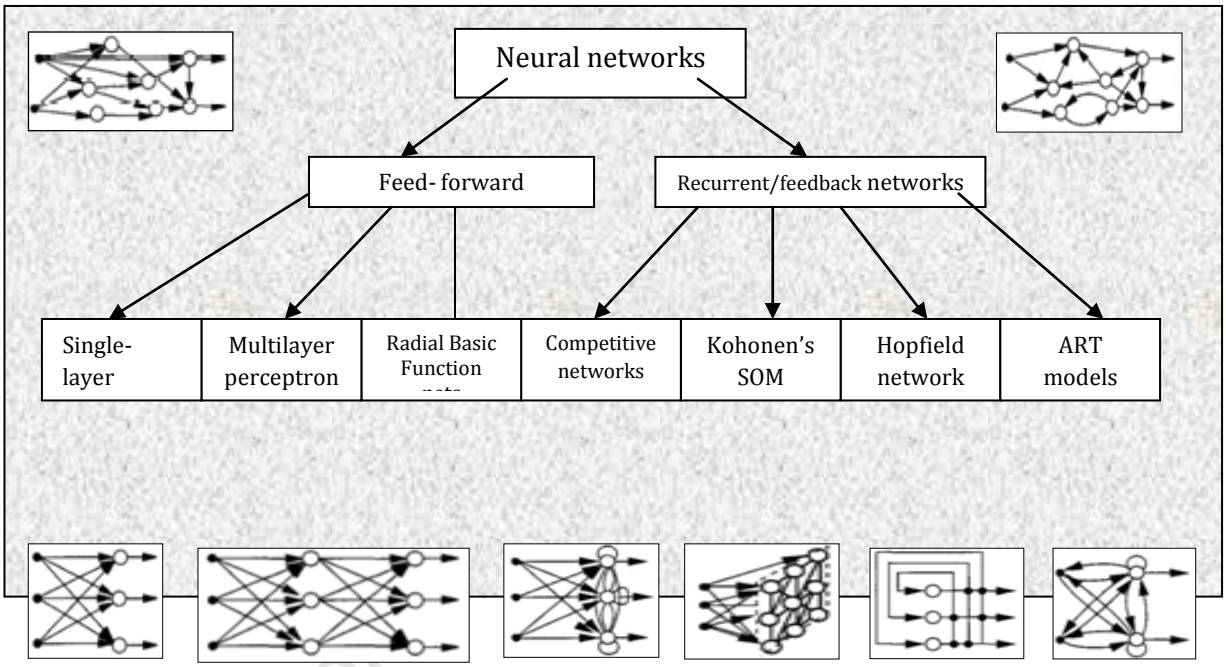

Figure 1.4: Artificial neural network architectures [30]

1.9 Voltage Standards under Engineering Practices

One of the measurements of good power quality of any utility is to operate at the normal standard and practices of engineering and keep the voltage at the customer site within a suitable range during normal operation. This normal voltage has been defined by different standard organizations such as, IEEE, IEC, CBEMA and SEMI [34]. These organizations have proposed standards for better operation and to reduce the possibility of shutting down of sensitive

equipment. Both the utilities and the electrical equipment manufacturers must comply with these standards, otherwise any deviation will result in poor power quality and damage of the equipment leading to financial losses for the customers.

The IEEE Standard 1159-2009, (IEEE Recommended Practice for monitoring Electric Power Quality) and European Standard EN-50160 indicate ±10% voltage variation from the nominal voltage is acceptable as the normal operating voltage [5], [35].

The International Electrotechnical Commission (IEC) and IEEE have introduced the concept of electromagnetic compatibility according to which electrical equipment should be compatible with the quality level of the power system. Figure 1.5 shows the well-known Computer Business Equipment Manufacturers Association (CBEMA) curve. The curve is a reference for equipment voltage tolerance as well as for severity of voltage dips. The "revised CBEMA curve" adopted by the Information Technology Industry Council (ITIC), the successor of CBEMA, is shown as a dashed line in Figure1.5 [34]. These curves can be used to monitor voltage events that occurred in power system.

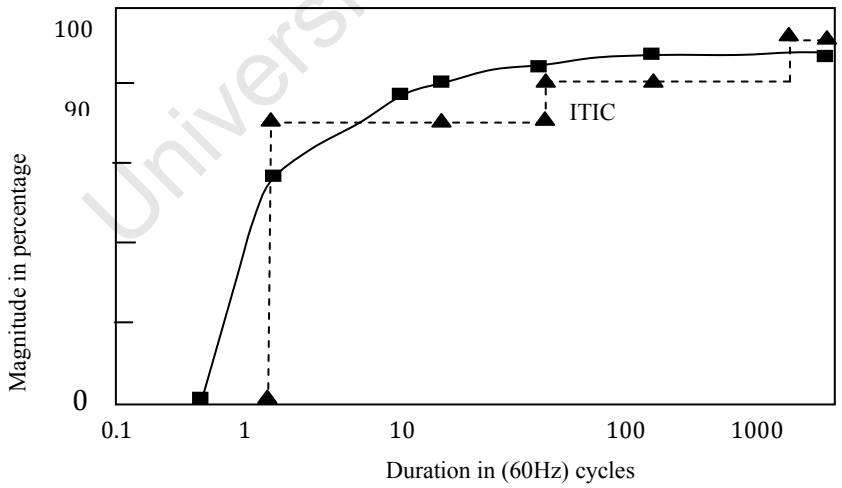

Figure 1.5: Voltage tolerance requirements for computing equipment [34]

1.10 Definitions of voltage dip phenomena

1.10.1 Description of Voltage Dip Event in Electric Power System

Voltage dip is a temporary reduction of voltage for a short time duration which is followed by the recovery of voltage to its normal value. This is associated with the occurrence and clearance of a short circuit or other current overloads or surges in an electric power system. Voltage dips might be experienced at the customer equipment even when short-circuit faults occur in the transmission system far away from the customer premise [36]. Voltage dip in British English is also known as voltage sag in American English, both having the same meaning. Voltage dip magnitude is measured as a percentage (%) or per unit (p.u.) of the nominal voltage. A voltage dip to 40% is equivalent to 40% of nominal voltage. However special attention should be paid when talking about voltage dip magnitude. For example, a 30% dip can refer to a dip that resulted in a voltage of 0.7 p.u. or 0.3 p.u., as this can be either voltage drop (missing voltage) or the remaining (retained) voltage. In most literature and in this thesis, the measurement of the remaining voltage is considered as the voltage dip magnitude as shown in Figure 1.6 below. In Figure 1.6, the nominal voltage is 1.0p.u., V_{th} is the threshold voltage (usually 90% of the declared or nominal voltage value) and V_{dip} is the depth of the reduced voltage during the event. The missing voltage magnitude is (V_{th} - V_{dip}), while the remaining voltage magnitude after disturbance is given by (V_{dip} - 0).

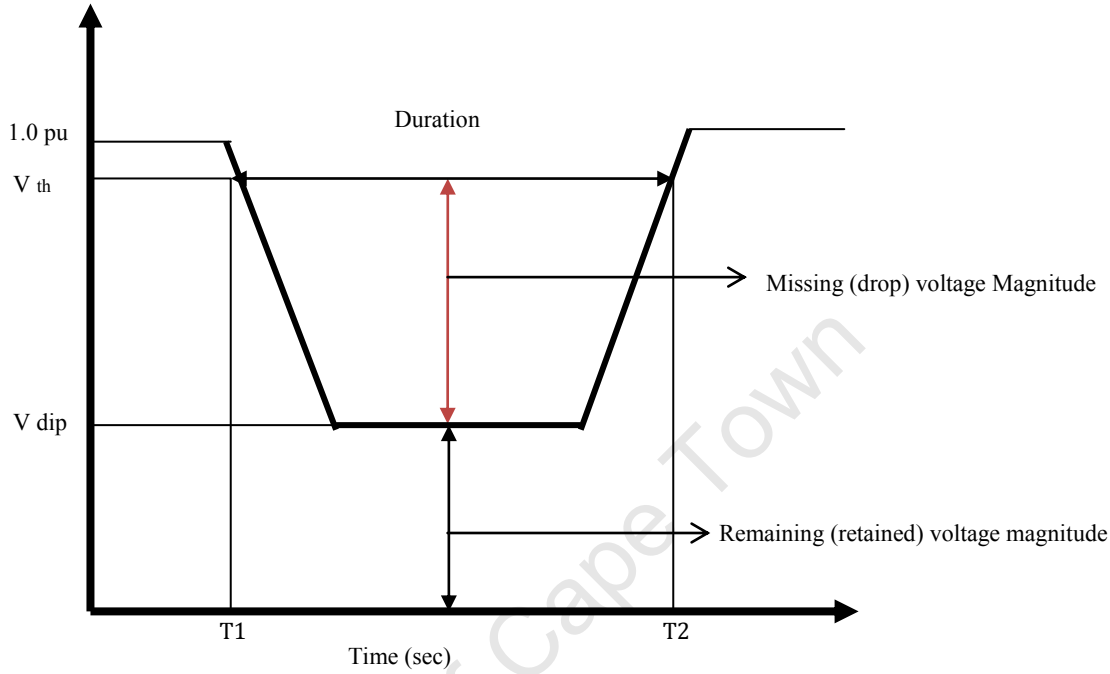

Figure 1.6: Voltage dip shown both the missing and the remaining voltage [40]

The definitions in The IEEE Std 1159-2009 IEEE Recommended Practice for Monitoring Electric Power Quality to label root mean square (r.m.s.) voltage disturbances are based upon their duration and voltage magnitude. Short duration r.m.s. variations are divided into the instantaneous, momentary and temporary time periods, while the voltage magnitude of the disturbance characterizes it as a dip, swell or interruption. A long-duration r.m.s. voltage variation is defined to last longer than 1 minute, and can be classified as a sustained interruption, under-voltage or over-voltage depending on its magnitude [36]. These disturbances are depicted in Figure 1.7.

The IEEE describes a voltage dip as a decrease in r.m.s. voltage between 0.1 p.u. and 0.9 p.u. for durations from 0.5 cycles to 1 min [5].

The International Electrotechnical Commission (IEC) defines a voltage dip as a sudden reduction of the voltage at a point in the electrical system, followed by a voltage recovery after a short period of time, from half a cycle to a few seconds [37], [38].

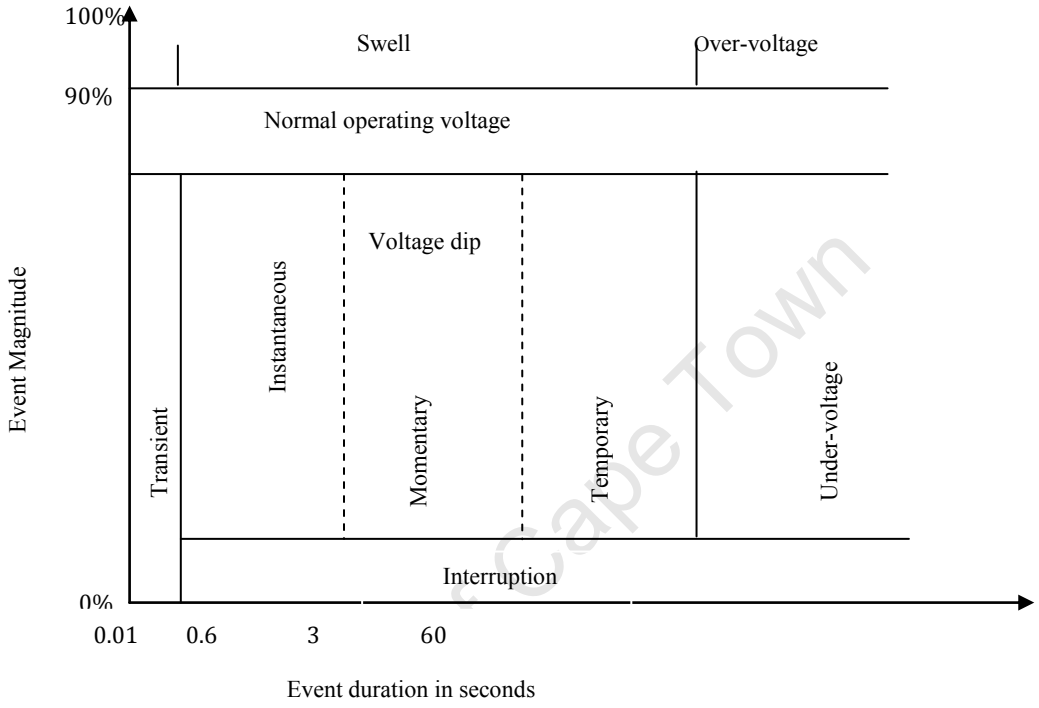

Figure 1.7: Definition of voltage dips according to IEEE Std. 1159-2009 [36]

1.10.2 Typical description of voltage dip

General voltage dip is defined as a sudden reduction of the supply voltage at the power frequency to a value between the ranges of 10% to 90% of nominal voltage followed by a voltage recovery after a short duration usually from 10 milliseconds up to 60 seconds [39]. An example of a typical voltage dip is shown in Figure 1.8 which is a modification of Figure 1.6 that shown the dip as a remaining (retained) voltage magnitude. The voltage dip commences when the declared voltage drops to a lower voltage than the threshold voltage V_{thr} (0.9 p.u. or 90 %.) at time T1, the lower voltage continues up to T2; at T2 the voltage recovers to a value a little over the threshold value. The magnitude of the voltage dip is V_{dip} and its duration is T2 -

T1 [40]. V_{dip} is the remaining voltage as explained earlier.

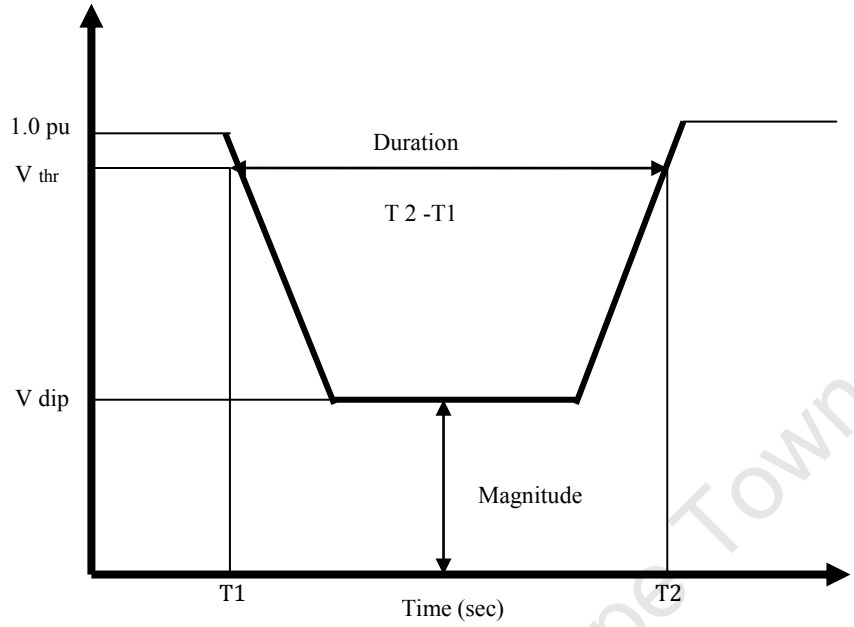

Figure 1.8: Voltage dip [40]

1.10.3 Alternative description of voltage dips

Defining a voltage dip by its magnitude and duration only usually leads to loss of information. For proper dip description phase angle shift and point on the wave must be considered. The description of a voltage dip includes pre-dip, during and post-dip magnitude. This extends the description of dip events beyond the magnitude and duration, and it is called dip segmentation [41]. An alternative description of voltage dips consists of transition segments and event segments. Figure.1.9 shows a typical voltage dip with no segments, and Figure 1.10 shows a voltage dip divided into five different segments, the pre-event segment, the first transition segment, the during-event segment, the second transition segment and the voltage recovery segment [42].

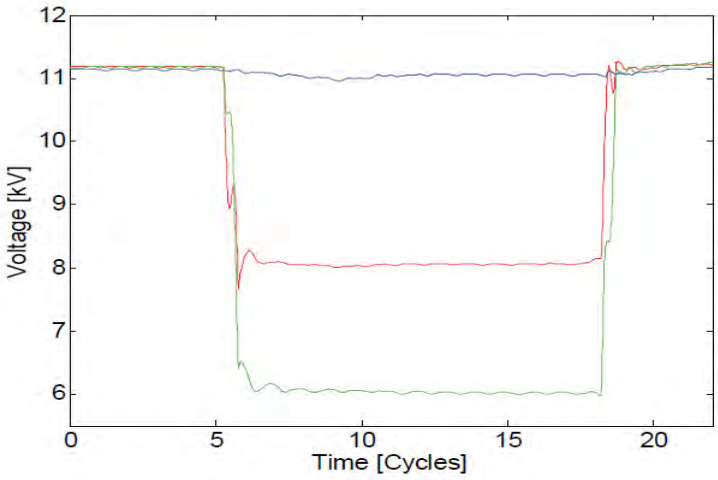

Figure 1.9: Typical voltage dip with no segments [42]

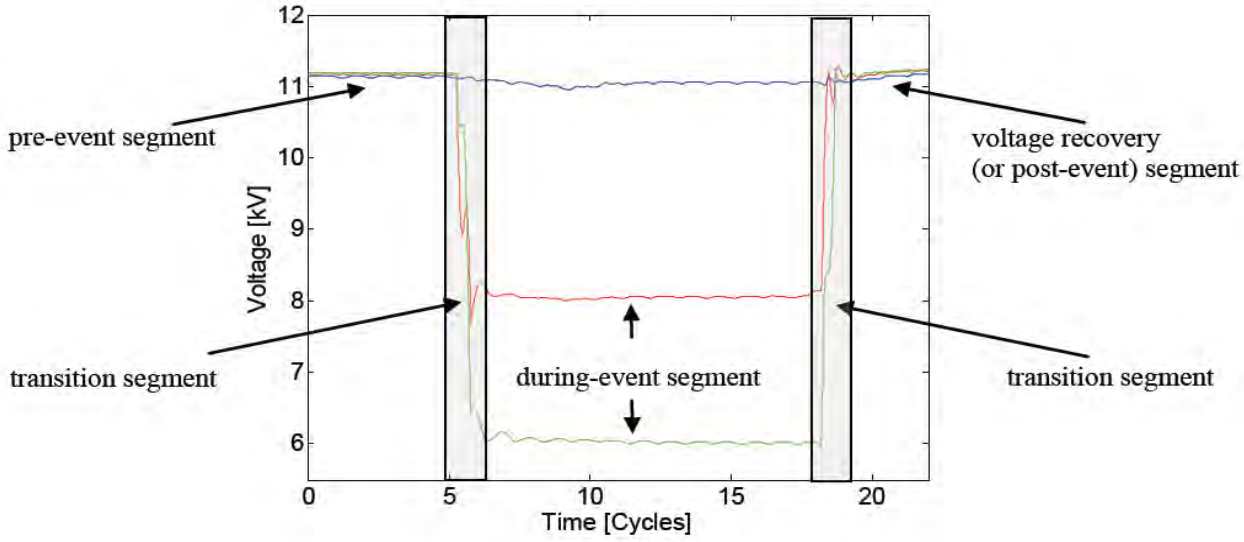

Figure 1.10: Typical voltage dip, with indicated event and transition segments [42]

1.10.4 Descriptions of Voltage dip segments

The pre-event segment is the area of the dip with balanced voltages of nearly nominal magnitude. The first sudden change from where the voltages start to drop from the nominal voltage is called the first transition segment. At this stage, the voltages change from being

nominal (or close to nominal) three-phase balanced to a system of unbalanced voltages whose magnitudes are lower than the nominal magnitude.

The third segment is called the during-event segment where there are unbalanced voltages of lower than nominal magnitudes.

Fourth segment is the second transition segment where the voltages start to recover and change back from a set of unbalanced lower voltages to a system of more or less balanced voltages with nominal or close to nominal magnitudes

The fifth segment, the voltage recovery segment is one during which the voltages are again balanced and with close to nominal magnitude [42].

1.11 Causes of Voltage Dip

The causes of voltage dip can be categorized into man-made and natural. Man-made causes (due to human activities on the power network) include switching operations or starting of large motors, power system faults (short circuit fault), power swings, sudden load changes, generating stations coming on/off line, unplanned load growth and indiscriminate integration of distributed generation. The natural causes include regulator dysfunction, bad weather, pollution, animals and birds, etc. [43]. All these operations could lead to voltage dip, when a voltage dip occurs on the transmission network; the voltage dip can be propagated directly to the distribution system (either the medium voltage or low voltage).

1.12 Factors influencing the severity of voltage dip

The severity of voltage dip can be influenced by many factors such as the type of fault, system configuration, fault location, system protection, etc. It is generally believed in an electrical power system that a three-phase short circuit fault is more severe than either a two-phase short circuit fault or a single-phase short circuit fault. Hence, the voltage dip produced by a three-phase short circuit fault will be more severe than either a two-phase or a single-phase short

circuit fault with the same condition. Fault impedance value also influences voltage dip severity as it will dictate the magnitude of fault current.

System design or configuration such as system impedance and transformer connections may change at the incidence of fault, which can result in tripping of protection systems. This might result in an alteration in system configuration leading to a more severe voltage dip. The presence of the distributed generators can also make voltage dip less severe, especially for sensitive loads. It is possible for some distributed generator to provide voltage support and can also supply reactive power. Fault location can as well influence voltage dip severity. Faults originating from transmission side of a power network will have more impact on the transmission level line than on a distribution level line. Equipment closer to the fault point will experience more severe dip than those located far away from the fault. Other factors are fault impedance, Pre-dip voltage level and Transformer connections.

1.13 Voltage dip characteristics

Many researchers believe that the two main properties that characterize voltage disturbances are residual voltage magnitude and the dip duration. Knowing the characteristics of voltage disturbances and their characterization in terms of magnitude and duration are important for proper analysis and mitigation of short-duration voltage variations like voltage dip [44]. In most cases, fault types, source and fault impedances define the dip magnitude, whereas fault clearing time defines the dip duration. Other characteristics include voltage dip phase-angle jump and point-on-wave of voltage dip [45].

1.13.1 Dip magnitude as a characteristic

Voltage dip magnitude depends on fault types, source impedance and the fault impedance. Most times the impedance between fault point and ground is always neglected, but it should not be practiced as a rule without investigating the impact of the value of this impedance on the nature and severity of the disturbance. The voltage dip magnitude is expressed in percentage or per unit of the remaining voltage and calculated by short-circuit analysis [46].

To find voltage dip magnitude at the equipment terminal in a radial system, the analysis is based on the voltage divider model has shown in Figure 1.11 below. The source voltage and impedance are given by E_S and Z_s respectively. Impedance between point- of-common coupling (point from which both the fault and the load are fed) and the fault is Z_f. The loads are assumed to be of constant impedance type, and it is assumed that there is no voltage drop between the load and the PCC. The voltage V_{pcc} at the PCC is thus given by equation 1.1 which is the dip magnitude of the remaining voltage and also the voltage that is experienced by the load during a three-phase fault [4].

$$V_{pcc} = V_{dip} = E_s \frac{Z_f}{Z_s + Z_f} \qquad 1.1$$

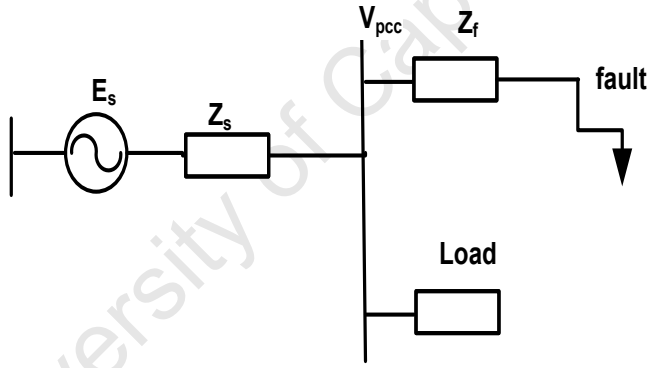

Figure 1.11: Voltage dip magnitude on a radial network [4]

1.13.2 Dip duration as a characteristic

Dip duration depends on the fault clearing time since voltage dip conditions last until the fault is cleared by a protective device. The moment a fault is cleared, the voltage returns to its previous nominal value. Fault clearing time depends upon the utility protection practices such as instantaneous fault clearing or intentional time delay fault clearing [47]. Voltage dip with longer time causes much damage to power system than those with shorter duration. In [46] dip duration is defined as the flow duration of the fault current in a network, and it is determined by the

characteristics of the system protection devices such as relays and circuit breakers. Faults on the transmission system are usually cleared faster than those on the distribution system because of higher fault current magnitudes in the former. When dip duration is too long, they might cause network instability. Hence, it is advised to have a fast response protection system with a short fault-clearing time. It is also important to have a voltage compensation system during the dip duration to avoid black-out. The fault-clearing times of various protective devices and fault-clearing times at various voltage levels for a USA utility are given in Table 1.3 and Table 1.4 respectively.

Table 1.3: Fault-clearing time of various protective devices [36]

Protective devices	**Fault-clearing time**
Current-limiting fuses	Less than one cycle
Expulsion fuses	10-1000ms
Distance relay with fast breaker	50-100ms
Distance relay in zone 1	100-200ms
Distance relay in zone 2	200-500ms
Differential relay	100-300ms
Overcurrent relay	200-2000ms

Table 1.4: Fault-clearing time for various voltage levels for a USA utility [36]

Voltage Level	**Best Case**	**Typical**	**Worse Case**
525 kV	33ms	50ms	83ms
345 kV	50ms	67ms	100ms
230kV	50ms	83ms	133ms
115kV	83ms	83ms	167ms
69kV	50ms	83ms	167ms
43.5kV	100ms	2 sec	3 sec
12.47kV	100ms	2 sec	3 sec

1.13.3 Other voltage dip characteristics

In April 2010, the CIGRE/CIRED/UIE joint working group C4.110, in their technical document, indicated that two different dips can have the same characteristics but have different effects on the customer equipment [42]. Therefore it is likely that only the magnitude and the duration might not characterize a voltage dip adequately.

Other characteristics include voltage dip phase-angle jump and point-on-wave where the voltage dip occurs. Whenever there is a short circuit fault on a power network, there is phase displacement of the voltage compared to the voltage before and after the fault. This phase-angle jump or phase shift is dependent on the relation between the source and fault impedance and is expressed as change of the X/R ratio (where X is the reactance and R is the resistance). Phase-angle jump may not affect most equipment but power electronic converters using phase-angle information for their firing may be affected [45], [48]. The phase shift is described in Figure 1.12 and is given as $T_b - T_a$.

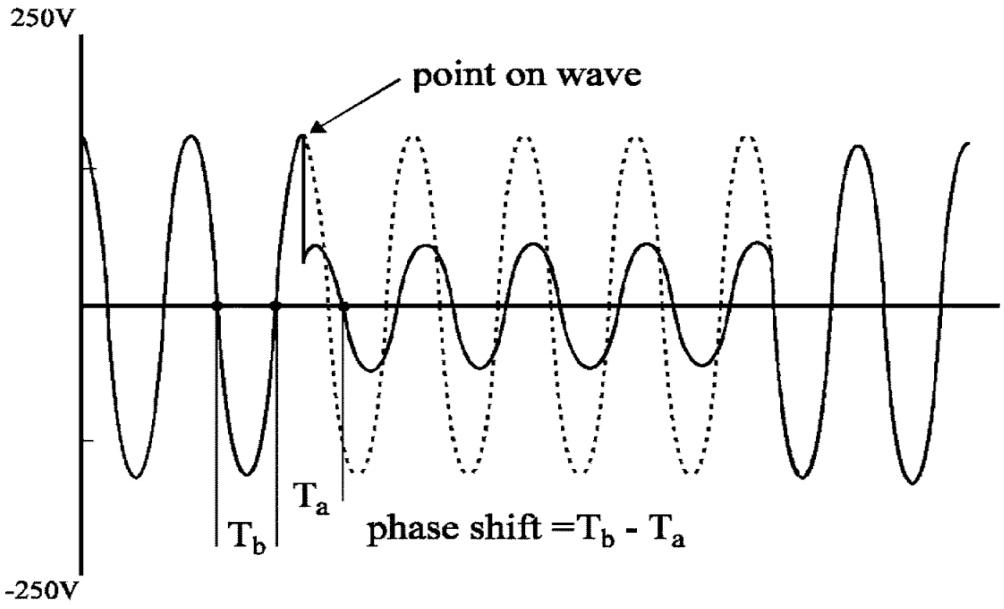

Figure 1.12: Voltage dip with phase shift [49]

The phase-angle jump can be calculated theoretically using the voltage divider model as shown in Figure 1.11. It is assumed that source voltage E_S before the fault is 1p.u., the fault and the source impedances Z_f and Z_s are complex quantities and rewritten as $Z_s = R_s + jX_S$ and $Z_s = R_s + jX_S$. Then equation 1.1 becomes equation 1.2 as shown below.

$$V_{dip} = \frac{Z_f}{Z_s + Z_f} \tag{1.2}$$

The phase-angle jump in voltage is given by equation 1.3

$$\Delta\phi = \arg\left(V_{dip}\right) = \arctan\left(\frac{X_f}{R_f}\right) - \arctan\left(\frac{X_s + X_f}{R_s + R_f}\right) \tag{1.3}$$

If $\frac{X_s}{R_s} = \frac{X_f}{R_f}$ then equation (3) becomes zero and there is no phase-angle jump.

The phase-angle jump will only be presented as the X/R ratio of the source and the feeder [36].

1.14 Methods for dip magnitude calculation

The magnitude of a voltage dip can be obtained from the r.m.s. voltages and this is done in different ways. The r.m.s. voltage which can be calculated from the sample time – domain voltages by using equation 1.4

$$V_{rms} = \sqrt{\frac{1}{N}\sum_{i=1}^{N} v_i^2} \tag{1.4}$$

where N is the number of samples per cycle and v_i is the sampled voltage in time domain.

Usually voltage samples are obtained with a certain sampling rate of 128 samples per cycle or 256 samples per cycle. If equation 1.4 is applied to the sampled voltage dip waveform shown in Figure 1.13, the result will be as Figure 1.14. The r.m.s. voltage over a window of one cycle

(256 samples) was used to obtain Figure 1.14. Half-cycle window can also be use but this usually leads to oscillations in the result when a second harmonic component is present [36].

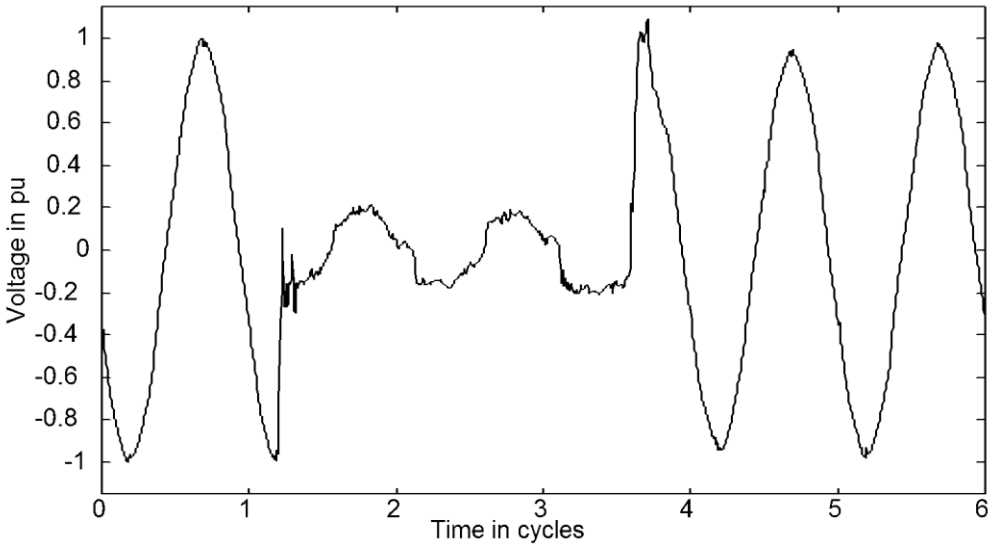

Figure 1.13: A voltage dip due to a short-circuit fault in time domain [36]

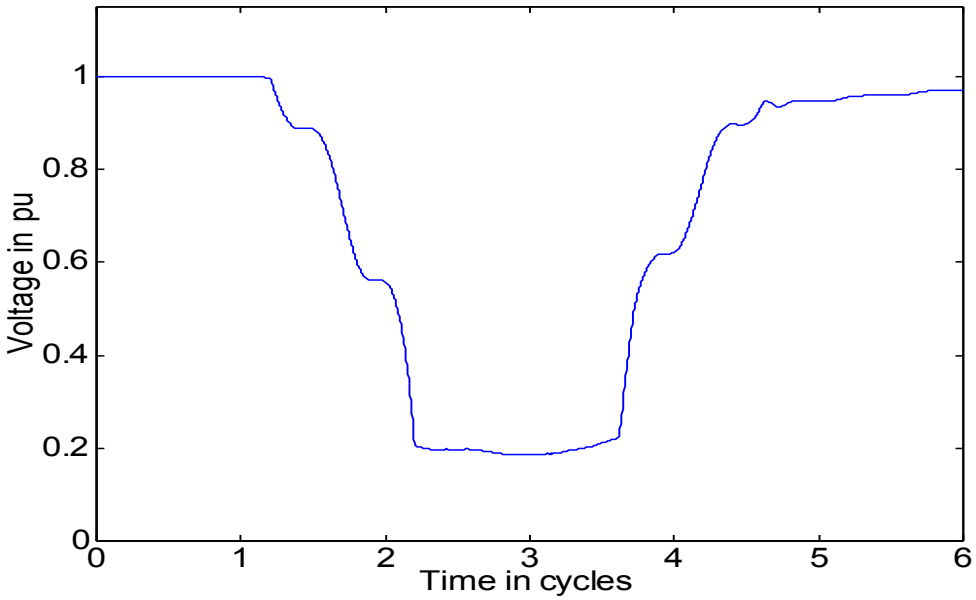

Figure 1.14: One-cycle r.m.s. voltage for the voltage dip shown in Figure. 1. 13 [36]

1.15 R.M.S vs. Instantaneous value

Many power signal processing techniques have been used in power quality detection and classification in recent times. The root mean square is one of the most-used tools because it gives a good approximation of the fundamental frequency amplitude profile of a waveform, it has simple algorithm, high speed of calculation and requires less memory, and can be stored periodically instead of per sample [50].

Many literature works and engineering bodies such as IEEE, ICE, etc. have indicated that voltage dip is a sudden reduction in r r.m.s. voltage within duration of 0.5 cycles to 60sec. Hence, it is preferred that the r.m.s.value be used for calculating the magnitude of a voltage dip. Figure 1.15 shows the instantaneous value of a voltage dip due to three-phase fault measured in instantaneous values compared to R.M.S values as shown in Figure 1.16 and measured on a busbar from simulation in DIgSILENT PowerFactory

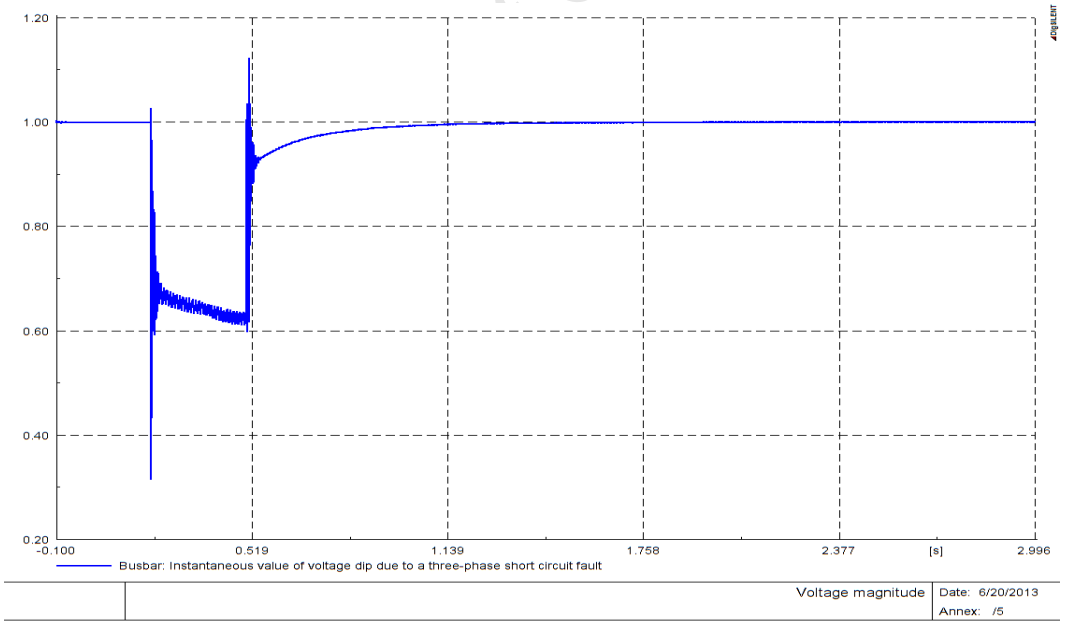

Figure 1.15: Instantaneous value of a voltage dip due to three-phase fault

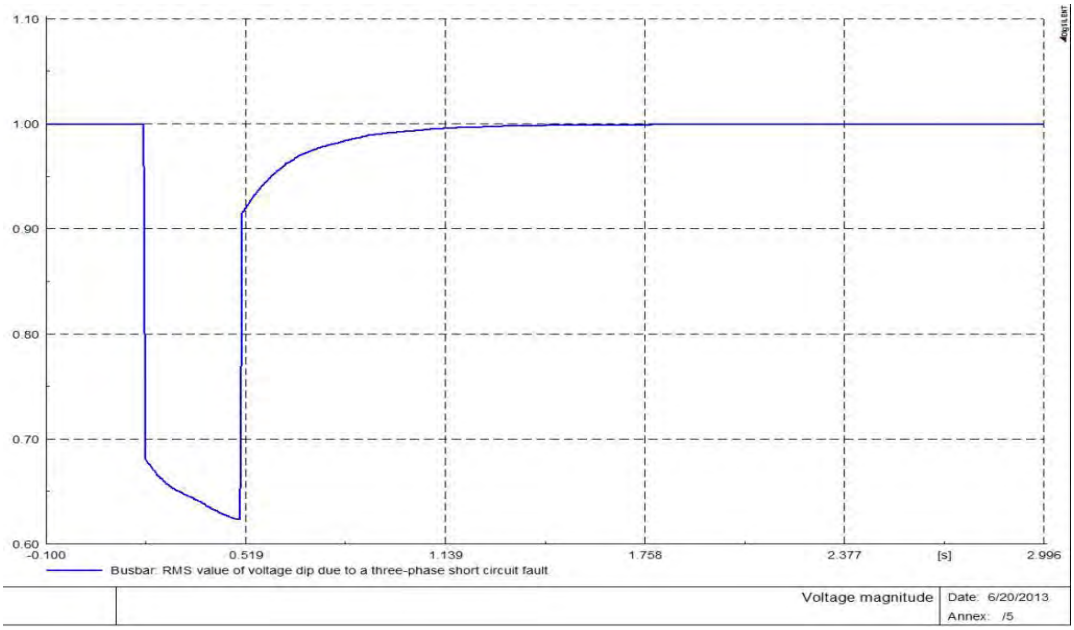

Figure 1.16*:* **R.M.S value of a voltage dip due to three-phase fault shown in Figure. 1. 15**

1.16 Existing Voltage Dip Classification

The method of extracting useful information from measurements that describe the voltage dip event without the need to retain every detail of the event is known as voltage dip characterization. The main characteristics of a voltage dip are its magnitude and duration. During analysis and mitigation of voltage dip, the characterization in terms of magnitude and duration is essential. However, Bollen *et al.* indicated that two different dips can have the same characteristics but have different effects on the customer equipment [42].

Different researches have been carried out on the classification of voltage dips according to their origins to helps utilities to determine location of fault [51]. Voltage dips can also be classified according to the reason why they occurred such a voltage dips due to faults, dips caused by motors, dips caused as a result of transformer energizing etc. [52], [53]. Reference [54] discusses different theoretical and practical methodologies currently used for definition and characterization of voltage dips.

1.16.1 The IEEE categories

The IEEE categorizes voltage dips into three groups depending on the dip duration. Dip duration between 0.5cycles to 30 cycles (10ms to 600 ms with power frequency of 50 Hz system) is classified as instantaneous with typical voltage magnitude between 0.1p.u. and 0.9 p.u. Voltage dip with duration between 30cycles and 3seconds is classified as momentary while dip duration between 3 seconds and 60 seconds is classified to be temporary [5]. The categories are indicated in Table 1.5.

Table 1.5: IEEE voltage dip categories

Categories	Typical dip duration	Typical voltage magnitude (p.u.)
Instantaneous	0.5–30 cycles	0.1–0.9
Momentary	30 cycles – 3 s	0.1–0.9
Temporary	>3 s – 60 s	0.1–0.9

1.16.2 The ABC Classification

The ABC classification is based on non-symmetrical faults and is one of the oldest classifications commonly used. It distinguishes between seven types of three-phase unbalanced voltage dips. The ABC classification can be used to generate and predict the dips that can be expected at the terminals of three-phase equipment. Its drawback includes incomplete assumptions, simulation-based and cannot be directly used to obtain the characteristics of measured dips [55]. The seven types of voltage dips were reported by many researchers [36], [56] and [57] and are defined by complex voltages and phasor diagrams based on the relations between the minimum phase-to-neutral voltage V_{PN} and the minimum phase-to-phase voltage V_{PP} [47]. Other authors such as Ignatova et al. Reference [6] suggests that two additional types are necessary, the dip types H and I. Voltage dip types B, D, F and H are characterized by a major drop in one of the phases, and they are called single phase voltage dips. C, E, G and I are

characterized by major drops in two of the phases and are called double phase dips while dip type A is called a three-phase dip. Table 1.6 shows the phasor diagrams for the nine types of three-phase unbalanced voltage dips while Table 1.7 shows equation form for the first seven types.

Table 1. 6: Nine types of three-phase unbalanced voltage dips according to the abc classification [6]

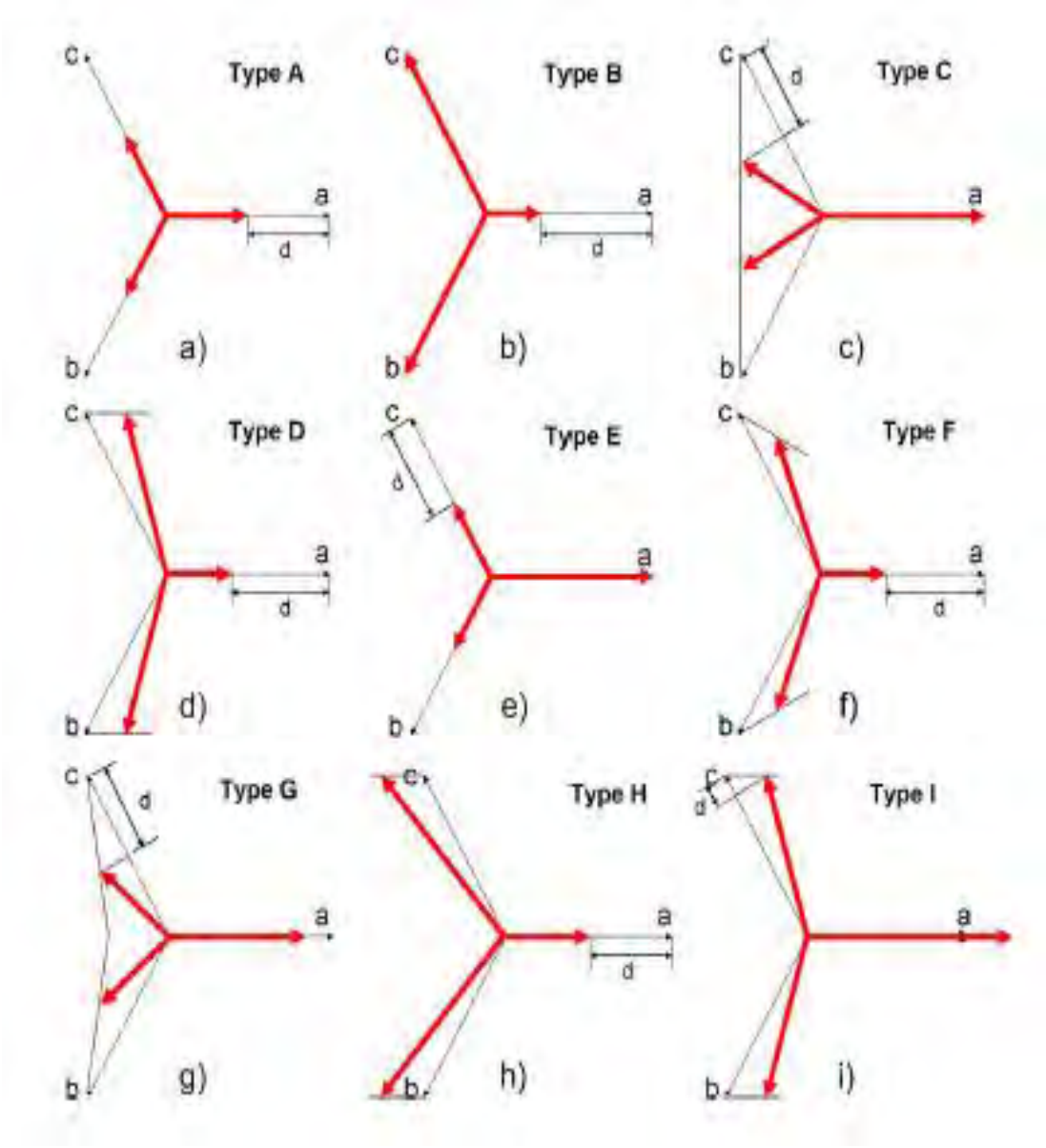

Table 1.7: Dips types in equation form [36]

Type A
$V_a = V$
$V_b = -\frac{1}{2}V - \frac{1}{2}jV\sqrt{3}$
$V_c = -\frac{1}{2}V + \frac{1}{2}jV\sqrt{3}$

Type B
$V_a = V$
$V_b = -\frac{1}{2} - \frac{1}{2}j\sqrt{3}$
$V_c = -\frac{1}{2} + \frac{1}{2}j\sqrt{3}$

Type C
$V_a = 1$
$V_b = -\frac{1}{2}V - \frac{1}{2}j\sqrt{3}$
$V_c = -\frac{1}{2}V + \frac{1}{2}j\sqrt{3}$

Type D
$V_a = V$
$V_b = -\frac{1}{2}V - \frac{1}{2}j\sqrt{3}$
$V_c = -\frac{1}{2}V + \frac{1}{2}j\sqrt{3}$

Type E
$V_a = 1$
$V_b = -\frac{1}{2}V - \frac{1}{2}Vj\sqrt{3}$
$V_c = -\frac{1}{2}V + \frac{1}{2}Vj\sqrt{3}$

Type F
$V_a = V$
$V_b = -\frac{1}{3} j\sqrt{3} - \frac{1}{2} V - \frac{1}{6} Vj\sqrt{3}$
$V_b = +\frac{1}{3} j\sqrt{3} - \frac{1}{2} V + \frac{1}{6} Vj\sqrt{3}$

Type G
$V_a = \frac{2}{3} + \frac{1}{3} V$
$V_b = -\frac{1}{3} - \frac{1}{6} V - \frac{1}{2} Vj\sqrt{3}$
$V_c = -\frac{1}{3} - \frac{1}{6} V + \frac{1}{2} Vj\sqrt{3}$

1.16.3 ESKOM voltage dip windows classification

The South African utility Eskom defines and categorizes voltage dips into seven classes Y, X1, X2, S, T, Z1 and Z2. This category is based on a combination of network protection characteristics and customer load compatibility [58]. Table 1.8 shows YXSTZ classification with the voltage magnitudes both in terms of the missing (drop) voltage magnitude ΔU and remaining (retained) voltage magnitude U_r, where U_d is the declared voltage [58].

Table 1.8: Characterization of depth and duration of voltage dips according to NRS 048-2 [58]

<table>
<tr><td>1</td><td>2</td><td>3</td><td>4</td><td>5</td></tr>
<tr><td rowspan="2">Range of dip Depth ΔU (expressed as a % of U_d)</td><td rowspan="2">Range of residual Depth U_r (expressed as a % of U_r)</td><td colspan="3">Duration t</td></tr>
<tr><td>20< t ≤ 150 ms</td><td>150 < t ≤ 600 ms</td><td>0.6 < t ≤ 3 s</td></tr>
<tr><td>$10 < \Delta U \leq 15$</td><td>$90 > U_r \geq 85$</td><td colspan="3">Y</td></tr>
<tr><td>$15 < \Delta U \leq 20$</td><td>$85 > U_r \geq 80$</td><td rowspan="2"></td><td rowspan="2"></td><td rowspan="2">Z1</td></tr>
<tr><td>$20 < \Delta U \leq 30$</td><td>$80 > U_r \geq 70$</td></tr>
<tr><td>$30 < \Delta U \leq 40$</td><td>$70 > U_r \geq 60$</td><td>X1</td><td rowspan="2">S</td><td rowspan="3">Z2</td></tr>
<tr><td>$40 < \Delta U \leq 60$</td><td>$60 > U_r \geq 40$</td><td>X2</td></tr>
<tr><td>$60 < \Delta U \leq 100$</td><td>$40 > U_r \geq 0$</td><td colspan="2">T</td></tr>
</table>

Figure 1.17 shows the Eskom voltage dip window according to remaining (retained) voltage magnitude Ur for the seven different classes.

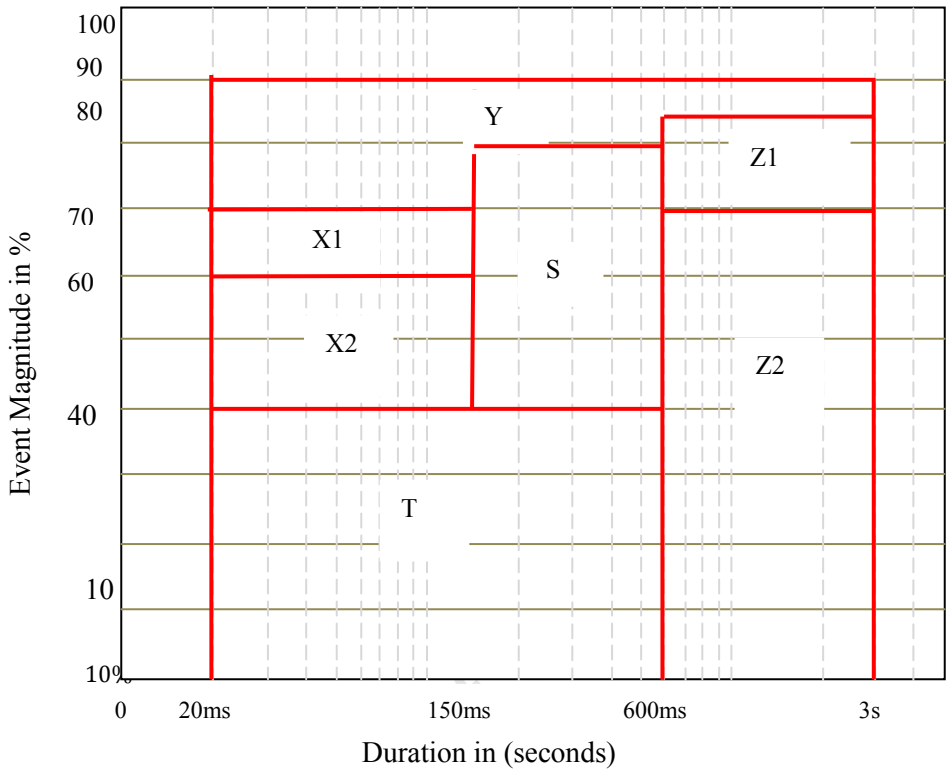

Figure 1.17: ESKOM voltage dip window according to remaining (retained) voltage magnitude U_r [34]

1.16.4 The EPRI-Electrotek classification

EPRI suggests, as listed in Table 1.9, the following five magnitudes and three duration ranges to characterize voltage thresholds. The duration ranges are based on the definition as specified by IEEE Std. 1159- 1995) [20], where the frequency is the number of events per year with magnitude below X.

Table 1.9: Characterization of voltage thresholds according to EPRl -Electrotek [20]

		Frequency for voltage threshold X: with					Duration between
1	RMS variation	<90%	<80%	<70%	<50%	<10%	0.5 cycle - 60 sec
2	Instantaneous RMS variation	<90%	<80%	<70%	<50%	-	0.5 cycle - 0.5 sec
3	Momentary RMS variation	<90%	<80%	<70%	<50%	-	0.5 sec - 3 sec.
4	Momentary RMS variation	-	-	-	-	<10%	0.5 cycle - 3 sec.
5	Temporary RMS variation	<90%	<80%	<70%	<50%	<10%	3 sec. - 60 sec.

1.16.5 The Canadian Electrical Association (CEA)

The Canadian Electrical Association (CEA) also recommends four difference indices for dip magnitude which is indicated by the remaining voltage of 85%, 70%, 40%and 1% [20].

1.16.6 Classification according to the reasons why they originate

Voltage dip can be classified according to the reasons why they originate. For example, they can be categorized according to dip caused by faults, dip caused as a result of electrical motor starting, transformer energizing, multistage voltage dips and voltage dips due to self-extinguishing faults [52], [59].

1.17 Economic loss and impact due to voltage dips in power systems

Some literatures have reported and claimed that voltage dips are the costliest of all power quality disturbances apart from interruptions. Annually, in USA, voltage dips and interruptions cause considerable financial loss to industry. It was estimated to be between U.S. $ 104 billion and U.S. $ 164 billion [60]. The document [61] shows the financial losses as a result of voltage dip associated from ranges of industries in Table 1.10 and another summary of the impact of

voltage sags on various industries from the US in Table 1.11. Effect of voltage dip usually causes disruption of manufacturing processes due to equipment being unable to operate correctly. In many industries, loss of vital pieces of equipment or manufacturing processes as a result of voltage dip may lead to a full shut down of production leading to significant financial losses as shown in Tables 1.10 and 1.11. Damages as result of voltage dip include, significant loss of material as well as the time taken to clean up and restart the process must also be considered.

Table 1.10: Typical financial loss for voltage dips based on industry [61]

Type of Industry	**Financial Loss in €**
Semiconductor Industry	3 800 000
Financial trading	6 000 000 per hour
Computer center	750 000
Telecommunications	30 000 per minute
Steel works	350 000
Glass Industry	250 000

Table 1.11: Impact of voltage dips on US industries [61]

Type of US Industry	**Financial Loss in $\$US$**
Paper Manufacturing	30 000
Chemical Industry	50 000
Automobile Industry	75 000
Equipment Manufacturing	100 000
Credit card processing	250 000
Semiconductor Industry	2 500 000

1.18 Distributed Generation Technology

In the last few decades, the amount of newly introduced DG has increased rapidly. Despite this rapid grow; voltage quality, especially voltage dip as a result of fault, poor power quality disturbances, and integration of both renewable and non-renewable distributed generation has remained a burden to consumers and utilities. Daily research works show the technical difficulties of controlling and managing these DGs especially the renewable DGs since they are being affected by external natural factors. Nevertheless, the DG units provide ancillary services support to both the grid and the load.

1.19 Distributed Generation Definition

Today distribution generation is relatively a developing and small-scale method of generating of electrical power when compare to the centralized generation. It is involving generation of electrical power close to the load being served; it is usually referred to as an electric power source connected directly to the distribution system (either the medium voltage or low voltage) or on the industrial facility grid at the customer site of the meter [62]. In the last decade, different terms have been used by researchers to describe and explain distribution generation. In Anglo-American countries, it is refered to as embedded generation and in North American countries, it is called dispersed generation while in Europe and parts of Asia, the term decentralized generation is used [63]. Some technical works define DG according to the purpose they are serving in a particular power network, their location, the power rating of DG, power delivery area, the technology, environmental impact, and mode of operation, ownership, and the penetration of distributed generation [64]. T. Ackermann *et al*. [63] defines distributed generation as an electric power source connected directly to the distribution network or on the customer site of the meter. Table 1.12 shows the definition of DG as presented by organizations and Table 1.13 presents definition of DG according to its rating by organizations.

There are different technologies that are available for distributed generation, such as micro-turbines, photovoltaic/ solar panels, wind turbines, and fuel cells, etc. In the recent years, the installation cost of distributed generation has reduced as a result of improvement in the technology involved [65].

Table 1.12: Definition of DG according to organizations [66]

Organization/ Institute	**Definition**
CIGRE working group	"All generation units with capacity of 50MW to 100MW, that are connected to the distribution network and that are neither centrally planned nor dispatched".
The IEEE	"Generation of electricity by facilities that are sufficiently smaller than central generating plants so as to allow interconnection at nearly any point in a power system".
CIRED	
IEA	"Units producing power on a customer's site or within local distribution utilities, and supplying power directly to the local distribution network".

Table 1.13: Definition of DG according to its rating by organizations reproduced from [63]

Organization/ Institute	**Definition**
Electric Power Research Institute	a few kilowatts up to 50 MW
Gas Research Institute	between 25 kW and 25 MW
Preston and Rastler	a few kW to over 100 MW
Cardell	500 kW and 1 MW
International Conference on Large High Voltage Electric Systems (CIGRE´)	smaller than 50 –100 MW

The capacity of DG unit depends on it application and the user load, and the use of a particular distribution generation technology is based on the availability and source of its energy to produce electricity. The energy source could be from wind, solar, hydro, etc.

The advantage of DG in the remote area cannot be overemphasized. Remote areas have limited power supply or sometimes no asses to the national grid; this is due to high cost of extending transmission lines, losses and low capacity form the centralized generator. The remote location can make use of the renewable distributed generation; especially when there is availability of

source energy at a reduced cost when compare to extend the national grid. In so many African, countries there are much such remote location.

1.20 Why Distributed Generation

The amount of newly introduced DG to the present power networks has increased exponentially and growing rapidly every day. The reasons might be due to factors such as voltage support, improved reliability, line loss reduction, and transmission and distribution capacity release as provided by the distribution generation [62], [67]. Despite this growing increase in DG, the operators of DG units have failed to consider DG rating, positioning and also both the technical and economic factors on the traditional power networks before installation of DG. This has contributed to poor power quality of today. In 2002, the IEA point out five reasons why there is a renewed interest in DG which include [66]:

1. Developments in distributed generation technologies,
2. Constraints on the construction of new transmission lines,
3. Increased customer demand for highly reliable electricity,
4. the electricity market liberalization and
5. Concerns about climate change.

Apart from these points there are some other technical and economic reasons responsible for increase in DG.

1.20.1 Why DG (technical reasons)

The supply of a good power quality and reliable power network cannot be overemphasis. Most of the developing countries in Africa found good and reliable power supply as a challenge. For example, in Nigeria, the unreliable power supply has led to shut down of many industries and the country's crude oil refineries. Since power is an important infrastructure, most industries and individual decide to invest in DG in other to have a reliable and uninterrupted power supply.

The present of distributed generation in a power network may provide ancillary services support for the grid there by lead to a more reliable and stable operation. Reactive power can also be supplied by DG, especially the synchronous DG and power electronic interface asynchronous DG. Distributed generations have helped to solve some power quality problems such as voltage dip by providing the missing voltage during the dip. DG can be used in remote areas where the national grid is not functioning or the grid is too weak to support the voltage level, energy security and system frequency. They can contribute to increase the grid capacity to meet up with growing increase demand for electrical power by delivering their excess power to the grid.

DG makes use of clean energy and renewable energy to produce electrical power, and it has high efficiency and environmental protection performance is excellent. It has high-energy efficiency up to 65% to 95% [68]. It is important to reduce the effect of poisonous gases from the atmosphere, especially the one cursed as a result of carbon compound from power plants. Environmental policies and regulations such as the Kyoto protocol on climate change (UNFCCC) have forced power producers to look for a cleaner way of generating electrical energy [66].

In summary literature indicates the following advantages of DG schemes as listed below [69]:

a) Improve power quality and reliability
b) Eliminate/reduce transmission and distribution losses due to close proximity to loads
c) Reduce or avoid the necessity to build new transmission/distribution lines or upgrade existing ones.
d) Diversify the range of energy sources in use and increase the reliability of the grid network.
e) Can be configured to provide premium power, when coupled with uninterruptible power supply (UPS)
f) Can be located close to the customer and can be installed in modular sizes to match the local load or energy requirement of the customer.

1.20.2 Why DG (economic reasons)

Distributed generation has a lower capital cost because of the small size when compare to centralized generation. The design and construction of some DG need not building of power transformer and distribution station [68]. DGs are well sized to be installed in small increments to provide the exact required customer load demand. They can be easily assembled and install within a short time, and the power delivered can be increased or decreased by additional or removing modules [67], [70].

Since DGs are connected very close to the load, they reduce the cost of building a new transmission and distribution lines. Additionally, their closeness to the load been served reduces the price of transporting electrical power to the load. According to [66] the IEA report shows that on-site production of electricity could result in cost savings of about 30% of electricity costs.

The energy delivered by many distribution generations connected to the distribution side of a power network is mainly to be consumed by the load within the distribution network. However, this is not usually the case sometimes when the DGs have excess power needed by the load. This excess power is always delivered to the grid. This will reduce the power price according to supply and demand law in economics, stated that the higher the supply the lower the demand and, the lower the price would be.

DG technology encourages different kinds of energy resources; this makes it easy and cheaper to use various available fuels to generate electrical power. There is no monopolizing of energy resources. Having distribution generation installed provides efficient use of cheap fuel opportunities like landfills and municipal solid waste [66]. In combined heat and power DGs waste can be used for heating, cooling or improving the efficiency of the DG through generation of more power.

1.21 Technical limitations of DG

The connection of distribution generation to the distribution side of a power network has changed the characteristics of the power network. This has seriously affected the distribution system design, control, operation, protection, and also affects reliability and security of the system. This requires planning method and making appropriate changes to the traditional distribution network [68].

No doubt that daily installation and power delivery of DG is growing; however it contribution in regard to power delivered to the utility grid remains small when compare to power deliver by centralized power plants. . In most cases, the availability of renewable energy, such as sun, water and wind determines the feasibility of a renewable-energy system [62].

It is known that electrical power flows from higher to lower voltage levels (from transmission to distribution) but the inclusion of distributed generation units within the power network has to induce power flow from the low voltage into the medium-voltage grid. This makes the electrical power to flow now in a directional. This situation always affects the power quality negatively. It can lead to power quality problems such as harmonic distortion, frequency deviation and change in voltage profile [62]. In addition, the power electronic interface in some DG technology is capable of producing and contributing to the system harmonics.

Directional power flow can also reduce the effectiveness of protection systems. This condition usually conflicts with the protection relay and breaker re-close. Other technical challenges of DG include voltage transients as a result of disconnection and the operation of the DG during faults. The operators of DG systems must ensure resynchronisation with the grid's voltage and frequency after a power disturbance or outage and make sure that no power is supplied to the grid during the time of the outage [66].

Other shortcomings of DG are increase in short circuit level and overloading of lines and equipment leading to thermal overloading.

1.22 Economical limitations of DG

The small size of distributed generation makes it to have a lower capital cost when compare to centralized generation. On the other hand, some researchers such as the International Energy Agency believe that it has a relatively high capital cost per kW installed power compared to large central plants [66].

The detection and clearing of power system fault on a system with DG units are more complicated and complex because of the bidirectional power flow within the network, therefore, a costly and more sophisticated protective device will be required [62].

1.23 The benefits and ancillary services support of DG systems to the grid

The existing electric grid was designed and created to safely and reliably distribute power from few concentrated power generation sources through highly monitored and controlled transmission lines to the distributed loads. Distributed Generation (DG) puts new demands on the existing electric infrastructure by introducing electric generation sources distributed throughout the distribution grid.

The operation of an electricity supply system in a reliable manner requires the provision of what are termed ancillary services. These technical services include reserves, reactive power, congestion management and black-start capability [71]. Ancillary services are being provided increasingly through market mechanisms, and wind generation has the potential to earn revenue from them. They can be contracted on a long-term basis in a competitive manner. They can be provided through centralized markets, for example, locational pricing for congestion management, and co-optimized energy and reserve markets [72].

Many works [73], [74] provided general discussion about DG impact on power system, and the ancillary services that it can perform. However, what a DG is really able to do depend not only on the kind of DG source, but also on working, loading and technological conditions. So, in most cases, detailed analyses have to be made. In fact, the question of power quality and

distributed generation is not straightforward. On one hand, Distributed Generation (DG) contributes to the improvement of power quality. In the areas where voltage support is difficult, DG offers significant benefits for the voltage profile and power factor corrections.

A wind turbine can provide reserve by not operating at its maximum power output for the wind available that is spilling wind. This may make economic sense in certain circumstances. The more modern wind turbines or wind farms can control reactive power and can participate in voltage control. Black-start capability is impossible for a wind turbine as it depends on wind availability [71].

In wind generation, there are three main used technologies: synchronous generator, asynchronous generator and power electronics converter interface. It is well known that fixed-speed wind turbines, employing pure-without power electronic converters-asynchronous generators, can lead to voltage collapse after a system fault or a trip of a nearby generator. They consume large amounts of reactive power during the fault, which impedes on the voltage restoration after it [75].

Variable-speed wind turbines with doubly-fed induction generators or synchronous generators, when connected to the grid by power electronics converters have positive impacts on the grid and can hardly have a risk of voltage collapse. The can resynchronize immediately after a fault, they do not contribute to the fault level, and they do not consume reactive power [75].

Like wind generation, solar generation also experiences intermittency, which is a combination of non-controllable variability and partial unpredictability, and depends on resource that is location dependent [76]. When integrating solar generation into the grid, the three distinct aspects earlier mentioned create distinct challenges for generation owners and grid operators. And as the presence of both wind and sunlight is temporally and spatially outside the human control, integrating wind and solar generation resources into the grid involves managing other controllable operations that may affect many other parts of the grid, including conventional generation. These operations and activities occur along a multitude of time scales, from seconds to years, and include new dispatch strategies for generation resources, load management,

provision of ancillary services for frequency and voltage control, and expansion of transmission capacity, etc. [77].

The essential insight to integration of variable Renewable Energy (RE) is that its variability imposes the need for greater flexibility on the rest of the grid, from other (controllable) generators to transmission capacity to loads. In fact, on the seconds to minutes time scale, grid operators must deal with fluctuations in frequency and voltage on the transmission system that, if left unchecked, would damage the system as well as equipment on it. To do so, operators may order generators to inject power (active and reactive) into the grid not for sale to consumers, but in order to balance the actual and forecasted generation of power, which is necessary to maintain frequency and voltage on the grid. For an impressionistic overview, the specific description of these ancillary services includes frequency regulation, spinning reserves; non-spinning reserves, voltage support, and black-start capacity [77].

Sustainable hydropower is a renewable, safe, clean and reliable source of energy. It already supplies energy to most of the countries around the world, and its development is most advanced in some of the richest and most environmentally aware nations. In fact, hydropower enables power to be effectively stored in freshwater reservoirs, allowing it to be released to meet peaks in demand or loss in supply from other sources. This makes it the natural renewable partner for other technologies such as wind, wave, tidal or solar, which do not themselves provide continuous supply [78].

In a mixed energy system, hydroelectric generation is recognized to have unique capabilities that offer to operate flexibility and cost advantages over other types of generation. However, hydropower's flexibility enables fossil-fuel plants to operate in a steady state at their highest efficiency, further reducing emissions. It also improves energy security.

In order to guarantee a level playing field for the generators and customers to access the transmission network, the Transmission System Operator (TSO) is required to be independent of other market participants. The ISO or TSO have acquired central coordination role and

carries out the important responsibility of providing ancillary services to ensure system reliability and security [78]. These services include the following: regulation and frequency response, reactive supply and voltage control, scheduling, system operation control and dispatch, energy imbalance service, operation reserves, and black start service. Table 1.14 shows the technological capabilities of distributed energy resources (DER) Unit

Table 1.14: Technological Capabilities DER Unit [79]

Ancillary services / DER Unit	WTG		PV	Hydro		CCHP				Storage	
						Thermal-driven		Electrify-driven			
frequency control		+	+		+		NO		++		++
Voltage control Congestion management, Optimization of grid losses	INV	++	++	INV	++	INV	+	INV	++	INV	++
	SG	++		SG	++	SG	+	SG	++	SG	++
	DFIG	+									
	IG	-		IG	-	IG	NO	IG	-	IG	-
Improvement of voltage quality	INV	++	++	INV	++	INV	++	INV	++	INV	++
	SG	NO		SG	NO	SG	NO	SG	NO	SG	NO
	DFIG	+									
	IG	NO		IG	NO	IG	NO	IG	NO	IG	NO
Block start	INV	+	+	INV	+	INV	NO	INV	++	INV	++
	SG	+		SG	+	SG		SG	+	SG	+
	DFIG	-									
	IG	NO		IG	NO	IG		IG	NO	IG	NO
Islanded operation	INV	+	+	INV	+	INV	NO	INV	++	INV	++
	SG	+		SG	+	SG		SG	++	SG	++
	DFIG	-									
	IG	NO		IG	NO	IG		IG	NO	IG	NO

legend		
	Grid coupling technology IG is directly-coupled induction generator SG is directly-coupled synchronous generator DFIG is double-fed induction generator CCHP is Combined Cooling Heating and Power IVN is inverter (including inverter- coupled IG and SG)	++ indicates very good capabilities + indicates good capabilities - indicates little capabilities No indicates very little capabilities WTG is wind turbine generator PV solar photovoltaic Hydro is hydro generator

1.24 Types of Distributed Generation

Many literatures and text books have shown various ways, types, groups and categories of distributed generation. These grouping of distributed generation can be classified either based on it construction. Technology involved such as prime mover used, engine turbines, and also based on fuel resources either renewable or non-renewable resources [80]. The advantage of these grouping helps to compare and make a decision with regard to which kind is more suitable to be chosen in different situations [70]. Figure 1.18 shows the distributed generation types and technologies used for distributed generation.

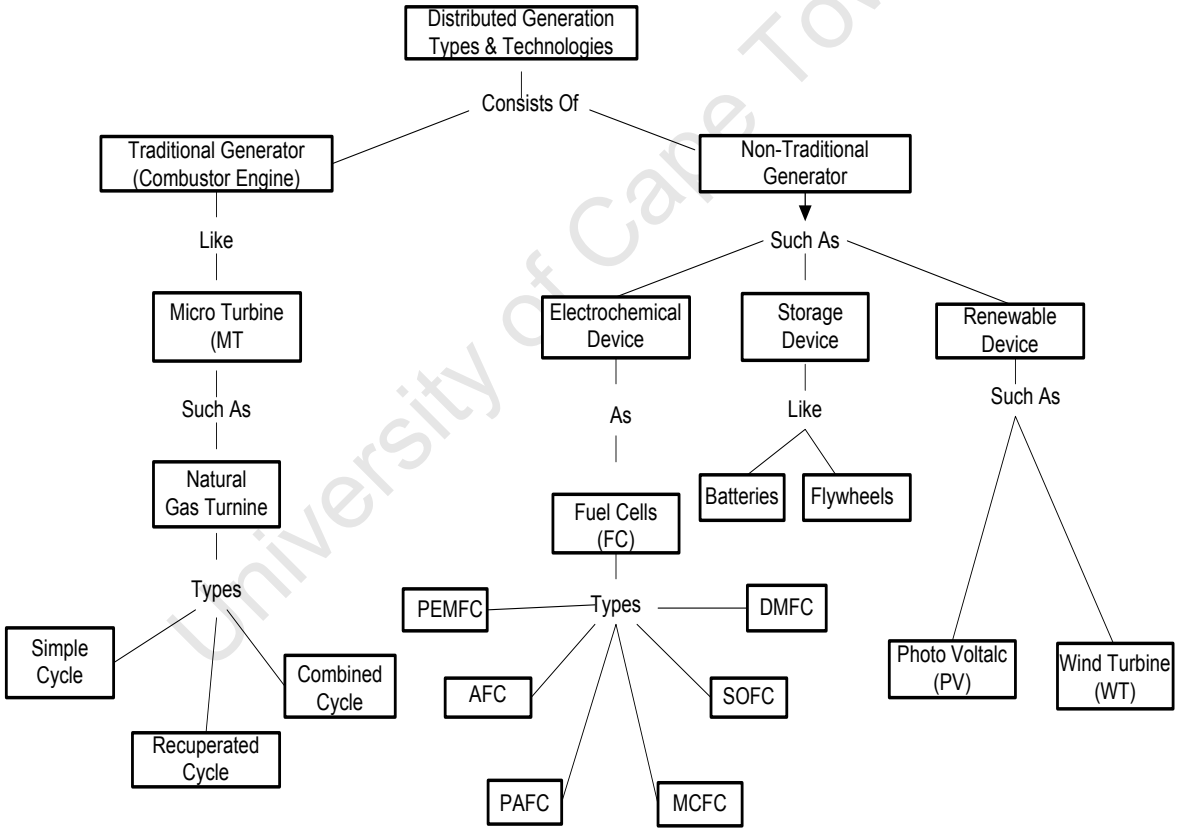

Figure 1.18: Distributed generation types and technologies [70]

1.25 Types of DG electricity/power generation technologies

Generally, three kinds of generator technologies are normally employed and involved in DG technology. The synchronous generator, inductor generator and power electronics converter interface.

1.25.1 Synchronous generator

Synchronous generators are machine that are driven at a speed that corresponds to the number of poles of the machine and the frequency of the electric power system with which it is connected [80]. They work at a constant speed related to the fixed frequency of the power system and their excitation can be adjusted to control its reactive power output.

1.25.2 Inductor generator / Asynchronous generator

The operation with this type of generator is different from the synchronous generator, especially when connected directly to the grid, as they are not capable of supplying reactive power instead they draw reactive power unless its interface with capacitors or power electronics. They are suited for variable-speed operation in the wind farms.

1.25.3 Power electronics converter interface

Some DG like photovoltaic modules, batteries, and fuel cells have no capacity to generate an AC voltage at power frequency of 50 Hz. Power electronic converters are needed to convert the DC voltage generated by these DGs to AC voltage. DG such as solar photovoltaic, fuel cells, well as battery storage systems are examples of a power electronics converter based distributed generation. Figure 1.19 shows power electronic circuits (inverter) converting DC into a specified AC frequency using fuel cells (FC). Since the power electronics converter based DG delivers dc power, it dynamic performance varies when compare to other types of DG [81]. It must be inverted and stepped up to be able to use for household applications as well as for distributed generation [82].

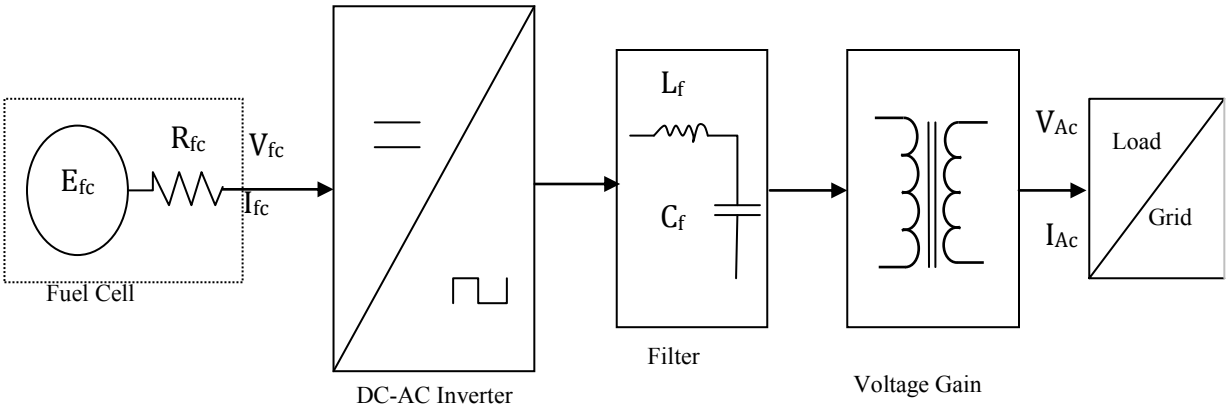

Figure 1.19: Single stage FC-based power supply system [82]

1.26 Renewable Distributed Generation Technology

Renewable distributed generation is one of the available cheap and alternative ways of generating clean and green energy in recent times. It makes use of renewable sources like sun, hydro and wind. However, the integration, management, system stability, voltage quality, active and reactive power flow control and coordination of RDG have always been concerned issues to power systems engineers. In recent times, a lot of significant researches have been going on in the area of renewable energy and low carbon technologies. In the report of reference [83], the three stage of the electrical energy supply chain was identified. These are low carbon electricity generation, low carbon electricity networks and low carbon electricity services.

1.27 Modes of Renewable Power Generation

1.27.1 Wind power

Wind power is produced by using wind turbine generators to harness the kinetic energy of wind. Wind turbine is made up of the rotor blades, shaft and the generator. The blades produce the rotation when the wind forces it to turn. Shaft is a rod that connects the rotor blades to the generator in other to transfer the rotational mechanical energy to the generator. The generator

finally converts the mechanical energy into electrical energy. The efficiency of wind turbine depends on wind power, the altitude, obstructions, the blade and the air temperature [84].

Wind energy is growing at a rapid rate, and it has been described as one of the fastest growing energy technologies. It has more than 30% yearly growth and at the end of 2008 about 121,000 MW has been installed globally. 45% of this installed capacity is located in EU countries [83]. Wind energy impact on electrical power generation is significant, and it is anticipated that more than 300GW of installed power, of which 120GW off-shore, will be installed throughout Europe in the year 2030.

1.27.2 Solar power

Solar power is the conversion of energy from sunlight into electricity. Sunlight produces the world largest energy of 170,000TWth; it is free, clean, endless and exploitable in almost every part of the world. Solar technologies can either use photovoltaic (PV) directly to produce electricity through photoelectric materials, or indirectly using concentrated solar power (CSP). CSP is also known as solar thermal electric, which is the production of electric power though heat generated as a result of solar radiation [85].

Grid-connected PV systems do not control the grid voltage; they only inject current into the utility. The voltage operating range for PV inverters is selected as a protection function that responds to abnormal utility conditions, not as a voltage regulation function [86].

1.27.3 Hydroelectric power

Hydroelectric plant converts the potential energy of water into electrical energy. This involves the movement of water from the source to the turbine flow-out which turns the electrical machinery. In 2001, hydroelectric power was the world's second largest of electricity. It was forecasted in reference [85] that the world output capacity of hydroelectric power will be 4,749 TWh by the year 2030.

1.27.4 Biomass

Biomass which accounted for 10.6% of the global primary energy supply throughout the year 2004 is the largest exploited source of renewable energy in the world. It has a large energy volume when compared with coal, oil and gas [85].

1.27.5 Geothermal energy

Electricity can be produced from geothermal energy. This is done through the heat from the earth heating water from the underground reservoirs. The temperature of water that can be used for generation of electricity is typically 225°F-600°F. There are currently three types of geothermal power plants that include dry steam, flash steam and binary cycle [87].Other renewables includes wave power, tidal power and nuclear power.

1.28 DG technologies can be classified into two categories based on the output power characteristics of DG

It is possible to determine the output power of non-renewable DG units by controlling the primary energy source while renewable DG energy cannot be controlled since the primary energy source is stochastic in nature [13]. Table 1.15 shown examples of both controllable and non-controllable DG. Distributed generation can be operated as standalone or grid-connected power systems.

Table 1.15: Controllable and Non-controllable classification of DG [13]

DG technology	Controllable	Non-controllable
Conventional fossil-fuel Based Generators	✓	
Micro turbines	✓	
Combined hydro-power (CHP) Plants		✓
Small hydro-power Plants		✓
Wind turbines		✓
Photovoltaic		✓
Fuel cells	✓	
Geothermal power plants	✓	
Biomass power plants	✓	

Tidal power plants		✓
Wave power plants		✓

1.29 Factors influencing the choice of DG technology

The location of renewable DGs such as hydro, wind, and solar units require certain geographical conditions. The choice of DG technology can be influenced by system design including DG placement and sizing [69]. These are as follows:

a) Energy costs and fuel availability
b) Electrical load size/factor/shape
c) Load criticality
d) Thermal load quality/size/shape
e) Special load considerations
f) Regulatory requirements

1.30 Impact of DG in a power network

There are many factors that affect the impact of DG in a power network such as location, size, etc. The location of DG depends on the availability of weather parameters. Different DG locations can have a positive or negative impact on the system, especially on voltage dip mitigation. The impact depends on positions of the load bus and position of DG installed in the system. The amount of power supply by DG depends on its capacity. Different capacities of DG can supply different powers to the power system during voltage dips. The impact also depends on the total load in the network. Chapter 2 reviews voltage dip mitigation techniques with different distributed generation sources and also the techniques for detection and classification of voltage dips in electricity networks.

1.31 Grid connection requirements for renewable distributed generation

1.31.1 Connecting renewable distributed generation to the Grid

The renewable distribution generation can be connected both at the distribution and transmission level of electric power network. There are guiding rules and standards that provide the mode of connection to the main grid which is known as grid code. It is very important to regulate and monitor how RDG is connected to the grid, because of the technical and procedural requirements needed for safety, reliable and efficient [88]. In the field of electrical engineering, these standards and codes are set by engineering bodies such as the IEEE, IEC 61400-21, 2001, and also by a national energy regulator. In South Africa, the national energy regulator of South Africa (NERSA) regulates, approves and amends grid codes. NERSA is the administrative authority for all codes.

1.31.2 South African Grid Code and Connection Requirements

Grid code is a technical detailed description of how electrical plant can be connected to the main grid in other to ensure safety and proper operation. Many countries have standard on how electricity should be generated, transmitted and distributed. Furthermore, grid code indicates trading of electricity, economic proper functioning and security of the electric system. The installation of RDG systems on our power network must not jeopardize or reduced power quality of the normal operation of our power grid.

Various aspects of grid code include voltage operation, and tolerances range, frequency requirement, active and reactive power requirement. These are usually specified by an authority responsible for electricity regulation, system integrity and network operation. Table 1.16 shows South Africa grid code requirements for different categories of renewable energy, which depends upon the size of power plant and connection voltage.

Table 1.16: Categories of renewable-energy facilities [89]

Categories	Connection voltage	Power range
A1	LV	$0 < X \leq 13.8KVA$
A2	LV	$13.8KVA < X < 100KVA$
A3	LV	$100KVA \leq X < 1MVA$
B	MV N/A	$0 < X < 1MVA$ $1MVA \leq X < 20MVA$
C	N/A	$\geq 20MVA$

Table 1.17: shows the differences between synchronous and asynchronous generators.

Table 1.17: Differences between synchronous and asynchronous generators [90]

Synchronous generators	Asynchronous generators
Can inject or absorb reactive power	Always absorbs reactive power
Can supply islanded networks, without the need for an external power supply.	An external source of reactive power is required
Operates at synchronous speed	Operates with a slip frequency above the synchronous speed. The magnitude of the slip determines the injected power.
Short-circuit contribution takes longer to decay due to the sub-transient and transient behavior of the generator	Short-circuit contribution reduces quickly, typically before the sub-transient time period has been exceeded
The power transmitted depends on the prime mover and the load angle between the rotor and the system	The power transmitted is dependent on the prime mover and the slip frequency
Requires synchronizing equipment	Connects to system when operating faster than system and with slip

Chapter 2

2.1 Review of voltage dip mitigation techniques with distributed generation in electricity networks

Researchers in the field of electric power quality are becoming increasingly concerned over the years, regarding voltage quality disturbance caused as a result of voltage dip. In recent times, the rising usage of sensitive electrical and electronic equipment has made the provision of good voltage quality mandatory for power utilities. In addition, power system faults, leading to unhealthy voltage dips, are stochastic in nature and cannot readily be eliminated from regular utility operation. Voltage dip is a major concern because it causes equipment malfunction, damage and financial loss, and reduces customer satisfaction [62], [69].

Different types of additional costs have been incurred by both the power utilities and the consumers as a result of voltage dip. Examples of costs incurred by a typical industrial consumer include, cost of lost in production, cost of damaged product, cost of maintenance and hidden cost. A number of technologies have been already employed to mitigate voltage dip in an electric power network both by the utility and the consumer. In power quality research literature, various methods and solutions have been proposed by power and energy researchers to alleviate voltage dip and other PQ disturbances.

The presence of distributed generation from renewable sources in the distribution network is quite useful in delivering different ancillary services to the utility such as voltage dip mitigation and improving the voltage profile at critical buses. These have proven a positive effect on the customer's sensitive equipment and the utility's quality of power supply. Technical literatures have shown that DG helps to maintain during-fault voltage in a power network close to nominal levels [91], [92]. The methods involve in voltage dip mitigation have been grouped into active and passive measures [93].

2.2 Active measures

Active measures are methods that reduce equipment sensitivity and also the number of voltage dips. These methods act on the operations that generate the disturbances that led to voltage dip, such as reducing the number of faults on the power network. Different active measures have been employed for voltage dip mitigation, as listed below [43]:

i. Implementing strict policy for maintenance and inspection;
ii. Mitigation through system improvement and improve network design;
iii. Having power system components of high quality;
iv. Underground cables instead of overhead lines;
v. Reducing the duration of faults;
vi. Increasing equipment immunity;
vii. Covered conductors instead of bare overhead lines;
viii. Changing the power system layout and
ix. Surge arresters instead of spark gaps.

During voltage dip mitigation, it is required to carefully observe the characteristics of the dip process, nature and its origin so that a proper and adequate mitigation measure can be taken. It is important to reduce the number of voltage dips by preventing the occurrence of faults by designing and installing appropriate protection schemes that minimize the impact of faults to acceptable level of power quality such as the system average r.m.s. (variation) frequency index (SARFI) which represents the average number of specific r.m.s. variation events that occur over the assessment period per customer served [94].

2.3 Passive measures

Generally, methods that compensate or balance for the missing voltage during the disturbance are referred to as passive measures. These methods keep the voltage at its nominal value during the dip. During the voltage dip process; there is a significant retained voltage, which is not useful for the sensitive load; however there are some voltage dip mitigation equipment such as automatic voltage stabilizer that can be used to mitigate voltage dip without energy storage

mechanism [91]. Voltage stabilizers rely on generating full voltage from the energy still available at reduced voltage during the dip. Examples of voltage stabilizers are electro-mechanical, ferro-resonant or constant voltage transformer (CVT), electronic step regulators, electronic voltage stabilizer (EVS), etc, [69].

Other methods involve energy generation and storage which can supply the missing voltage, this include distributed generation, battery and capacitor banks. Research is going on for the utilization of distributed generation for mitigating of voltage dip problems and several methods or schemes have been reported and proposed with DG.

2.4 Previous work on voltage dips mitigation using distribution generation schemes.

The effect of distributed generation from renewable sources on voltage dips in a power network depends on the design of the protection system and the coordination between the different protective devices [95]. It is important to find the best location for DG placement, design, and capacity for optimum mitigation of voltage dip. Other factors such as the DG generated power type and DG supply duration also have an impact during voltage dip mitigation.

Many research works such as [96] have shown the effects of DG location on voltage dip mitigation and [19] shows how various DGs types can be used to mitigate the effect of voltage dip. The ability of a DG to mitigate voltage dips depends on its location. Therefore, the first step for employing DGs to mitigate voltage sags is to find the most suitable location for them to be used for this purpose [97].

2.4.1 Application of converter-based DG, synchronous and asynchronous generators

Many technical literatures have shown that the presence of grid-connected distributed generation can have a positive effect on the retained voltage during the voltage dip. The authors of [4] investigate and compare the effects of converter-based DG units, synchronous and asynchronous generators on the retained voltage during voltage dips in low voltage distribution

grids. The positive effect of the synchronous and power electronics equipped induction generators connected to the grid is generally known to be favourable. These generators provide reactive power for the grid as a result of voltage dip and this surely increases the retained voltage during the dip. However, in the low-voltage distribution grids, the impact and the behaviour of converter-based DG is negligible as a result of their unitary power factor, and the currents injected into the grid are limited to the nominal current of the converter [4]. The provision of reactive power and injection of voltage during voltage dip depends on the type of DG and it location. The presence of a DG unit on the distribution network will mitigate the voltage dips as experienced by the load connected close to the DG as compare with a DG unit connected to the sub-transmission network or far away from the distribution network. Contrary to the reported impacts of synchronous and asynchronous generators on voltage dips in high to medium voltage networks, their influence on voltage dips in low voltage networks is rather minimal. Converter-based DG is found to have a similar effect on voltage dips in low voltage networks, in opposition to high-voltage networks [62].

The effect of DG units on voltage dip was investigated using the voltage divider model in a radial system [4]. The analysis is based on voltage dips caused by short circuit fault as shown in Figure 2.1. The model consists of source impedance Z_s at the point of common coupling (PCC) and the impedance between PCC and the fault, Z_f. All the loads are constant impedance type. The voltage V_{pcc} at the PCC is thus given by equation 2.1 which is the dip magnitude at the PCC.

$$V_{pcc} = E_s \frac{Z_f}{Z_s + Z_f} \qquad 2.1$$

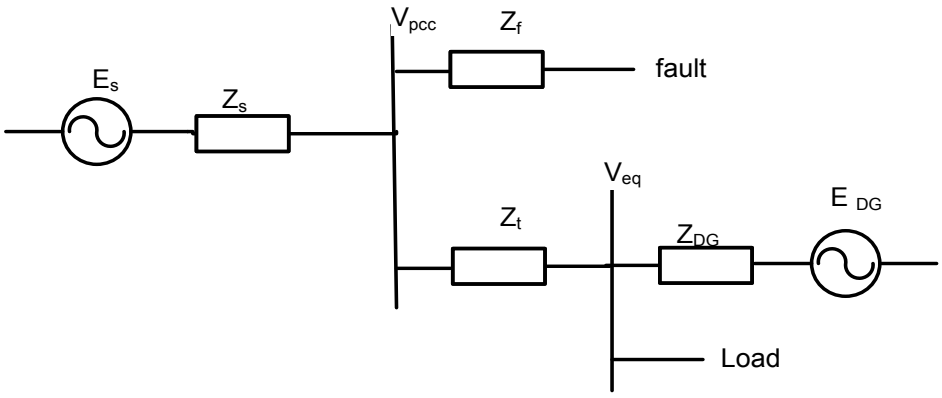

Figure 2.1: Voltage divider model [4]

An additional branch is added at the PCC with impedance Z_t which is the impedance between the PCC and the equipment terminals. The voltage at the equipment terminals V_{eq} will be strongly dependent on the behavior of the connected DG unit, represented in the scheme of Figure 2.1 by a voltage source E_{DG} and impedance Z_{DG}. The voltage at the equipment terminals is given by equation 2.2

$$V_{eq} = V_{pcc}\frac{Z_{DG}}{Z_t + Z_{DG}} + E_{DG}\frac{Z_t}{Z_t + Z_{DG}} \qquad 2.2$$

The positive impact of grid-connected wind DG, with different modes of excitation is studied and analyzed during voltage dip by [48]. The analysis was done with DG and without DG when for a three phase fault condition. The result shows that the during-fault voltage magnitude was improved with DG connected in the system. In addition, voltage dip is less severe with the synchronous generator during the dip. Also, a synchronous generator with PI controller has less impact on voltage sag compared to other types of synchronous generators. Lastly it was found that voltage dip magnitude is highest for induction generator followed by synchronous generator with power factor control.

The impact of synchronous generator on voltage dips caused as a result of faults in a small distribution network was investigated by the authors of [91]. It was established that DG can improve the voltage magnitude during voltage dip if the fault duration is no longer than 2s.

Ramos *et.al* [98] reports simulation of symmetrical and asymmetrical faults in systems with DG with different fault location using the ANAFAS tool. The simulation was based on the capacity of DG unit. Three capacities of synchronous generator DGs were considered for the study viz., 9 MVA, 2.25 MVA and 45 kVA.

It was observed that the voltage magnitude at the load bus was greatly influenced by the presence of DG compared to when there was no DG connected in the system. The smallest DG of 45 kVA DG had almost a negligible impact as compared to 2.25 MVA and 9 MVA DG units. Both kept the voltage magnitude at the load bus above 0.48 p.u. for all fault conditions. The improvement of the voltage magnitude during the voltage dip was better for larger DG as shown by the difference between the 2.25 MVA DG unit and the 9 MVA DG units. However, the investigation do not mention the highest level of DG penetration that would be sufficient for voltage dip mitigation and whether that might exceed the allowed level of DG penetration to a system.

The technical work of [99] reports on a technique to mitigate the voltage unbalance in LV distribution grids using DG. The approach uses a central battery storage bank as the DG and three inverters, these inverters can be controlled and adjusted individually according to voltage dip in each of the lines. The injection of voltage and power in every line of the distribution system was generated according to an imposed condition in other to balance and mitigate the voltage at the PCC.

The impacts of DG on voltage dip assessment in a distribution system were investigated with and without DG installed in the system by [100]. The impact of DG on voltage dip assessment depends on characteristics of DG such as the size of DG and location. The location of DG can also have impact on mitigating voltage dip severity, when DG is installed at the same feeder or very close to the fault. It was observed that the area of vulnerability (AOV), voltage dip frequency and voltage dip index are improved when DG is installed in a distribution system [100]. However, when installed at a different feeder the performance of a DG in voltage dip mitigation is lower, but it is still better than without DG installed in the system [62].

2.4.2 Mitigation of voltage dips through grid-connected distributed generation in series configurations

Series compensation is defined as insertion of reactive power elements into transmission lines and provides the benefits such as reducing the line voltage drops, limiting the load-dependent voltage drops and also increasing system stability [101].The world's first static series compensator (SSC) was installed on the Duke Power distribution system on August 26, 1996 to protect sensitive loads against voltage dips [102]. This technique has been used widely with DG to mitigate the effects of voltage dip.

Voltage dip can be mitigated by using a grid-connected converter for DG unit is in series between the PCC and the load. This will inject the missing voltage and provide the frequency and phase needed to compensate the voltage dip. The series-connected voltage source converter (VSC) is known as the dynamic voltage restorer (DVR) [103].

A DVR is a power electronics converter-based device which protects sensitive loads against different kinds of disturbances such as voltage dip and under-voltage. DVR is usually connected in series with a distribution feeder and is capable of generating or absorbing real and reactive power at its AC terminals. It is made up of a voltage source inverter, a switching control scheme, a DC energy storage device that may be supplied by DG, output filter and an injection or coupling transformer is connected in series with the AC system [62], [104].

The application of DVR was demonstrated by [105] using a wind power supported distributed generation. The proposed method is based on the symmetrical components estimation, which ensures the correction of positive sequence amplitude during dip and it ensures that sensitive loads are compensated against voltage dip.

Mitigation of voltage dips with DVR on the distribution system with DG was investigated by X. Liu *et al*. [104]. The authors of [104] investigated the dynamic analysis of a DVR when applied

to correct the voltage distortion in distribution system and show how DVR can inject appropriate voltage components along the distribution feeder. The configuration of distribution system with DVR and DG is shown in Figure 2.2 while Figure 2.3 shows the flow diagram for the detection process of the voltage compensation.

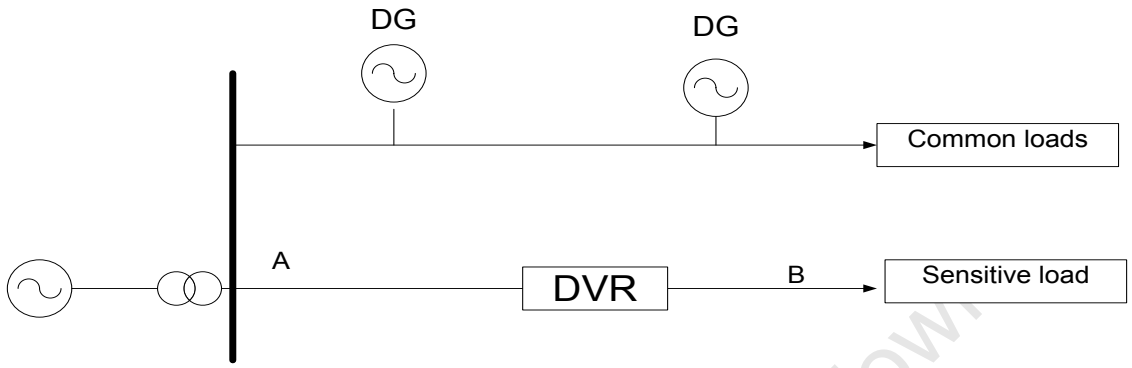

Figure 2.2: Configuration of distribution system with DVR and DG [104]

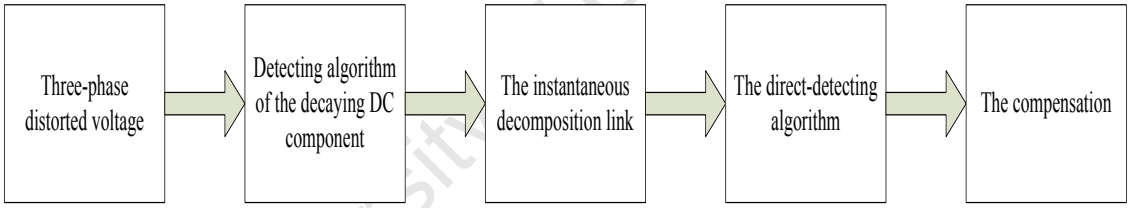

Figure 2.3: Flow diagram of voltage compensation detection method [104]

In the technical work of K.J.P. Macken *et al*. [19], it is shown that series compensation requires active power and also a voltage source inverter that has to be connected in series with the grid. The distributed generation power electronic converter can be connected to a series compensator as shown in Figure 2.4. During a voltage dip, it is possible to inject a voltage in series with the distribution grid during this process the distributed generation systems play an important role.

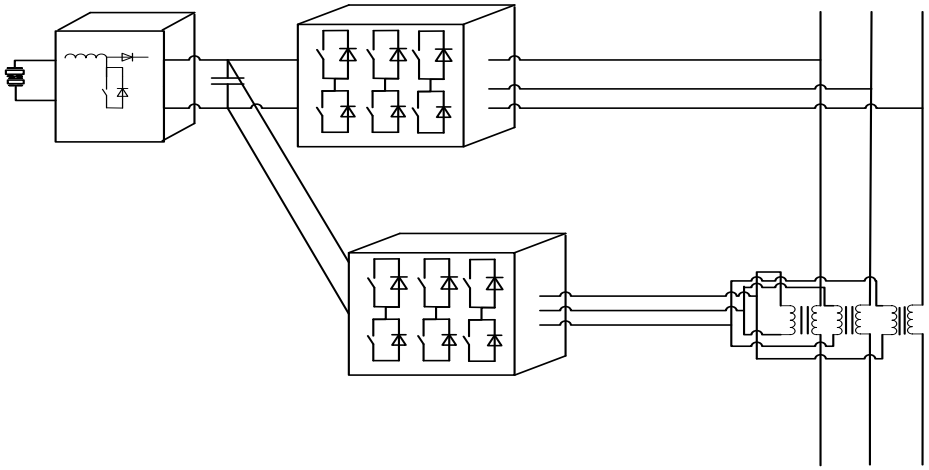

Figure 2.4: A grid-interfaced distributed generation system extended with a series compensator [19]

The advantage of series interconnection is that it helps to prevent inadvertent islanding of DG unit. Also it is economical due to the use of only one set of voltage source converter and it can be used to regulate the voltage level during normal conditions [103].

Series compensator is capable to compensate severe voltage dip but its capability of compensation is depends on active power of supply.

However, the series compensation schemes cannot be used during interruptions as the shunt configuration does. It cannot be used during voltage dips that exceed the rating of the series converter and the complicated protection system is another drawback of series compensation. They are expensive and require more power electronic components [62], [106].

2.4.3 Mitigation of voltage dips through grid-connected distributed generation system in shunt configurations

Voltage dip can be reduced by parallel interconnection of a shunt connected voltage source converter which inject a current of desired amplitude, frequency and phase into the grid. Shunt-connected voltage source converter is also called distribution STATCOM or DSTATCOM [103]. DSTATCOM (Distribution STATCOM) is made up of 6-pulse semi-conductor bridge like in conventional STATCOM (Static Synchronous Compensator) systems applied in HV

transmission networks. The different between DSTATCOM and the conventional STATCOM is in their power, the type of semi-conductor switches applied and their control systems. DSTATCOM operates in a current control mode, and its controllers are usually designed for distribution grids and they are adequate for mitigation of voltage dip at the distribution side of power network [62]. DSTATCOM compensator topology and control consist of a 3-phase 6-pulse voltage source inverter which is connected to the network through a reactor and supplied by a DC capacitor [69].

Reference [107] demonstrated how DSTATCOM compensator with DG can be used to reduce voltage dips coming from the supplying network in a typical rural network. DSTATCOM compensation generates appropriate reference currents that achieve the desired performance. It injects a set of three unbalanced compensating currents to the network such that the network current becomes sinusoidal balanced and in phase with the voltage. The voltage dip mitigation capacity of a shunt connected voltage source converter depends on the capacity of the DG unit and the current rating of the converter [103].

In [108], a three-phase voltage source converter (VSC) is implemented as a front end of a wind generator DG unit as shown in Figure 2.5. This is due to the control system of the DG unit in a rotating *dq*-frame which can be synchronized with the voltage at the PCC and its output power quality.

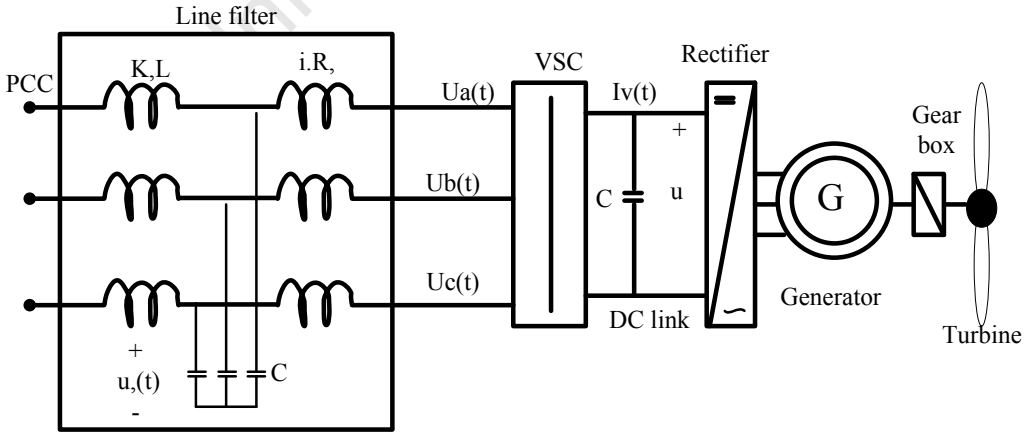

Figure 2.5: DG unit utilizing wind power

A shunt connected voltage source converter can be used during interruptions unlike the series scheme which cannot be used [103]. DSTATCOM compensator can operate both in current control mode and voltage control mode, in voltage control mode it works as a voltage stabilizer while in the current control mode for compensating voltage variation, unbalance and reactive power [62].

The shunt configuration is not suitable for mitigating the deep voltage dips [103]. The unbalance compensation in 4-wire network requires 4-leg device to be applied, whereas the remaining tasks may be effectively performed by 3-leg compensator. Furthermore, the problems with integration of DG technology using renewable energy such as sun, wind and hydro may limit and deteriorate power quality considerably [69].

Voltage dips compensation using distributed generation with voltage source converter as a front end can enhance weak grid power quality as observed by the customers. However it is limited in voltage regulation margin due to the limited rating of the DG unit [108].

2.4.4 Mitigation of voltage dips through combined compensation strategy using series and shunt configurations for distribution network with distributed generation.

The authors of [109] investigated a combined compensation strategy using both the series and shunt configurations with distributed generation. This method is proposed to reduce the active power generation of series compensator using the shunt compensation. Shunt compensation are usually limited by its small power capacity. It is advisable not to use shunt compensation during severe voltage dip alone [109]. The combined compensation strategy is shown in Figure 2.6.

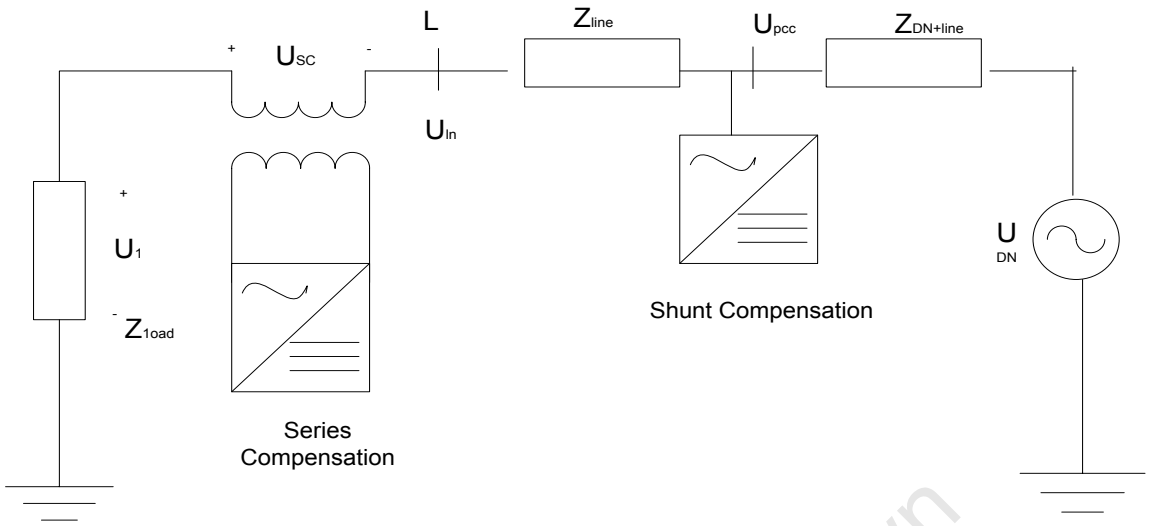

Figure 2.6: Combined compensation strategy [109]

Where:

U_{ln} = the voltage at the feeder end node L

$Z_{DN+line}$ = the voltage at the pcc

U_1 = the voltage at the load node

U_{pcc} = the voltage at the pcc

U_{DN} = the source voltage of the distribution network

U'_{ln} = the normal voltage

U'_{dip} = the voltage dip

The active power generation of series compensation is given by equation 2.3

$$P_{sc} = [1-(1-U_{dip})\cos(\varphi+\omega)]P_{load}/\cos\varphi \qquad 2.3$$

Where U_{dip} is a three-phase balanced voltage dip, ω is the phase angle jump, φ the load angle and the P_{load} is the total active power of the load.

It is know that DVR is capable of generating or absorbing reactive power but the active power injection of the device must be provided by an external energy source or energy storage system.

The response time of both DVD and D-STATCOM is very short and is limited by the power electronics devices and the voltage sag detection time. The expected response time is about 25 milliseconds, and which is much less than some of the traditional methods of voltage correction such as tap-changing transformers [110].

2.4.5 Shunt Active Filter with Energy Storage (SAFES)

Mitigation of voltage dips at the load side using a shunt active filter with energy storage (SAFES) in the presence of DG was theoretically analyzed and investigated by [111] within a micro-grid. This control strategy is based on the state space pole placement design. Voltage mitigation is achieved by calculating the reference fundamental current for the SAFES and it works in conjunction with local distributed generation to control the voltage at the pcc. This provides short term compensation for voltage dip by injecting appropriate current to the line [62].

The use of shunt active filter with energy storage in the presence of DG provides for voltage dip compensation within a micro-grid and this scheme is able to quickly recover the grid voltage after a local load change [69].

2.4.6 Transfer to Micro-grid Operation during Dips

In a transfer to micro-grid operation during dips scheme, the DG units are usually designed for and operated in both the grid-connected and micro-grid (islanded) mode. They are connected through a power electronic converter to the grid as shown in Figure 2.7. An additional power electronic controller is inserted between the utility supply side and the load side. This power electronic controller is a three-phase static transfer switch which comprises back-to-back thyristors. The converter controller of the DG system regulate the current during grid-connected operation (current-mode control), while the controller regulates the voltage during micro-grid operation (voltage-mode control) [62], [69], [19].

At the incidence of the voltage dip, the static transfer switch will open and isolate the sensitive load from the utility supply side, i.e. the micro-grid operation. During the voltage dip event, the distributed generation system at the load side regulates the voltage and supply all the power

needed at the load side. This operation is assumed to be seamless and the dip will not affect the sensitive load since it is isolated from the utility supply. When the voltage dip event is over and the supply voltage recovers the static transfer switch is closed and the DG system switches from micro-grid operation back to grid-connected operation. Synchronization of the DG system with the grid is important and must be done at the same frequency and voltage with the grid [19], [69].

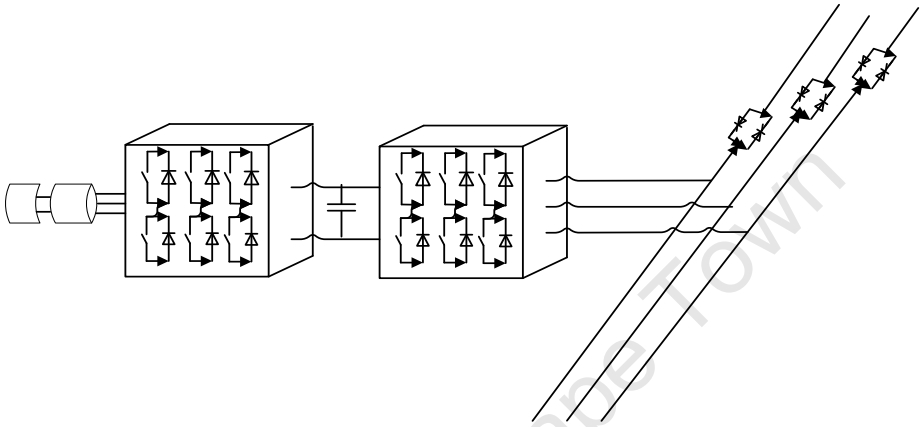

Figure 2.7: A grid-interfaced DG system which is isolated from the utility supply during dips by a static transfer switch [19], [69]

The advantage of this scheme is that it can be used during severe voltage dips and interruptions. The power electronics involve is lesser than some other schemes making it a cheaper solution. Nevertheless, the integration and synchronization of large amounts of renewable-based DG system is still a challenge and its operation during voltage dip is less reliable than the series compensator [69], [112].

2.4.7 Fault Decoupling Device (FDD)

Fault decoupling device (FDD) is a resonant device that is installed between the substation and the loads. Reference [113] presented and analyzed by means of computer simulations how FDD can be used to mitigate voltage dips due to faults or large induction motor in the presence of DG units in the system. The schematic structure of FDD is shown in Figure 2.8. It consists of series-connected inductors and capacitors which are designed in order to realize parallel resonance at the fundamental frequency [113]. If current above a threshold is detected by the control system,

the static devices in series with the capacitors are turned off, while the ones in parallel with the inductors are fired in order to shortcut them. During a short circuit on a feeder supplied by the substation, the control system inserts the FDD by turning off the static devices on the faulted line and turning on those in series with the capacitors [113].

The advantages and benefits of FDD include a reduction of the short-circuit current on the faulted line and mitigation of the voltage dip at the point of common coupling (PCC). There is a decrease in the short-circuit current drawn from the DG connected to the distribution system [62].

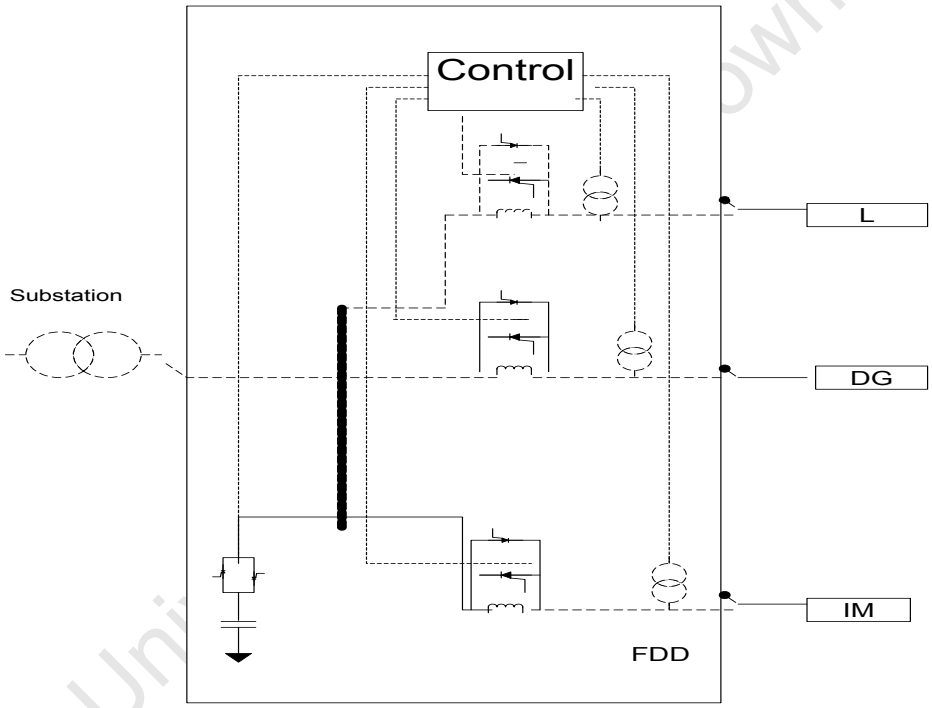

Figure 2.8: One-phase FDD circuit, with load (L), distributed generation (DG) unit, and induction motor (IM) [113]

2.5 Artificial Intelligent Approach for Voltage Dip Detection and Classification with DG

An intelligent system is any system that perceives its environment and accordingly responds or acts to maximize its chances of success. These systems and techniques are known as Artificial Intelligence (AI). Examples of common AI tools are fuzzy logic (FL), artificial neural network

(ANN), genetic algorithm (GA), expert system (ES) and support vector machine (SVM) [33]. Artificial intelligent approach to mitigation of voltage dip using DG is still a new area in the field of power quality research. Various technical works like [96], [114] and [115], are inclined toward voltage dip mitigation using AI have only focused on the optimal location and sizing of DG to mitigate voltage dip in the distribution network.

In addition, work has been done in the area of detection and classification of voltage dips using different AI tools such as in [55], [116], and [117]. These technical research works are not including or investigating on how AI tool can be used to enhance mitigation of voltage dip during or after the detection or classification of voltage dips with DG. These simulations results might be good enough; however, no guidelines or decisions are given on how the detected or classified voltage dips can be mitigated either with DG or otherwise. This thesis investigates and shows how the auxiliary services of GRDGs can be used to mitigate voltage dips through early detection and classification using ANN.

Furthermore, the thesis provides insight about voltage dip severity as a result of classifying dips into classes according to their retained voltage magnitude, phase-angle shift and dip duration. Other methods such as in [51] and [52] classified voltage dips according to the causes or the reason why they originated and [6], [55] and [118], classify voltage dips according to symmetrical component classification based on the decomposition of the three-phase voltages in symmetrical components, generally known as ABC classification.

2.6 AI techniques for voltage dip detection and classification

Detection and classification of voltage dip automatically from a large number of voltage disturbances signal is important for good power quality. I.Y.H. Gu *et al.* [117], addresses how voltage dips can be detected, and it is based on the Neyman–Pearson criterion. A statistical-based sequential method for fast online detection of fault-induced voltage dips. The method consists of dip detection when a half-cycle r.m.s. voltage drops below a threshold followed by analysis windows of different length. The technique used by [119] is based on unscented Kalman smoother for voltage dip detection. It was used to estimate state variables of measured

voltage; it has a good result. However, harmonics and noise cause to increase estimation process.

In addition, the work of authors of [116] showed that voltage dip can be detected and identified based on phase-shift using radial basis (RBF) neural network. The RBF has been developed here for voltage dip classification according to the causes leading to the dips. Though the proposed method is simple, yet it only classifies dips according to the cause and does not provide any possibility for classifying them according to their three-phase nature. A. Deihimi *et al.* [120] presented ANN-based expert system to classify voltage dips using three-phase voltage measurements. The classification algorithm is intended to identify two voltage dip types C and D and the flow chart for the expert system is shown in Figure 2.9. In this work, the ANNs are trained individually for type C and type D dips, as shown in the Figure 2.10. A major limitation of this method is training of an individual ANN. The training of three ANNs consumes a lot of time when compared to train just one ANN model, since a longer time is use in training each of them.

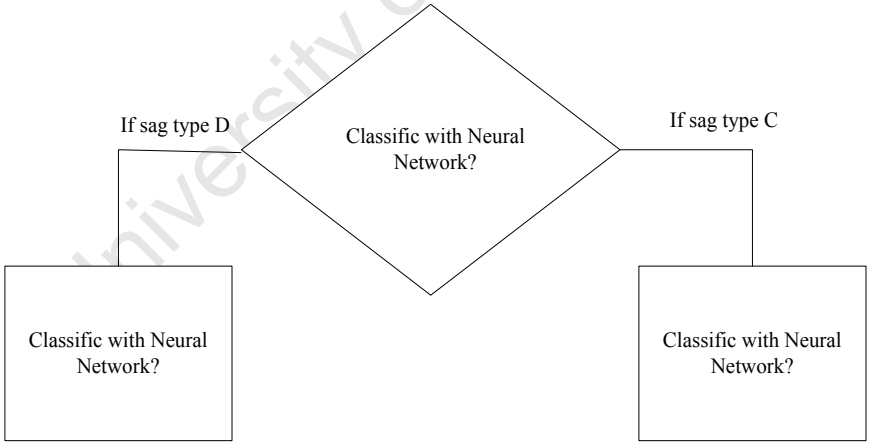

Figure 2.9: Chart of the expert system [120]

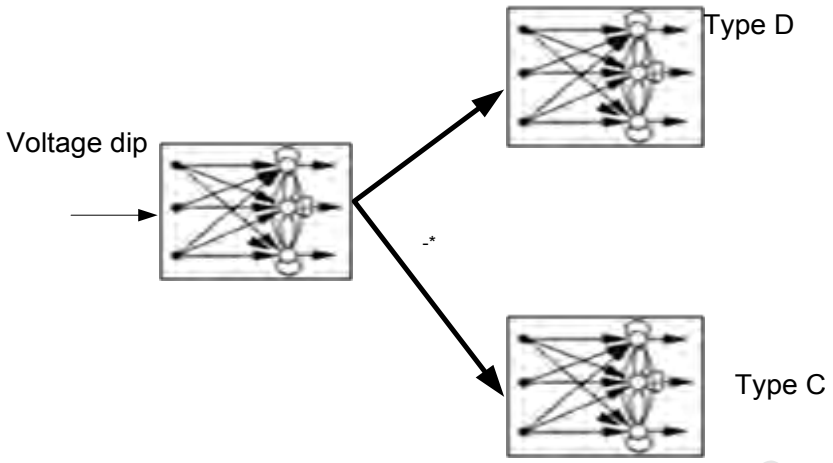

Figure 2.10: Classification scheme [120]

Reference [118] proposed dip classification using ANN classifier for dip types A, B, C and D. J. Melendez *et.al* [51] presented a statistical method for dip classification based on their point of origin such as downstream or upstream. This work is based on their waveform similarity and the goal is to obtain a statistical model. The main advantage of this method is that it has a voltage dip register which is used to compare voltage dip without comparing directly its waveforms. However, its limitation is that it can only locate the origin of the voltage dips this makes the method inadequate for detecting the incidence or occurrence.

2.7 AI techniques used for voltage dip mitigation with DG

2.7.1 Optimal DG allocation and sizing for mitigating voltage sag in distribution systems

The appropriate placement of DG in the distribution network can reduce the negative effects of voltage dips in an electric power network. The severity, features and quality of voltage dip in distribution networks caused by faults are highly influenced by the placement and size of DG. The frequently-used optimization tool in this regard is the genetic algorithm (GA). GA is a well-

known optimization tool in power system research for planning and optimization. It is a computational model that relies on concepts of evolutionary processes.

M.J. Jahromi *et al*. [115] presented mitigation of voltage dip by optimal DG allocation using genetic algorithm (GA) on a MV distribution network. This solution considerable improved the voltage dip by adding a number of DG units at the right place. Furthermore, reference [114] also uses the GA for optimal placement and sizing of DG units in a highly loaded 20KV feeder to support 30% of the feeder load for loss reduction and voltage dip mitigation.

A new method was formulated by reference [121] using GA, the idea is to reduce and mitigate voltage dips in low voltage distribution networks. The DG placement algorithm is able to demonstrate and simultaneously determine suitable number of DGs, their sizes and locations on the feeder. The new algorithm considers both the technical and the economic objectives involved in voltage dip mitigation [62].

The optimal siting and sizing of DG in distribution systems is presented by [122], the aim being to compare genetic algorithm with particle swarm optimization (PSO) in terms of solution quality and number of iterations. The outcome shows that the PSO algorithm is better compare with the GA algorithm.

The similarity between PSO and continuous GA algorithms is that both begin with a random population matrix. However, PSO has no evolution operators such as crossover and mutation unlike GA. This is a major difference between the two techniques. PSO is easy to implement and there are few parameters to adjust when compare with GA [96].

The authors of [96] proposed the use of PSO technique to establish the optimal DG allocation and sizing on a distribution network for proper mitigation of voltage dip. Voltage dip depends on parameters such as sensitivity of loads, location of faults and loads and impedances of the network. It is important to consider all of these parameters in order to mitigate voltage dip through the determination of the best DG location. The use of PSO technique shows an improvement on voltage dip mitigation when DG was optimally positioned and sized [62].

2.7.2 Dynamic Voltage Restorer (DVR) with Artificial Intelligence (AI)

The compensation provided by a DVR depends on its maximum voltage injection ability and the amount of stored energy available and also on its control strategy. This is due to the nonlinearity of the DVR dynamic characteristics. Its configuration and control scheme varies depending upon the nature and characteristics of the load to be protected [123]. In [124], fuzzy logic control is proposed to enhance the compensating performance of a DVR when compared to the traditional PI control during voltage dip mitigation. Fuzzy logic can be described as computing with words rather than numbers, it controls with sentence rather than equations.

References [125], [126] also investigated the use of DVR with fuzzy logic to mitigate voltage dip both at the distribution side and also at the industrial customer site.

The mitigation of voltage dip using adaptive neural network with DVR was demonstrated by M.R. Banaei *et al*. [123]. Because of the limitation of energy storage capacity of DC link in the DVR it is important to minimize energy injection from DVR. This was done using a simple structure feed forward neural network for separating the negative sequence components from fundamental sequence components in unbalance voltage dip and also correct the voltage dip in a distribution feeder [62].

2.8 Conventional schemes used by energy utilities

Energy utilities also use some other means to improve the voltage profile on the power system. Many years back, fixed or mechanically switched capacitors and rotating synchronous condensers were used for improving the voltage profile through reactive power compensation. However, in recent years, static VAR compensators are being employed for the same purpose [127]. This might be as a result of its instantaneous response time and because of the development of reliable high-speed power electronics, powerful analytical tools, advanced control and microcomputer technologies, Flexible AC Transmission Systems (FACTS), have been developed and represent a new concept for the operation of power transmission systems [128], [129], [130]. The following is some of the voltage dip compensating devices used by power utilities.

2.8.1 Shunt capacitors

Voltage profile can be corrected or improved through the supply of necessary reactive power, which can be done through either shunt compensation or series compensation. They are used to modify the natural electrical characteristics of AC power systems [127]. The basic difference between these two approaches is that series compensation modifies the transmission or distribution system parameters; while shunt compensation changes the equivalent impedance of the load [131], [132]. Among the reactive power compensation based solutions the static synchronous compensators have confirmed the superior performance due to the possibility of using all rated power exclusively to voltage support [133].

Voltage regulation is one of the main reasons that shunt capacitors are installed in a power network. It is made up of HV shunt capacitor, serial reactor, switch (insulation switch, grounding switch), arrester, fuse, etc. It controls the voltage within required levels. The shunt capacitor banks are connected to the bus and can be switched as needed. Switching can be based on time, if load variation is predictable, or can be based on voltage, power factor, or line current. The Salt River Project (SRP), a public power utility serving more than 720,000 (April 2000) customers in central Arizona, USA utilizes this method coupled with the load tap changer transformers to compensate for the voltage dip on their power network. Its disadvantages include:

1. Slow switching time;
2. It is a summer peaking system. After each summer peak, a capacitor study is performed to determine the capacitor requirements for the next summer. The burden of performing the routine check cost time and money each summer.

2.8.2 Series capacitor compensation

Series compensation was first installed in that late 1940s. They act directly on the series reactance of the line. It reduces the transfer reactance between supply point and the load, thereby reducing the voltage drop. Series capacitor can be thought of as a voltage regulator.

It adds a voltage proportional to the load current and thereby improves the load voltage. Some problems like self-excitation of motors during starting, ferro-resonance, steady hunting of synchronous motors discourage the wide use of series compensation in power systems. It is not also economical to design the capacitors to withstand the currents and voltages associated with faults.

2.8.3 Static Var control (SVC)

Static VAR compensators, also known as SVCs, are shunt connected devices. Its reactive power can be varied by switching the reactive impedance components by means of power electronic controls. The main components of an SVC are thyristor valves, reactors, the control system, and the step-down transformer. An SVC can compensate voltage dip durations between 10ms and 60ms for load variations and maintain constant voltage by controlling the duration of current flow in each cycle through the reactor. The capacitor is switched on and off by mechanical breaker, and the time delay is usually ten cycles or more than 200ms

2.8.4 Static compensator (STATCOM)

The first demonstration STATCOM of ±100 MVAr rating was installed at the Tennessee Valley Authority's Sullivan substation in USA in 1994. It consists of voltage source inverter using gate turn off thyristors (GTOs). The new VAR compensator technology is based on power electronics converters and digital control schemes [134]; voltage dip can also be mitigated using the present time high performance power system controllers such as Static Synchronous Compensator (STATCOM), the Static Synchronous Series Compensator (SSSC), the Dynamic Voltage Restorer (DVR), the Unified Power Flow Controller (UPFC), the Interline Power Flow Controller (IPFC) and the Superconducting Magnetic Energy Storage (SMES).

This thesis presents a novel corrective scheme that can detect and classify voltage dip based on Eskom voltage dip windows and mitigation through the voltage support provide by the GRDGs. It is able to provide guidelines for the automatic processing of different voltage dip types in terms of voltage level, dip duration time, and effectiveness of GRDGs during and after the voltage dip mitigation.

Chapter 3

3.0 Artificial Neural Network System Modeling

3.1 Introduction

Today, there are different power system analysis software such as Power System Toolbox in MATLAB®, DIgSILENT Power Factory, Real Time Digital System Simulator (RTDS), Power Systems Analysis Toolbox (PSAT), Power System Dynamic Simulation (PSDS), Simulation Programs for Integrated Circuits (SPICE), etc. These software are capable of processing and simulating electrical power system behavior under normal and abnormal conditions. This research work has been performed using Matlab 2011a and DIgSILENT PowerFactory Version 14.1. DIgSILENT has been used to model the various power system networks while Matlab Neural Network Toolbox7.0™ is used for the modeling of voltage dip detector and classifier intelligent systems. Many of these software have been used by researchers and engineers for design and detailed analysis of electrical power systems. In addition, they are capable of simulation of steady state and high-speed transient analyses and optimization. However, several investigated PQ disturbances presented in many research literatures were done and based on simulated data obtained using power system analysis software instead of practical site data [135].

The software, Digital Simulator for Electrical Network popularly known as DIgSILENT Power Factory, is widely used by South African utility, ESKOM for power system modeling, analyses and simulation power their own planning and operation. DIgSILENT performs steady state and transient power system analyses using built-in libraries and blocks for modeling conventional and renewable energy related (e.g. RDG) electrical components within a power system [136].

If not done prudently, grid integration of RDG systems might disturb the delivery of quality power to the PQ (power quality) sensitive loads connected to the grid. The challenge becomes serious with the increasing use of voltage-sensitive electronic equipment in industries, offices

and households [137]. However, existing literature show that grid-integrated RDG systems can be effectively used to provide ancillary services to support the grid operation (within the framework of the grid codes) during contingencies, of which voltage dip mitigation is one.

To achieve good power quality and maintain an uninterrupted power supply at the load terminals, the voltage disturbances must be adequately monitored. It is a good practice to determine and record the sources and causes of a disturbance such that appropriate mitigating action can be taken [138]. Voltage disturbance monitoring is a complex task, and the use of an intelligent system can be helpful in achieving the same. It has been established that power quality disturbance waveform recognition is often difficult because the decision boundaries of disturbance features may overlap [138].

Detection of voltage dip events by analyzing the r.m.s. voltage is an important task. Presently, utilities are using dip recorder's data for detection, analysis and mitigation of voltage dips. Utilities in many countries such as South Africa, Zambia, etc., use the 10-minute r.m.s. value(s) to determine the highest or the lowest voltage magnitude of all the samples taken during a 10-minute period [58], [139]. This is a long duration of time, which does not facilitate early mitigation of the dip. Early detection and classification of voltage dip for severity are necessary to reduce its effects and provide a timely and practical mitigation measure for power networks.

Nevertheless, it was reported that the frequencies of occurrences of voltage dips are highly unpredictable both in time and place [140]. Therefore, getting rid of voltage dip fully from the present power networks might be practically impossible, as a result of unforeseen causes of voltage dip events.

Most power quality disturbances such as voltage dip are non-stationary and transitory, and the classification has proven to be very demanding. However, it is possible that the use of artificial intelligence (AI) such as Artificial Neural Network (ANN) in voltage dip mitigation can greatly improve the efficiency, reliability and robustness of the power system through the timely detection and classification of voltage dips [62]. ANNs are among the newest detection and

classification tools nowadays. ANN is a nonlinear statistical model identification technique which learns and does not need to be reprogrammed [141]. Other qualities of ANN that help in voltage dip detection and classification are its ability to generalize at high speed (for voltage dip needs to be identified and classified in time for effective mitigation) and it can handle noisy and incomplete data.

This PhD work is based on the proposition that ANN-based voltage dip mitigation technique with grid-connected RDG will help the power utilities to design and plan RDG integration and operate their systems appropriately to ensure good voltage quality to the customers. A correctly planned and operated grid-connected RDG will in turn reduce the possibilities of shut-down of sensitive equipment leading to loss of production or services with direct financial impact for the affected customers. The main emphasis of this thesis is on voltage quality only.

3.2 Artificial neural network Modeling

Artificial neural networks (ANNs) are the artificial modeling of the complicated, versatile and powerful human central nervous system (CNS). They try to mimic some important functions of the human brain, and researchers have implemented these model neurons in hardware as electronic circuits [142], [143]. ANNs are applied to solve complex and nonlinear engineering problems and are capable of machine learning and pattern recognition.

ANNs are made up many simple processing elements called neurons, which operate in parallel that has a natural propensity for storing experiential knowledge and making it available for use [32],[53],[144]. Figure 1.4 in Chapter 1 shows the ANN architecture which is based upon the connection pattern. ANN can be categorized into two groups, viz., feed-forward or recurrent. In a feed-forward ANN the graphs have no loops unlike the recurrent ANN which have loops as a result of feedback connections [145]. Figure 3.1 is re-presentation of Figure 1.4 showing the ANN architectures.

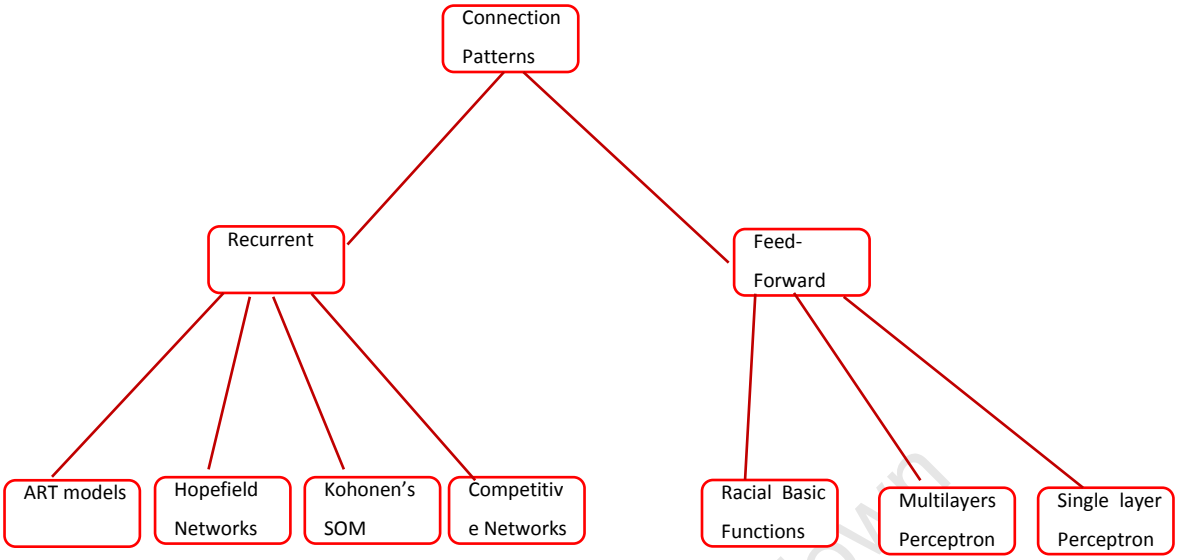

Figure 3.1: Artificial neural network architectures [30]

3.3 A single neuron

The fundamental building block or the basic computational element for neural networks is the neuron. It is capable of receiving input information from other neurons or from an external source. Each neuron in the network is only aware of signals it periodically receives and the signal it periodically sends out to other neurons after computation as shown by Figure 3.2 [146].

The artificial neurons are built into ANNs and are made up of the weights, inputs, activation function and output. The weight function applies weights to an input to get weighted input, as specified by a particular function. A stronger input will have a positive or higher weight while a weaker input has a negative weight, and this will inhibit the input.

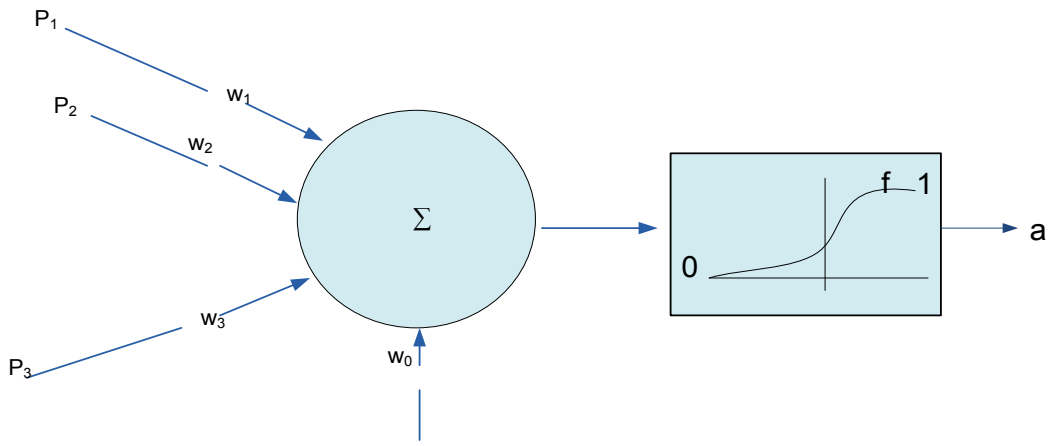

Figure 3.2: Basic model of an artificial neuron [147]

The behavior of an ANN depends on both the weights, and the input-output function called activation function or transfer function. This function can be linear, nonlinear or binary. The choice of the activation function depends on the nature of the problem that the neuron is attempting to solve [146].

3.4 The mathematical models of neuron and neural network

The mathematical analysis of a single-input neuron is shown schematically in Figure 3.3. The single input n is the sum to two separate input functions, p multiplied by its weight w and 1 multiplied by a bias b. Input n is expressed by equation 3.1.

$$n = (wp + b) \tag{3.1}$$

n is passed through the activation function f to produce the neuron output a, as in equation 3.2.

$$a = f(wp + b) \tag{3.2}$$

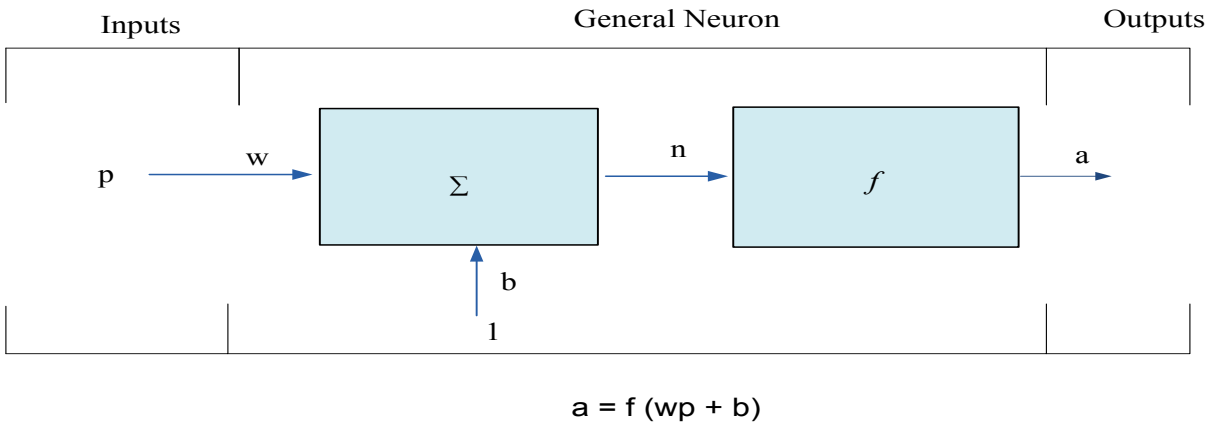

Figure 3.3: Single –input neuron [144]

For multiple-input neuron shown in Figure 3.4, input *n* is given by equation 3.3 and Figure 3.4.

$$n = (w_{1,1}p_1 + w_{1,2}p_2 + w_{1,3}p_3 + \ldots w_{1,R}p_R + b) \quad 3.3$$

In matrix form, the matrix **W** has one row for single neuron and R for R numbers of an element in input vector shown in Figure 3.4.

$$\mathbf{n = (Wp + b)} \quad 3.4$$

The neuron output is given as.

$$\mathbf{a = \mathit{f}(Wp + b)} \quad 3.5$$

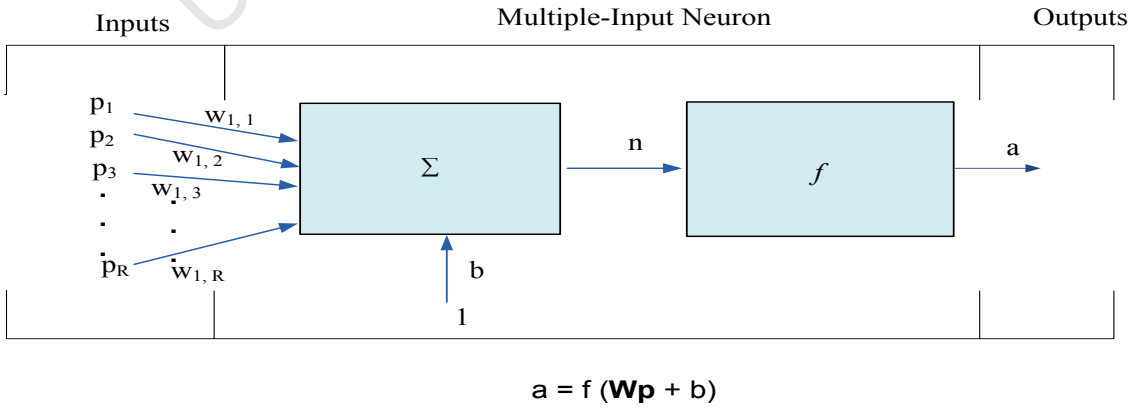

Figure 3.4: Multiple-Input Neuron [146]

3.5 Types of artificial neural networks

The authors of reference [148] states that ANNs can be realized by both hardware based and software based systems; they also comment that ANNs learn from experience and generalize at high speed to produce a meaningful solution even when the input data contain errors or is incomplete [148]. They can be classified depending on the topology of network, the activation function used, and the training algorithm [147]. Different types of ANNs include feed-forward neural network, radial basis function (RBF) network, recurrent neural network, self-organizing network, learning vector quantization, etc. Perceptron is the first simplest form of feed-forward neural network with one layer where inputs are fed directly to the output unit via the weighted connections. Its limitation is its inability to recognize many classes of pattern, which is overcome in multi-layer perceptron (MLP). MLP has massive interconnectivity, nonlinear processing elements and is capable of approximating arbitrary functions [149]. Another method like PLS (partial least squares) can overcome the problem of over-fitting and might give roughly the same results as with ANN [257].

The best and optimal ANN architecture is the one that will give the best performance both in terms of error minimization and require minimum time to perform a task, while retaining a simple and compact structure.

3.6 Steps in designing neural networks for voltage dip detection and classification

ANN can be and has been used to detect and classify many power quality problems. Authors of [26], [150] and [151] demonstrated how ANN can be used to detect and classify power quality disturbances. In addition, [26] showed that ANN is more accurate and efficient when compared to fuzzy logic. RTeference [152] observes that the design of a neural network involves the selection of its architecture, i.e., number of layers, connectivity pattern, learning algorithm, and activation functions for its neurons according to the application. This work , its application includes the detection of the voltage dip incidence and classification. Literatures have shown that designing ANN with too many neurons in the hidden layer will make the network to memorize instead of learning and generalization. However higher number of neuron will help to

adjust to larger fluctuation of target function and allow the model to consider the presence of volatilities in the data [149].

The flow chart of ANN implementation is as follows [153]

1 Collect data

2 Create the network

3 Configure the network

4 Initialize the weights and biases

5 Train the network

6 Validate the network

7 Use the network / implementation

In general, the designer of ANNs chooses the best network topology, activation function and the learning rule.

3.7 Selection of an ANN Model for voltage dip detection and classification

To create an ANN for voltage dip detection and classification it is necessary to determine how many inputs the network need to have, how many layers are needed, how many neurons are needed per layer and how many training, test and validation data are needed. The two basic models of ANN commonly used are the multilayer feed-forward networks and radial basis functions. The data is usually fed through the input layer to the hidden layer(s) where the learning process commences and also continues at the output layer which finally, output the result.

3.7.1 Input layer

The input layer to ANN is usually determined by the input features considered in the problem. For the task of detection and classification of voltage dip, the voltage dip magnitude, dip

duration and phase angle shift are considered as the input features to the ANN. Input layer takes in information from the environment or the system and propagates it through the network.

3.7.2 Hidden layer

The hidden layer takes their input from the input layer. The design of the hidden layer has no rule or formula for calculating the number of hidden neurons [152]. This has remained a challenge in ANN modeling, and the best numbers of hidden neuron are usually determined by a hit-and-trial method [154]. The input to an ANN is usually determined by the number of features consider in a particular problem while the output is decided by the number of classes. Presently, there is no formal way to determine the size of the hidden layer [155]. The best number of hidden neurons is the one with minimal error and highest accuracy. Therefore the network must be trained many times with different numbers of hidden neurons before an acceptable network is found [156]. However, reference [156] provided a method called coarse to fine search technique and also reported that two techniques can be used to determine the number of hidden neurons in an ANN. These include the network growing and network pruning. In addition the literature survey done by [157] has shown some existing methods such as estimation theory, Akaike's information criteria, etc. have limitations. These drawbacks include long training and testing time. Furthermore there is no guarantee that the network with a given number of hidden units will find the correct weights and provide optimal solution [157].

In this work, the most suitable number of hidden neuron is based upon the number of inputs and outputs and the complexity of the function to be learned. The best number of hidden neurons with minimal error and highest accuracy was selected. Random selection of a number of hidden neurons might cause either over-fitting or under-fitting problems. Using too few numbers of hidden units will result in high training but low generalization error due to under-fitting, while too many hidden units will give low training but a high generalization error due to over-fitting [158].

3.7.3 Output layer

The output layer outputs the result of the ANN to the environment or to another system. The output of the detector ANN is the presence of a voltage dip while that of classifier ANN is any of the Eskom voltage dip classes to which the dip belongs. The concerned of this work is Eskom voltage dip classes, and its will help to improve voltage quality in the South African network. The proposed technique using ANN systems for voltage dip mitigation was tested and validated on a typical Eskom network using generic data from Eskom.

3.7.4 Activation Functions

The activation function acts as a squashing function; it controls whether a neuron is active or inactive [159]. The learning ability of ANN to detect or classify voltage dips depends upon its activation function. As already stated, activation functions may be linear, threshold or sigmoid. In this dissertation, the hyperbolic tangent sigmoid function is used as the activation or transfer function for the hidden layers of the detector ANN. This is due to its good converging results when compared to other activation functions in addition to its fast approximation [152].

For the output layer, which must be in binary codification, the activation function is chosen to be sigmoid since it has the ability to assume values between 0 and 1 for either "dip" or "no dip" condition. The threshold 1's and 0's indicating voltage dip and no voltage dip respectively.

The radial basis transfer function is used as the transfer function for the hidden layers of the ANN classifier because it is good for pattern recognition and classification. This is due to its advantages such as low computational complexity and low memory requirement [160]. Sigmoid function was used as the activation function for its output layer. This is because its output varies continuously but not linearly as the input changes. Sigmoid function bears a greater resemblance to real neurons within the brain when compared to the other activation functions [161]. These activation functions can be expressed as follows:

Hyperbolic tangent sigmoid transfer function

$$f(x) = \frac{2}{1+e^{-2x}} - 1 \qquad 3.6a$$

Radial basis transfer function

$$f(x) = e^{-x^2} \tag{3.6b}$$

Sigmoid transfer function

$$f(x) = \frac{1}{1+e^{-x}} \tag{3.6c}$$

3.8 Training of artificial neural networks

Learning is acquiring or enhancing knowledge; knowledge is acquired by the ANN through a training process. There are three main types of learning, supervised learning, unsupervised learning and reinforcement learning [162]. Reinforcement learning occurs through trial and error. In reinforcement learning, the presence of the teacher is only to indicate if the computed output is right of wrong and the teacher is not involved in the learning process. Unsupervised learning is when the ANN system is not provided with the correct results during the training and no teacher is present. The ANN system learns on its own by adapting to the structural feature of the input pattern.

Supervised learning or associative learning is the one in which the ANN network is trained by providing it with input and matching output patterns [159]. In this type of learning the correct result is already known, and the learning process takes place through comparison between the network output and the correct expected output which generate the error. The ANN parameter is changed according to the error by comparing the system output to the desired output in order to improve the network. Data is divided into the training, test and validation data sets. The nature of data for training, test and validation include the features that were selected for detection and classification of voltage dip. These include the voltage magnitude, dip duration and the phase angle shift. The detection and classification of voltage dip in this work use supervised learning. These methods are usually fast and accurate and give correct results when a new data is given without knowing the target [158]. Figure 3.5 shows the learning methods and their rules for ANN.

Learning rules are algorithms or equations that control changes in the weight of connections in a network. Learning rules can be trained with or without a teacher, and they have a particular architecture and learning algorithm. Examples of basic types of learning rules are Error correction rules, Boltzmann rules, Hebbian rules and Competitive learning rules. Learning rules such as delta rule, generalized delta rule and back propagation incorporate error reduction or correction procedure [163]. The approach to supervised learning in ANNs is the back propagation algorithm and has proven to be very efficient for a number of non-linear problems [162].

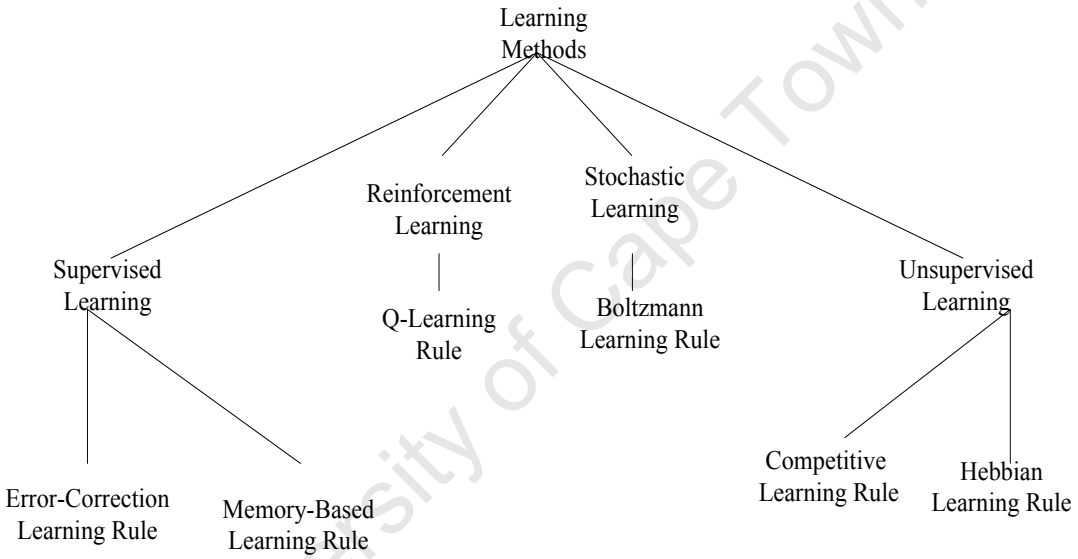

Figure 3.5: Learning rules of ANN [162]

3.9 Training or teaching algorithms

In many cases, it is difficult to know which training algorithm is appropriate for a particular problem as this depends on the complexity of the problem, whether the network is being used for pattern recognition or function approximation and some other factors [146]. Technical literatures have reported the use of very simple algorithms, such as the least mean square or error back-propagation (EBP) to train neural networks. However, these algorithms converge very slowly in comparison to second-order methods [164]. The EBP uses the first-order stochastic gradient method. This has been used extensively in multilayer perceptron training but

its main drawback is slow speed of convergence [165]. The training speed of EBP might be improved using dynamic learning rates [166]. However, today there is improvement and a fast speed of convergence and mapping accuracy as compared to the EBP [167]. Better performance techniques include quasi-newton, neuron-by-neuron (NBN) algorithm, scaled conjugate gradient back-propagation [SCG], resilient back-propagation (RP) and Levenburg-Marquardt (LM) algorithm.

LM algorithm is fast and powerful for training neural networks with a realistic function approximation and nonlinear regression problem as compared to other algorithms, which have difficulties in convergence [168]. It combines gradient descent algorithm with Gauss-Newton method. This makes it easier to switch between the two algorithms during the training process. It has both local convergence of Gauss-Newton method and global character of the gradient descent algorithm [169]. Nevertheless, its limitations include sensitivity to the initial network weights, and it does not consider the output data which most time leads to overfitting noise. In addition, its performance is relatively poor on pattern recognition problems [146]. RP and SCG algorithms are often very fast back-propagation algorithms and are highly recommended as a first-choice supervised algorithm for a realistic pattern recognition and nonlinear discriminant analysis problem. They are regarded as one of the most efficient training algorithms.

The propagation algorithms used during this research to teach the neural networks are the scaled conjugate gradient algorithm and the resilient back-propagation. Fewer steps are required during the training of ANN with RP algorithm when compared to other back-propagation algorithms and only the signs of the derivatives are used during training in other to adjust the weights instead of its values; these make RP faster than the other methods [170]. Furthermore, RP has the ability of escaping flat areas of the error surface and less dependent on the initialization of the weights as a result RP is more robust than other types of back-propagation algorithms [170]. The scaled conjugate gradient algorithm is another method to estimate the step size in order to minimize the multivariable error function of the weights [171]. It is an improvement over the conjugate gradient algorithm; they converge faster more than the steepest descent method and also avoid the calculation of the Hessian matrix and inversion in quasi-Newton method [172].

3.10 Resilient propagation algorithm

The resilient propagation algorithm steps involve performing the feed-forward, processing the level backwards to determine the error gradients at each level and finally adjusting the weight to the changes. The RP algorithm is as follows for all weights and biases [173]. The following parameters are used in resilient propagation algorithm Δ_0 , $\Delta_{\max}$, Δ_{mim}

Δ_0 is the initial value of the delta update, Δ_{ij} , $\Delta_{\max}$ is the maximum value a delta update, Δ_{ij}, Δ_{mim} is the minimum value a delta update, Δ_{ij}, $\frac{\partial E}{\partial w_{ij}}$ is the error gradient

An update-value is weight Δ_{ij} is introduced for every weight w_{ij} which determines the size of the weight update. The values of η^+ and η^- are the two values use by RP algorithm as the increase and decrease factors respectively.

$$
\begin{aligned}
&if \quad \left(\frac{\partial E}{\partial w_{ij}}(t-1) X \frac{\partial E}{\partial w_{ij}}(t) \quad > \quad 0 \right) \quad then \\
&\{ \\
&\Delta_{ij}(t) \quad = \quad \min\left(\eta^+ X \Delta_{ij}(t-1), \Delta_{\max}\right) \\
&\Delta w_{ij}(t) = \quad - \quad sign\left(\frac{\partial E}{\partial w_{ij}}(t) \right) X \Delta_{ij}(t) \\
&\Delta w_{ij}(t+1) = w_{ij}(t) + \Delta w_{ij}(t) \\
&\} \\
&else\ if \quad \left(\frac{\partial E}{\partial w_{ij}}(t-1) X \frac{\partial E}{\partial w_{ij}}(t) \quad < \quad 0 \right) \quad then \\
&\{ \\
&\Delta_{ij}(t) \quad = \quad \max\left(\eta^- X \Delta_{ij}(t-1), \Delta_{\min}\right) \\
&\Delta w_{ij}(t+1) = \quad w_{ij}(t) \quad - \Delta w_{ij}(t-1) \\
&\frac{\partial E}{\partial w_{ij}}(t) = \quad 0 \\
&\} \\
&else\ if \quad \left(\frac{\partial E}{\partial w_{ij}}(t-1) X \frac{\partial E}{\partial w_{ij}}(t) \quad = \quad 0 \right) \quad then \\
&\{ \\
&\Delta w_{ij}(t) = \quad - \quad sign\left(\frac{\partial E}{\partial w_{ij}}(t) \right) X \Delta_{ij}(t) \\
&\Delta w_{ij}(t+1) = \quad w_{ij}(t) \quad + \Delta w_{ij}\ \}(t) \\
&\}
\end{aligned}
$$

3.11 Scaled conjugate gradient (SCG) propagation algorithm

The SCG propagation algorithm is given by the steps below [174], [175].

k is the iteration, w is the weights

x_1 is the weight vector , Δk is the scale parameter

p_1 is the initial conjugate, r_1 is the steepest descent direction

λ_k is the error

1. Initialize the weight vector at the first iteration, x_1, and set the values of

   $\sigma > 0,\ \lambda_1 > 0\ and\ \bar{\lambda}_1 > 0.$ set the initial conjugate solution, p_1, and the steepest descent direction, r_1, equal to the error surface gradient, $p_1 = r_1 = -\nabla f(x_1)$. set success = true.

2. If success = true, then calculate the curvature information, $\nabla^2 f(x_k)$:

$$\sigma_k = \frac{\sigma}{|p_k|}$$

$$\nabla^2 f(x_k) = \frac{\nabla f(x_k + \sigma_k p_k) - \nabla f(x_k)}{\sigma_k}$$

$$\delta_k = p_k^T$$

3. Scale $\nabla^2 f(x_k)\ \ and\ \ \delta_K$:

$$\nabla^2 f(x_k) = \nabla^2 f(x_k) + (\lambda_k - \overline{\lambda_k}) P_k$$

$$\delta_K = \delta_K + (\lambda_k - \overline{\lambda_k}) P_k$$

4. If $\delta_k \le 0$, make the Hessian matrix positive definite:

$$\nabla^2 f(x_k) = \nabla^2 f(x_k) + \left(\lambda_k - 2\frac{\delta_k}{|p_k|^2}\right) p_k$$

$$\overline{\lambda_k} = 2\left(\lambda_k - \frac{\delta_k}{|p_k|^2}\right)$$

$$\delta_k = \delta_k + \lambda_k |p_k|^2, \lambda_k = \overline{\lambda_k}$$

5. Calculate the step size, μ_k :

$$\mu_k = p_k^T r_k, \alpha_k = \frac{\mu_k}{\delta_k}$$

6. Calculate the comparison parameter, Δk:

$$\Delta k = \frac{2\delta_k (f(x_k) - f(x_k + \alpha_k p_k))}{\mu_k^2}$$

7. If $\Delta k \geq 0$, then a successful reduction in error can be made. Update the weight vectors, $x_k + 1$, and the steepest descent direction, $r_k + 1$:

$$x_{k+1} = x_k + \alpha_k p_k$$
$$r_{k+1} = -\nabla f(x_{k+1})$$
$$\overline{\lambda_k} = 0, \quad success = true$$

   a. Check, whether the direction is still acceptable with k mod N = 0. If acceptable:

   $$p_{k+1} = r_{k+1}$$

   b. Else, create a new conjugate direction:

   $$\beta_k = \frac{|r_{k+1}|^2 - r_{k+1} r_k}{\mu_k}$$

   $$p_{k+1} = r_{k+1} + \beta_k p_k$$

8. If $\Delta_k \geq 0.75$ then reduce the scale parameter $\lambda_k = \frac{1}{2}\lambda_k$,

9. Else a reduction in the error is impossible:

   $\overline{\lambda}_k = \lambda_k$, $success = false$

10. If $\Delta k < 0.25$, then increase the scale parameter $\lambda_k = 4\lambda_k$

11. If the steepest descent direction $r_k \neq 0$, then set k =k + 1 and go to step 2. Else, terminate optimization and return x_{k+1} as the desired weights.

3.12 The activities of neuron during propagation

The objective of the ANN training algorithm in voltage dip detection and classification is to reduce the error and the training time in order to produce a better result. This process includes tuning the values of the weights and biases of the network to optimize network performance [176]. The error function *E* is given as

$$E = \frac{1}{P}\sum_{P=1}^{P} E_P \tag{3.7}$$

where P is the total number of training pattern, E_P is mean square error (MSE) for a pattern p which is given as the average squared difference between the network outputs a_i and the target outputs t_i. It is obtained by the equation 3.8.

$$MSE_p = E_P = \frac{1}{N}\sum_{i=1}^{N}(a_i - t_i)^2 \tag{3.8}$$

where N is the total number of output neurons.

Assuming each neuron has a sigmoid activation function as given in equation 3.6c above and is repeated then it is given by

$$f(x) = \frac{1}{1+e^{-x}} \tag{3.6c}$$

the input to a neuron j is calculated as

$$net_j = \sum_i w_{ij}x_i + \theta_j \tag{3.9}$$

Where x_i is the output from the preceding layer, w_{ij} is the weight connecting neuron, i to neuron j, and θ_j is the bias.

Computing the weight update with back-propagation learning.

$$w_{ij}(t+1) = w_{ij}(t) + \Delta w_{ij}(t) \tag{3.10}$$

In regular gradient descent the weight update rule is,

$$\Delta w_{ij}(t) = -\eta \frac{\partial E}{\partial w_{ij}}(t) \tag{3.11}$$

where η is the learning rate which scales the derivative and also determines the step size. The momentum term is introduced to get rid of the problem arising from learning rate. When the

learning rate is too small then many steps are needed to get to an acceptable solution and when it is too large, it can lead to oscillation [177]. With the momentum coefficient term μ, the rule now becomes.

$$\Delta w_{ij}(t) = -\eta \frac{\partial E}{\partial w_{ij}}(t) + \mu \Delta w_{ij}(t-1) \qquad 3.12$$

3.13 The resilient propagation

Resilient propagation does not have training parameters unlike other training algorithms and are not usually changed from their default values. The advantage of RP is to eliminate the influence of the size or magnitude of the partial derivative on the weight step, which resulted in using the only sign of the derivatives as mentioned above. To accomplish this process an update-value is weight Δ_{ij} is introduced for every weight w_{ij} which determines the size of the weight update and the RP learning rule is given by [173], [178].

$$\Delta_{ij}(t) = \begin{cases} \eta^{+} \cdot \Delta_{ij}(t-1) & if \quad \frac{\partial E}{\partial w_{ij}}(t) \cdot \frac{\partial E}{\partial w_{ij}}(t-1) > 0 \\ \eta^{-} \cdot \Delta_{ij}(t-1) & if \quad \frac{\partial E}{\partial w_{ij}}(t) \cdot \frac{\partial E}{\partial w_{ij}}(t-1) < 0 \\ \eta \Delta_{ij}(t-1) & Otherwise \\ & \\ & 0 < \eta^{-} < 1 < \eta^{+} \end{cases} \qquad 3.13$$

The values of η^{+} and η^{-} are the two values use by RP algorithm as the increase and decrease factors respectively. These parameters are set in most cases at $\eta_{-} = 0.5$ and $\eta_{+} = 1.2$.

The weight-step rule is

$$\Delta_{ij}(t)=\begin{cases}+\Delta_{ij}(t) & if \quad \frac{\partial E}{\partial w_{ij}}(t)>0\\ -\Delta_{ij}(t) & if \quad \frac{\partial E}{\partial w_{ij}}(t)<0\\ 0 & Otherwise^{+}\end{cases} \qquad 3.14$$

The exception is when the partial derivative changes sign then the previous weight-update will be reverted.

$$\Delta w_{ij}(t)=-\Delta w_{ij}(t-1), \qquad if \frac{\partial E}{\partial w_{ij}}(t-1)\cdot\frac{\partial E}{\partial w_{ij}}(t)<0 \qquad 3.15$$

To avoid double punishment then $\frac{\partial E}{\partial w_{ij}}(t)=0$ 3.16

3.14 Capabilities and inabilities of using ANN in voltage dip detection and classification

ANNs are known for their ability to learn without the help of a teacher. For example, it is possible to have two voltage dips of the same magnitude but with different duration. These two dips with the same magnitudes may have a different impact on the sensitive equipment. Therefore, each contingency must be treated separately. ANN has a great capability of high-dimensional pattern recognition and the ability to handle noisy data [179]. The neurons in ANN are nonlinear device and are appropriate for non-linear modeling based on the training data samples. It has the ability to generalize at a high speed; since quick assessment of the system is needed during system disturbances such as a voltage dip [180]. It can be operated in real time operation since computations are been done in parallel, and special hardware devices are being designed and manufactured, which take advantage of this capability.

3.15 ANN system modeling for voltage dip detection and classification

The daily improvements on the monitoring of power quality disturbances have significant economic values to both the utilities and the customers with power quality sensitive loads [181]. Voltage dip has been identified as one of the expensive PQ disturbances [60], for any system to detect its occurrence in a power system the difference between the nominal voltage, and the actual voltage must be calculated and known. In the 70's voltmeters are used to monitor power quality, oscilloscopes and graphics were used in the 80's while digital signal processing, computer and mass storage are use in 90's. Presently, the power utilities are now incorporating smart pattern recognition and decision-making systems [50].

Various methods and techniques have been proposed in the literatures for voltage dip magnitude calculation which can also be used for dip magnitude detection. A voltage dip detection technique detects the occurrence of the dip, the start point, the end point, dip magnitude and phase shift. The exiting common voltage dip detection methods include the peak value, root mean square (r.m.s.), Fourier transform (FT) and space vector [182], [183]. Technical works have indicated other techniques for power quality classification such as support vector machine and the least square support vector machine [184], [185].

When the r.m.s. value is used, the voltage waveforms are either sampled at a sampling rate of 128 samples per cycle (half-cycle) or 256 samples per cycle (one-cycle). Both the one-cycle and half-cycle r.m.s. voltage can be used to detect voltage dip, however, the half-cycle r.m.s. detects voltage dip faster than the one-cycle r.m.s. since it moves faster to new voltage state [117]. Reference [186] reported that the half-cycle r.m.s. was equally fast as Kalman filter order 1 as compare to higher-order Kalman filter.

It is possible to model the root mean square method for voltage dip detection. A voltage signal can also be modeled as a sine-wave [137], [187], since PQ is maintaining sinusoidal waveform of the load voltage at a specified magnitude usually 1p.u. and at the power frequency. Nominal voltage is given by the sinusoidal waveform as shown in equation 3.17.

$$u(t) = A\sin(2\pi ft + \phi) \ , \quad 0 \le t < T \tag{3.17}$$

Where A is the magnitude of the nominal voltage, f is the frequency of the power signal usually 50Hz or 60Hz, T is the duration, and ϕ is the phase angle. All these parameters vary with time, and they depend upon the factors such as load changes, faults, etc. [188].

The missing or drop voltage A_1 is given by $A_1 = \alpha A$ with $0.1 \le \alpha < 0.9$,

Where α represents the magnitude of the dip and $\omega = 2\pi ft$

Assuming A = 1, then signal model describing voltage dip as the missing or drop voltage magnitude is express as,

$$u(t) = \begin{cases} (1-\alpha)\sin(2\pi ft + \phi) & t_1 \le t \le t_2 \\ A\sin(2\pi ft + \phi) & t < t_1, t > t_2 \end{cases} \quad 0.01s < t_2 - t_1 < 60s \tag{3.18}$$

At a phase shift of 90^0 , The addition of the square of ideal sinusoidal signal in equation 3.17 above [116]

$$u^2(t) + u^2(t - T/4) = A^2 \tag{3.19}$$

The equation 3.19 will be zero for sinusoidal signal but will surely be non-zero for dip.

Each type of Eskom voltage dip windows is characterized with different voltage dip magnitude and duration. The mathematical expressions for the Eskom voltage dip windows Y, X1, X2, S, T, Z1 and Z2 is given by

For Y

$$u(t) = \begin{cases} (1-\alpha)\sin(2\pi ft + \phi) & t_1 \le t \le t_2 \\ A\sin(2\pi ft + \phi) & t < t_1, t > t_2 \end{cases} \quad 0.02s < t_2 - t_1 < 3s \qquad 3.20$$

The missing or drop voltage A_1 is given by $A_1 = \alpha A$ with $0.7 \le \alpha < 0.9$,

For X1

$$u(t) = \begin{cases} (1-\alpha)\sin(2\pi ft + \phi) & t_1 \le t \le t_2 \\ A\sin(2\pi ft + \phi) & t < t_1, t > t_2 \end{cases} \quad 0.02s < t_2 - t_1 < 0.15s \qquad 3.21$$

The missing or drop voltage A_1 is given by $A_1 = \alpha A$ with $0.6 \le \alpha < 0.7$,

For X2

$$u(t) = \begin{cases} (1-\alpha)\sin(2\pi ft + \phi) & t_1 \le t \le t_2 \\ A\sin(2\pi ft + \phi) & t < t_1, t > t_2 \end{cases} \quad 0.02s < t_2 - t_1 < 0.15s \qquad 3.22$$

The missing or drop voltage A_1 is given by $A_1 = \alpha A$ with $0.4 \le \alpha < 0.6$,

For S

$$u(t) = \begin{cases} (1-\alpha)\sin(2\pi ft + \phi) & t_1 \le t \le t_2 \\ A\sin(2\pi ft + \phi) & t < t_1, t > t_2 \end{cases} \quad 0.15s < t_2 - t_1 < 0.6s \qquad 3.23$$

The missing or drop voltage A_1 is given by $A_1 = \alpha A$ with $0.4 \le \alpha < 0.8$,

For T

$$u(t) = \begin{cases} (1-\alpha)\sin(2\pi ft + \phi) & t_1 \le t \le t_2 \\ A\sin(2\pi ft + \phi) & t < t_1, t > t_2 \end{cases} \quad 0.2s < t_2 - t_1 < 0.6s \qquad 3.24$$

The missing or drop voltage A_1 is given by $A_1 = \alpha A$ with $0.0 \le \alpha < 0.4$,

For Z1

$$u(t) = \begin{cases} (1-\alpha)\sin(2\pi ft + \phi) & t_1 \le t \le t_2 \\ A\sin(2\pi ft + \phi) & t < t_1, t > t_2 \end{cases} \quad 0.6s < t_2 - t_1 < 3s \qquad 3.25$$

The missing or drop voltage A_1 is given by $A_1 = \alpha A$ with $0.7 \le \alpha < 0.85$,

For Z2

$$u(t) = \begin{cases} (1-\alpha)\sin(2\pi ft + \phi) & t_1 \le t \le t_2 \\ A\sin(2\pi ft + \phi) & t < t_1, t > t_2 \end{cases} \quad 0.6s < t_2 - t_1 < 3s \qquad 3.26$$

The missing or drop voltage A_1 is given by $A_1 = \alpha A$ with $0.0 \le \alpha < 0.7$

The r.m.s.voltage V_{rms} which can be calculated from the sample time – domain voltages by using equation 1.4 in chapter 1.

$$V_{\text{r.m.s.}} = \sqrt{\frac{1}{N}\sum_{i=1}^{N} v_i^2} \qquad 1.4$$

Where N is the number of samples per cycle and v_i is the sampled voltage in the time domain. This method of voltage dip detection is based on comparing the $V_{r.m.s.}$ with a threshold voltage V_{thr} (0.9 p.u. or 90 % of the nominal voltage) as indicated in figure 1.6 in chapter 1.

This thesis provides an additional step towards this direction by using the ANN for the detection of voltage dip. For the ANN detector; it decides the voltage dip occurrence when the r.m.s. voltage is lower than 90 % of the nominal voltage.

Electrical power system is a dynamic and nonlinear system [189]. Each power quality problem has its own unique features that distinguish it from another disturbance [25]. When a fault occurs, different power system parameters change in the power network such as the voltage magnitude, phase angle and the reactive power. In order to identify the incident of voltage dip effectively the r.m.s. voltage magnitude and phase angle was monitored and acquired at the busbars of interest, computed and compared with the required voltage magnitude and the phase angle. If the magnitude of the r.m.s. value is between 10% and 90% of the nominal voltage and for duration of 10ms to 60sec, then the voltage is computed to signify the occurrence of a voltage dip [62]. This method is implemented by using Neural Networks in Matlab.

Under such circumstances, artificial neural network (ANN) was applied for detecting the dip incident. For detection at the beginning of an incident is necessary for adequate mitigation. It is necessary to extract the important features that identify and classify voltage dips [190]. The features selected for detection and classification of voltage dip and used as the training data for the different ANN are the voltage magnitude, dip duration and the phase angle shift and their performance is also evaluated. The possibility of this technique was demonstrated by comparing with other techniques and an extensive simulation of different of dip types was simulated.

ANN is a promising and novel method of processing and solving complex power system problems [8], [191]. In this dissertation, ANN was used to classify voltage dips according to the new seven voltage dip windows of ESKOM. This will help in taking an adequate and proper mitigation measure at the occurrence of the voltage dips. If a wrong mitigation measure is taken it can also lead to a more terrible power quality problem. Figure 3.6 shows the architecture of

the proposed intelligent voltage dip detection and classification system. This proposed method requires fewer numbers of features as compared with other methods. The model is based on voltage amplitude estimation and it duration. The input patterns of the ANN are obtained by windowing the samples within the class of the dip duration and the voltage dip magnitude. The output of the ANN must shows which voltage dip class or classes that are present.

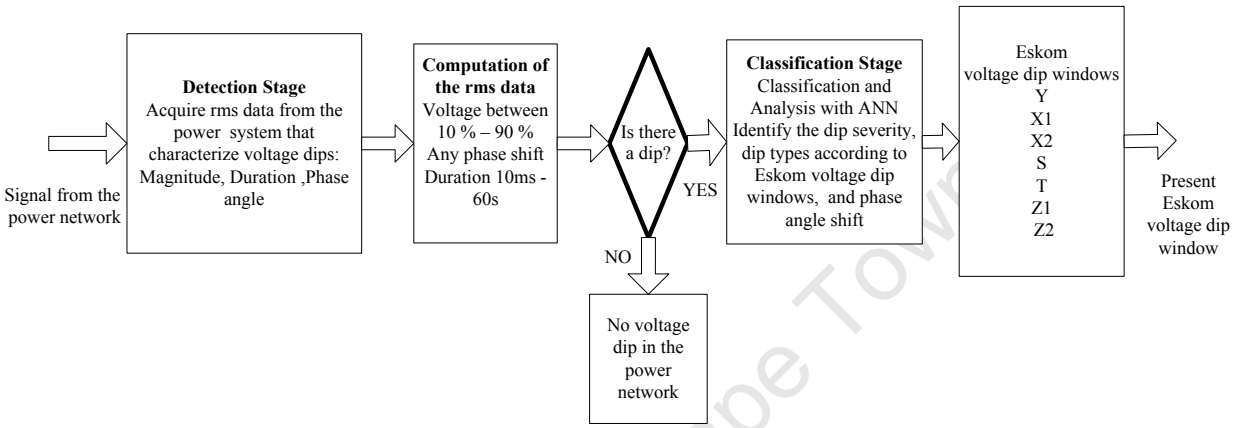

Figure 3.6: Architecture of the proposed intelligent voltage dip detection and classification system

3.16 Features extraction

Feature extraction is defined as changing of original signal to a new form which is suitable for the extraction of useful information. Features can be extracted from r.m.s.values, Fourier, wavelet, s-transform, etc. Fourier transform do not give information about component appearance time but about the existence of a certain frequency component. Both FT and STFT are unsuitable for non-stationary signals; in addition STFT has the limitation of a fixed window width. S-transform also involves a significant amount of computational resources [192], [150].

The r.m.s. value gives a good speed of calculation and requires less space. It gives an approximation of the fundamental frequency amplitude profile of a waveform and it algorithm is simple and requires less memory [50]. However, it does not recognize difference fundamental frequency and harmonics; this makes it suitable for event analysis and automatic classification of disturbance such as voltage dip. Fast Fourier transform (FFT) can be used to transform a signal from the time domain to the frequency domain. One of it disadvantages is window

dependency resolution. However, it is good for estimation of periodic signals in a stationary state but very poor for defection of suddenly or fast changes in the waveform of a signal such as voltage dips [50].

3.17 Neural network structure and design

The model of ANN used in this dissertation is a Multilayer Feed-forward Neural Network (MFNN). An MFNN neural network is a type of network where data flows in forward direction only, i.e. from input to output and is usually trained with the back-propagation learning algorithm. MFNN is made up of multiple layers that are more than one, and it is related to multilayer perceptron (MLP) [193]. It consists of a set input at the input layer, one or more hidden layers, and an output layer. MFNN can solve problems such as prediction, recognition, approximation and classification. They are usually multi-input, multi-output and are nonlinear systems [167]. The findings from this work have shown that FFNN models produce satisfactory results and took negligible time to detect and classify voltage dip once the network had been trained. There are several and well-known classification techniques that have shown useful in the areas of detection and classification of power quality disturbances. Examples are probabilistic neural networks (PNN), radial base function (RBF) and generalized regression neural network (GRNN).

PNN is derived from Bayes Decision Networks, and they are forward feed networks built with three layers. PNN is easily trained without delay; the execution time is slow, and it requires a large amount of space in memory [195]. Reference [27] shows that S-Transform based PNN classifier is simple and learning efficiency is very fast had compared with feed-forward multilayer back propagation and learning vector quantization. This might be due to superior properties of S-Transform during classification of PQ disturbances [196]. RBF is a special case of multilayer feed-forward with only two layers and its hybrid or varieties of learning algorithms converges faster than the back propagation algorithm. However, in many application problems, it has a slower speed due to a large number of hidden units [145].

GRNN and PNN are often used for function approximation and classification problems. However, they cannot easily converge unless they are given enough training data. Both the

GRNN and PNN are slower than MFNN during computation [144]. Both require more memory space to process and store information [197]. These make both PNN and GRNN unsuitable for voltage dip detection and classification since dip needs to be detected and classified as fast as possible.

The workflow for the FFNN neural network includes:

Collection of data from DigSILENT through Microsoft excel

Saved in CSV (comma delimited)

All input files must be in CSV format with only numbers in the entries

Creating columns and rows from the feature data,

Specifying the training, testing and validation set

Creating the network, configuring the network, initializing the weights and biases, train the network, validating the network (post-training analysis) and using the network [144].

A feed-forward neural network (FFNN) is made up of series of layers. The first neuron layers which are the input layer which connect to the hidden layer. FFNN supports feed-forward neural networks with any number of hidden layers and any number of neurons in each hidden layer. The numbers of hidden layers determine whether the FFNN is single, two-layer feed-forward or multilayer feed-forward neural network. The data is fed through the input layer to the hidden layer where the learning process commences and also continues at the output layer which finally, output the result as shown in the Figure 3.7.

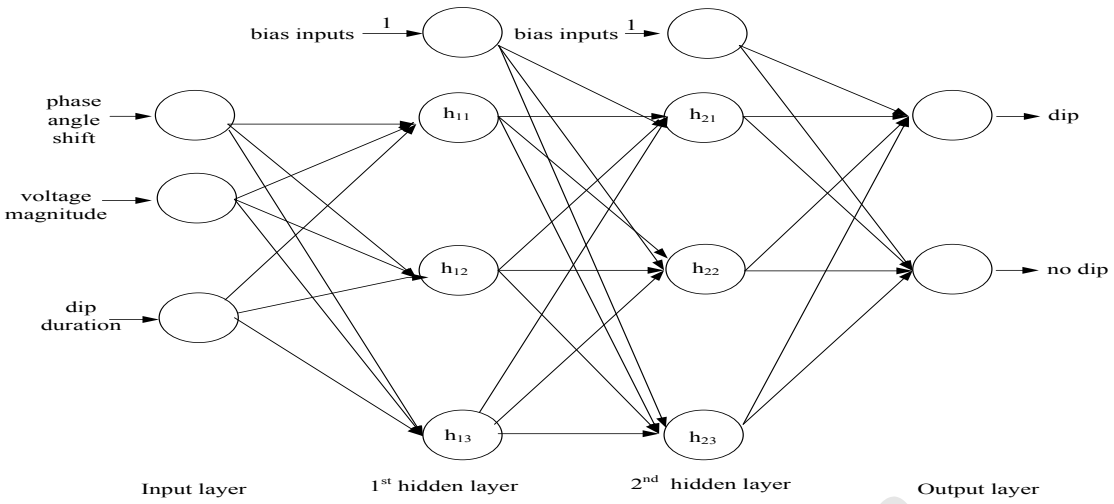

Figure 3.7: A three-layer feed-forward neural network for voltage dip detection with configuration 3-3-3-2

3.18 MATLAB ANN tool box

Today, there are different kinds of software for neural network modeling. The common types are the Matlab Neural Network Toolbox™ (MNNT), JavaNNS and Stuttgart Neural Network Simulator (NNS) [198]. Modeling and design of ANN involve the optimization of the maximization of network capacity and the minimization of neural architecture [199]. Neural networks are good pattern recognition and classification tool. Voltage dip identification and classification was done using Matlab codes. The ANN models were implemented using a combination of Matlab Simulink Toolbox models and programming in Matlab function code.

In this research work, Matlab code was used to create, train, and simulate a customized neural network for both detection of voltage dip and classification of voltage dip according to ESKOM voltage dip windows with the presence of RDG ancillary services support. The ANN detector and classifier were trained with sample data generated through simulation in DIgSILENT. These intelligent systems can be used by power utility for detection and classification of voltage dip on their power network. The MNNT provides graphical user interfaces (GUI) or command-line operations or simple coding by using m-file, and it is possible to design, create, train, and simulate neural networks. Matlab provides high-level neural network creation functions like *newlin* that is used to create a linear layer, *newp* create a perceptron and *newff* will create a feed -forward back-propagation [200].

The training, testing and validating data are generated and collected from DIgSILENT through Microsoft excel. With different sample data of voltage dip classes were simulated with various starting time, duration and distortion magnitude. Collaboration was made with Eskom to use generic data also for the simulation [201].

In the case of dip detection, voltage dips of different types were simulated. The data are organized into two matrices, the input matrix and the target matrix which defines the desire network output. The target data is generated when there is a fault or disturbance on the power network and hence the voltage dip occurs within the system which might be a short circuit fault. The following short circuit faults were investigated. Three phases short-circuit (3P) fault, Two phases short-circuit (2P) fault, Single phase-to-ground (SLG) Fault and Two phase-to-ground (2LG) Fault. Each column of the input matrix has 3 elements representing the voltage dip feature. The column of the target matrix has two elements (1's and 0's) indicating voltage dip and no voltage dip conditions respectively.

For voltage dip classification, each column of the input matrix has 15 elements, which are seven voltage magnitudes and seven phase angle shift and the dip duration. These represent the features for classification. Each corresponding column of the target matrix has seven elements indicating the Eskom voltage dip windows, consisting of six 0's and a 1 in the location of the associated with a particular dip class.

3.19 Feed-forward ANN architecture

Feed-forward ANN architecture is of the form

$$\mathbf{A - B_1h_1 - \ldots - B_mh_n X- C}$$

Where A is the number of input features, C is the numbers of output target. h_1 represent the first hidden layer with "B_1" number of neurons, and h_n is the nth hidden layer with "B_m" number of neurons. Hence, n= 2, 3...n. and m = 0, 1, 2, 3…m. Where n and m are positive integers.

In a single-layer feed-forward network, B1 =0 at the first hidden layer h_1, therefore, $B_m h_n = 0$. Then it is represented by **A - C.** since the first hidden layer is zero that second layer is zero and non-existing. Assuming A = 5 and C= 2, then the neural network is a single-layer feed-forward of the form 5 – 2.

A 4 layer feed-forward ANN with A=11, B_1=4 at h_1, B_2=6 at h_2, B_3=5 at h_3, and C = 3. The model will be represented as

11 - 4 - 6 - 5 - 3

In this research, the detector ANN is of the form (3 - B_1h_1 - … B_mh_n - 2) while the classifier ANN has the form (15 - B_1h_1 - … B_mh_n - 7)

3.20 Missing data restoration

The field of research always experiences the issue of corrupted and missing data. Missing data may be due to equipment malfunction, and certain data may not be considered important at the time of entry. There has been many ways to decide missing data. It could be through complete or available case analysis, substitution using the mean value, regression substitution, matching imputation. However, the technique to use depends upon the data [158]. In this work, a missing data restoration (MDR) algorithm, which can be used in case of faulty input data, error signals and loss of signal from the system, was used. This will help to identify missing and corrupted data.

3.21 Performance evaluation of ANN

There are different methods to judge the performances of the neural network. The common measures are the performance plot and the confusion matrix. The performances of the ANN detector and classifier were judged using the performance plot and the confusion matrix. Performance is measured in terms of mean squared error (MSE). This is given as the average squared difference between the network outputs and the target outputs. Lower values of mean squared error are better while zero means no error.

3.22 Software implementation

The simulation was done on a PC with a processor Intel(R) Core(TM) i7- 2600 CPU@ 3.40GHz and RAM of 16.0 GB. The code was modeled using the programming in Matlab function code.

3.23 The proposed algorithms for voltage dip detection and classification

This algorithm is capable of detecting and classifying voltage dips according to Eskom voltage dip windows. The inputs to the algorithm are the r.m.s. retained voltage magnitude, phase angle and the dip duration. The detector ANN architecture is made up of two-layer FFNN with 3-27-2 input-neuron-output structure. The three inputs are the r.m.s. retained voltage magnitude, phase angle and the dip duration, while the output is either dip occurrence or no dip occurrence. The classifier ANN has fifteen inputs, 20 neurons and 7 outputs, which is 5-20-7. The fifteen inputs are the r.m.s. retained voltage magnitude and phase angle of the seven voltage dip classes and the dip duration. The output is the seven dip classes. The algorithm for detection and classification of voltage dip is shown follow:

VOLTAGE DIP DETECTION ALGORITHM

Training of Neural Network

a) Load INPUT A[r, c]

b) Initialize OUTPUT B[r, c]]

c) Training using Scaled Conjugate Gradient Algorithm

```
n = total no of columns
r = row no
c = column no
r = 1
For c=1 to n
{
        If (A[r, c] is between 0.1 and 0.899999)
        {
                Train B[r, c] = 1;
                Train B[r+1, c] = 0;
        }
        Else If (A[r, c] is between 0.9 and 1.0)  {
                Train B[r, c] = 0;
                Train B[r+1, c] = 1;
                }
```

Validating Training with Input Data

d) Load INPUT D[r, c]

```
Initialize OUTPUT C[r, c]]
n = total no of columns
r = row no
c = column no
r = 1
For c=1 to n
{
```

```
        If (D[r, c] is between 0.1 and 0.899999)
        {
                Output Result C[r, c] = 1;
                Output Result C[r+1, c] = 0;
        }
        Else If (A[r, c] is between 0.9 and 1.0) {
                Output Result C[r, c] = 0;
                Output Result C[r+1, c] = 1;
        }
Else


        }
```

Checking Results

```
For r = 1 to n
{
        For c=1 to n
        {
                If (B[r, c] == C[r, c])

                        Print -> Neural network is well trained for voltage dip detection
                Else
                        Print -> Neural network misclassified voltage dip.
        }

}
```

Testing a Fresh Input Data

e) Load TestInput X[r, c]
   n = total no of columns

```
r = row no
c = column no
r = 1

For c=1 to n
{
        If (X[r, c] is between 0.1 and 0.899999)
        {
                Output TestResult Y[r, c] = 1;
                Output TestResult Y[r+1, c] = 0;
        }
        Else If (X[r, c] is between 0.9 and 1.0)   {
                Output TestResult Y[r, c] = 0;
                Output TestResult Y[r+1, c] = 1;
        }
}
```

VOLTAGE DIP CLASSIFICATION ALGORITHM

a) Load DIP INPUT Data
b) Load DIP OUPUT Data
c) Training using Resilient Algorithm

n = total no of columns
r = row no
c = column no
r = 0
t_1= dip starting time
t_m = dip end time
A[r,c] = Voltage Magnitude
A[r+1, c] = Phase Angle shift j ($\Delta\theta = \theta - \theta_i$) {i=1,2,3,…k.}
A[r+2, c] = Dip duration T ($\Delta t = t_m - t_1$)

```
For c=1 to n
{
    If (A[r, c] is between 0.7 & 0.9 and A[r+1, c] is Δ θ  and A[r+2, c] is  Δ t < 2980
    {
        Train B[r, c] = 1;
        Train B[r+1, c] = 0;
        Train B[r+2, c] = 0;
        Train B[r+3, c] = 0;
        Train B[r+4, c] = 0;
        Train B[r+5, c] = 0;
        Train B[r+6, c] = 0;
    }

    Else if (A[r, c] is between 0.6 & 0.7 and A[r+1, c] is Δ θ and A[r+2, c] is Δ t <
130)
    {
        Train B[r, c] = 0;
        Train B[r+1, c] = 1;
        Train B[r+2, c] = 0;
        Train B[r+3, c] = 0;
        Train B[r+4, c] = 0;
        Train B[r+5, c] = 0;
        Train B[r+6, c] = 0;
    }
    Else if (A[r, c] is between 0.4 & 0.6 and A[r+1, c] is Δ θ and A[r+2, c] is Δ t <
130)
    {
        Train B[r, c] = 0;
        Train B[r+1, c] = 0;
        Train B[r+2, c] = 1;
```

Train B[r+3, c] = 0;
Train B[r+4, c] = 0;
Train B[r+5, c] = 0;
Train B[r+6, c] = 0;
}

Else if (A[r, c] is between 0.4 & 0.8 and A[r+1, c] is Δ θ and A[r+2, c] is Δ t < 450)
{
Train B[r, c] = 0;
Train B[r+1, c] = 0;
Train B[r+2, c] = 0;
Train B[r+3, c] = 1;
Train B[r+4, c] = 0;
Train B[r+5, c] = 0;
Train B[r+6, c] = 0;
}

Else if (A[r, c] is between 0.0 & 0.4 and A[r+1, c] is Δ θ and A[r+2, c] is Δ t < 580)
{
Train B[r, c] = 0;
Train B[r+1, c] = 0;
Train B[r+2, c] = 0;
Train B[r+3, c] = 0;
Train B[r+4, c] = 1;
Train B[r+5, c] = 0;
Train B[r+6, c] = 0;
}

Else if (A[r, c] is between 0.70 & 0.85 and A[r+1, c] is Δ θ and A[r+2, c] is Δt < 2400)

```
        {
                Train B[r, c] = 0;
                Train B[r+1, c] = 0;
                Train B[r+2, c] = 0;
                Train B[r+3, c] = 0;
                Train B[r+4, c] = 0;
                Train B[r+5, c] = 1;
                Train B[r+6, c] = 0;
        }
        Else if (A[r, c] is between 0.0 & 0.7 and A[r+1, c] is Δ θ and A[r+2, c] is Δ t <
2400)
        {
                Train B[r, c] = 0;
                Train B[r+1, c] = 0;
                Train B[r+2, c] = 0;
                Train B[r+3, c] = 0;
                Train B[r+4, c] = 0;
                Train B[r+5, c] = 0;
                Train B[r+6, c] = 1;
        }
Else
 print -> wrong data input.
}
```


3.24 Voltage dip detection and classification flow chart

Voltage dip detection and classification flow chart is shown as follows.

VOLTAGE DIP DETECTION ALGORITHM

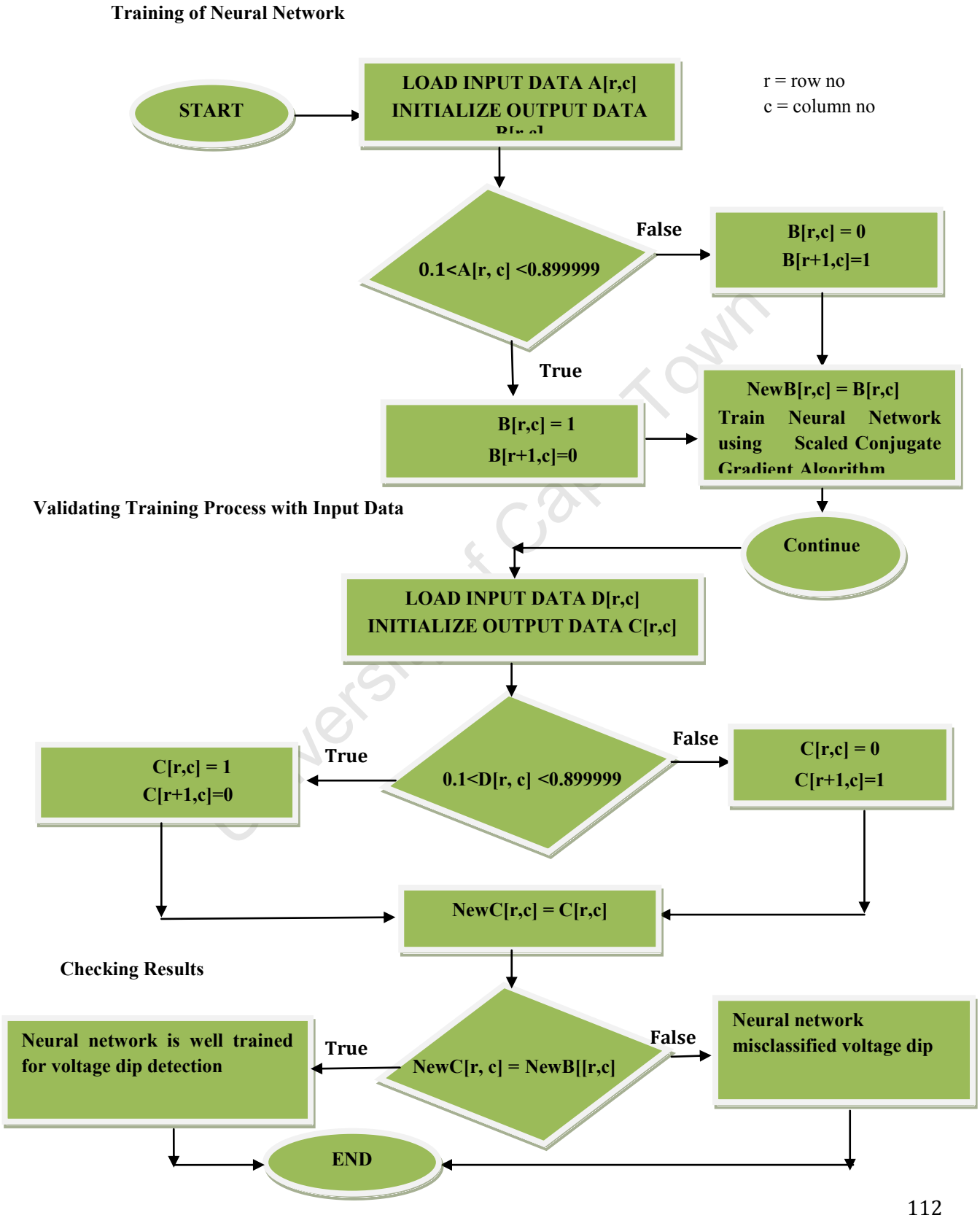

Testing a Fresh Input Data

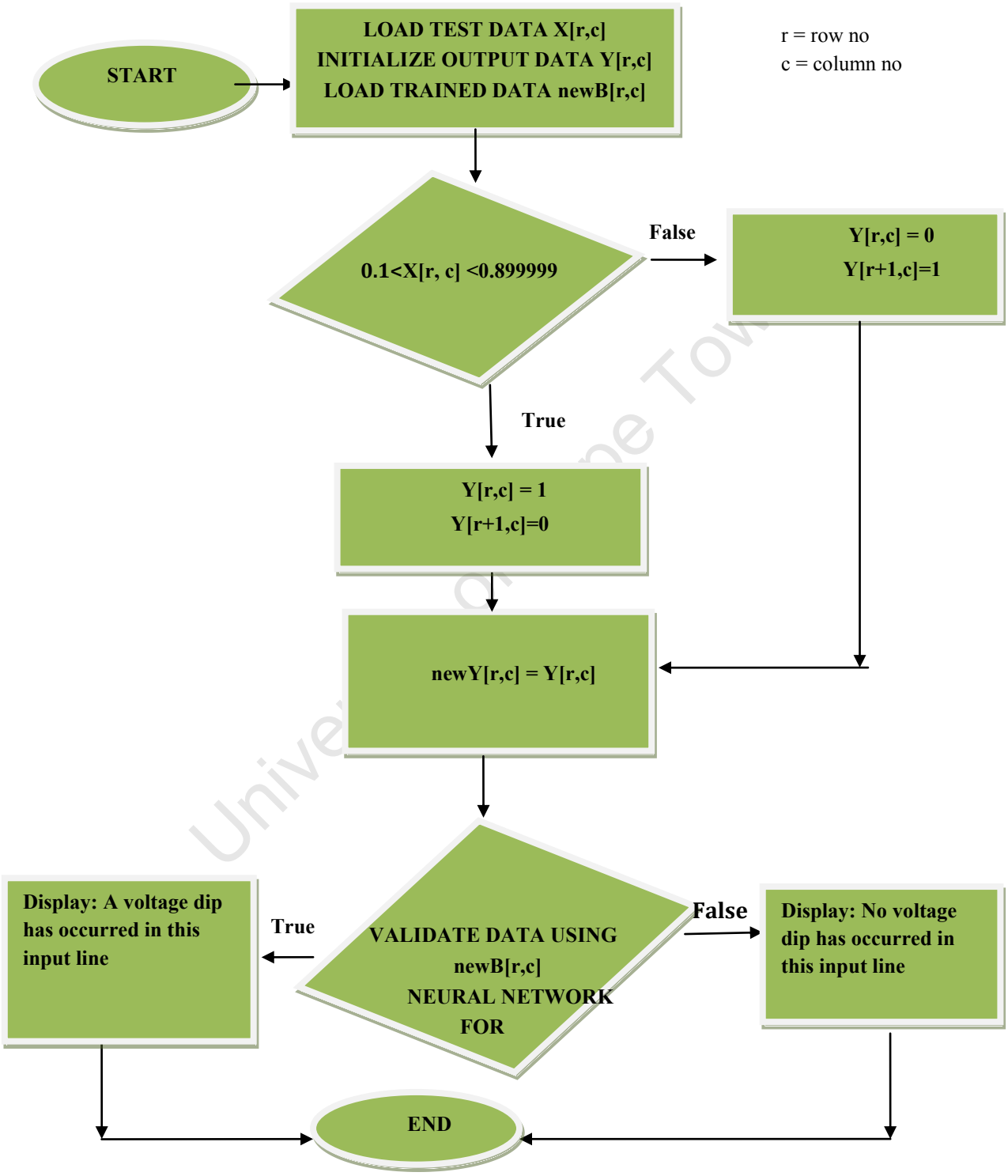

VOLTAGE DIP CLASSIFICATION ALGORITHM

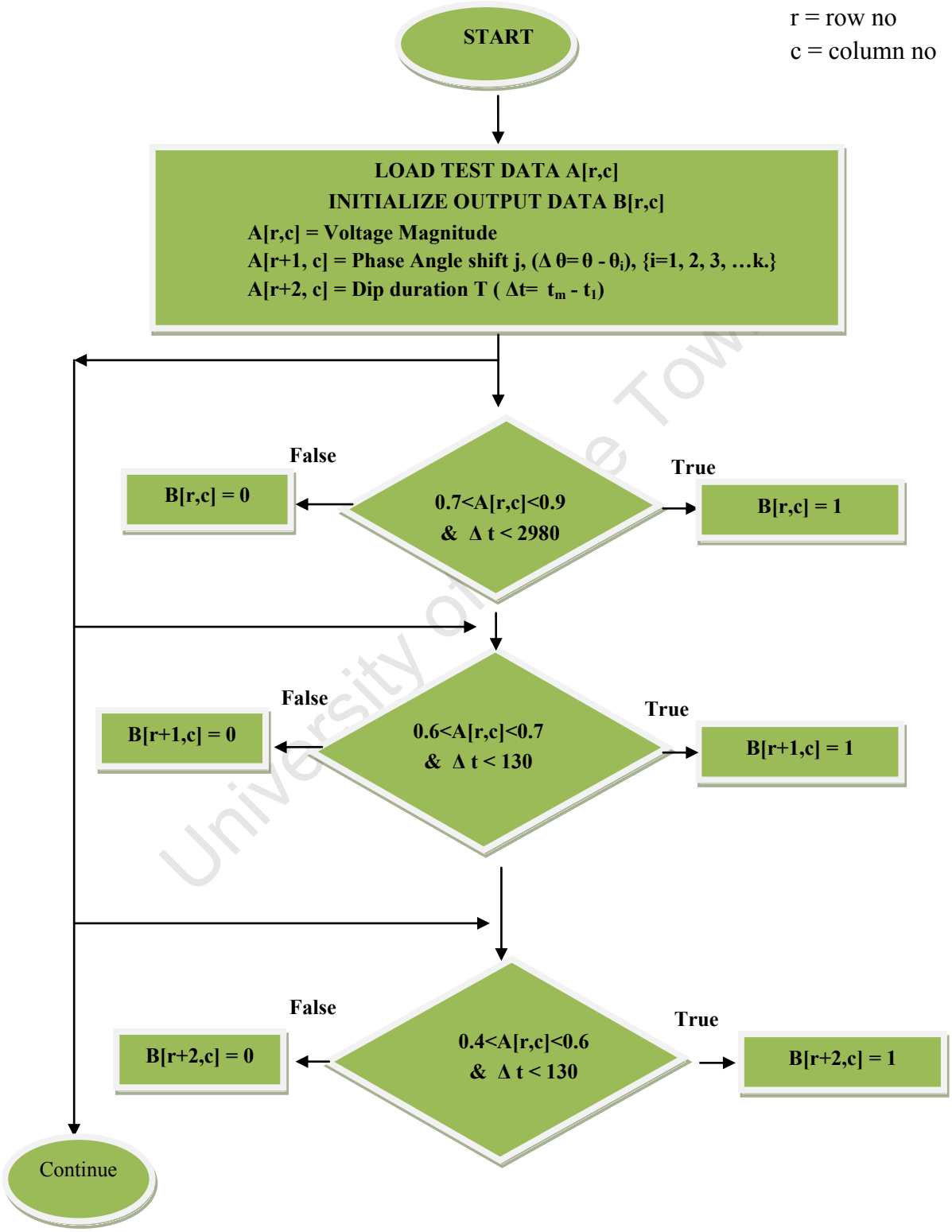

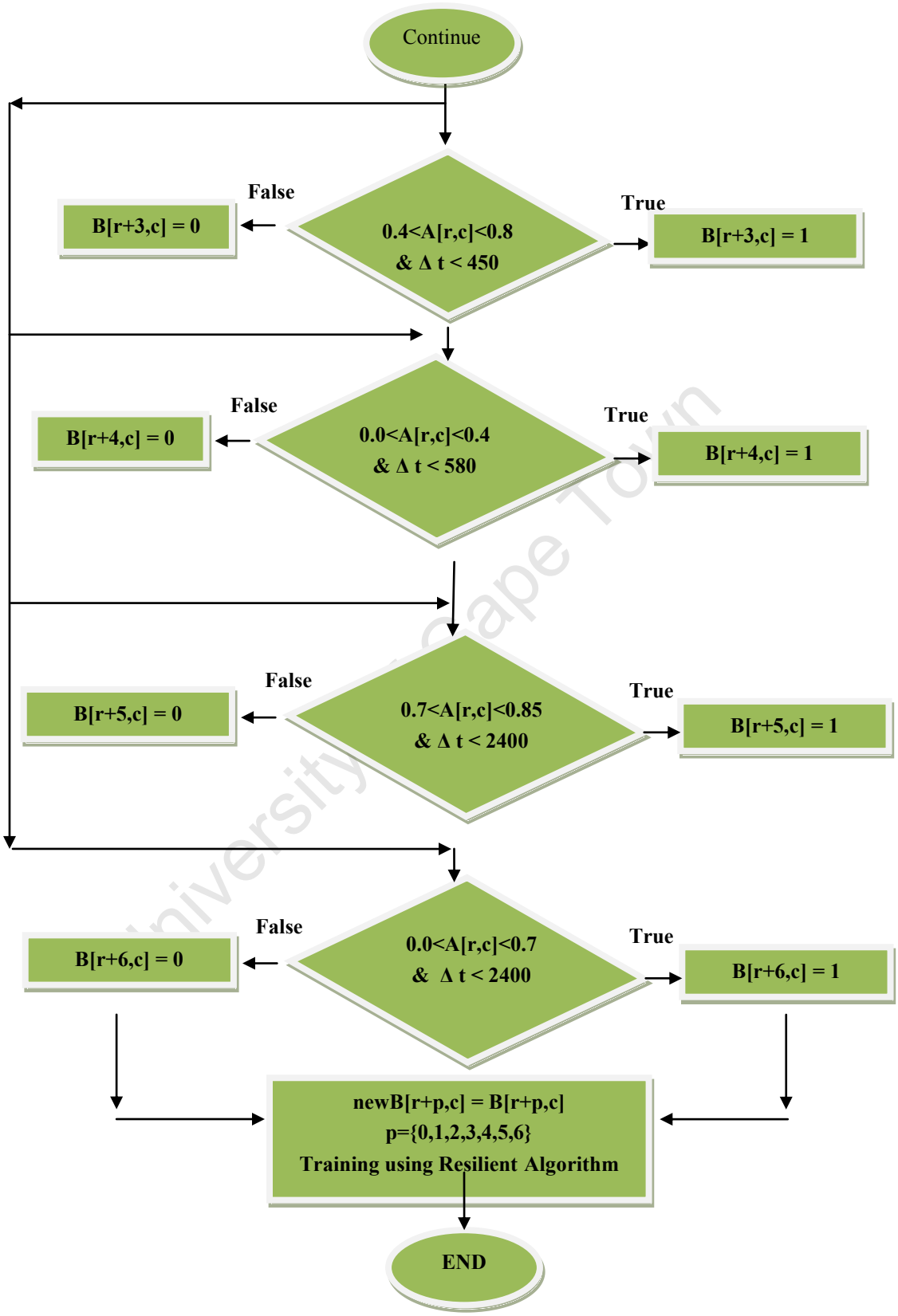

Chapter 4

4.1 Test Network Description and Modeling in DIgSILENT Power Factory

DIgSILENT is integrated power system analysis software that combines reliable and flexible system modeling capabilities, features analysis and operation of any aspect of the power system. It is industrial and academic power system simulation software that provides a comprehensive library of models, and it is in use in many countries around the world such as National Grid (UK), ESKOM (RSA), Swissgrid, Tennet, ETRA, Dong, Terna, EON, EDF, etc. It has been used to address most power system analysis issues, and it provides users all the required models and techniques of modern power systems [202]. DIgSILENT library provides basic models of many electrical power components such as grid models or external grid, power sources, electrical loads, modeling of various grid-connected renewable distributed generations, etc. DIgSILENT offers data management and many reporting options such as exporting its result data to other software programs such as Microsoft excel, Microsoft access, Notepad, etc. This has made it possible to process or analyze the result obtained from simulations in DIgSILENT.

PowerFactory is capable of modelling the following; external grid in form of meshed and radial AC systems with single, two, and three-phases and model validity from HV to MV and LV. Renewable generators and power sources can either be modelled as AC voltage source and DC voltage source using DIgSILENT machines such as synchronous, asynchronous, doubly-fed induction generator and static generator (for wind, hydro, solar generator, etc.). Loads can be a general load model (for MV- feeders and LV-feeders), complex load model Low voltage load. Branch models such as the line (Overhead line and cable models) and transformers.

4.2 Description of the test network

The test network is a generic model that was built, modeled, and simulated in DIgSILENT PowerFactory. It is modelled after a typical South African power network. The model is developed as a combination of the generic model from the South African power utility model and IEEE 9 bus test system. The specifications are provided in Appendix 4. Test network is

made up of individual network components such as lines, grid-connected renewable distributed generators with a number of control systems, transformers, electrical loads, utility generators and busbars or buses, etc. It also comprises the external grid, the transmission grid and the distribution grid as shown in Figure 4.1.

In this thesis, the IEEE 9 bus system is modelled as the transmission network as it closely resembles the Eskom transmission network in terms of voltage levels. It transmits electricity at high-voltage three-phase alternating current of 230kV; this is to reduce the energy loss in long-distance transmission. For this thesis, it was coupled with the grid and the distribution network, both modelled using data available from the South African power utility, Eskom [201]. The transmission and the sub-transmission systems have nominal voltages of 230kV, 66kV, 22kV and 11kV. The 66kV, 11 kV and 22 kV are most commonly used in South Africa. Both the transmission and the distribution networks are made up of overhead lines, which make the lines prone to overhead line faults. The power network lines are homogeneous which means that there is no joining of different types of conductor sizes and hence that the line impedance is distributed uniformly on the whole length.

The external grid operates at a constant voltage of 230kV, and it injects 370 MW of power to the transmission grid, and it is connected at substation busbar10 through line7. The transmission system is also connected at the substation busbar24 through line15. The IEEE 9 bus system has four different voltage levels of 230kV, 18kV, 16.5kV and 13.8kV. It has three synchronous generators, three loads, three transformers and six lines with nine bus bars. It supplies the distribution grid through line8 and line15. Line7 and line8 take the power to the substation, and the voltage is stepped down from 230kV to sub-transmission and distribution voltages of 66kV and 11kV on busbar27 and busbar11 respectively. Furthermore, the voltage at 230kV is also stepped down at another substation on busbar23 to 11kV. The 66kV was further stepped down to 22kV on busbar25. All these voltages were further stepped down to a distribution voltage of 0. 415kV. The detailed description of the system parameters and analysis can be found in Appendix 4.

The transmission network is fed from two sides, busbar10 and busbar24. The advantage of this type of configuration is to allow the distribution network to receive power when one of the substations cannot supply power. With this looped network, the customers do not experience power interruption. In addition to the grid-connected RDG systems which are located close to the sensitive loads. Basically, the first step to take in installation of the grid-connected RDG is to identify a suitable location and it economic viability. However, the locations of the grid-connected RDG units are determined according to the natural presence of the energy source in a particular area.

4.3 Placement and type of RDGs in the test network

In Africa, a meaningful number of RDG exists, and they are generally connected at the distribution network. In places like Swaziland, Lesotho, South Africa and some other parts of Africa, the utility operates and owns a large number of the distributed generators; however, in Nigeria, it is mainly operated privately by independent power producers. This might be due to the incapability of the Power Holding Company in Nigeria to manage and maintain the present distributed generators.

The RDG systems that exist in Sothern African region include the hydro, wind and solar power plants. This region is dominated by hydro-power plant as a result of endowed rivers around the region, and many dams have been built for different usage such as for power, irrigation, water supply, etc. Wind power plants are also present in areas such as the Western Cape and there are ongoing projects in Eastern Cape and Northern Cape such as Coega wind farm and Nobelsfontaine wind farm respectively. PV plants are usually installed in areas such as rural area or remote area from the grid. There is ongoing 50MW solar project in Touwsrivier, Western Cape, as well as 75MW in Kalkbult, Northern Cape.

Many techniques and methods for sizing and placement of RDG systems have been published in technical literature. These methods include analytical method, particle swarm optimization, Monte Carlo approach, etc., [203], [204], [205], [206]. However, most of these techniques and methods depend on some economic, environmental and technical factors that affect the

positioning of RDG systems. Most importantly, the placement of RDG systems is guided by local availability of the energy source in an area and other factors affecting the deployment.

The economic factor includes the cost of the electric power from the generating station through the transmission to the distribution side, the fuel cost and cost of providing a particular type of RDG plant in an area and cost of managing its emission and waste. Waste Management, greenhouse gas emissions and sound pollution are the common environmental factors that might affect RDG placement. Furthermore, the technical motivators might include improving power quality of the system, reduction in line loss and stand-alone or grid-connected system. The economic advantages of RDG system placement are reduction of transmission and distribution cost, electricity price and saving of fuel. The environmental advantages entail reductions of sound pollution and emission of greenhouse gases, while the technical advantages involve line loss reduction and better power quality [207].

As mentioned previously, RDG placement depends on the availability of energy source in a particular locality. Renewable energy sources cannot be transported, and therefore, the electricity must be generated at the location where the energy source is available. For example, hydropower plant will be sited only in areas where water bodies or rivers are present, the solar power generators are mostly located where the intensity of solar radiation is high and where there is enough space for the solar panels. Moreover, the wind power plants are sited where the wind velocity is at its highest and more or less constant over the year. The same condition holds in South Africa and RDGs must be located where the energy sources are available. The test network model in this dissertation takes into account the importance of placement of RDG systems as guided by the local availability of the energy sources.

The types of grid-connected RDG installed within the test power system include wind plants, PV plants and the hydro plants. These various power plants use different generator technologies such as synchronous generator, induction generator and fully rated power electronics converter interfaced generators. In the power network model used in this thesis, the hydro power plants are modeled as synchronous generators while the PV plants are modeled as static generators

with power electronics converter interfaces. The wind energy conversion systems models are made up of different wind farms. They are modeled as synchronous generators, induction generators and static generators with fully rated converters.

These grid-connected RDGs are connected at both sub-transmission sides of high-voltage industrial facility, and at the distribution system either at medium voltage or low voltage or on the industrial facility grid at the customer site of the meter. They are usually connected close to the load, and their power flow being in the direction opposite to that of the centralized generators.

In the test network in Figure 4.1, generators RDG01, RDG02, RDG08, RDG09, RDG010 and RDG011 are represented as hydro-electric generators which are non-conventional permanent magnet synchronous generators; RDG03, RDG04, RDG05, RDG06 and RDG07 are represented as PV generators; RDG012 to RDG026 are represented as the wind generators. Of these, RDG012, RDG013, RDG014, RDG015 and RDG016 are modelled as variable-speed doubly-fed induction generators; RDG017, RDG018, RDG019 and RDG020 are modelled as static generators with fully rated power electronics converters; RDG021, RDG022, RDG023, RDG024, RDG025, and RDG026 are represented as variable-speed permanent magnet synchronous wind generators. The parameters of these generators are shown in the Appendix 4.

4.4 Electrical Load category

There are different kinds of load models in the network, such as balanced or unbalanced load, critical or non-critical load, inductive or capacitive load, general or complex load and their input modes. Practical industrial, commercial, office and domestic loads are simulated as inductive loads. Examples are ballast, welding, lighting, heating, motors, transformers, computers, etc. Capacitive loads are not so common unlike inductive loads. Load such as synchronous motors and capacitor banks are examples of capacitive loads. In the test network used in the thesis, all the loads are assumed to be balanced loads except loads designated as ‘Load 7’, ‘Load 9’ and ‘Load 10’ which are unbalanced loads. Only two loads, ‘Load 4’and ‘Load F’, are designated as

capacitive loads while all other loads are inductive load. The details of these loads are given in Appendix 4.

4.5 Limitations and assumption in the test network

This thesis only focuses on intelligent voltage dip mitigation with RDG through the early detection and classification of voltage dip in a power network. This provides distinctive characteristics of each class and guides the utility in selecting judiciously an RDG-based voltage dip mitigation scheme. This study is carried out using generic data provided by South African utility, Eskom 201]. However, data for some power network components are assumed. For the transmission grid, IEEE 9 bus test system was assumed as Eskom transmission network as it has a close resemblance to the Eskom transmission network in terms of voltage level. Some data such as transmission line and load parameters were obtained from the Eskom transmission system on the website [208]. The IEEE 9 bus test system parameters such as for the generators, lines, transformers, etc. are selected from DIgSILENT library [209] as indicated in Appendix 4. The events leading to voltage dip are simulated as electrical power systems faults such as three-phase short-circuit (3P) fault, two-phase short-circuit (2P) fault, single phase-to-ground (SLG) fault and two phase-to-ground (2LG) fault. The steady state load flow study is carried out to satisfy that the test network is within the required limits of voltages and loading. The allowed standards of voltage limits are 0.950p.u. and 1.05p.u.

It is assumed that there is absent of stability problems, and the ancillary service is provided by the GRDG and PV generators only supply active power. It is also assumed that the protection devices do not fail during the dip events and there is no fault current from the RDG units. The fault currents are negligible compared to that from utility generators. The size of the RDGs is lesser compared to the size of the utility generators, when a short circuit study is conducted to compare the RDG and utility fault currents. It is also assumed that the power network lines are homogeneous. There is no joining of different types of conductor size so that the line impedance is distributed uniformly on the whole length.

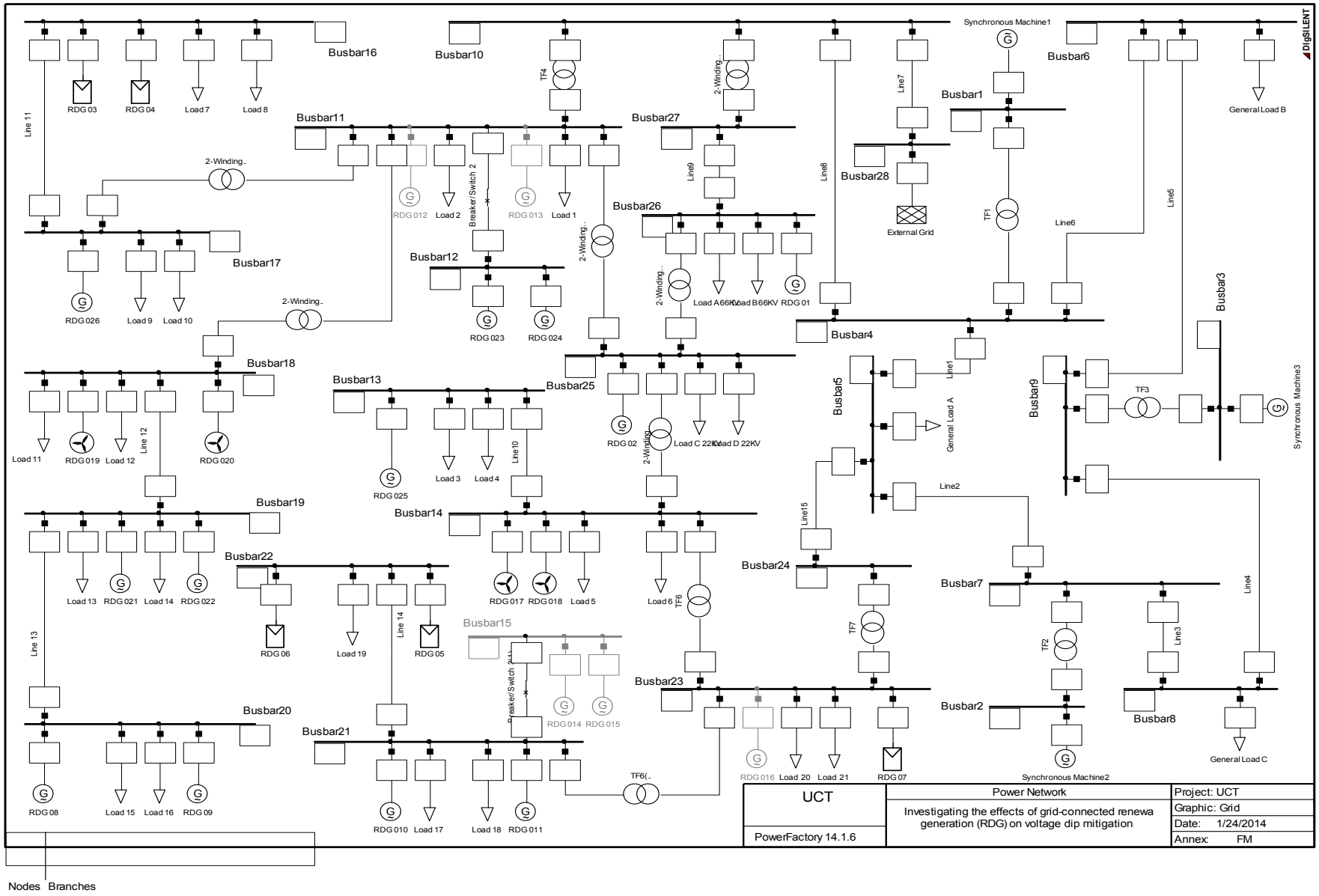

Figure 4.1: Test network with RDG

4.6 Modeling and simulation of individual network components

4.6.1 Modeling of a synchronous generator

The test network in Figure 4.1 has the following synchronous generators installed.

1. All the hydro-electric generators (RDG01, RDG02, RDG08, RDG09, RDG010 and RDG011) are non-conventional permanent magnet synchronous generators.
2. The three generators of the IEEE 9 bus test systems are also modelled as conventional synchronous generators.
3. Some wind generators are modelled as variable-speed permanent magnet synchronous wind generators (RDG021, RDG022, RDG023, RDG024, RDG025, and RDG026)

The model setup of a synchronous generator in DIgSILENT PowerFactory is such that the generator can be defined by different parameters such as type data (rated power, voltage, power factor, reactance, inertia, time constants, saturation characteristic, etc.), element data (PQ, PV or SL machine, dispatched power, voltage or reactive power, MVAr limits, reference to station controller & secondary controller, virtual power plant, etc.).

A synchronous generator requires a DC excitation and both frequency and amplitude of the induced voltage depend on the actual rotor speed. On the contrary, an induction generator relies completely on the power system for excitation to create the rotating magnetic field on the rotor [90]. Synchronous generators are driven at a speed that corresponds to the number of poles of the generator and the frequency of the electric power system with which it is connected. They have a synchronous speed, which is defined by equation 4.1.

$$N_S = \frac{120f}{p} \tag{4.1}$$

where N_s is the synchronous speed in rpm, p is the number of pole pairs and f is the frequency. One difference between synchronous generators and asynchronous generators is in their operational speed. This difference in speed is called the slip and is given as equation 4.2.

$$s = \frac{N_s - N_m}{N_s} \tag{4.2}$$

where s is the slip N_s is the synchronous speed in rpm and N_m machine speed in rpm.

The magnetic flux in synchronous generator's rotor is usually described by a vector, based on the assumption that the magnetic flux distribution around the rotor is sinusoidal. This type of model is called the Park model and can be represented in a rotor-oriented d-q-reference frame, and the equivalent circuits for the d and q models are shown in Figure 4.2 and Figure 4.3 [210]. According to Figures 4.2 and 4.3, the stator and rotor voltage equations are given by equations 4.3 to 4.7.

$$v_d = R_a i_d + \dot{\psi}_d - \omega\psi_q \tag{4.3}$$

$$v_q = R_a i_q + \dot{\psi}_q + \omega\psi_d \tag{4.4}$$

$$v_E = R_E i_E + \dot{\psi}_E \tag{4.5}$$

$$0 = R_D i_D + \dot{\psi}_D \tag{4.6}$$

$$0 = R_Q i_Q + \dot{\psi}_Q \tag{4.7}$$

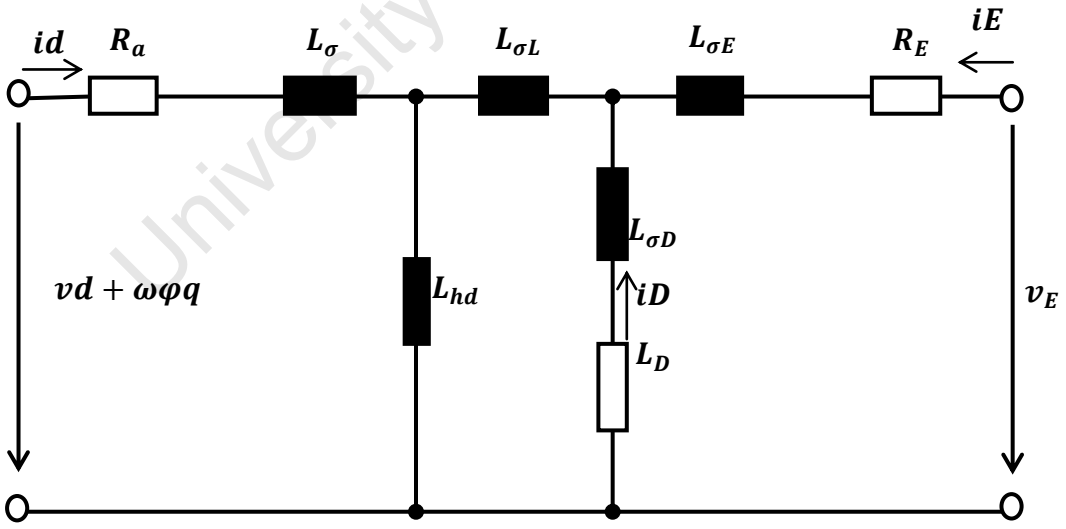

Figure 4.2: d-axis synchronous machine model [210]

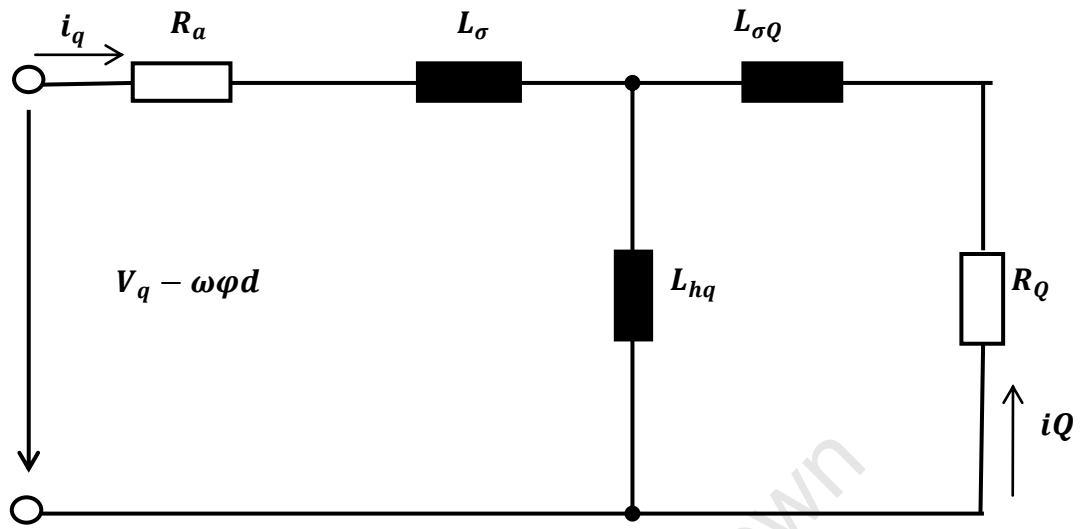

Figure 4.3: q-axis synchronous machine model [210]

If the stator and rotor transient terms are neglected, then the rotor voltage equations of a synchronous generator are shown by the equations 4.8 to 4.10, and the stator voltage equations are shown in equations 4.11 and 4.12 below [211].

$$\dot{\psi}_{fd} = V_{fd} - R_{fd} I_{fd} \quad 4.8$$

$$\dot{\psi}_{KD} = -R_{KD} I_{KD} \quad 4.9$$

$$\dot{\psi}_{KQ} = -R_{KQ} I_{KQ} \quad 4.10$$

$$\dot{\psi}_{d} = V_{d} + R_s I_d^{gen} + \omega_s \psi_q \quad 4.11$$

$$\dot{\psi}_{d} = V_{q} + R_s I_q^{gen} - \omega_s \psi_d \quad 4.12$$

where V_{fd} is the exciter field voltage, I_{fd} is the exciter field current, R_{fd} is the field winding resistance, R_{KD} and R_{KQ} are equivalent d-axis and q-axis damper winding resistance, I_{KD} and I_{KQ} are the d-axis and q-axis rotor damper winding currents, ψ_{fd}, ψ_{KD} and ψ_{KQ} are the flux-linkages

of the field winding and the d-axis and q- axis damper windings. V_d and V_q are the d-axis and q-axis stator output voltages, R_s is the phase resistance of the stator winding, ψ_d and ψfq are the d-axis and q-axis flux-linkages of the stator winding. The synchronous angular frequency of the generator is ω_s. The mechanical model of the synchronous generator is represented by its torque equation in equation 4.13 [212].

$$2H\frac{dw}{dt} = T_m - T_e - T_D \tag{4.13}$$

Damping torque T_D is given as $D\Delta w$, where H is the inertia constant measure in seconds, w is angular velocity of rotor in [rad/sec], T_m is mechanical torque in [N.m], T_e is electrical torque in [N.m], T_D is damping torque in [N.m] D is the damping coefficient and Δw is change in angular velocity of rotor in [rad/sec].

4.6.2 Modeling of synchronous PMSG

All the synchronous generators as mentioned in section 4.6.1 above in the test network are permanent magnet synchronous generators. Modeling of Permanent Magnet Synchronous Generator (PMSG) is given by the voltage equation 4.14 and 4.15 [213].

$$\frac{di_{ds}}{dt} = \frac{1}{L_d}[-V_{ds} - R_s i_{ds} + \omega L_q i_{qs}] \tag{4.14}$$

$$\frac{di_{ds}}{dt} = \frac{1}{L_d}[-V_{qs} - R_s i_{qs} - \omega L_d i_{ds} + \omega \phi_m] \tag{4.15}$$

where,

V_{ds} and V_{qs} are the (d-q)-axis machine voltages.

i_{ds} and i_{qs} = the (d-q)-axis machine currents.

R_s = the stator resistance

ω = electrical angular frequency

L_q and L_q = direct axis inductance and quadrature inductance

$Ø_m$ = amplitude of the flux linkages

4.6.3 Modeling of electrical loads

In this thesis, the load is modeled as a general active and reactive load in DIgSILENT. General load model can be defined as having a constant active and reactive power, P and Q. However, the load can also be defined to be voltage-dependent. The test network has different load models types. They are modeled as balanced loads, capacitive, inductive and with different input modes like PQ, $P\cos(phi) \quad and \quad Q\cos(phi)$.

Electrical load modeling can be categorized into static load models, which are not dependent on time and dynamic load models, which are dependent on time. These various types of load models have a different impact on the voltage profile [214]. Loads are assumed both as constant active and reactive power loads and constant R-L loads. Modelling the load in terms of *dq-axis* current components as obtained from the absorbed active and reactive power is given in equations 4.16 and 4.17 [215].

$$I_d = \frac{V_d P}{V_d^2 + V_q^2} + \frac{V_q Q}{V_q^2 + V_q^2} \tag{4.16}$$

$$I_q = \frac{V_q P}{V_d^2 + V_q^2} + \frac{V_d Q}{V_q^2 + V_q^2} \tag{4.17}$$

Assuming the resistance R for the constant R-L load is connected in series with the load inductance L. The load current is I_L and the voltage drop across the load V_L can be given by equation 4.18 [215].

$$V_L = RI_L + L\frac{dL_L}{dt} \tag{4.18}$$

4.6.4 Power electronics converters modeling

DIgSILENT PowerFactory library provides for different types of power electronic converters for both the grid-side converter and the generator-side converter. Power electronic interfaces are needed in most RDG systems either as an inverter or as a rectifier. They can be modeled, design and use for a specific and appropriate model. Examples of power electronic converters available in DIgSILENT are inverters, pulse-width modulated (PWM) converters, rectifiers, soft-starter, etc. [216]. Electrical generators such as synchronous generator, solar generators, DFIG, etc., use power electronic interfaces for converting the generated voltage to the required AC voltage at power frequency of 50 Hz or 60 Hz. In many synchronous generators, the generator must be connected to the grid through the power converter called frequency converter, and there is an infinite way to realize this frequency converter in synchronous generators [210]. In DFIG and converter-driven synchronous generator (CDSG) models, the rotor part is usually connected to the grid via the PWM converters, and the converter is connected back to back as shown in Figure 4.4. The CDSG model usually has two PWM converters, one connected to the stator and the generator on the generator's side while the other is connected with the rotor to the grid. The grid side PWM acts as an inverter that converts the DC voltage from the generator to an AC voltage at the desired power frequency. If the DC voltage is assumed to be ideal and ideal PWM modulation, therefor the relationship between line-to-line AC and DC r.m.s. values are given by the equations 4.19 and 4.20 [210].

$$|v_{ac}| = \frac{\sqrt{3}}{2\sqrt{2}} m v_{dc} \tag{4.19}$$

$$v_{dc} i_{dc} + \sqrt{3}\,\mathrm{Re}(v_{ac} i_{ac}^{*}) = 0 \tag{4.20}$$

where v_{dc} and i_{dc} are the direct current (DC) voltage and current respectively, and v_{ac} and i_{ac} are the alternating current (AC) voltage and current respectively. m is the modulation index and it varies between zero and one (i.e. $0 \leq m \geq 1$).

From the equations above, equations 4.19 and 4.20 it is assumed that the converter is a loss-less converter, and the angle of the AC voltage is determined by the PWM converter since it has a very high switching frequency.

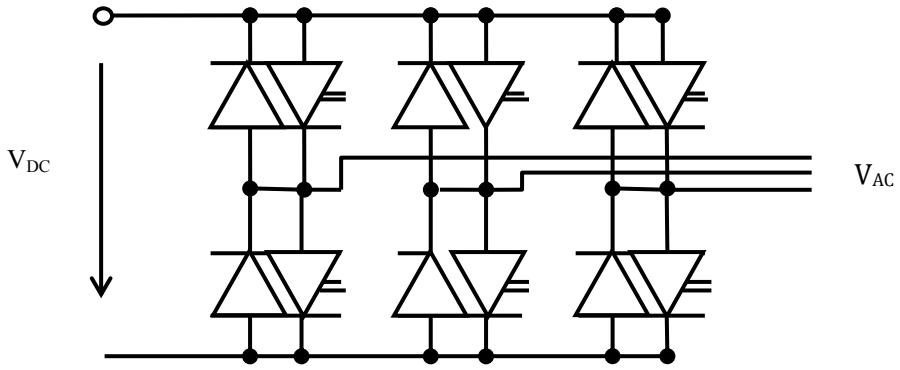

Figure 4.4: PWM converter circuit [210]

Figure 4.5 shows both the generator side converter which operates as a rectifier and the grid side converter which operates as an inverter. The two converters are identical.

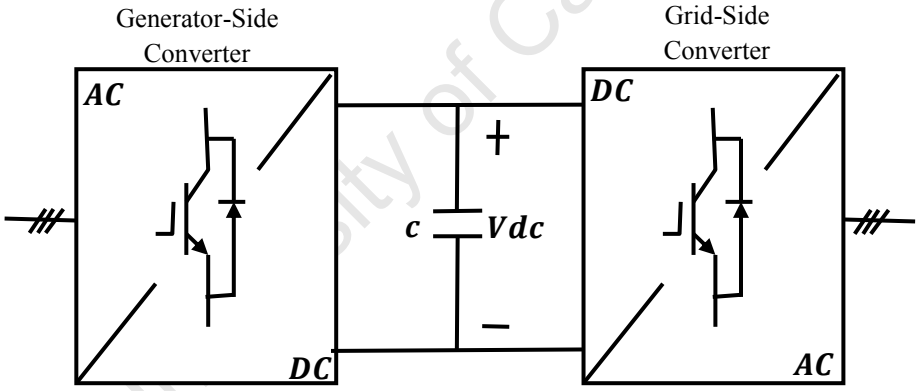

Figure 4.5: Generator side converter and the grid side converter [253]

Diodes can be used for the generator side as a rectifier. A rectifier converts the AC voltage into a DC voltage while the inverter converts the DC voltage into the AC voltage.

4.6.5 Transformers

Transformers can be modeled both as 2-winding and 3-winding transformer using the DIgSILENT library blocks. A 2-winding transformer has a two-port element connecting the power system while a 3-winding transformer has a three-port element connecting the the power system [216]. Most transformers at the generating stations are step-up transformers since bulk power transmission voltage needs to be much higher than generation voltage in order to reduce the bulk of transmission conductors and reduce the line losses. However, transformers at the transmission, sub-transmission and distribution levels are usually step-down transformers. This is to enable effective usage by the customer's equipment. The 2-winding transformer can be found at the generation, transmission and distribution networks while the DFIG wind energy conversion system uses the 3-winding transformer for its grid side connection. In addition, three winding transformers are also used for harmonic suppression in power networks. Please check and write this here. The representation of the positive sequence equivalent diagram for a 3-winding transformer is shown in Figure 4.6.

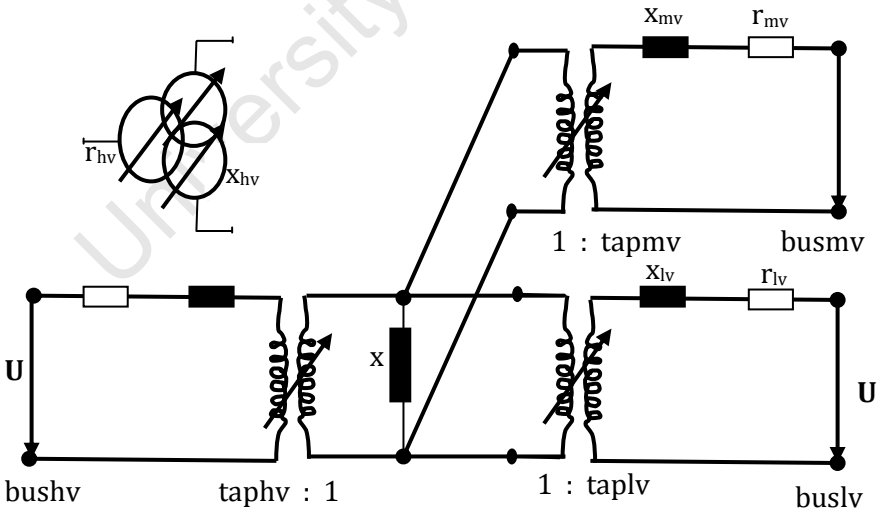

Figure 4.6: Positive sequence 3-windings transformer equivalent model [216]

All the input parameters for the DIgSILENT 3-phase transformer model blocks used the simulation of the test network are adopted from Eskom data. These parameters include MVA rating, voltage levels, copper losses etc.

4.6.6 Grid model

The external grid can be modelled as an ideal symmetrical three-phase voltage source as shown in Figure 4.7. External grid is assumed to be an infinite bus that can supply the network with a constant voltage and power. For the test network, the external grid operates at a constant voltage of 230kV. It is a reference value used for all other generators. The relevant details of the external grid components are listed in Appendix 4.

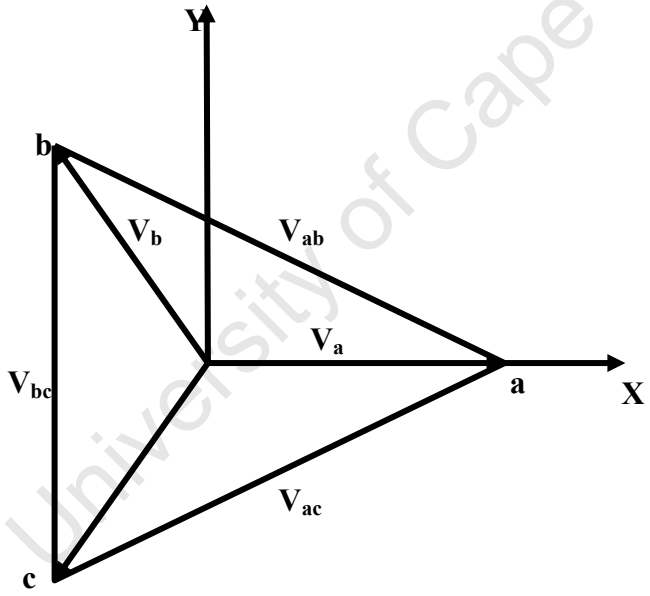

Figure 4.7: Symmetrical three-phase system [218]

A simple power system can be modeled as a source with load and electrical power line. Assuming the load is a PQ represented by *p(1+jk)* with line impedance *(0 + jX)*. Load power is given by *(S =p +jq)* and *I* is the current. E is the voltage supply by the source and V is the voltage at the load [219].

$$V = E - jXI \quad 4.21$$

$$S = \frac{j}{X}(EV\cos\delta + jEV\sin\delta - V^2) \quad 4.22$$

$$p = -\frac{EV}{X}\sin\delta \quad 4.23$$

$$q = -\frac{V^2}{X} + \frac{EV}{X}\cos\delta \quad 4.24$$

Equations 4.21 to 4.24 are based on quasi-steady state, which reduces the power flow equations.

4.6.7 Modeling of grid-connected wind energy conversion system

It is no longer news that grid-connected wind generators are rapidly growing. The total wind installed capacity throughout the world was total at 120.8 GW at the end of 2008 [220]. In July 2008, Department of Energy in the USA indicated that USA may receive 20% of its electrical energy from wind by 2030 [221]. This is likely to have a positive impact on the grid by augmenting the grid generation and by providing ancillary support to the grid. Rapid development in wind energy conversion systems has been marked by different types of wind generation technologies being developed by researchers and manufacturers across the globe. Wind turbine generators can be connected at the low, medium, high or extra-high voltage grid levels and are usually equipped with transformers, power electronic interfaces/controllers and protective devices [222].

The early wind energy conversion systems would consist of the fixed-speed and the variable-speed wind turbine generators. The early fixed-speed wind turbine generators would include a standard squirrel-cage induction generator (SCIG) and a multi-stage gearbox, directly connected to the grid [220]. They are known as constant speed or fixed speed turbine because rotor speed would vary with the amount of power generated and are generally small such as two-percent.

They always consume reactive power and can be compensated by capacitors in order to achieve a power factor close to one.

The variable-speed wind turbine generators can have a geared-drive system or direct-drive system. In a DFIG, the back-to-back voltage source converter feeds the three-phase rotor winding and helps to match the electrical stator and rotor frequency. The direct-drive systems are direct-drive electrical excited synchronous generator (EESG) and drive-drive permanent magnet synchronous generator (PMSG) [220]. The technological roadmap of wind turbine generator systems is shown in Figure 4.8.

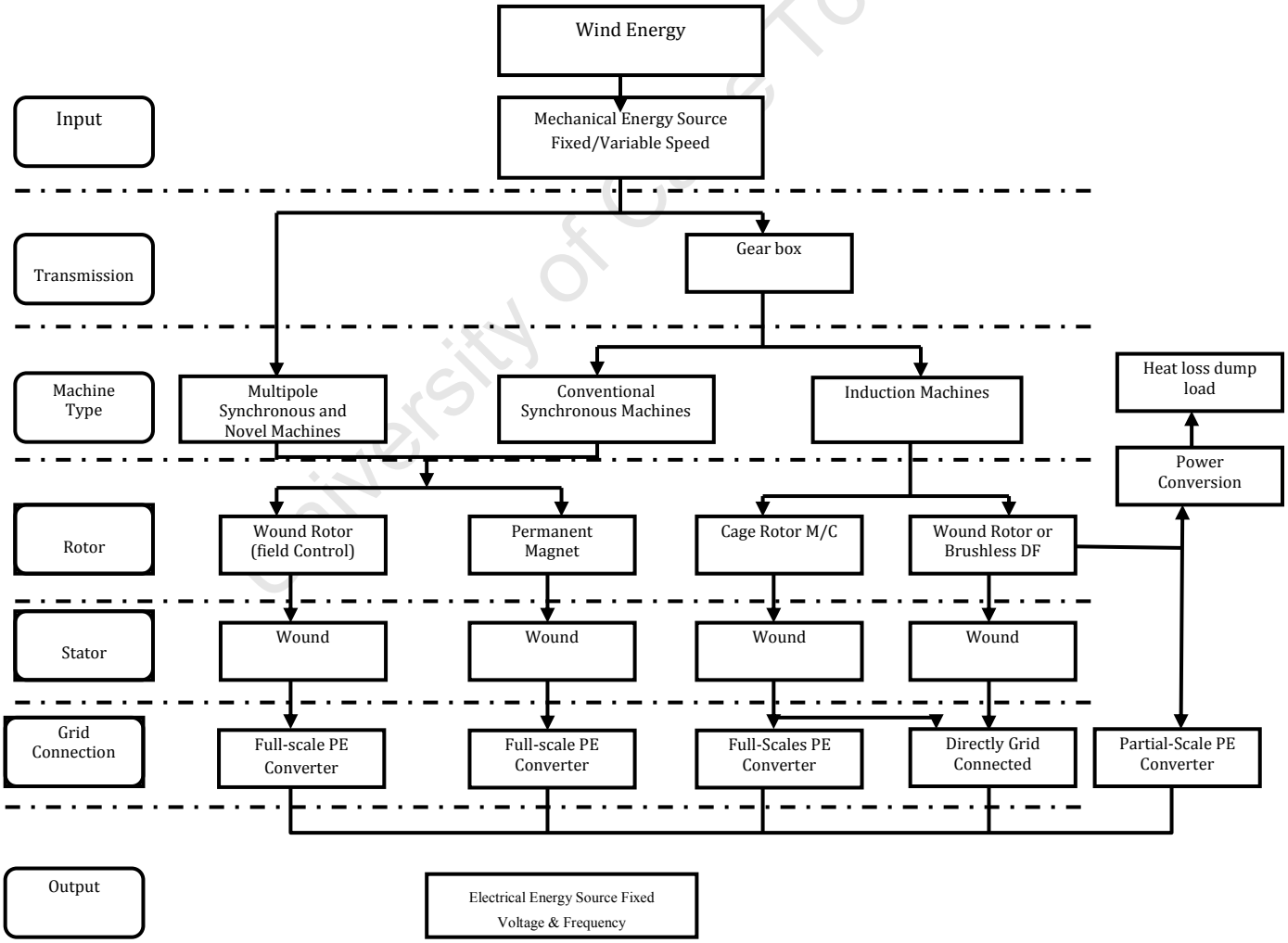

Figure 4.8: Roadmap of wind turbine technologies [223]

The authors of [224], [225], [226] indicated that wind turbines can be classified into four basic types, which include.

- Type 1: Fixed-speed wind turbines
- Type 2: Variable-speed wind turbines
- Type 3: Doubly-fed induction generator (DFIG) wind turbines
- Type 4: Full-converter wind turbines

However, the main technologies of wind generator used are the synchronous generator, asynchronous generator and power electronic converter interface. In addition, the full converter based wind generation systems can be configured with fixed-speed and variable-speed wind generators. Figures 4.9 to 4.11 shows various wind generator technologies [75].

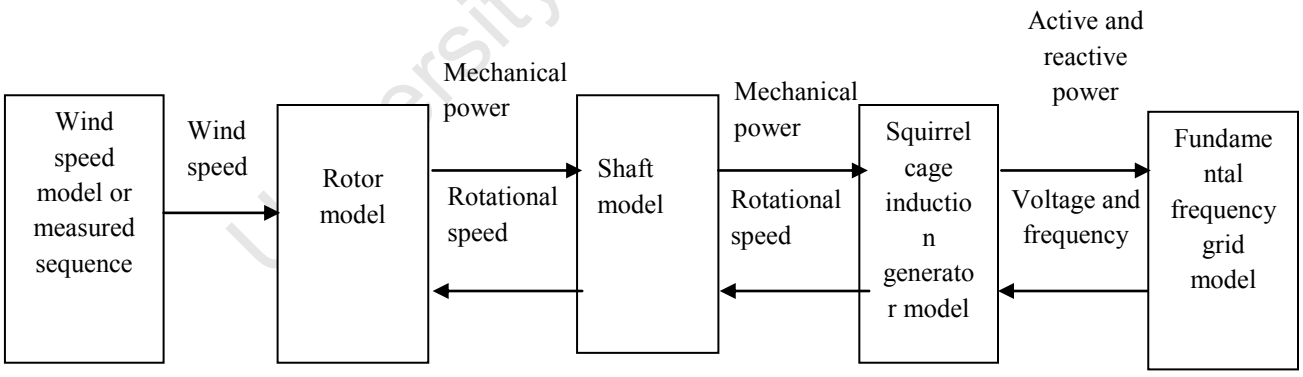

Figure 4.9: Fixed-speed wind turbine model [227]

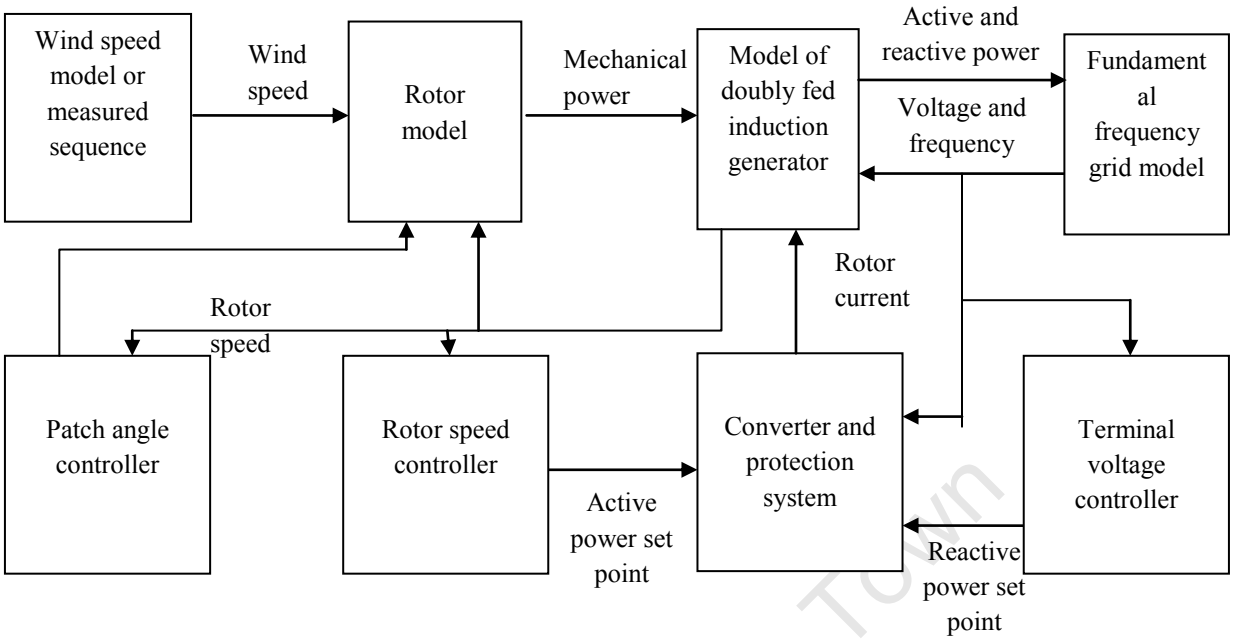

Figure 4.10: Variable-speed wind turbine model [228]

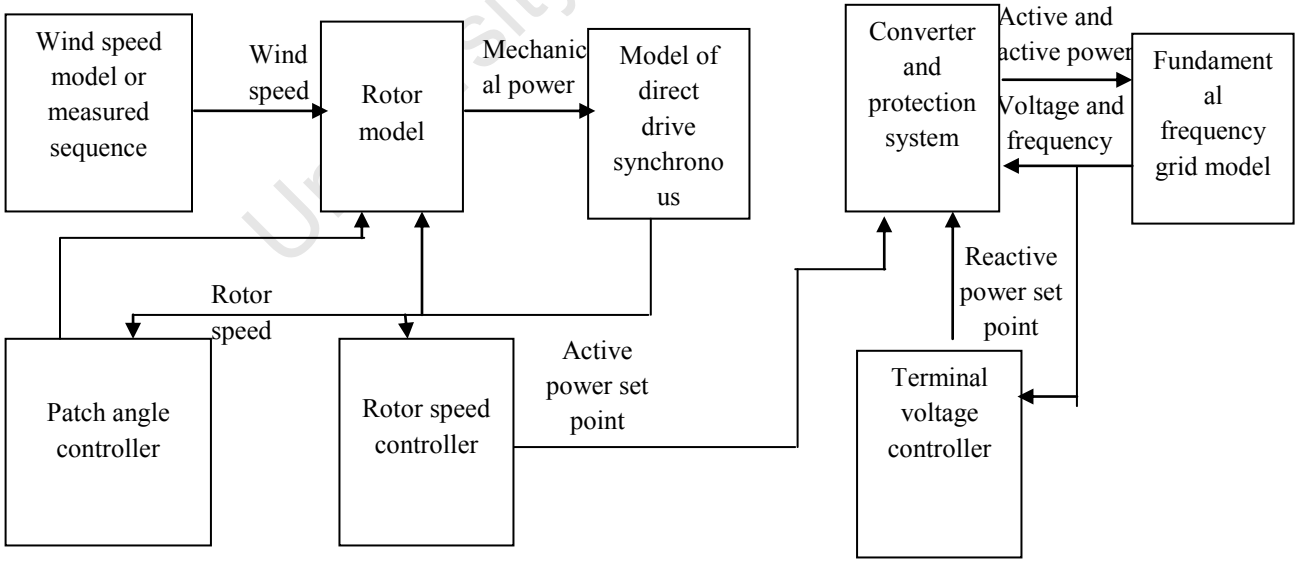

Figure 4.11: Direct drive synchronous wind turbine model [228]

Fixed-speed wind turbines are known as the squirrel cage induction wind turbine or constant speed generator have a very little variation in turbine rotor speed and are usually operated with less than 1% variation in rotor speed while the variable-speed wind turbines are operated at a wide range of rotor speeds. Both the doubly-fed induction generator (DFIG) wind turbines and full-converter wind turbines require power converters to interface the wind turbine and the grid, and this allows independent real and reactive power control [224]. The most widely use grid-connected wind generator is the variable-speed wind turbines this might be as a result of its advantageous characteristics during operation [229].

DIgSILENT provides basic dynamic simulation, and modeling of different wind generator models and the electrical components of the wind-turbine model are present in the DIgSILENT library and are written in the dynamic simulation language DSL of DIgSILENT. These allow the users to create new blocks or modify the existing models [216]. Grid-connected wind distributed generation are characterized with fluctuation as a result of variations of the wind power, and this affects the output power from the generator. Dynamic simulation language DSL provides a realistic simulation and implementation of a control system for wind generators during continuous operation [136]. The most widely used grid-connected wind turbines are modeled and implemented using DIgSILENT PowerFactory for the purposes of this research. The model is based on parameters from a typical South African network, and the specifications are provided in Appendix 4.

4.6.8 Modeling of the wind turbine generator

Wind turbine generator extracts kinetic energy from the wind passing through its blades and converts that into electrical energy in the generator coupled to the turbine. Power produced by the wind turbine generator depends on interaction between the wind-turbine rotor and the wind [230], [231]. This is given by equation 4.25.

$$P = \frac{1}{2} C_p \rho V^3 A \qquad 4.25$$

where ρ is air density, A is area swept area of blades ($A = \pi.R^2$), the rotor power coefficient C_P and V is the wind speed in (m/s) and R the blade radius in [m].

Wind turbine generators are characterized by their Cp - λ curve. The tip-speed ratio λ is the ratio between the linear speed of the tip of the blade to the wind speed and power coefficient C_p [232].

Mathematically the tip-speed ratio λ is expressed as

$$\lambda = \frac{\omega_t R}{V} \tag{4.26}$$

where ω_t (rad/sec) is the turbine speed.

4.6.9 Modeling the mechanical parts of wind turbine generator

The drive train is made up of low-speed shaft, gearbox, high-speed shaft, and wind generator rotor as shown in Figure 4.12 [232]. It is modeled as a series of rigid disks connected through massless shafts [233], [234]. Drive train plays a major role during power fluctuations, and the model is implemented as a DSL model in DIgSILENT [216]. The arrangement of the mass corresponding to the large turbine rotor inertia made up of the blades and the hub while the small inertia representing the rotor mass of the generator [229]. Other parts of the mechanical model arrangement are neglected such as tower and the flap bending modes. The three differential equations that describe the dynamic of the mechanical model are given by equations 4.27, 4.28 and 4.29.

$$\dot{\theta}_{rot} = \omega_{rot} \tag{4.27}$$

$$\dot{\theta}_k = \omega_{rot} - \frac{\omega_{gen}}{n_{gear}} \tag{4.28}$$

$$\dot{\omega}_{rot} = (T_{rot} - T_{shaft}) / J_{rot} \tag{4.29}$$

Equations 4.27 and 4.28 are measured in *rad/s* while equation 4.29 is in *rad/s*^{2}

where $\theta_k = \theta_{rot} - \frac{\theta_{gen}}{n_{gear}}$ is the angular difference between the two ends of the flexible shaft.

The acceleration is given by first-order differential equation in equation 4.30, where J is the total inertia of the equivalent shaft, T_g is the torque from the gearbox, and f is the friction coefficient of the equivalent shaft.

$$J\frac{d\Omega}{dt} = T - T_g - f\Omega_t \tag{4.30}$$

The aerodynamic power from the slow rotating turbine shaft can be increased by the gearbox to a fast rotating shaft through the gear ratio G, which drives the generator at the mechanical speed Ω [229]. This is represented in the equation 4.31 and 4.32. The electromagnetic torque of the generator is given as T_{em}

$$T_{em} = \frac{T_g}{G} \tag{4.31}$$

$$\Omega_t = \frac{\Omega}{G} \tag{4.32}$$

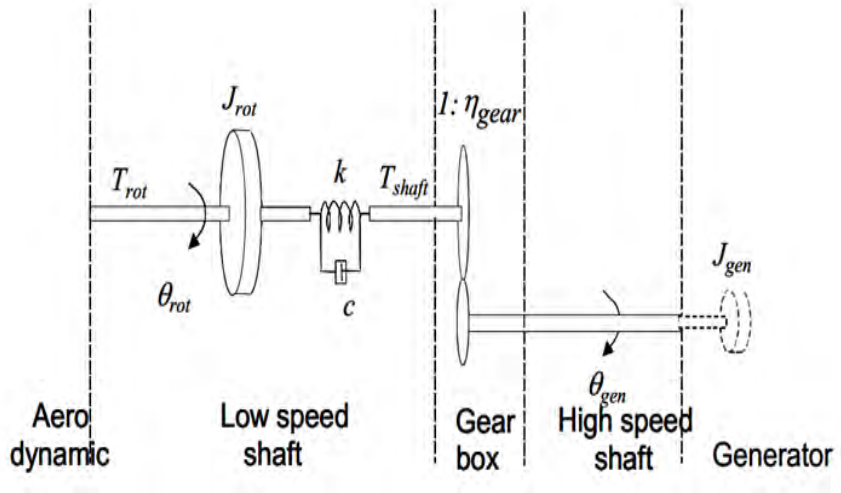

Figure 4.12: Drive train model in DIgSILENT [216].

4.6.10 Static characteristics of a wind turbine generator

The schematic diagram of wind turbine integrated into the power network is shown in Figure 4.13.

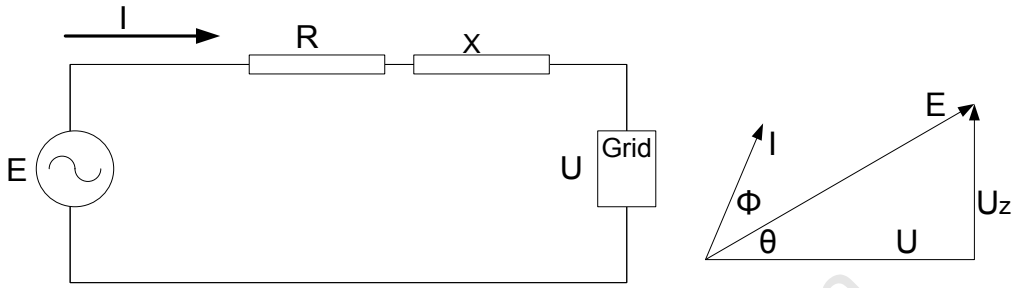

Figure 4.13: Schematic diagram of wind turbine integrating into the power network [235]

E is the voltage phasor at the wind generator terminal, U is the grid voltage phasor, R and X are the resistance and reactance of power line, and I is the current [235].

The grid voltage phasor $\dot{U}$ according to [235] is represented by equation 4.33

$$\dot{U} = E - \frac{PR + QX}{E} - j\frac{PR + QR}{E} \tag{4.33}$$

where P and Q the active and reactive output power

$$U_Z^2 = U^2 + E^2 - 2EU\cos\theta = I^2(R^2 + X^2) \tag{4.34}$$

$$\text{If } \; I^2E^2 = P^2 + Q^2$$

Therefore

$$\frac{P^2 + Q^2}{E^2}(R^2 + X^2) = U^2 + E^2 - 2UE\cos\theta \tag{4.35}$$

From the phasor diagram of Figure 4.13

$$E = U\ \cos\theta + RI\cos\phi - XI\sin\phi \tag{4.36}$$

4.6.11 Modelling the doubly-fed induction generator (DFIG)

The dynamic model of DFIG provided by the DIgSILENT library uses the steady-state parameters and a *d-q* model as given by the differential equations 4.37 and 4.38 as below [216].

$$u_s = R_s i_s - j\omega_{syn}\psi_s + \frac{d}{dt}\psi_s \quad 4.37$$

$$0 = R_r i_r + j(\omega_{syn} - \omega_r)\psi_r + \frac{d}{dt}\psi_r \quad 4.38$$

In the aforesaid equations, *s* is the suffix used stator quantities while *r* is the suffix used in the rotor quantities. *d* - *q* represent the direct and quadrature axis component respectively and *v* is the voltage in (V), R is the resistance in (Ω), while *i* is the current in (A) and ω the stator electrical frequency in (rad/s), ψ the flux linkage (Vs). ω_{syn} is the synchronous speed, while ω_r is the angular speed of the rotor.

Using the generator convention and neglecting the stator transients in a DFIG as shown in equivalent circuits of d and q-axis in Figure 4.14 and Figure 4.15 respectively, the voltage equations can be written as per equations 4.39 and 4.40 [217], [237].

$$v_{ds} = -R_s i_{ds} - \omega_s \varphi_{qs} + \frac{d}{dt}\varphi_{ds} \quad 4.39$$

$$v_{qs} = -R_s i_{qs} + \omega_s \varphi_{ds} + \frac{d}{dt}\varphi_{qs} \quad 4.40$$

$$v_{dr} = -R_r i_{dr} - s\omega_s \varphi_{qr} + \frac{d}{dt}\varphi_{dr} \quad 4.41$$

$$v_{qr} = -R_r i_{qr} + s\omega_s \varphi_{dr} + \frac{d}{dt}\varphi_{qr} \quad 4.42$$

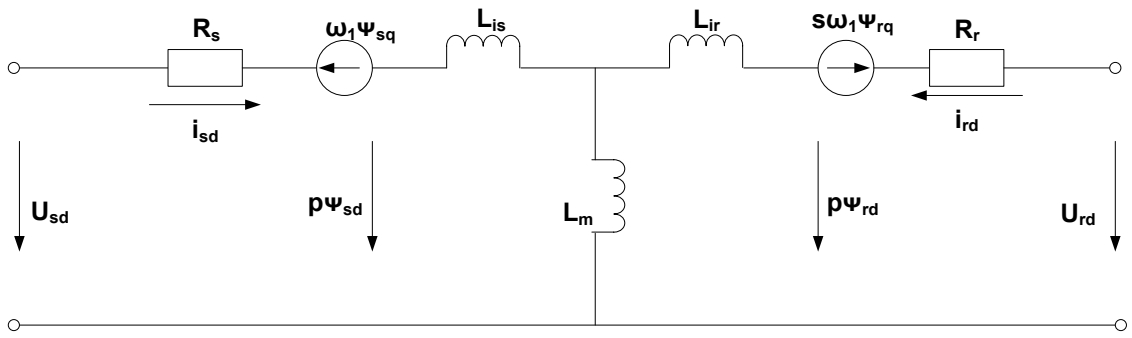

Figure 4.14: *d*-axis equivalent circuits of DFIG in the synchronous reference frame [256]

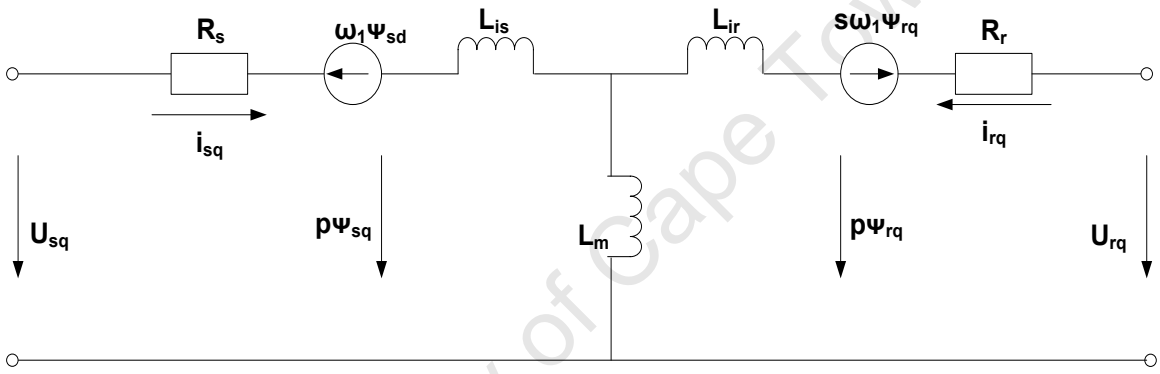

Figure 4.15: *q*-axis equivalent circuits of DFIG in the synchronous reference frame [256]

Equations 4.43, 4.44 and 4.45 indicate the reactive and active power at the rotor and stator of a DFIG generator.

$$Q_r = u_{qr} i_{dr} - u_{dr} i_{qr} \quad 4.43$$

$$P_r = u_{dr} i_{dr} + u_{qr} i_{qr} \quad 4.44$$

$$P_s = u_{ds} i_{ds} + u_{qs} i_{qs} \quad 4.45$$

The mechanical equation for DFIG is given by [216]

$$J\dot{\omega}_r = T_e - T_m \quad 4.46$$

where J is generator inertia, T_e is the electrical torque, T_m is the mechanical torque. The mechanical equation can be rated to the nominal torque T_n.

$$T_n = P_n / [\omega_n (1 - s_n)] \quad 4.47$$

The acceleration time constant is T_{ag}

$$T_{ag} = \frac{J(1 - s_n)\omega_n^2}{P_n} \quad 4.48$$

where ω_n is the nominal electrical angular frequency which is measured in rad/s, and s_n is the nominal slip.

The flux linkage-current relationships are [237], [238]:

$$\psi_{sd} = -L_{ss} i_{sd} - L_m i_{rd} \quad 4.49$$

$$\psi_{sq} = -L_{ss} i_{sq} - L_m i_{rq} \quad 4.50$$

$$\psi_{rd} = -L_m i_{sd} - L_{rr} i_{rd} \quad 4.51$$

$$\psi_{rq} = -L_m i_{sq} - L_{rr} i_{rq} \quad 4.52$$

In the equations above v, i, ψ, R, L and L_m are the voltage, current, flux linkage, winding resistance, leakage inductance and s the mutual inductance respectively. ω is the electrical angular speed, the subscripts 's' and 'r' represent the stator and rotor side while 'd' and 'q' refer to the d-axis and q-axis respectively.

The DFIG systems are usually provided with different controllers such as the current controller, current measurement, active power reduction, pitch control etc. The parameter of some of its controller is given by Eskom [201] and was used in the modeling in PowerFactory. Some of these are shown in Table 4.1 to Table 4.7.

Table 4.1: Speed-Controller parameter

Kptrq : Speed Controller Proportional Gain	1.000000
Kitrq : Speed Controller Integral Gain[1/s]	0.100000
Tpc : Output Limiter Time Constant[s]	0.500000
p_min : Active Power Lower Limit [p.u.]	0.100000
dp_min : dP/dt Lower Limit [p.u./s]	-99.000000
p_max : Active Power Upper Limit [p.u.]	1.100000
dp_max : dP/dt Upper Limit [p.u./s]	99.000000

Table 4.2: Current Controller parameter

Kq : Gain reactive current controller [-]	1.000000
Tq : Integrator time constant reactive current ctrl [s]	0.002000
Kd : Gain active current controller [-]	1.000000
Td : Integrator time constant active current ctrl [s]	0.002000
Tm : Current filter time constant [s]	0.000000

Table 4.3: Current measurement parameter

Urrated : Rated Rotor Voltage [V]	1863.000000
Srated : Rated Apparent Power [kVA]	4000.000000

Table 4.4: Irot-Ctirl parameter

Kd :	0.049600
Td :	0.012800
Kq :	0.049600
Tq :	0.012800

Table 4.5: Active power reduction parameter

fUp : Start of Act. Power Reduction [Hz]	50.200000
fLow : End of Act. Power Reduction [Hz]	50.050000
PHz : Gradient of Act. Power Reduction [%/Hz]	50.000000
Tfilter : PT1-Filter Time Constant [s]	0.010000
negGrad: Neg Gradient for Power Change[p.u./s]	-0.100000
postgrad : Pos Gradient for Power Change[p.u./s]	0.100000

Table 4.6: Pitch Control parameter

Kpp : Blade Angle Controller Gain [p.u.]	150.000000
Kip : Blade Angle Controller Time Constant [s]	25.000000
Tp : Servo Time Constant[s]	0.010000
speed_max	1.200000
beta_min Min. beta[deg]	0.000000
dbeta_min Min. dbeta/dt [deg/s]	-10.000000
beta_max Max. beta [deg]	27.000000
dbeta_max Max. dbeta/dt [deg/s]	10.000000

Table 4.7: Shaft parameter

H	4.020000
Ptbase	2.220000
Pgbase	1.947000
Ktg	80.270000
Dtg	1.500000
ombase	1.745000

4.6.12 Modeling of squirrel cage induction generator (SCIG)

The SCIG is not used in the test network in Figure 4.1; however it was used in the test network in Figure 5.12 to investigate different types of wind energy conversions systems. SCIGs are usually directly connected to power grid and are coupled to the wind turbine through a gear box.

They are operated at a fixed speed because the rotor slip is very small [240]. There are several equivalent circuits that can be used for the parameters of an induction generator model in DIgSILENT. The general equivalent circuit of the SCIG is shown in Figure 4.16, where R_s is the stator winding resistance, X_s is the stator leakage reactance, X_m is the magnetising reactance and Z_{rot} is the rotor impedance.

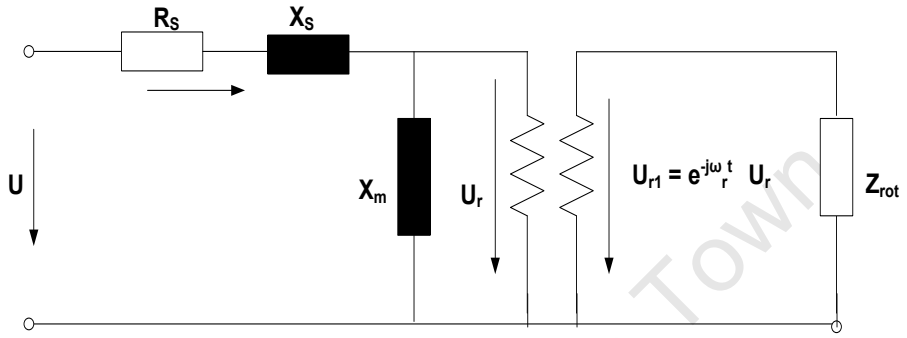

Figure 4.16: The general model equivalent circuit of an induction generator [216]

The wind-turbine generators have the mechanical power of the wind as the prime mover input. This kinetic power obtained from the wind, and the drive train of the wind-turbine generator is given by [240],

$$P = \frac{1}{2} C_P \rho V^3 A \tag{4.53}$$

$$2H_r . \frac{d\omega}{dt} = T_{wt} - T_{mec} - D_r \omega_r \tag{4.54}$$

$$2H_G . \frac{d\omega}{dt} = T_{mec} - T_e - T_G \omega_G \tag{4.55}$$

$$T_{mec} = D_{mec} . (\omega_r - \omega_G) + K_{mec} . \int (\omega_r - \omega_G) dt \tag{4.56}$$

where ρ is air density (kg/m^3)

A denotes the rotor disk area (m^2)

V is wind speed (m/s)

λ is the tip speed ratio of wind turbine θ denotes the pitch angle

C_P is the power coefficient that is nonlinear function of λ and θ

H the inertia constant of wind turbine (s)

H_G the inertia constant of generator (s)

ω_r the rotation speed of wind turbine (m/s)

ω_G the rotor speed of generator (m/s)

e' the internal voltage of induction generator (p.u.)

D_r the damping coefficient of wind turbine

D_G the damping coefficient of generator

D_{mec} the damping coefficient of mechanical coupling

K_{mec} the stiffness of mechanical coupling

T_{wt} the mechanical torque from the wind turbine rotor shaft

T_e the generator electrical torque

T_{mec} the mechanical torque from the generator shaft

The electrical behaviors, dynamic and algebraic model of SCIG wind turbine are represented by equation 4.57 to equation 4.60, and the schematic diagram is shown Figure 4.17.

$$\frac{de'_d}{dt} = \frac{1}{T'_o}.(e'_d - (X_s - X'_s).i_{qs}) + s.\omega_s.e'_q \qquad 4.57$$

$$\frac{de'_q}{dt} = \frac{1}{T'_o}.(e'_q - (X_s - X'_s).i_{ds}) - s.\omega_s.e'_q \qquad 4.58$$

$$T_e = \frac{1}{\omega_s}.(e'_d.i_{ds} + e'_q.i_{qs}) \qquad 4.59$$

$$\dot{I}_g = \dot{I}_s - \frac{1}{X_c}\dot{U}_g \qquad 4.60$$

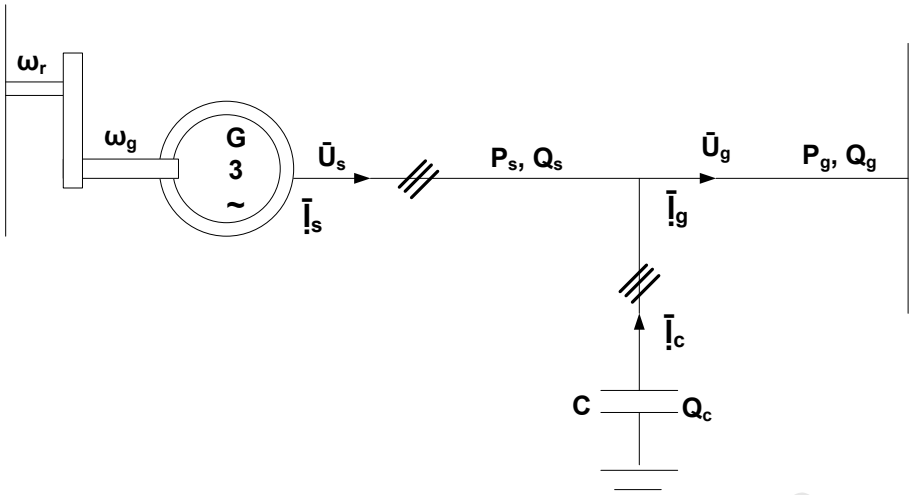

Figure 4.17: Schematic diagram of SCIG [240]

4.6.13 Modeling of grid-connected fully rated static wind generator

Application of power electronic converters in wind turbine technologies has enhanced power quality in regard to voltage regulation, energy storage interface, reactive power, etc. [75]. However, their main disadvantage is that they generate harmonics, which might deteriorate the power quality. In wind turbine generators, the power electronic interface is connected to the rotor of the generator, and the power electronics converters are used to control the steady, dynamic and reactive power flow to and from an electrical generator [241]. It comprises controller models such as current controller, current measurement, and active power reduction, pitch control, etc. The PQ and over-frequency power reduction controllers' parameters are given in Table 4.8 to Table 4.9 for the fully rated converter control of the wind generator.

Table 4.8: PQ Controller parameter for static generator

Kp	: Active Power Control Gain [p.u.]	0.500000
Tp	: Active Power Control Time Constant [s]	0.002000
Kq	: Reactive Power Control Gain [p.u.]	0.500000
Tq	: Reactive Power Control Time Constant [s]	0.020000
Xm	: Magnetizing reactance @Pbase [p.u.]	0.000000
deltaU	: Voltage Dead Band [p.u.]	0.100000

i_EEG : 0 = acc. E.ON; 1 = acc. SDLWindV	1.000000
Tudelay : Voltage Support Delay [s]	0.010000
K_del : Reactive support gain	2.000000
i_max : Combined current limit [p.u.]	1.000000
ramp : Active Power Ramp for e.ON Mode [%/s]	500.000000
u_max : max. allowed internal voltage [p.u.]	1.100000
X : Coupling Reactance [%]	10.000000
id_max : id current limit [p.u.]	1.000000
iq_max : iq current limit [p.u.]	1.000000

Table 4.9: Over-frequency power reduction parameter for static generator

fUp	Start of Act. Power Reduction [Hz]	50.200000
fLow	End of Act. Power Reduction [Hz]	50.050000
PHz	Gradient of Act. Power Reduction [%/Hz]	40.000000
Tfilter	PT1-Filter Time Constant [s]	0.050000
negGrad	Neg Gradient for Power Change [p.u./s]	-0.250000
posGrad	Pos Gradient for Power Change [p.u./s]	0.250000

4.6.14 Modeling of grid-connected hydro distributed generation system

The hydroelectric power plants considered in this thesis are represented by synchronous generators. In a hydroelectric power plant, the hydro turbine converts the kinetic energy of falling water into mechanical energy. The mechanical power produced by the turbine is proportional to the product of the flow rate, the head and the efficiency, as expressed in equation 4.61.

$$P = QH\eta\rho g \qquad 4.61$$

where P is the output power in [W], Q the flow rate [m3/s], and H is the effective head [m], η the overall efficiency, ρ the density of water [kg/m^3], and g the gravitational constant [m/s^2].

The efficiency of the turbine depends upon the turbine characteristics and the fluid flow rate and is defined as the ratio of power delivered at the shaft to the power taken from the flow. The efficiency is usually given as the ratio of power supplied by the turbine (mechanical power transmitted by the turbine shaft) to the absorbed power (hydraulic power equivalent to the measured discharge under the net head) [236].

The turbine efficiency is given by equation 4.62 as below.

$$\eta = \frac{BH\omega}{\gamma Q H_O} = \frac{P}{\gamma Q H_O} \tag{4.62}$$

where P (W) is still the power in, BH (N.m) is the torque, ω (rad/s) is the angular velocity, Q (m^3/s) is the flow rate, Ho is the net head on the turbine and *γ is* the friction coefficient.

The relationship between the turbine dynamics and the generator dynamics is given by equation 4.63.

$$P_m = \frac{n}{\omega_s} m_m \tag{4.63}$$

m_m is the mechanical torque and at synchronous speed $n = \omega_s$ therefore

$$P_m = m_m \tag{4.64}$$

4.6.15 Modeling the grid-connected solar photovoltaic distributed generation system

Solar power just like other renewable-energy resources is a reliable and environment-friendly source of energy nowadays [244]. Grid-connected PV systems are usually modeled as static generators in DIgSILENT and are connected through the inverter to the distribution grid. The inverter that is used is called the DC to AC inverter, and it converts the DC voltage from the PV stored in a battery to AC voltage that is useful for the AC grid. However, in some cases the PV systems are connected to the grid without the present of a storage device such as battery. They are connected through a maximum power point tracker (MPPT) in order to optimize the DC

output power from the PV model [242]. This is shown in Figure 4.18. The inverter also helps the synchronization of the PV system with the grid in voltage and frequency.

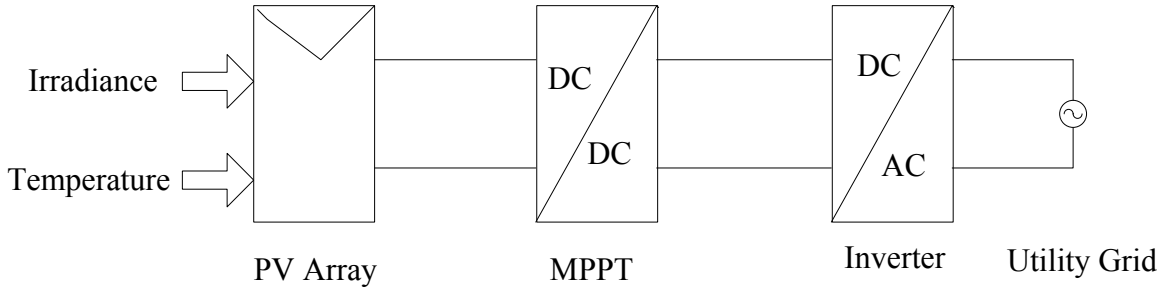

Figure 4.18: Block diagram of grid-connected PV distribution generation [242]

Photovoltaic distributed generation systems do not usually supply electrical power at night; it is likely that loads supply by photovoltaic distributed generation systems might experience a blackout when the sun is not available.

PV systems have poor voltage regulation and low power quality this is due to the absent of inertia constant of the PV systems. They also lack reactive power capability and do not supply reactive power to the grid. However, the inverter within the PV system helps to export or import reactive power and can be modeled as voltage source inverters. [243]

The DIgSILENT library has different element and building block for modeling the photovoltaic generators. This could be a DC current source, DC voltage source or static generator model in the library of DIgSILENT.

In this work, the generic photovoltaic system used contains also a DSL model of the PV cell. There are five photovoltaic distributed generation plants in the power network shown in Figure 4.1. They are connected at different voltage levels at different voltage levels (0.415kV and 22kV). The content of PV plants is made up of photovoltaic model, power measurement, DC busbar , capacitor model, controller and the static generator.

4.6.16 Mathematical model for a photovoltaic module

PV module is a made up of several solar cells connected together either in parallel or in series in other to produce electrical power.

The power produce by a grid-connected solar PV can be calculated using the equation 4.65.

$$P = VI \tag{4.65}$$

In equation 3.76 above P is the power in watts, V the voltage in volts, and I is the current in ampere. Figure 4.19 shows a single mechanism four parameters equivalent circuit.

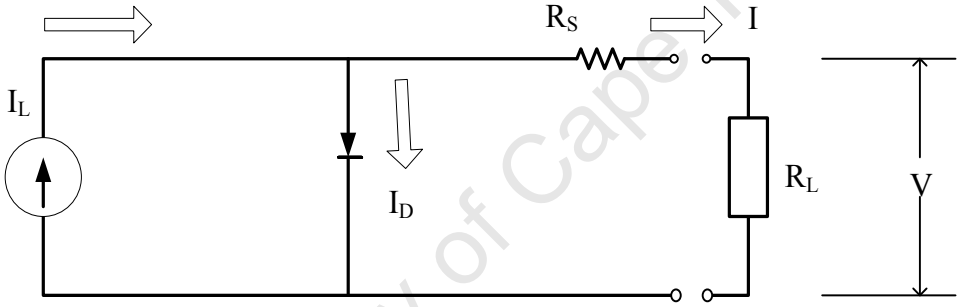

Figure 4.19 : Single mechanism for four-parameter model of solar cell equivalent circuit [244]

The output current I that flow through the load is calculated as the difference between I_L, the light-generated current and I_D is diode or junction current. This is indicated by equation 4.66.

$$I = I_L - I_D \tag{4.66}$$

The light-generated current depends on the impinging radiation, the cell temperature and the materials of the PV cell and is given by

$$I_L = \frac{\Phi}{\Phi_{REF}}(I_{L,REF} + \mu_{ISC}(T_C - T_{C,REF})) \tag{4.67}$$

Where Φ is the irradiance at the new conditions, and Φ_{REF} is irradiance at the reference condition.

$I_{L,REF}$ is light current, in amps, at the reference condition, μ_{ISC} is the manufacturer-supplied temperature coefficient of short circuit current in amps per degree and T_C,$T_{C,REF}$ is the cell temperature at the new and reference conditions and V is the output voltage. Using Shockley equation, for the circuit in Figure 4.19, the current-voltage relationship is given by,

$$I_D = I_O\left[\exp\left(\frac{q(V+IR_S)}{\gamma k T_C}\right)\right]-1 \qquad 4.68$$

where k: Boltzmann's constant t $(1.38 \times 10^{-23}$ J/K); q: Electron charge $(1.602 \times 10^{-19}$ C)
Tc: reference cell operating temperature, R_s : Series resistance of cell (Ω);
V is the voltage across the diode, α, β: Parameters which define Band gap energy of the semiconductor (eV/K2 , K), a is the diode ideality constant.

Where I_O is the saturation current, γ = A x (NCS) and R_S is the series resistance. If we substitute equation 4.68 into equation 4.66 we have equation 4.69

$$I = I_L - I_O\left[\exp\left(\frac{q(V+IR_S)}{\gamma k T_C}\right)\right]-1 \qquad 4.69$$

And I_O depends on temperature is given by

$$I_O = I_{O,R}\left(\frac{T_C}{T_{C,R}}\right)^3 \exp\left[\left(\frac{q\varepsilon_G}{kA}\right)\left(\frac{1}{T_{C,R}}-\frac{1}{T_C}\right)\right] \qquad 4.70$$

4.6.17 PV module and array model

In a grid-connected PV array, the PV array could be made up of several connected PV modules of solar cells connected in series and parallel. This is to increase the output power and achieve the required voltage and current [245]. This can be represented by equation 3.82, and the equation parameters can be obtained from manufacturer's datasheet [242], [246].

$$I = N_{PP} I_L - N_{PP} I_O \left[\exp\left(\frac{V + IR_S\left(\frac{N_{SS}}{N_{PP}}\right)}{V_t a N_{SS}} \right) - 1 \right] - \frac{V + IR_S\left(\frac{N_{SS}}{N_{PP}}\right)}{R_P\left(\frac{N_{SS}}{N_{PP}}\right)} \quad 4.71$$

$V_t = \left(\frac{N_S kT}{q} \right)$ is the thermal voltage of the array (mV);

Where R_S is series resistance, R_P is parallel resistance; a is the diode ideality constant; NPP is the number of PV modules connected in parallel, and N_{SS} is the number of PV modules connected in series. Figure 4.20 shows the mathematical modeled of PV array.

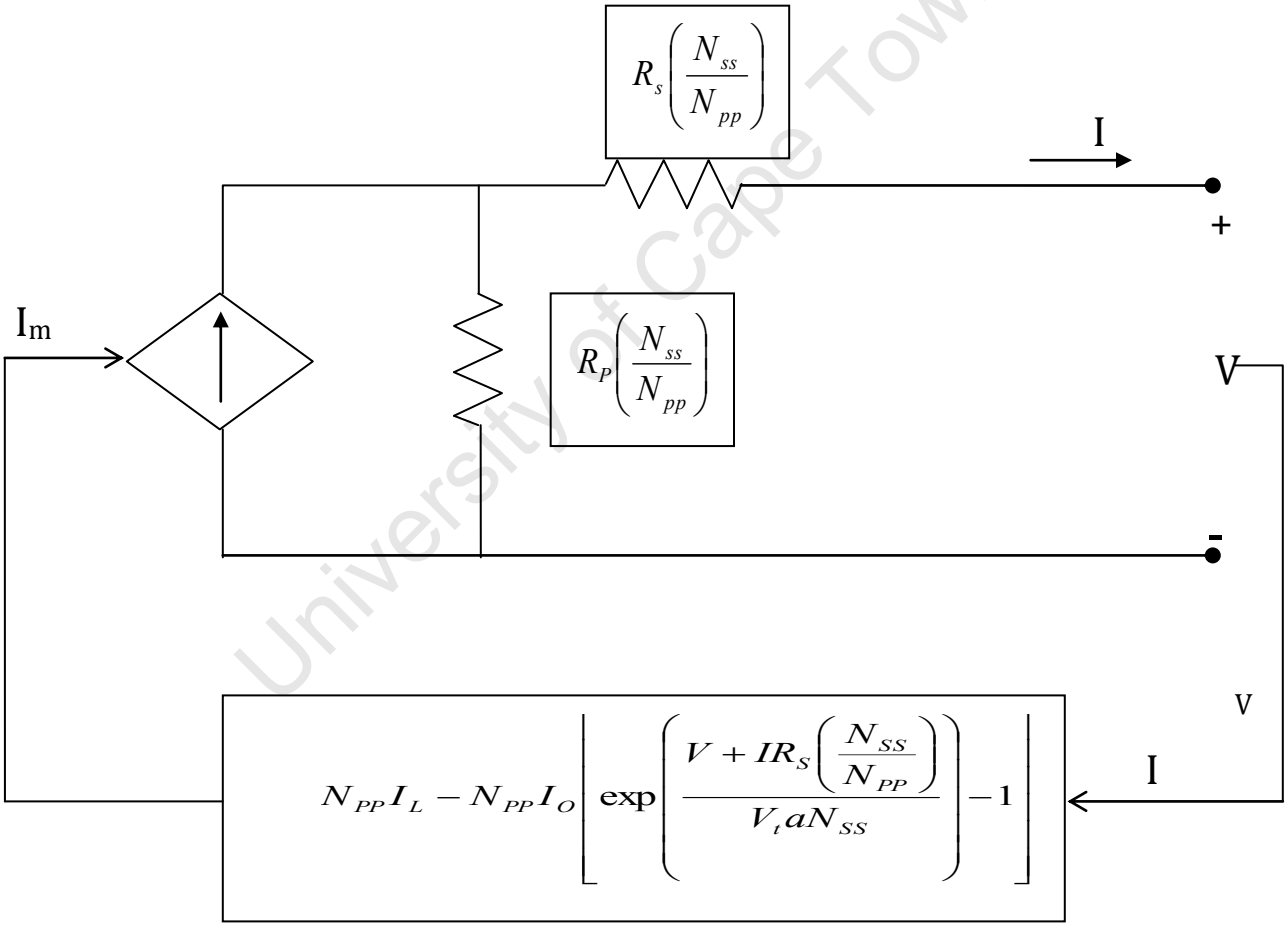

Figure 4.20: PV array mathematical modeling [242]

$$I = N_{PP} I_L - N_{PP} I_O \left[\exp\left(\frac{\frac{V}{N_{SS}} + IR_S\left(\frac{1}{N_{PP}}\right)}{V_t a} \right) - 1 \right] - \frac{V\left(\frac{N_{PP}}{N_{SS}}\right) + IR_S}{R_P} \quad 4.72$$

Assume the parameters in equation 4.72 for ideal condition of solar cell where R_S is very small or 0, and R_P is very large or infinity and a is 1 [239]. Therefore, equation 4.72 can be rewritten as equation 4.73.

$$I = N_{PP} I_L - N_{PP} I_O \left[\exp\left(\frac{V.\frac{1}{N_{SS}}}{V_t} \right) - 1 \right] \quad 4.73$$

The modeling and implementation of grid-connected PV generator are based upon the equations above and can be represented in PowerFactory using the dynamic simulation language DSL of DIgSILENT. This makes it possible for electrical engineers to model elements that are not in the library when the parameters of the generator are known. The PV systems are modeled as a static generator since they are non-rotating generators. A static generator is made up of the PV panels and inverter this could be connected to the grid through the transformer.

Some of the solar PV power plant parameters are given in the Tables 4.10, 4.11 and 4.12 below [201].

Table 4.10: The PV array model definition

Ul0 : Open-circuit Voltage (STC) of Module [V]	43.800000
Umpp0 : MPP Voltage (STC) of Module [V]	35.000000
Impp0 : MPP Current (STC) of Module [A]	4.580000
Ik0 : Short-ciruit Current (STC) of Module [A]	5.000000
au : Temperature correction factor (voltage) [1/K]	-0.003900
ai Temperature correction factor (current) [1/K]	0.000400
nSerialModules Number	20.000000
nParallelModules Number	140.000000
Tr Time Constant of Module [s]	0.000000

Table 4.11: The PV controller parameter

Kp Gain, Active Power PI-Controller [-]	0.005000
Tip Integration Time Constant, Active Power PI-Controller) [s]	0.030000
Tr Measurement Delay [s]	0.001000
Tmpp Time Delay MPP-Tracking [s]	5.000000
Deadband Deadband for AC Voltg. Support [p.u.]	0.100000
Droop Static for AC Voltg. Support [-]	2.000000
i_EEG : 0 = acc. TC2007; 1 = acc. SDLWindV	1.000000
id_min Min. Active Current Limit [p.u.]	0.000000
U_min minimal allowed DC-voltage [V]	333.000000
iq_min Min. Reactive Current Limit [p.u.]	-1.000000
id_max Max. Active Current Limit [p.u.]	1.000000
iq_max Max. Reactive Current Limit [p.u.]	1.000000
maxAbsCur Max. allowed absolute current [p.u.]	1.000000
maxIq Max.abs reactive current in normal operation[p.u.]	1.000000

Table 4.12: DC busbar and capacitor

Capacity of capacitor on DC busbar [s]	0.017200
Udc0 Initial DC-voltage [V]	700.000000
UdcN Nominal DC Voltage [kV]	1.000000
Pnen Rated Power [MW]	0.500000

4.7 Modeling and simulation of voltage dip phenomena

Voltage dip is defined as a short-duration reduction in r.m.s. magnitude of the declared voltage in any or all the three-phases of a power network. It is believed to be one of the most expensive power quality problems which usually lead to equipment damage and loss of revenue. Voltage dip is caused as a result of power system faults, starting of big motors, load variation, energizing of transformers, etc. [36]. Voltage dips are characterized by features such as magnitude, duration, phase-angle jump and shape. Voltage dip magnitude and phase-angle shift

depend on the fault location and line impedance, while the voltage dip duration depends on fault clearing time.

In this work, the causes of voltage dips are simulated in DIgSILENT in the form of power system faults such as three-phase short-circuit (3P) fault, two-phase short-circuit (2P) fault, single phase-to-ground (SLG) fault and two phase-to-ground (2LG) fault in this thesis. Different fault impendences can be selected to produce different types and magnitudes of voltage dip at the fault point [247]. Nominal voltage wave can be modeled by a sinusoidal waveform as shown in equation 4.74. Therefore, voltage dip can be modeled using equation 4.75 as follows [248].

$$u(t) = \sin(\omega t) \qquad 0 \le t < T \tag{4.74}$$

$$u(t) = \begin{cases} (1-\partial)\sin(\omega t) & t_1 \le t \le t_2 \\ \sin(\omega t) & t < t_1, t > t_2 \end{cases} \qquad 0.01s < t_2 - t_1 < 60s \tag{4.75}$$

According to IEEE Std 1159-2009, using the sine-wave voltage, the r.m.s. value is given as equation 1.4 in chapter 1 and renumbered as 4.76 in this chapter.

$$V_{rms} = \sqrt{\frac{1}{N}\sum_{i=1}^{N} v_i^2} \tag{4.76}$$

where N is the number of samples per cycle and v_i is the sampled voltage in time domain.

Theoretical voltage dip can be modeled and calculated using the voltage divider model of Figure 1.11 in chapter 1 and is given by equation 1.1 in chapter 1 but renumbered as 4.77 in this chapter.

$$V_{pcc} = V_{dip} = E_s \frac{Z_f}{Z_s + Z_f} \tag{4.77}$$

where Z_F is the feeder impedance between PCC and the fault point, Z_S is source impedance between the source and pcc and E is the source voltage.

4.8 Steps of extraction of input parameter from the simulation to be used in ANN detector and classifier

In electrical power systems, various types of signal processing techniques such as Least Error Square, Discrete Fourier transforms, etc., have been used for extracting waveform information features. In addition, the root mean square value has been used and applied broadly in power system monitoring, identification and measurement [119]. In this thesis, the root mean square (r.m.s.) value of the basic features and parameters from the simulation of voltage dip (according to IEEE definition of voltage dip) in addition to artificial neural network was used to estimate and monitor the amplitude and duration of voltage dip for detection and classification of voltage dip.

The input to both the ANN detector and classifier are the r.m.s. voltage dip magnitude, dip duration and the phase-angle shift.

Data is collected from DIgSILENT simulation of voltage dip in time domain using the windows clipboard, and it is exported to Microsoft Excel. This data is saved in CSV (comma delimited) format, and the required columns and rows are created for training of ANN in Matlab environment. Table 4.13 below shows sample of voltage dip data for classes Y,X1, X2, S, T, Z1, and Z2.

Table 4.13: Sample of voltage dip data

	S type				**T type**				**X1 type**	
Time	Angle	Magnitude		Time	Angle	Magnitude		Time	Angle	Magnitude
4.851761	-1.7969	0.961443		5.671761	-1.7969	0.961443		3.911761	-1.7969	0.961444
4.861761	-1.7969	0.961443		5.681761	-1.7969	0.961443		3.921761	-1.7969	0.961444
4.871761	-1.7969	0.961443		5.691761	-1.7969	0.961443		3.931761	-1.7969	0.961444
4.881761	-1.7969	0.961443		5.701761	-1.7969	0.961443		3.941761	-1.7969	0.961444
4.891761	-1.7969	0.961443		5.711761	-1.7969	0.961443		3.951761	-1.7969	0.961444
4.901761	-1.7969	0.961443		5.721761	-1.7969	0.961443		3.961761	-1.7969	0.961444
4.911761	-1.7969	0.961443		5.731761	-1.7969	0.961443		3.971761	-1.7969	0.961444
4.921761	-1.7969	0.961443		5.741761	-1.7969	0.961443		3.981761	-1.7969	0.961444
4.931761	-1.7969	0.961443		5.751761	-1.7969	0.961443		3.991761	-26.6991	0.605935
4.941761	-1.7969	0.961443		5.761761	-1.7969	0.961443		4.001761	-26.6974	0.605909
4.951761	-1.7969	0.961443		5.771761	-1.7969	0.961443		4.011761	-26.6948	0.605869
4.961761	-1.7969	0.961443		5.781761	-1.7969	0.961443		4.021761	-26.6923	0.605829
4.971761	-1.7969	0.961443		5.791761	0	0		4.031761	-26.6898	0.60579
4.981761	-1.7969	0.961443		5.801761	0	0		4.041761	-26.6872	0.60575
4.991761	-21.7595	0.621861		5.811761	0	0		4.051761	-26.6847	0.60571
5.001761	-21.7582	0.621838		5.821761	0	0		4.061761	-26.6821	0.605671
5.011761	-21.7563	0.621803		5.831761	0	0		4.071761	-26.6796	0.605631
5.021761	-21.7544	0.621769		5.841761	0	0		4.081761	-26.6775	0.605598
5.031761	-21.7525	0.621734		5.851761	0	0		4.091761	-1.78275	0.960554
5.041761	-21.7506	0.621699		5.861761	0	0		4.101761	-1.78275	0.960554
5.051761	-21.7487	0.621665		5.871761	0	0		4.111761	-1.78275	0.960554
5.061761	-21.7468	0.62163		5.881761	0	0		4.121761	-1.78276	0.960554
5.071761	-21.7449	0.621595		5.891761	0	0		4.131761	-1.78276	0.960555
5.081761	-21.743	0.621561		5.901761	0	0		4.141761	-1.78277	0.960555
5.091761	-21.7411	0.621526		5.911761	0	0		4.151761	-1.78277	0.960555
5.101761	-21.7392	0.621491		5.921761	0	0		4.161761	-1.78278	0.960555
5.111761	-21.7373	0.621457		5.931761	0	0		4.171761	-1.78278	0.960556
5.121761	-21.7354	0.621422		5.941761	0	0		4.181761	-1.78279	0.960556
5.131761	-21.7335	0.621387		5.951761	0	0		4.191761	-1.78279	0.960556
5.141761	-21.7316	0.621353		5.961761	0	0		4.201761	-1.7828	0.960557
5.151761	-21.7296	0.621318		5.971761	0	0		4.211761	-1.7828	0.960557
5.161761	-21.7277	0.621284		5.981761	0	0		4.221761	-1.78281	0.960557
5.171761	-21.7258	0.621249		5.991761	0	0		4.231761	-1.78281	0.960558
5.181761	-21.7239	0.621214		6.001761	0	0		4.241761	-1.78282	0.960558
5.191761	-21.722	0.62118		6.011761	0	0		4.251761	-1.78282	0.960558
5.201761	-21.7201	0.621145		6.021761	0	0		4.261761	-1.78283	0.960558
5.211761	-21.7182	0.621111		6.031761	0	0				

5.221761	-21.7163	0.621076		6.041761	0	0				
5.231761	-21.7144	0.621041		6.051761	0	0				
5.241761	-21.7125	0.621007		6.061761	0	0				
5.251761	-21.7106	0.620972		6.071761	0	0				
5.261761	-21.7087	0.620938		6.081761	0	0				
5.271761	-21.7068	0.620903		6.091761	0	0				
5.281761	-21.7049	0.620869		6.101761	0	0				
5.291761	-21.703	0.620834		6.111761	0	0				
5.301761	-21.7011	0.6208		6.121761	0	0				
5.311761	-21.6992	0.620765		6.131761	0	0				
5.321761	-21.6973	0.62073		6.141761	0	0				
5.331761	-21.6954	0.620696		6.151761	0	0				
5.341761	-21.6935	0.620661		6.161761	0	0				
5.351761	-21.6916	0.620627		6.171761	0	0				
5.361761	-21.6897	0.620592		6.181761	0	0				
5.371761	-21.6878	0.620558		6.191761	0	0				
5.381761	-21.6859	0.620523		6.201761	0	0				
5.391761	-21.684	0.620489		6.211761	0	0				
5.401761	-21.6821	0.620454		6.221761	0	0				
5.411761	-21.6806	0.620426		6.231761	0	0				
5.421761	-1.7436	0.958091		6.241761	0	0				
5.431761	-1.74362	0.958092		6.251761	0	0				
5.441761	-1.74363	0.958093		6.261761	0	0				
5.451761	-1.74365	0.958095		6.271761	0	0				
5.461761	-1.74367	0.958096		6.281761	0	0				
5.471761	-1.74369	0.958097		6.291761	0	0				
5.481761	-1.74371	0.958098		6.301761	0	0				
5.491761	-1.74372	0.958099		6.311761	0	0				
5.501761	-1.74374	0.9581		6.321761	0	0				
5.511761	-1.74376	0.958101		6.331761	-1.84942	0.964746				
5.521761	-1.74378	0.958102		6.341761	-1.8494	0.964745				
5.531761	-1.7438	0.958104		6.351761	-1.84939	0.964744				
5.541761	-1.74381	0.958105		6.361761	-1.84937	0.964743				
5.551761	-1.74383	0.958106		6.371761	-1.84935	0.964742				
5.561761	-1.74385	0.958107		6.381761	-1.84933	0.964741				
5.571761	-1.74387	0.958108		6.391761	-1.84932	0.96474				
5.581761	-1.74388	0.958109		6.401761	-1.8493	0.964738				
5.591761	-1.7439	0.95811		6.411761	-1.84928	0.964737				

	Y type				**Z1 type**				**Z2 type**	
Time	Angle	Magnitude		Time	Angle	Magnitude		Time	Angle	Magnitude
0.31	-1.7969	0.961444		7.361761	-1.7969	0.961443		11.44176	-1.79689	0.961443
0.32	-1.7969	0.961444		7.371761	-1.7969	0.961443		11.45176	-1.79689	0.961443
0.33	-1.7969	0.961444		7.381761	-1.7969	0.961443		11.46176	-1.79689	0.961443
0.34	-1.7969	0.961444		7.391761	-1.7969	0.961443		11.47176	-1.79689	0.961443
0.35	-1.7969	0.961444		7.401761	-1.7969	0.961443		11.48176	-1.79689	0.961443
0.36	-1.7969	0.961444		7.411761	-1.7969	0.961443		11.49176	-1.79689	0.961443
0.37	-1.7969	0.961444		7.421761	-1.7969	0.961443		11.50176	-1.79689	0.961443
0.38	-1.7969	0.961444		7.431761	-1.7969	0.961443		11.51176	-1.79689	0.961443
0.39	-1.7969	0.961444		7.441761	-1.7969	0.961443		11.52176	-1.79689	0.961443
0.4	-1.7969	0.961444		7.451761	-1.7969	0.961443		11.53176	-1.79689	0.961443
0.41	-1.7969	0.961444		7.461761	-1.7969	0.961443		11.54176	-27.7718	0.585366
0.42	-1.7969	0.961444		7.471761	-1.7969	0.961443		11.55176	-27.7702	0.585341
0.43	-1.7969	0.961444		7.481761	-1.7969	0.961443		11.56176	-27.7677	0.585304
0.44	-1.7969	0.961444		7.491761	-13.9396	0.76629		11.57176	-27.7651	0.585268
0.45	-1.7969	0.961444		7.501761	-13.9386	0.766261		11.58176	-27.7626	0.585231
0.46	-1.7969	0.961444		7.511761	-13.9371	0.766219		11.59176	-27.7601	0.585194
0.47	-1.7969	0.961444		7.521761	-13.9357	0.766177		11.60176	-27.7576	0.585157
0.48	-1.7969	0.961444		7.531761	-13.9342	0.766134		11.61176	-27.7551	0.58512
0.49	-1.7969	0.961444		7.541761	-13.9327	0.766092		11.62176	-27.7526	0.585083
0.5	-1.7969	0.961444		7.551761	-13.9312	0.76605		11.63176	-27.7501	0.585047
0.50505	-9.58546	0.803852		7.561761	-13.9298	0.766008		11.64176	-27.7476	0.58501
0.511761	-9.58488	0.803832		7.571761	-13.9283	0.765965		11.65176	-27.7451	0.584973
0.521761	-9.58401	0.803801		7.581761	-13.9268	0.765923		11.66176	-27.7426	0.584936
0.531761	-9.58314	0.80377		7.591761	-13.9254	0.765881		11.67176	-27.7401	0.584899
0.541761	-9.58228	0.80374		7.601761	-13.9239	0.765839		11.68176	-27.7376	0.584863
0.551761	-9.58142	0.803709		7.611761	-13.9224	0.765796		11.69176	-27.7351	0.584826
0.561761	-9.58055	0.803679		7.621761	-13.921	0.765754		11.70176	-27.7325	0.584789
0.571761	-9.57969	0.803648		7.631761	-13.9195	0.765712		11.71176	-27.73	0.584752
0.581761	-9.57882	0.803617		7.641761	-13.9181	0.76567		11.72176	-27.7275	0.584715
0.591761	-9.57796	0.803587		7.651761	-13.9166	0.765628		11.73176	-27.725	0.584679
0.601761	-9.5771	0.803556		7.661761	-13.9151	0.765585		11.74176	-27.7225	0.584642
0.611761	-9.57623	0.803526		7.671761	-13.9137	0.765543		11.75176	-27.72	0.584605
0.621761	-9.57537	0.803495		7.681761	-13.9122	0.765501		11.76176	-27.7175	0.584568
0.631761	-9.57451	0.803465		7.691761	-13.9107	0.765459		11.77176	-27.715	0.584532
0.641761	-9.57365	0.803434		7.701761	-13.9093	0.765417		11.78176	-27.7125	0.584495
0.651761	-9.57278	0.803403		7.711761	-13.9078	0.765375		11.79176	-27.71	0.584458
0.661761	-9.57192	0.803373		7.721761	-13.9063	0.765333		11.80176	-27.7075	0.584421

0.671761	-9.57106	0.803342		7.731761	-13.9049	0.76529		11.81176	-27.705	0.584384
0.681761	-9.5702	0.803312		7.741761	-13.9034	0.765248		11.82176	-27.7025	0.584348
0.691761	-9.56934	0.803281		7.751761	-13.902	0.765206		11.83176	-27.7	0.584311
0.701761	-9.56848	0.803251		7.761761	-13.9005	0.765164		11.84176	-27.6975	0.584274
0.711761	-9.56762	0.80322		7.771761	-13.899	0.765122		11.85176	-27.695	0.584237
0.721761	-9.56675	0.80319		7.781761	-13.8976	0.76508		11.86176	-27.6925	0.584201
0.731761	-9.56589	0.803159		7.791761	-13.8961	0.765038		11.87176	-27.69	0.584164
0.741761	-9.56503	0.803129		7.801761	-13.8947	0.764996		11.88176	-27.6875	0.584127
0.751761	-9.56417	0.803098		7.811761	-13.8932	0.764954		11.89176	-27.685	0.58409
0.761761	-9.56332	0.803068		7.821761	-13.8918	0.764912		11.90176	-27.6825	0.584054
0.771761	-9.56246	0.803038		7.831761	-13.8903	0.76487		11.91176	-27.68	0.584017
0.781761	-9.5616	0.803007		7.841761	-13.8888	0.764828		11.92176	-27.6775	0.58398
0.791761	-9.56074	0.802977		7.851761	-13.8874	0.764786		11.93176	-27.675	0.583943
0.801761	-9.55988	0.802946		7.861761	-13.8859	0.764744		11.94176	-27.6725	0.583907
0.811761	-9.55902	0.802916		7.871761	-13.8845	0.764702		11.95176	-27.67	0.58387
0.821761	-9.55816	0.802885		7.881761	-13.883	0.76466		11.96176	-27.6675	0.583833
0.831761	-9.5573	0.802855		7.891761	-13.8816	0.764618		11.97176	-27.665	0.583796
0.841761	-9.55645	0.802825		7.901761	-13.8801	0.764576		11.98176	-27.6625	0.58376
0.851761	-9.55559	0.802794		7.911761	-13.8786	0.764534		11.99176	-27.66	0.583723
0.861761	-9.55473	0.802764		7.921761	-13.8772	0.764492		12.00176	-27.6575	0.583686
0.871761	-9.55388	0.802734		7.931761	-13.8757	0.76445		12.01176	-27.655	0.583649
0.881761	-9.55302	0.802703		7.941761	-13.8743	0.764408		12.02176	-27.6525	0.583613
0.891761	-9.55216	0.802673		7.951761	-13.8728	0.764366		12.03176	-27.65	0.583576
0.901761	-9.55131	0.802643		7.961761	-13.8714	0.764325		12.04176	-27.6475	0.583539
0.911761	-9.55045	0.802612		7.971761	-13.8699	0.764283		12.05176	-27.645	0.583502
0.921761	-9.54959	0.802582		7.981761	-13.8685	0.764241		12.06176	-27.6425	0.583466
0.931761	-9.54874	0.802552		7.991761	-13.867	0.764199		12.07176	-27.64	0.583429
0.941761	-9.54788	0.802521		8.001761	-13.8656	0.764157		12.08176	-27.6375	0.583392
0.951761	-9.54703	0.802491		8.011761	-13.8641	0.764115		12.09176	-27.635	0.583356
0.961761	-9.54617	0.802461		8.021761	-13.8627	0.764073		12.10176	-27.6325	0.583319
0.971761	-9.54532	0.80243		8.031761	-13.8612	0.764032		12.11176	-27.63	0.583282
0.981761	-9.54446	0.8024		8.041761	-13.8598	0.76399		12.12176	-27.6275	0.583245
0.991761	-9.54361	0.80237		8.051761	-13.8583	0.763948		12.13176	-27.625	0.583209
1	-9.54291	0.802345		8.061761	-13.8569	0.763906		12.14176	-27.6225	0.583172
1.00505	-9.54248	0.80233		8.071761	-13.8554	0.763864		12.15176	-27.62	0.583135
1.011761	-9.5419	0.802309		8.081761	-13.854	0.763823		12.16176	-27.6175	0.583099
1.021761	-9.54105	0.802279		8.091761	-13.8525	0.763781		12.17176	-27.615	0.583062
1.031761	-9.5402	0.802249		8.101761	-13.8511	0.763739		12.18176	-27.6125	0.583025
1.041761	-9.53934	0.802219		8.111761	-13.8496	0.763697		12.19176	-27.61	0.582988
1.051761	-9.53849	0.802188		8.121761	-13.8482	0.763656		12.20176	-27.6075	0.582952
1.061761	-9.53764	0.802158		8.131761	-13.8467	0.763614		12.21176	-27.605	0.582915

1.071761	-9.53679	0.802128		8.141761	-13.8453	0.763572		12.22176	-27.6025	0.582878
1.081761	-9.53593	0.802098		8.151761	-13.8438	0.76353		12.23176	-27.6	0.582842
1.091761	-9.53508	0.802068		8.161761	-13.8424	0.763489		12.24176	-27.5975	0.582805
1.101761	-9.53423	0.802038		8.171761	-13.8409	0.763447		12.25176	-27.595	0.582768
1.111761	-9.53338	0.802007		8.181761	-13.8395	0.763405		12.26176	-27.5925	0.582732
1.121761	-9.53253	0.801977		8.191761	-13.838	0.763364		12.27176	-27.59	0.582695
1.131761	-9.53168	0.801947		8.201761	-13.8366	0.763322		12.28176	-27.5875	0.582658
1.141761	-9.53083	0.801917		8.211761	-13.8352	0.76328		12.29176	-27.585	0.582622
1.151761	-9.52997	0.801887		8.221761	-13.8337	0.763239		12.30176	-27.5825	0.582585
1.161761	-9.52912	0.801857		8.231761	-13.8323	0.763197		12.31176	-27.58	0.582548
1.171761	-9.52827	0.801827		8.241761	-13.8308	0.763155		12.32176	-27.5776	0.582512
1.181761	-9.52742	0.801796		8.251761	-13.8294	0.763114		12.33176	-27.5751	0.582475
1.191761	-9.52658	0.801766		8.261761	-13.8279	0.763072		12.34176	-27.5726	0.582438
1.201761	-9.52573	0.801736		8.271761	-13.8265	0.763031		12.35176	-27.5701	0.582402
1.211761	-9.52488	0.801706		8.281761	-13.825	0.762989		12.36176	-27.5676	0.582365
1.221761	-9.52403	0.801676		8.291761	-13.8236	0.762947		12.37176	-27.5651	0.582328
1.231761	-9.52318	0.801646		8.301761	-13.8222	0.762906		12.38176	-27.5626	0.582292
1.241761	-9.52233	0.801616		8.311761	-13.8207	0.762864		12.39176	-27.5601	0.582255
1.251761	-9.52148	0.801586		8.321761	-13.8193	0.762823		12.40176	-27.5576	0.582218
1.261761	-9.52064	0.801556		8.331761	-13.8178	0.762781		12.41176	-27.5551	0.582182
1.271761	-9.51979	0.801526		8.341761	-13.8164	0.76274		12.42176	-27.5526	0.582145
1.281761	-9.51894	0.801496		8.351761	-13.815	0.762698		12.43176	-27.5501	0.582108
1.291761	-9.51809	0.801466		8.361761	-13.8135	0.762657		12.44176	-27.5476	0.582072
1.301761	-9.51725	0.801436		8.371761	-13.8121	0.762615		12.45176	-27.5452	0.582035
1.311761	-9.5164	0.801406		8.381761	-13.8106	0.762574		12.46176	-27.5427	0.581998
1.321761	-9.51555	0.801376		8.391761	-13.8092	0.762532		12.47176	-27.5402	0.581962
1.331761	-9.51471	0.801346		8.401761	-13.8078	0.762491		12.48176	-27.5377	0.581925
1.341761	-9.51386	0.801316		8.411761	-13.8063	0.762449		12.49176	-27.5352	0.581888
1.351761	-9.51301	0.801286		8.421761	-13.8049	0.762408		12.50176	-27.5327	0.581852
1.361761	-9.51217	0.801256		8.431761	-13.8035	0.762366		12.51176	-27.5302	0.581815
1.371761	-9.51132	0.801226		8.441761	-13.802	0.762325		12.52176	-27.5277	0.581778
1.381761	-9.51048	0.801196		8.451761	-13.8006	0.762284		12.53176	-27.5252	0.581742
1.391761	-9.50963	0.801166		8.461761	-13.7991	0.762242		12.54176	-27.5227	0.581705
1.401761	-9.50879	0.801136		8.471761	-13.7977	0.762201		12.55176	-27.5203	0.581669
1.411761	-9.50794	0.801106		8.481761	-13.7963	0.762159		12.56176	-27.5178	0.581632
1.421761	-9.5071	0.801076		8.491761	-13.7948	0.762118		12.57176	-27.5153	0.581595
1.431761	-9.50626	0.801046		8.501761	-13.7934	0.762077		12.58176	-27.5128	0.581559
1.441761	-9.50541	0.801016		8.511761	-13.792	0.762035		12.59176	-27.5103	0.581522
1.451761	-9.50457	0.800987		8.521761	-13.7905	0.761994		12.60176	-27.5078	0.581485
1.461761	-9.50373	0.800957		8.531761	-13.7891	0.761953		12.61176	-27.5053	0.581449
1.471761	-9.50288	0.800927		8.541761	-13.7877	0.761911		12.62176	-27.5028	0.581412

1.481761	-9.50204	0.800897		8.551761	-13.7862	0.76187		12.63176	-27.5004	0.581376
1.491761	-9.5012	0.800867		8.561761	-13.7848	0.761829		12.64176	-27.4979	0.581339
1.501761	-9.50036	0.800837		8.571761	-13.7834	0.761787		12.65176	-27.4954	0.581302
1.511761	-9.49951	0.800807		8.581761	-13.7819	0.761746		12.66176	-27.4929	0.581266
1.521761	-9.49867	0.800778		8.591761	-13.7805	0.761705		12.67176	-27.4904	0.581229
1.531761	-9.49783	0.800748		8.601761	-13.7791	0.761663		12.68176	-27.4879	0.581193
1.541761	-9.49699	0.800718		8.611761	-13.7777	0.761622		12.69176	-27.4854	0.581156
1.551761	-9.49615	0.800688		8.621761	-13.7762	0.761581		12.70176	-27.483	0.581119
1.561761	-9.49531	0.800658		8.631761	-13.7748	0.76154		12.71176	-27.4805	0.581083
1.571761	-9.49447	0.800628		8.641761	-13.7734	0.761498		12.72176	-27.478	0.581046
1.58	-9.49377	0.800604		8.651761	-13.7719	0.761457		12.73176	-27.4755	0.58101
1.58505	-9.49335	0.800589		8.661761	-13.7705	0.761416		12.74176	-27.473	0.580973
1.591761	-9.49279	0.800569		8.671761	-13.7691	0.761375		12.75176	-27.4705	0.580936
1.601761	-9.49195	0.800539		8.681761	-13.7676	0.761334		12.76176	-27.4681	0.5809
1.611761	-9.49111	0.800509		8.691761	-13.7662	0.761292		12.77176	-27.4656	0.580863
1.621761	-9.49027	0.80048		8.701761	-13.7648	0.761251		12.78176	-27.4631	0.580827
1.631761	-9.48943	0.80045		8.711761	-13.7634	0.76121		12.79176	-27.4606	0.58079
1.641761	-9.48859	0.80042		8.721761	-13.7619	0.761169		12.80176	-27.4581	0.580754
1.651761	-9.48775	0.80039		8.731761	-13.7605	0.761128		12.81176	-27.4556	0.580717
1.661761	-9.48691	0.800361		8.741761	-13.7591	0.761087		12.82176	-27.4532	0.58068
1.671761	-9.48607	0.800331		8.751761	-13.7577	0.761045		12.83176	-27.4507	0.580644
1.681761	-9.48523	0.800301		8.761761	-13.7562	0.761004		12.84176	-27.4482	0.580607
1.691761	-9.4844	0.800272		8.771761	-13.7548	0.760963		12.85176	-27.4457	0.580571
1.701761	-9.48356	0.800242		8.781761	-13.7534	0.760922		12.86176	-27.4432	0.580534
1.711761	-9.48272	0.800212		8.791761	-13.752	0.760881		12.87176	-27.4407	0.580498
1.721761	-9.48188	0.800182		8.801761	-13.7505	0.76084		12.88176	-27.4383	0.580461
1.731761	-9.48105	0.800153		8.811761	-13.7491	0.760799		12.89176	-27.4358	0.580425
1.741761	-9.48021	0.800123		8.821761	-13.7477	0.760758		12.90176	-27.4333	0.580388
1.751761	-9.47937	0.800094		8.831761	-13.7463	0.760717		12.91176	-27.4308	0.580351
1.761761	-9.47854	0.800064		8.841761	-13.7448	0.760676		12.92176	-27.4283	0.580315
1.771761	-9.4777	0.800034		8.851761	-13.7434	0.760635		12.93176	-27.4259	0.580278
1.781761	-9.47687	0.800005		8.861761	-13.742	0.760594		12.94176	-27.4234	0.580242
1.791761	-9.47603	0.799975		8.871761	-13.7406	0.760553		12.95176	-27.4209	0.580205
1.801761	-9.4752	0.799945		8.881761	-13.7392	0.760512		12.96176	-27.4184	0.580169
1.811761	-9.47436	0.799916		8.891761	-13.7377	0.760471		12.97176	-27.4159	0.580132
1.821761	-9.47353	0.799886		8.901761	-13.7363	0.76043		12.98176	-27.4135	0.580096
1.831761	-9.47269	0.799857		8.911761	-13.7349	0.760389		12.99176	-27.411	0.580059
1.841761	-9.47186	0.799827		8.921761	-13.7335	0.760348		13.00176	-27.4085	0.580023
1.851761	-9.47102	0.799797		8.931761	-13.7321	0.760307		13.01176	-27.406	0.579986
1.861761	-9.47019	0.799768		8.941761	-13.7306	0.760266		13.02176	-27.4035	0.57995
1.871761	-9.46935	0.799738		8.951761	-13.7292	0.760225		13.03176	-27.4011	0.579913

1.881761	-9.46852	0.799709		8.961761	-13.7278	0.760184		13.04176	-27.3986	0.579877
1.891761	-9.46769	0.799679		8.971761	-13.7264	0.760143		13.05176	-27.3961	0.57984
1.901761	-9.46685	0.79965		8.981761	-13.725	0.760102		13.06176	-27.3936	0.579804
1.911761	-9.46602	0.79962		8.991761	-13.7235	0.760061		13.07176	-27.3912	0.579767
1.921761	-9.46519	0.799591		9.001761	-13.7221	0.76002		13.08176	-27.3887	0.57973
1.931761	-9.46436	0.799561		9.011761	-13.7207	0.759979		13.09176	-27.3862	0.579694
1.941761	-9.46352	0.799532		9.021761	-13.7193	0.759939		13.10176	-27.3837	0.579657
1.951761	-9.46269	0.799502		9.031761	-13.7179	0.759898		13.11176	-27.3813	0.579621
1.961761	-9.46186	0.799473		9.041761	-13.7165	0.759857		13.12176	-27.3788	0.579584
1.971761	-9.46103	0.799443		9.051761	-13.7151	0.759816		13.13176	-27.3763	0.579548
1.981761	-9.4602	0.799414		9.061761	-13.7136	0.759775		13.14176	-27.3738	0.579511
1.991761	-9.45937	0.799384		9.071761	-13.7122	0.759734		13.15176	-27.3714	0.579475
2.001761	-9.45854	0.799355		9.081761	-13.7108	0.759694		13.16176	-27.3689	0.579438
2.011761	-9.45771	0.799325		9.091761	-13.7094	0.759653		13.17176	-27.3664	0.579402
2.021761	-9.45688	0.799296		9.101761	-13.708	0.759612		13.18176	-27.3639	0.579366
2.031761	-9.45605	0.799267		9.111761	-13.7066	0.759571		13.19176	-27.3615	0.579329
2.041761	-9.45522	0.799237		9.121761	-13.7052	0.75953		13.20176	-27.359	0.579293
2.051761	-9.45439	0.799208		9.131761	-13.7037	0.75949		13.21176	-27.3565	0.579256
2.061761	-9.45356	0.799178		9.141761	-13.7023	0.759449		13.22176	-27.354	0.57922
2.071761	-9.45273	0.799149		9.151761	-13.7009	0.759408		13.23176	-27.3516	0.579183
2.081761	-9.4519	0.79912		9.161761	-13.6995	0.759367		13.24176	-27.3491	0.579147
2.091761	-9.45107	0.79909		9.171761	-13.6981	0.759327		13.25176	-27.3466	0.57911
2.101761	-9.45024	0.799061		9.181761	-13.6967	0.759286		13.26176	-27.3441	0.579074
2.111761	-9.44941	0.799031		9.191761	-13.6953	0.759245		13.27176	-27.3417	0.579037
2.121761	-9.44859	0.799002		9.201761	-13.6939	0.759205		13.28176	-27.3392	0.579001
2.131761	-9.44776	0.798973		9.211761	-13.6925	0.759164		13.29176	-27.3367	0.578964
2.141761	-9.44693	0.798943		9.221761	-13.691	0.759123		13.30176	-27.3343	0.578928
2.151761	-9.4461	0.798914		9.231761	-13.6896	0.759083		13.31176	-27.3318	0.578891
2.161761	-9.44528	0.798885		9.241761	-13.6882	0.759042		13.32176	-27.3293	0.578855
2.171761	-9.44445	0.798855		9.251761	-13.6868	0.759001		13.33176	-27.3268	0.578819
2.181761	-9.44362	0.798826		9.261761	-13.6854	0.758961		13.34176	-27.3244	0.578782
2.191761	-9.4428	0.798797		9.271761	-13.684	0.75892		13.35176	-27.3219	0.578746
2.201761	-9.44197	0.798768		9.281761	-13.6826	0.758879		13.36176	-27.3194	0.578709
2.211761	-9.44115	0.798738		9.291761	-13.6812	0.758839		13.37176	-27.317	0.578673
2.221761	-9.44032	0.798709		9.301761	-13.6798	0.758798		13.38176	-27.3145	0.578636
2.231761	-9.43949	0.79868		9.311761	-13.6784	0.758758		13.39176	-27.312	0.5786
2.241761	-9.43867	0.798651		9.321761	-13.677	0.758717		13.40176	-27.3096	0.578563
2.251761	-9.43784	0.798621		9.331761	-13.6756	0.758676		13.41176	-27.3071	0.578527
2.261761	-9.43702	0.798592		9.341761	-13.6742	0.758636		13.42176	-27.3046	0.578491
2.271761	-9.43619	0.798563		9.351761	-13.6728	0.758595		13.43176	-27.3022	0.578454
2.281761	-9.43537	0.798534		9.361761	-13.6714	0.758555		13.44176	-27.2997	0.578418

2.291761	-9.43455	0.798504		9.371761	-13.67	0.758514		13.45176	-27.2972	0.578381
2.301761	-9.43372	0.798475		9.381761	-13.6685	0.758474		13.46176	-27.2947	0.578345
2.311761	-9.4329	0.798446		9.391761	-13.6671	0.758433		13.47176	-27.2923	0.578309
2.321761	-9.43208	0.798417		9.401761	-13.6657	0.758393		13.48176	-27.2898	0.578272
2.331761	-9.43125	0.798388		9.411761	-13.6643	0.758352		13.49176	-27.2873	0.578236
2.341761	-9.43043	0.798358		9.421761	-13.6629	0.758312		13.50176	-27.2849	0.578199
2.351761	-9.42961	0.798329		9.431761	-13.6615	0.758271		13.51176	-27.2824	0.578163
2.361761	-9.42878	0.7983		9.441761	-13.6601	0.758231		13.52176	-27.2799	0.578126
2.371761	-9.42796	0.798271		9.451761	-13.6587	0.75819		13.53176	-27.2775	0.57809
2.381761	-9.42714	0.798242		9.461761	-13.6573	0.75815		13.54176	-27.275	0.578054
2.391761	-9.42632	0.798213		9.471761	-13.6559	0.758109		13.55176	-27.2725	0.578017
2.401761	-9.4255	0.798184		9.481761	-13.6545	0.758069		13.56176	-27.2701	0.577981
2.411761	-9.42468	0.798154		9.491761	-13.6531	0.758029		13.57176	-27.2676	0.577945
2.421761	-9.42386	0.798125		9.501761	-13.6517	0.757988		13.58176	-27.2652	0.577908
2.431761	-9.42303	0.798096		9.511761	-13.6503	0.757948		13.59176	-27.2627	0.577872
2.441761	-9.42221	0.798067		9.521761	-13.6489	0.757907		13.60176	-27.2602	0.577835
2.451761	-9.42139	0.798038		9.531761	-13.6475	0.757867		13.61176	-27.2578	0.577799
2.461761	-9.42057	0.798009		9.541761	-13.6461	0.757827		13.62176	-27.2553	0.577763
2.471761	-9.41975	0.79798		9.551761	-13.6447	0.757786		13.63176	-27.2528	0.577726
2.481761	-9.41893	0.797951		9.561761	-13.6433	0.757746		13.64176	-27.2504	0.57769
2.491761	-9.41811	0.797922		9.571761	-13.6419	0.757706		13.65176	-27.2479	0.577653
2.501761	-9.4173	0.797893		9.581761	-13.6406	0.757665		13.66176	-27.2454	0.577617
2.511761	-9.41648	0.797864		9.591761	-13.6392	0.757625		13.67176	-27.243	0.577581
2.521761	-9.41566	0.797835		9.601761	-13.6378	0.757585		13.68176	-27.2405	0.577544
2.531761	-9.41484	0.797806		9.611761	-13.6364	0.757544		13.69176	-27.2381	0.577508
2.541761	-9.41402	0.797777		9.621761	-13.635	0.757504		13.70176	-27.2356	0.577472
2.551761	-9.4132	0.797748		9.631761	-13.6336	0.757464		13.71176	-27.2331	0.577435
2.561761	-9.41238	0.797719		9.641761	-13.6322	0.757424		13.72176	-27.2307	0.577399
2.571761	-9.41157	0.79769		9.651761	-13.6308	0.757383		13.73176	-27.2282	0.577363
2.581761	-9.41075	0.797661		9.661761	-13.6294	0.757343		13.74176	-27.2258	0.577326
2.591761	-9.40993	0.797632		9.671761	-13.628	0.757303		13.75176	-27.2233	0.57729
2.601761	-9.40912	0.797603		9.681761	-13.6266	0.757263		13.76176	-27.2208	0.577254
2.611761	-9.4083	0.797574		9.691761	-13.6252	0.757222		13.77176	-27.2184	0.577217
2.621761	-9.40748	0.797545		9.701761	-13.6238	0.757182		13.78176	-27.2159	0.577181
2.631761	-9.40667	0.797516		9.711761	-13.6224	0.757142		13.79176	-27.2135	0.577145
2.641761	-9.40585	0.797487		9.721761	-13.621	0.757102		13.80176	-27.211	0.577108
2.651761	-9.40503	0.797458		9.731761	-13.6196	0.757062		13.81176	-27.2085	0.577072
2.661761	-9.40422	0.797429		9.741761	-13.6183	0.757021		13.82176	-27.2061	0.577036
2.671761	-9.4034	0.7974		9.751761	-13.6169	0.756981		13.83176	-27.2036	0.576999
2.681761	-9.40259	0.797371		9.761761	-13.6155	0.756941		13.84176	-27.2012	0.576963
2.691761	-9.40177	0.797342		9.771761	-13.6141	0.756901		13.85176	-27.1987	0.576927

2.701761	-9.40096	0.797313		9.781761	-13.6127	0.756861		13.86176	-27.1962	0.57689
2.711761	-9.40015	0.797285		9.791761	-13.6115	0.756828		13.87176	-27.1938	0.576854
2.721761	-9.39933	0.797256		9.801761	-1.56405	0.946792		13.88176	-27.1913	0.576818
2.731761	-9.39852	0.797227		9.811761	-1.56414	0.946798		13.89176	-27.1889	0.576781
2.741761	-9.3977	0.797198		9.821761	-1.56422	0.946803		13.90176	-27.1868	0.576752
2.751761	-9.39689	0.797169		9.831761	-1.5643	0.946808		13.91176	-1.43586	0.93872
2.761761	-9.39608	0.79714		9.841761	-1.56438	0.946813		13.92176	-1.436	0.938729
2.771761	-9.39526	0.797111		9.851761	-1.56446	0.946818		13.93176	-1.43613	0.938737
2.781761	-9.39445	0.797083		9.861761	-1.56454	0.946823		13.94176	-1.43625	0.938744
2.791761	-9.39364	0.797054		9.871761	-1.56462	0.946828		13.95176	-1.43638	0.938752
2.801761	-9.39283	0.797025						13.96176	-1.4365	0.93876
2.811761	-9.39201	0.796996						13.97176	-1.43662	0.938768
2.821761	-9.3912	0.796967						13.98176	-1.43675	0.938776
2.831761	-9.39039	0.796939						13.99176	-1.43687	0.938784
2.841761	-9.38958	0.79691						14.00176	-1.437	0.938791
2.851761	-9.38877	0.796881						14.01176	-1.43712	0.938799
2.861761	-9.38796	0.796852						14.02176	-1.43725	0.938807
2.871761	-9.38715	0.796823						14.03176	-1.43737	0.938815
2.881761	-9.38634	0.796795						14.04176	-1.43749	0.938823
2.891761	-9.38553	0.796766						14.05176	-1.43762	0.93883
2.901761	-9.38472	0.796737						14.06176	-1.43774	0.938838
2.911761	-9.38391	0.796709						14.07176	-1.43787	0.938846
2.921761	-9.3831	0.79668						14.08176	-1.43799	0.938854
2.931761	-9.38229	0.796651						14.09176	-1.43811	0.938862
2.941761	-9.38148	0.796622						14.10176	-1.43824	0.938869
2.951761	-9.38067	0.796594						14.11176	-1.43836	0.938877
2.961761	-9.37986	0.796565						14.12176	-1.43848	0.938885
2.971761	-9.37905	0.796536						14.13176	-1.43861	0.938893
2.981761	-9.37824	0.796508						14.14176	-1.43873	0.938901
2.991761	-9.37744	0.796479						14.15176	-1.43886	0.938908
3.001761	-9.37663	0.79645						14.16176	-1.43898	0.938916
3.011761	-9.37582	0.796422						14.17176	-1.4391	0.938924
3.021761	-9.37501	0.796393						14.18176	-1.43923	0.938932
3.031761	-9.37421	0.796365						14.19176	-1.43935	0.93894
3.041761	-9.3734	0.796336						14.20176	-1.43947	0.938947
3.051761	-9.37259	0.796307						14.21176	-1.4396	0.938955
3.061761	-9.37179	0.796279						14.22176	-1.43972	0.938963
3.071761	-9.37098	0.79625						14.23176	-1.43984	0.938971
3.081761	-9.37017	0.796222						14.24176	-1.43997	0.938978
3.091761	-9.36937	0.796193						14.25176	-1.44009	0.938986
3.101761	-9.36856	0.796164						14.26176	-1.44021	0.938994

3.111761	-9.36776	0.796136						14.27176	-1.44033	0.939002
3.121761	-9.36695	0.796107						14.28176	-1.44046	0.939009
3.131761	-9.36615	0.796079						14.29176	-1.44058	0.939017
3.141761	-9.36534	0.79605						14.30176	-1.4407	0.939025
3.151761	-9.36454	0.796022						14.31176	-1.44083	0.939033
3.161761	-9.36373	0.795993						14.32176	-1.44095	0.93904
3.171761	-9.36293	0.795965						14.33176	-1.44107	0.939048
3.181761	-9.36213	0.795936						14.34176	-1.44119	0.939056
3.191761	-9.36132	0.795908						14.35176	-1.44132	0.939063
3.201761	-9.36052	0.795879						14.36176	-1.44144	0.939071
3.211761	-9.35972	0.795851						14.37176	-1.44156	0.939079
3.221761	-9.35891	0.795822						14.38176	-1.44168	0.939087
3.231761	-9.35811	0.795794						14.39176	-1.44181	0.939094
3.241761	-9.35731	0.795765						14.40176	-1.44193	0.939102
3.251761	-9.35651	0.795737						14.41176	-1.44205	0.93911
3.261761	-9.35571	0.795708						14.42176	-1.44217	0.939117
3.271761	-9.3549	0.79568						14.43176	-1.4423	0.939125
3.281761	-9.3541	0.795651						14.44176	-1.44242	0.939133
3.291761	-9.3533	0.795623						14.45176	-1.44254	0.939141
3.301761	-9.3525	0.795595						14.46176	-1.44266	0.939148
3.311761	-9.3517	0.795566						14.47176	-1.44279	0.939156
3.321761	-9.3509	0.795538						14.48176	-1.44291	0.939164
3.331761	-9.3501	0.795509						14.49176	-1.44303	0.939171
3.341761	-9.3493	0.795481						14.50176	-1.44315	0.939179
3.351761	-9.3485	0.795453						14.51176	-1.44327	0.939187
3.361761	-9.3477	0.795424						14.52176	-1.4434	0.939194
3.371761	-9.3469	0.795396						14.53176	-1.44352	0.939202
3.381761	-9.3461	0.795368						14.54176	-1.44364	0.93921
3.391761	-9.3453	0.795339						14.55176	-1.44376	0.939217
3.401761	-9.3445	0.795311						14.56176	-1.44388	0.939225
3.411761	-9.34371	0.795283						14.57176	-1.444	0.939233
3.42	-9.34305	0.795259						14.58176	-1.44413	0.93924
3.42505	-1.7969	0.949406						14.59176	-1.44425	0.939248
3.431761	-1.7969	0.949411						14.60176	-1.44437	0.939256
3.441761	-1.7969	0.949415								
3.451761	-1.7969	0.949419								
3.461761	-1.7969	0.949423								

	X2 type	
Time	Angle	Magnitude
4.011761	-1.7969	0.961444
4.021761	-1.7969	0.961444
4.031761	-1.7969	0.961444
4.041761	-1.7969	0.961444
4.051761	-1.7969	0.961444
4.061761	-1.7969	0.961444
4.071761	-1.7969	0.961444
4.081761	-1.7969	0.961444
4.091761	-1.7969	0.961444
4.101761	-1.7969	0.961444
4.111761	-1.7969	0.961444
4.121761	-1.7969	0.961444
4.131761	-1.7969	0.961444
4.141761	-1.7969	0.961444
4.151761	-1.7969	0.961444
4.161761	-1.7969	0.961444
4.171761	-1.7969	0.961444
4.181761	-1.7969	0.961444
4.191761	-1.7969	0.961444
4.201761	-1.7969	0.961444
4.211761	-23.8604	0.429528
4.221761	-23.8598	0.429521
4.231761	-23.859	0.429511
4.241761	-23.8581	0.429501
4.251761	-23.8573	0.429491
4.261761	-23.8564	0.429481
4.271761	-23.8555	0.429471
4.281761	-23.8547	0.429461
4.291761	-23.854	0.429453
4.301761	-1.79145	0.961101
4.311761	-1.79145	0.961101
4.321761	-1.79145	0.961101
4.331761	-1.79145	0.961101
4.341761	-1.79146	0.961101
4.351761	-1.79146	0.961101
4.361761	-1.79146	0.961101

	X2 type	
Time	Angle	Magnitude
4.011761	-1.7969	0.961444
4.021761	-1.7969	0.961444
4.031761	-1.7969	0.961444
4.041761	-1.7969	0.961444
4.051761	-1.7969	0.961444
4.061761	-1.7969	0.961444
4.071761	-1.7969	0.961444
4.081761	-1.7969	0.961444
4.091761	-1.7969	0.961444
4.101761	-1.7969	0.961444
4.111761	-1.7969	0.961444
4.121761	-1.7969	0.961444
4.131761	-1.7969	0.961444
4.141761	-1.7969	0.961444
4.151761	-1.7969	0.961444
4.161761	-1.7969	0.961444
4.171761	-1.7969	0.961444
4.181761	-1.7969	0.961444
4.191761	-1.7969	0.961444
4.201761	-1.7969	0.961444
4.211761	-23.8604	0.429528
4.221761	-23.8598	0.429521
4.231761	-23.859	0.429511
4.241761	-23.8581	0.429501
4.251761	-23.8573	0.429491
4.261761	-23.8564	0.429481
4.271761	-23.8555	0.429471
4.281761	-23.8547	0.429461
4.291761	-23.854	0.429453
4.301761	-1.79145	0.961101
4.311761	-1.79145	0.961101
4.321761	-1.79145	0.961101

Chapter 5

5.1 Investigating the effects of grid-connected renewable distributed generation (GRDG) on voltage dip mitigation in an electric power network

This chapter investigates the effects of various grid-connected renewable distributed generations (GRDG) in a power network. The existence of GRDG in electrical power networks today has a positive effect on the retained voltage during voltage dips in a power network apart from the reduction of greenhouse gases and carbon emissions. Its impact on the retained grid voltage is strongly dependent on the voltage level, and thus the grid impedance. Different research works have been done in this area [4], [48], [91] and power systems faults, as a probable cause of voltage dip events, in the distribution network were considerably investigated, since most of the GRDG is usually connected at the distribution level voltages such as 0.415kV, 11 kV and 22 kV.

However, the researchers have not emphasized considerably on the impacts of multiple voltage dips within a short time, caused by faults, especially in the transmission grid and distribution grid. Furthermore, the effects of multiple voltage dips on different phases were also not investigated. The various types of grid-connected wind energy conversion systems was not also studied individually such as the fixed-speed squirrel cage induction wind generator (SCIWG), variable-speed doubly-fed induction wind generator (DFIWG) and variable-speed synchronous wind generator (SWG) for voltage dip mitigation, and the applicability of these wind-energy technologies as regard mitigation of voltage dips are not evaluated and compared with different fault resistance and fault reactance in previous studies.

However, in this research work, all the aforesaid cases are investigated and applicability of various GRDG using a typical South African network data [201]. In addition, the impact of increasing penetration level of different wind energy conversion systems in a power network on mitigation of multiple voltage dips.

The author proposes to determine the best range of GRDG capacities and penetration level for mitigation of voltage dip in a power network, and this work aims to help the power utilities in determining the optimal penetration level for mitigation of voltage dips while planning grid-integration of renewable distributed generation. In this context, possible scenarios of various voltage dip conditions in power networks containing GRDG are simulated and analysed in this thesis with the aim to generate the database for the ANN module for voltage dip mitigation as per the proposal of the thesis.

The GRDG can be connected at the sub-transmission network, distribution feeder or at the customer load side. Grid-integrated or grid-connected RDG systems can have either positive or negative effects on both the grid and the sensitive equipment. These effects depend on the power network operating characteristics and the RDG characteristics. Investigations have shown that some level of RDG units can be integrated on the power system without a major change to the system, but a high level of RDG penetration may require careful planning additional control, storage and structural changes [75]. GRDG can provide services like voltage quality disturbance compensation such as voltage dip mitigation, power system restoration services, etc. [249].

In this work, the ancillary services provided by GRDG are assumed to be without any stability problems. It is also assumed that there is no failure of protection devices during faults conditions and there is no fault current from the RDG units. The solar PV is assumed generating active power only. The grid-connected wind plants are assumed to have low voltage ride-through (LVRT) capability. The power network transmission lines are homogeneous, i.e., there is no joining of different types of conductor sizes so that the line impedance is distributed uniformly on the entire length.

5.2 Test network description

The description of the test network in Figure 4.1 has been given in chapter 4 and renamed as Figure 5.1 in this chapter. The test network with GRDGs modeled in DIgSILENT and based on generic data collected from Eskom [201]. This network is used to investigate the effects of

various GRDGs on multiple voltage dips caused by various power system faults. The three types of GRDGs considered in the test power system include the wind power plants, solar PV plants and the hydro-electric plants. They all use different technologies as mentioned in chapter 4. The hydro plants are modeled as permanent magnet synchronous generators; the solar PV plants are modeled as static generators with power electronics interface. The wind power plants are modelled with different types of generators such as wind variable-speed doubly-fed induction generators, wind static generators with fully rated power electronics converters and variable-speed permanent magnet synchronous wind generators.

However, a second test network as shown in Figure 5.12 later is adopted for investigating the impact of types of wind energy conversion systems and their levels of penetration on voltage dip mitigation. The different types of wind generators investigated are fixed-speed squirrel cage induction wind generator (SCIWG), variable-speed doubly-fed induction wind generator (DFIWG), variable-speed synchronous wind generator (SWG) and static generators with fully rated converters.

Different types of voltage dip studies are conducted and investigated on the test network shown in Figure 5.1, and the voltage dips are measured at the load busbars at different times. The depth of the multiple voltage dips and residual voltage during the faults and the voltage profile after the faults have been observed and carefully recorded.

The data recorded are saved in Microsoft Excel. These data are later presented and used as synthesized historical data for the ANN module.

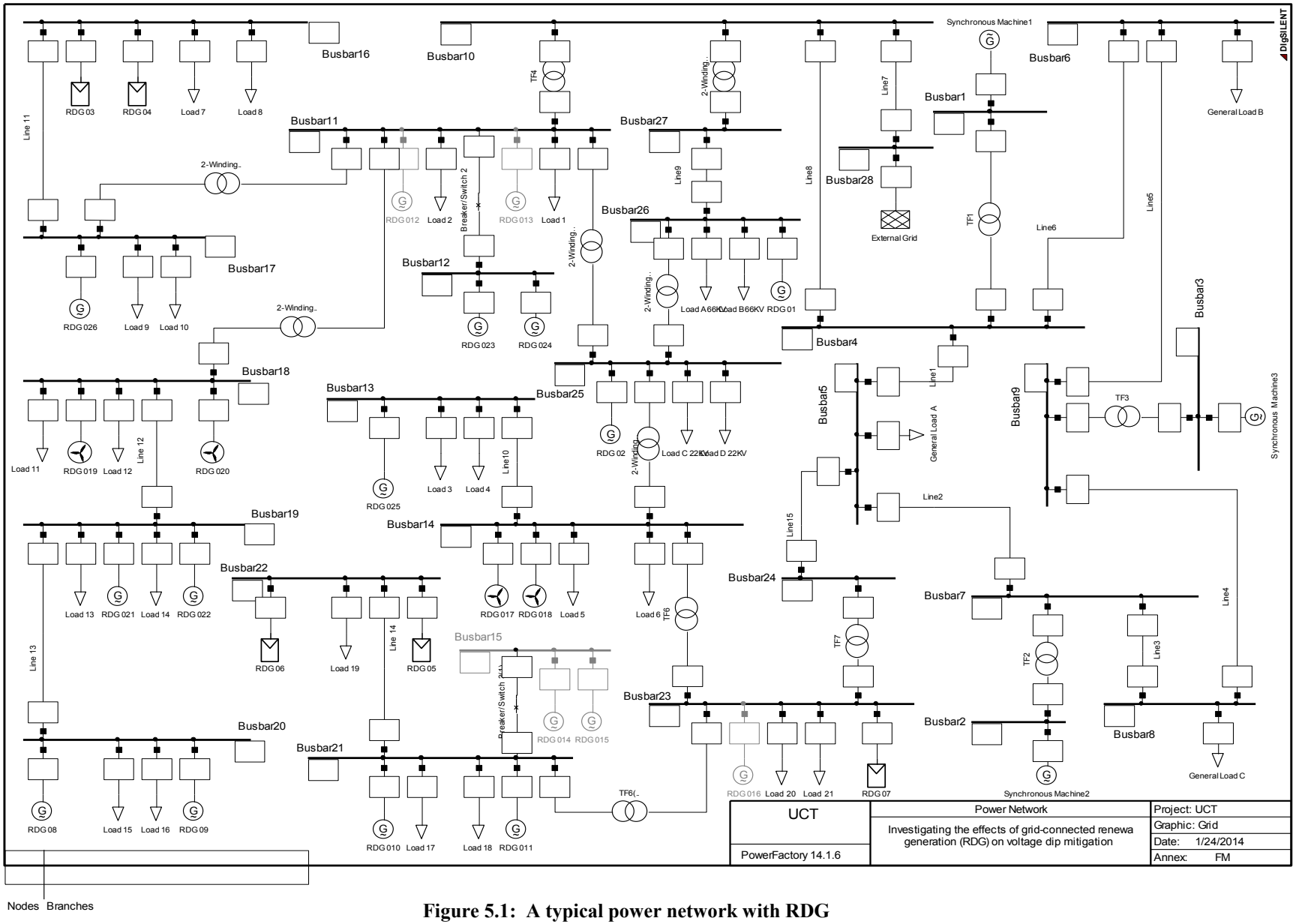

Figure 5.1: A typical power network with RDG

5.3 List of scenarios investigated

The different scenarios that are investigated in this thesis are as follows:

Scenario 1

1. The base case performs the steady-state load flow study on the test network of Figure 5.1 to monitor the load busbar voltage magnitude in p.u. without and with the RDGs. The results are tabulated in Table 5.1.

Scenario 2

2. This scenario investigates the effect of multiple voltage dips at the load busbars caused by disturbances in the transmission side of the test network, simulated as different types of faults, with different locations and durations. Multiple voltage dips are cause as a result of faults that occur one after the other within short duration. During this fault study, two scenarios of study are conducted as follows:
   a. The first fault, a 2P fault, occurs on line8 at 0. 80sec and was cleared at 1.10sec, followed by the second fault, a 3P fault, on line15 at 1.50sec and was cleared at 1.80sec. These faults are applied at fault locations 10%, 50% and 90% on each of the lines one after the other. GRDGs were not present when the fault studies were done. The result is presented in Table 5.2, and the retained voltage magnitude is measured at t=0.95sec, t=1.65sec and t=3.00sec.
   b. The first fault SLG fault occurs on line8 at 0.80sec and was cleared at 1.10sec, follow by the second fault which was a 2LG fault on line15 at 1.50sec and was cleared at 1.80sec. These faults are applied at fault locations 10%, 50% and 90% on each of the lines one after the other. GRDGs were not present when the fault studies were done. The result is presented in Table 5.3, and the retained voltage magnitude is a measured at t=0.95sec, t=1.65sec and t=3.00sec.

Scenario 3

3. This scenario investigates the effect of multiple voltage dips at the load busbars caused by disturbances in the distribution side of the test network, simulated as different types of faults. The fault location is at 50% for all of the lines. First fault is applied at time t=0.80sec followed by second fault at t=1.50sec, the faults are cleared at t=1.10sec and t=1.50sec respectively. GRDGs were not present when the fault studies were done. The result is presented in Table 5.4, and the retained voltage magnitude is a measured at t=0.95sec, t=1.65sec and t=3.00sec for all the cases. This fault study include:

a. Effects of 2P fault followed by SLG fault on line10 and line13.
b. Effects of 3P fault followed by 2LG fault on line12 and line14 and
c. Effects of SLG fault followed by 2P fault on line9 and line11.

Scenario 4

4. This scenario investigates the impact of various GRDGs on mitigation of multiple voltage dips due to faults in the transmission side of the test network. The different cases of GRDGs considered are:
   a. Grid-connected wind power plants (DFIG, PMSG and static generator)
   b. Grid-connected hydro-electric power plants
   c. Grid-connected solar PV power plants
   d. Grid-connected wind and hydro-electric generators
   e. All the GRDGs together

Scenario 5

5. This scenario investigates the impact of various GRDGs on mitigation of multiple voltage dips due to faults in the distribution side of the test network. The different cases of GRDGs considered are:
   a. Grid-connected wind power plants (DFIG, PMSG and static generator)
   b. Grid-connected hydro-electric power plants
   c. Grid-connected solar PV power plants
   d. Grid-connected wind and hydro-electric generators
   e. All the GRDGs together

Scenario 6

6. This scenario performs the following investigation on the test network shown in Figure 5.12. Another test network is adopted to investigate the impacts of different types of wind energy conversion systems (WECS) such as SCIWG, DFIWG and SWG. The impact of connecting each of these generators is assessed to establish their effects on mitigation of multiple voltage dips on the load busbars. The first fault 2LG (F1) is applied on line 4, at t=0.75sec and is cleared at t=1.25sec follow by the second fault 3P (F2) on line 2 at t=1.85sec and was cleared at t=2.45sec. F1 fault location is at 10% of line 4 and F2 fault location is at 50% of line 2 with different fault resistance and fault reactance as follows:
   a. F1 is 0Ω and 0Ω , F2 is 0Ω and 0Ω
   b. F1 is 2.5Ω and 1.8 Ω, F2 is 1.77Ω and 0.45

c. F1 is 10Ω and 5 Ω, F2 is 8Ω and 3 Ω

The result of this study is shown in Tables 5.15, Table 5.16, Table 5.17 and Table 5.18.

Scenario 7

7. This scenario investigates the effects of faults from different phases that cause voltage dips. First fault 2P (F1) is applied on line 3, at t=0.75sec and is cleared at t=1.25sec follow by the second fault 3P (F2) on line 1 at t=1.85sec and was cleared at t=2.45sec. F1 fault location is at 50% of line 3 follow by F2 fault location is at 10% of line 1 with and the fault impedance set to 0Ω in this study for both faults. However the WECS was not connected. The different phases are as follow:

a. F1 on 'phase a-b' follow by F2 on 'phase a', and repeated on 'phase b' and 'phase c'
b. F1 on 'phase b-c' follow by F2 on 'phase a', and repeated on 'phase b' and 'phase c'
c. F1 on 'phase c-a' follow by F2 on 'phase a', and repeated on 'phase b' and 'phase c'

The result of this study is shown in Tables 19, Table 20 and table 21.

Scenario 8

8. The effects of high penetration level of different wind energy conversion systems (SCIWG, DFIWG and SWG) during voltage dip mitigation.

The investigation and results for each of the case studies are present in a comparative manner as follows:

5.4 Scenario 1: Base Case

In the base case, load flow study is performed on the test network of Figure 5.1 to determine the load busbar voltages (in p.u.) without and with GRDGs. The results are tabulated in Table 5.1. The simulation is run for 5s. The lowest limit of allowed standard nominal voltage is 0.950p.u. while the highest limit of allowed nominal voltage is 1.050p.u.

Table 5.1: Voltage magnitude at load busbars without and with GRDG systems

Load busbar	Voltage (p.u.) without any GRDG	Voltage (p.u.) with WECS only	Voltage (p.u.) with HP only	Voltage (p.u.) with PV only	Voltage (p.u.) with all GRDG
Busbar5	0.998	1.029	1.020	1.011	1.010
Busbar6	0.993	1.000	1.000	0.997	1.003
Busbar8	0.978	0.999	0.990	0.985	1.008

Busbar11	0.992	1.011	1.001	0.993	1.008
Busbar13	0.974	1.019	1.002	0.997	1.001
Busbar14	0.974	1.010	1.002	0.997	1.001
Busbar16	0.972	1.002	0.999	0.974	1.000
Busbar17	0.972	1.002	0.999	0.974	1.000
Busbar18	0.952	0.988	1.021	0.953	1.025
Busbar19	0.952	0.988	1.021	0.953	1.025
Busbar20	0.952	1.000	1.021	0.953	1.020
Busbar21	0.976	1.011	1.002	0.999	1.009
Busbar22	0.976	1.011	1.002	0.999	1.009
Busbar23	0.976	1.011	1.002	1.000	1.009
Busbar25	0.973	0.984	1.001	0.983	1.003
Busbar26	0.957	0.984	1.001	0.962	1.003

5.5 Simulation of Power System Faults Leading to Voltage Dip without GRDG

Voltage dips are short-duration reduction of the r r.m.s. voltage magnitude in any or all the three-phases. They are usually caused as a result of energizing of transformers, switching operations, starting of large motors or bulk loads and electrical power systems faults such as three phases short-circuit (3P) fault, two phases short-circuit (2P) fault, single phase-to-ground (SLG) fault and two phase-to-ground (2LG) fault. Voltage dips are defined both as lost voltage and retained voltage. However, for this study, the retained voltage (remaining voltage magnitude) is used in the thesis for measuring the voltage dip.

Each of these fault types produces different types of voltage dip at the fault point and voltage dip effects in adjacent busbars [247]. The nature and behavior of an electrical fault depend on its cause. A fault may be a balanced or symmetric fault or an unbalanced or unsymmetrical fault. The balanced fault, such as a three-phase fault, will produce a balanced voltage dip, which will affect each of the three phases equally. The unbalanced faults, such those involving single or two phases, do not affect the three phases equally and usually produce unbalanced voltage dips.

The three-phases short-circuit fault occurs very rarely and causes the highest magnitude of fault current and the most severe voltage dip affecting all the three phases equally. Three-phase voltage dips usually occur due to starting large motors, switching or tripping of a three-phase circuit breaker, switch or recloser. They occur mostly at the medium voltage and low voltage distribution systems [55]. The common unbalanced faults are single phase-to-ground fault, two

phases short-circuit fault and two phase-to-ground fault which are common in transmission and distribution network. .

In this thesis, both balanced and unbalanced faults have been considered for simulating voltage dips. When a fault occurs, it produces different dip type as it propagates through the power network, such as type A, type B, etc.A three-phase short-circuit fault produces a type A dip characterized by dip equally affecting all three phaseswhile type B and type D dips can occur due to single-phase-to-ground faults. These dips are characterized by a major voltage drop in the afflicted phase and are called single phase dips. Dip types C and E occur as a result of either two-phase short circuit fault or two phase-to-ground fault and are characterized by major drop in the two afflicted phases and are called double phase dips.

5.6 Scenario 2: Investigating the effect of multiple voltage dips caused by disturbances in the transmission side of the test network

This scenario investigates the effect of multiple voltage dips caused by disturbances in the transmission side of the test network on the load busbars, the disturbances are simulated as different types of faults, with different fault locations 10%, 50% and 90% as mentioned in the list of scenarios above. Multiple voltage dips are cause as a result of faults that occur one after the other within short duration. Voltage dip magnitude is measured in p.u. in terms of the retained voltage at the load busbars. Three-phase short circuit (3P) faults rarely occur within the transmission network. This is due to the nature and design of transmission network. Majority of faults occur within the distribution network. Faults that occur on the transmission lines are approximately 5% symmetrical faults and are relatively rare; the popular faults are the single-phase faults.

For the scenarios 2 and 3, three-phase short-circuit fault (3P), two-phase short-circuit fault (2P), single phase-to-ground (SLG) fault and two phase-to-ground fault (2LG) have been considered for simulating different types of voltage dips and investigating their effects on load busbars containing critical and non-critical loads. However, faults SLG and 2LG fault are considered during the investigation of the effects of GRDGs due to fault from the transmission network. This is based on the assumption that 3P faults are not common on the transmission network as compare with other faults such as SLG and 2LG faults. Nevertheless, all the fault 3P, 2P, SLG and 2LG are considered for disturbance from distribution network.

The multiple voltage dips are generated in the transmission system of Figure 5.1 first by the inception of a 2P fault on line8 (between Busbar10 and Busbar4) at t=0.80sec and clearance of the same at t=1.10sec; this is followed by a second 3P fault on line15 (between Busbar5 and Busbar2) at t=1.50sec and cleared at t=1.80sec. Before the faults were applied the pre-fault nominal voltages at the load busbars are recorded as shown in Table 5.1.

The studied for this scenario are divided into two parts: a. Effects of 3P and 2P faults and b. Effects of SLG and 2LG faults.

5.6.1 Scenario 2a: Effects of 3P and 2P faults

This fault study is performed by applying the 2P and 3P faults at three different locations on the two transmission lines. In the first instance, the faults are applied at 10% of line length on both the lines, in the second instance at 50% of line length on both the lines and in the third instance 90% of line length on both the lines. The percentage line lengths for both lines are measured from the transmission side. This means that for line8, the percentage line length is measured from busbar10 while for line15; the same is measured from busbar5. Thus, fault location at 10% line length will be closer to the transmission side, at 50% line length will be at midpoint of the lines and at 90% line length will be closer to the distribution side. In this scenario, the fault resistance and reactance are both set to 0 Ω in order to produce the most severe fault current. Simulation is run for 5.00sec.Also no GRDGs are assumed to be connected to the test network for this scenario.

The results are tabulated in Table 5.2, which are the retained r.m.s. voltages at the load busbars are measured at times t=0.95sec, t=1.65sec and at t=3.00sec. At t=0.95sec, 3P fault is continuing and not yet cleared. At t=1.65sec, 3P fault is cleared and 2P fault is continuing and not yet cleared. At t=3.00sec, all the faults have been cleared in the test network.

Table 5.2: Voltage magnitude at the load busbars after 2P and 3P faults applied on line8 and line15

Load busbar	Voltage magnitude (p.u.) with fault at 10% of the lines at t=			Voltage magnitude (p.u.) with fault at 50% of the lines at t=			Voltage magnitude (p.u.) with fault at 90% of the lines at t=		
	0.95s	1.65s	3.00s	0.95s	1.65s	3.00s	0.95s	1.65s	3.00s
Busbar5	0.554	0.081	0.935	0.642	0.306	0.955	0.679	0.440	0.965
Busbar6	0.508	0.562	0.927	0.619	0.665	0.948	0.683	0.723	0.958
Busbar8	0.626	0.482	0.910	0.712	0.604	0.931	0.752	0.675	0.940
Busbar11	0.594	0.640	0.957	0.545	0.694	0.969	0.490	0.722	0.975
Busbar13	0.549	0.150	0.920	0.590	0.126	0.936	0.582	0.087	0.945

Busbar14	0.549	0.150	0.920	0.590	0.126	0.936	0.582	0.087	0.945
Busbar16	0.582	0.627	0.938	0.533	0.680	0.949	0.480	0.707	0.955
Busbar17	0.578	0.627	0.938	0.533	0.680	0.949	0.480	0.707	0.955
Busbar18	0.566	0.614	0.919	0.522	0.666	0.930	0.470	0.693	0.936
Busbar19	0.566	0.614	0.919	0.522	0.666	0.930	0.470	0.693	0.936
Busbar20	0.566	0.614	0.919	0.522	0.666	0.930	0.470	0.693	0.936
Busbar21	0.547	0.116	0.919	0.597	0.087	0.936	0.596	0.043	0.945
Busbar22	0.547	0.116	0.919	0.597	0.087	0.936	0.596	0.043	0.945
Busbar23	0.548	0.116	0.920	0.597	0.087	0.936	0.597	0.043	0.946
Busbar25	0.565	0.423	0.930	0.552	0.444	0.943	0.500	0.443	0.951
Busbar26	0.563	0.525	0.920	0.533	0.562	0.932	0.479	0.576	0.938

5.6.2 Scenario 2b: Effects of SLG and 2LG Faults

A similar fault study as scenario 2a is conducted with single phase-to-ground (SLG) fault and two phase-to-ground (2LG) fault applied in line8 and line15 respectively at 10%, 50% and 90% line lengths. The line lengths are measured in the same way as detailed for scenario 2a. The SLG fault is applied on line8 at t=0.80sec and was cleared at t=1.10sec. This is followed by the 2LG on line15 at t=1.50sec and cleared at t=1.80sec. The multiple voltage dips are recorded during the faults at t=0.95sec, at t=1.65sec and at t=3.00sec. Table 5.3 lists the retained r.m.s. voltage magnitudes at the same load busbars measured at the aforesaid time instants.

Table 5.3: Voltage magnitude at the load busbars after SLG and 2LG faults applied on lines line8 and ine15

Load busbar	Voltage magnitude (p.u.) with fault at 10% of the lines at t=			Voltage magnitude (p.u.) with fault at 50% of the lines at t=			Voltage magnitude (p.u.) with fault at 90% of the lines at t=		
	0.95s	**1.65s**	**3.00s**	**0.95s**	**1.65s**	**3.00s**	**0.95s**	**1.65s**	**3.00s**
Busbar5	0.421	0.090	0.953	0.604	0.330	0.968	0.671	0.466	0.975
Busbar6	0.344	0.616	0.945	0.580	0.710	0.962	0.682	0.761	0.969
Busbar8	0.578	0.539	0.929	0.716	0.655	0.945	0.773	0.718	0.953
Busbar11	0.383	0.669	0.968	0.281	0.716	0.976	0.086	0.739	0.981
Busbar13	0.404	0.165	0.935	0.514	0.136	0.948	0.518	0.093	0.954
Busbar14	0.404	0.165	0.935	0.514	0.136	0.948	0.518	0.093	0.954
Busbar16	0.376	0.654	0.949	0.275	0.700	0.957	0.085	0.722	0.961
Busbar17	0.376	0.654	0.949	0.275	0.700	0.957	0.085	0.722	0.961
Busbar18	0.368	0.638	0.929	0.269	0.683	0.937	0.085	0.705	0.941

Busbar19	0.368	0.638	0.929	0.269	0.683	0.937	0.085	0.705	0.941
Busbar20	0.368	0.638	0.929	0.269	0.683	0.937	0.085	0.705	0.941
Busbar21	0.406	0.131	0.935	0.532	0.096	0.948	0.549	0.048	0.954
Busbar22	0.406	0.131	0.935	0.532	0.096	0.948	0.549	0.048	0.954
Busbar23	0.406	0.130	0.936	0.532	0.095	0.948	0.549	0.047	0.955
Busbar25	0.387	0.443	0.942	0.376	0.457	0.953	0.267	0.452	0.958
Busbar26	0.374	0.545	0.931	0.314	0.575	0.940	0.163	0.584	0.944

Table 5.2 and Table 5.3 indicate that the distance of fault location from the load busbars affects the severity of the voltage dip. Voltage dip magnitude increases (and retained voltage magnitude decreases) with the decrease in the fault distance from the affected load busbars. Buses which are closer to the faults experience worst voltage dip as compared to the buses far away from the fault location. It is also seen that the effects of these transmission line faults are also experienced at the low voltage distribution buses through propagation along the transformers. However, the voltage dip propagation is not severe at the distribution side when compare to the transmission side. This is due to the fault type, fault location or the clearing time.

The results listed in Tables 5.2 and 5.3 validate this if one considers separately the transmission side busbars and the distribution side busbars. At the distribution side of the network, as the faults locations move closer along the lines towards the load busbars in the distribution network, the multiple voltage dip magnitudes tend to deteriorate with more and more closeness of the location. The experience is also similar to the sub-transmission load busbar11, busbar25 and busbar26 to that of the distribution busbars. However, at the transmission load busbar5, busbar6 and busbar 8, the impact and severity of the multiple voltage dips become less severe as the multiple faults' location moves closer (from 10% to 90%) to the distribution load busbars.

The nature and type of faults are also found to affect multiple dip magnitudes. The SLG fault on a transmission line is more severe than the 2P fault on the same line with the same fault resistance and fault reactance values. The impact of SLG is more than that of 2P at 90% of line8. This is experienced as an interruption instead of a dip since is below 10% of the declared

voltage as define by IEE Standard 1159-2009 [5]. This is shown in Table 5.3 as indicated by busbars 16, 17, 18, 19, and 20.

5.7 Scenario 3: Investigating the effect of multiple voltage dips caused by disturbances in the distribution side of the test network

This scenario investigates the magnitude of multiple voltage dips at the load busbars caused by disturbances in the distribution side of the test network, simulated as different types of faults, with different locations and durations. Most fault types occur on the distribution side of power network as compared to the transmission side. This is due to many factors such as the design of the distribution system, the distribution system, etc. Research work reported that conducted on power utilities in China shown that more than 70% fault in a power distribution system is single-phase-to-ground [250].

These scenarios include three separate studies with different fault types and fault locations as follows and discussed in the following sub-sections:

a. Effects of 2P fault followed by SLG fault,

b. Effects of 3P fault followed by 2LG fault and

c. Effects of SLG fault followed by 2P fault.

5.7.1 Scenario 3a:

In scenario 3a, a multiple voltage dip is simulated by applying a 2P fault on line10 followed by a SLG fault on line13 in the distribution side of the test network. The 2P fault is applied at 50% of length of line10 at t=0.80sec and cleared at t=1.10sec. The following SLG fault is applied at 50% of length of line13 at t=1.50sec and cleared at t=1.80sec. Voltage magnitudes at the load busbars are measured at t=0.95sec (when 2P fault is not yet cleared), at t=1.65sec (when 2P fault is cleared but SLG fault is not yet cleared) and at t=3.00sec (after all the faults are cleared). In this case, the test system does not include any GRDGs. The results are tabulated in Table 5.4.

5.7.2 Scenario 3b:

In scenario 3b, a multiple voltage dip is simulated by applying a 3P fault on line12 followed by a SLG fault on line14 in the distribution side of the test network at 50% line lengths for both the lines. The 3P fault is applied at t=0.80sec and cleared at t=1.10sec. The following SLG fault is applied at t=1.50sec and cleared at t=1.80sec. Voltage magnitudes at the load busbars are

measured at same time instants as 3a. In this case also, the test system does not include any GRDGs. The results are tabulated in Table 5.4.

5.7.3 Scenario 3c:

In scenario 3c, a multiple voltage dip is simulated by applying a SLG fault on line9 followed by a 2P fault on line11. The fault application and clearance times and fault location are kept same as in 3a and 3b. Line9 is a 66kV line at sub-transmission level. In this case also, the test system does not include any GRDGs. The results are tabulated in Table 5.4.

Table 5.4: Voltage magnitudes at the load busbars for different fault types on distribution lines at 50% of each line

Load busbar	Voltage magnitude (p.u.) with 2P and SLG faults on line10 and line13 respectively at t=			Voltage magnitude (p.u.) with 3P and 2LG faults on line12 and line14 respectively at t=			Voltage magnitude (p.u.) with SLG and 2P faults on line9 and line11 respectively at t=		
	0.95s	**1.65s**	**3.00s**	**0.95s**	**1.65s**	**3.00s**	**0.95s**	**1.65s**	**3.00s**
Busbar5	0.680	0.925	0.993	0.910	0.615	0.983	0.867	0.919	0.995
Busbar6	0.835	0.927	0.988	0.911	0.824	0.979	0.904	0.920	0.990
Busbar8	0.807	0.928	0.972	0.919	0.791	0.962	0.910	0.924	0.975
Busbar11	0.794	0.749	0.988	0.738	0.790	0.986	0.713	0.779	0.991
Busbar13	0.477	0.870	0.971	0.854	0.202	0.961	0.710	0.867	0.973
Busbar14	0.477	0.870	0.971	0.854	0.202	0.961	0.710	0.867	0.973
Busbar16	0.778	0.733	0.968	0.723	0.773	0.966	0.698	0.483	0.971
Busbar17	0.778	0.733	0.968	0.723	0.773	0.966	0.698	0.483	0.971
Busbar18	0.763	0.000	0.948	0.000	0.755	0.946	0.682	0.748	0.951
Busbar19	0.762	0.000	0.948	0.000	0.755	0.946	0.682	0.748	0.951
Busbar20	0.762	0.000	0.948	0.000	0.755	0.946	0.682	0.748	0.951
Busbar21	0.465	0.879	0.972	0.863	0.000	0.962	0.742	0.875	0.974
Busbar22	0.465	0.879	0.972	0.863	0.000	0.962	0.742	0.875	0.974
Busbar23	0.465	0.879	0.973	0.863	0.161	0.962	0.742	0.875	0.974
Busbar25	0.588	0.803	0.969	0.791	0.527	0.963	0.458	0.816	0.972
Busbar26	0.670	0.781	0.953	0.770	0.646	0.950	0.000	0.769	0.956

The voltage dip as a result of 2P fault (line 10) is not as severe when compare to the SLG fault (line 13) on the load busbar18, busbar19 and busbar20 as shown in Table 5.4. For example,

busbar13 and busbar14 connected through line10 did not experience a voltage dip magnitude of 0.00p.u. at inception of 2P fault unlike busbars 18, 19 and 20 when SLG fault is applied on line 13. However, the inception of SLG fault on line13 causes busbar18, busbar19 and busbar20 to experience 0.00p.u. voltage dip at t=1.65sec. This is due to fault closer to these busbars, unlike the 2P fault which is not close to the busbars.

In scenario 3b, the inception of a 3P fault on line12 causes the retained voltage magnitude of 0.00p.u. at busbar18, busbar19 and busbar20 at t=0.95sec. This is as a result of the fault closer to the busbars on the line (line12) connecting the two busbars. The same level of severity is experienced following an SLG fault on line14 on busbar21 and busbar22 at t=1.65sec. However, the voltage recovers (0.962p.u.) at t=3.00sec.

Scenario 3c in Table 5.4 shows the effect of SLG fault from the sub-transmission line 9 followed by a 2P fault on line11 within the distribution network. The sub-transmission SLG fault has more impact on the transmission busbar26 than any other busbars in the test network at t=0.95sec. This is because the fault emanated from the sub-transmission. However, the 2P fault on line11 from the distribution does not have much impact on the transmission busbars such as busbar5 (0.919p.u.), busbar6 (0.920p.u.), and busbar8 (0.919p.u.) at t=1.65sec compare to distribution busbars such as busbar16 (0.483p.u.), busbar17 (0.483p.u.) and busbar19 (0.748p.u.)

5.8 Impact of various grid-connected renewable distributed generations (GRDG) on mitigation of multiple voltage dips

In this section, the effect of different grid-connected renewable distributed generations on mitigation of voltage dip is investigated. Those that were studied are the hydro-electric, solar photovoltaic and wind plants. The hydro-electric plants are modeled as hydro synchronous generators and hydro-turbo generators. The wind generators were modeled as wind energy farms, which include static generators with fully rated converter, variable-speed doubly-fed induction generator and variable-speed synchronous generator. The solar plants were modeled as static generators.

All these generators have a different impact on the voltage profile during voltage dip. New wind energy conversion systems technologies have reduced the problems arising and associated with wind power generators through the power-electronics-converter based device such as AVR, DVR, etc. The variable-speed wind generators have power electronic converters that help to

reduce the negative effects of wind generators on power systems. The grid-connected wind energy conversion systems are connected to the power network at the sub-transmission level, the MV-grid and LV-grid.

Scenario 4:

5.9 Scenario 4: Impact of GRDGs on mitigation of multiple voltage dips due to faults in the transmission side of the test network

This scenario investigates the impact of various GRDGs on mitigation of multiple voltage dips due to faults in the transmission side of the test network. The different cases of GRDGs considered are:

a. Grid-connected wind power plants
b. Grid-connected hydro-electric power plants
c. Grid-connected solar PV power plants
d. Grid-connected wind and hydro-electric generators
e. All the GRDGs together

5.9.1 Scenario 4a: Grid-connected wind power plants

In this scenario, the wind power plants are included in the test network as the only GRDGs. These are wind power plants name from RDG012 to RDG026. The wind power plants RDG012 and RDG013 are connected to busbar11; wind power plants RDG014 and RDG015 are connected to busbar15, and RDG016 is connected to busbar23.

In addition, wind power plants RDG017 and RDG018 are connected to busbar14. RDG019 and RDG020 are connected to busbar18. The wind power plants RDG021 and RDG022 are connected to busbar19. RDG023 and RDG024 are connected to busbar12. RDG025 is connected to busbar13, and RDG026 is connected to busbar17.

The effects of grid-connected wind generators are investigated using the multiple fault conditions in Table 5.3 which considers SLG and 2LG faults. This choice is based on the assumption that 3P faults are not common in the transmission network as compared to other faults such as SLG and 2LG faults.

In this study, all the grid-connected wind power plants remain connected to the network before, during and after the faults. The effect of connecting these GRDGs on multiple voltage dips

caused by the faults in the transmission lines are observed and the mitigation of the same is ascertained from any increase in the voltage magnitude at the load busbars with respect to the magnitudes without the GRDGs as in the results of Table 5.3 for scenario 2b. The application and clearance of faults and recording times for voltage magnitudes in the load busbars are same as in scenario 2a. The results are tabulated in Table 5.5. Figure 5.2 shows the percentage voltage improvement or deterioration of the voltage profile by comparing the two tables (Table 5.3 and Table 5.5). The voltage profile is improved better during the SLG fault as compare to the 2LG fault when the wind generators are connected.

The percentage improvement due to present of GRDG is given in equation 5.1 as ($\%VD_{imp}$)

$$\%VD_{imp} = \frac{A_{r.m.s.} - B_{r.m.s.}}{B_{r.m.s.}} \; x100 \qquad 5.1$$

Where

r.m.s. retained voltage magnitude with the present of GRDG during voltage dip is $A_{r.m.s.}$

r.m.s. retained voltage magnitude without the present of GRDG during voltage dip is $B_{r.m.s.}$

The voltage magnitude is increased and improved more at the distribution grid as compared to the sub-transmission grid. A voltage elevation of 68.35% was experienced at busbar16 and busbar17 during SLG fault at location 10% of the two lines (line8 and line15). In the same way, 110.18% were recorded on the same busbars during SLG fault at 50% of the two lines. Furthermore, during fault at 90% of the two lines, a 427.06% increase in voltage profile from 0.085p.u. to 0.448p.u. was experienced on both busbar16 and busbar17.

Table 5.5: Mitigation of multiple dips with grid-connected wind generators as a result of SLG and 2LG faults from the transmission lines (line8 and line15) measured at 0.95sec and 1.65sec during and 3.00sec after the multiple dips

Load busbar	Voltage magnitude with fault at 10% of the lines in (p.u.) at t=			Voltage magnitude with fault at 50% of the lines in (p.u.) at t=			Voltage magnitude with fault at 90% of the lines in (p.u.) at t=		
	0.95s	**1.65s**	**3.00s**	**0.95s**	**1.65s**	**3.00s**	**0.95s**	**1.65s**	**3.00s**
Busbar5	0.485	0.168	0.967	0.670	0.362	0.984	0.737	0.477	0.988
Busbar6	0.349	0.556	0.922	0.591	0.682	0.938	0.694	0.725	0.942
Busbar8	0.602	0.513	0.914	0.743	0.641	0.937	0.799	0.695	0.942
Busbar11	0.464	0.624	0.957	0.367	0.724	0.947	0.158	0.739	0.948
Busbar13	0.582	0.300	1.012	0.688	0.280	1.022	0.696	0.205	1.024
Busbar14	0.582	0.300	1.012	0.688	0.280	1.022	0.696	0.205	1.024

Busbar16	0.633	0.726	1.014	0.578	0.817	0.995	0.448	0.830	0.997
Busbar17	0.633	0.726	1.014	0.578	0.817	0.995	0.448	0.830	0.997
Busbar18	0.565	0.639	0.935	0.505	0.731	0.935	0.372	0.761	0.934
Busbar19	0.565	0.639	0.935	0.505	0.731	0.935	0.372	0.761	0.934
Busbar20	0.565	0.639	0.935	0.505	0.731	0.935	0.372	0.761	0.934
Busbar21	0.562	0.256	1.002	0.685	0.221	1.013	0.705	0.142	1.015
Busbar22	0.562	0.256	1.002	0.685	0.221	1.013	0.705	0.142	1.015
Busbar23	0.562	0.255	1.002	0.685	0.220	1.013	0.705	0.141	1.015
Busbar25	0.486	0.465	0.963	0.477	0.519	0.958	0.366	0.497	0.960
Busbar26	0.444	0.527	0.931	0.384	0.603	0.924	0.214	0.600	0.925

For the 2LG fault, during the 10% of the two lines fault the mitigation was poor as compare to locations 50% and 90% of the two lines. The highest mitigation at 10% fault on the two lines was at busbar23 from 0.130p.u. to 0.255p.u. This is 96.15% improvement in the voltage profile; however, at busbar6 the voltage dip was worsened from 0.616p.u. to 0.556p.u. This is a further worsen and deteriorating in the voltage profile which might be due to the negative effect from the grid-connected wind generators. The records at locations 50% and 90% of the two lines when multiple faults were applied indicated that the voltage profile was increased from 0.095p.u. to 0.220p.u. and 0.047p.u. to 0.141p.u. which are 131.58% and 200% improvement in voltage profile at 50% and 90% of faults on the lines respectively at busbar23. The voltage magnitude also gets worst at busbar6 for the two cases. The wind generators also have negative effects on the voltage profile after the dip, the voltage magnitude did not improve after the dip on some busbars such as busbar6, busbar8 and busbar11 when the multiple faults was applied at any of the locations (10%, 50% and 90%). In addition, the voltage magnitude deteriorated as the location increases from 10% to 90%

The detail percentage improvement due to mitigation of multiple dips with grid-connected wind generators as a result of SLG and 2LG faults from the transmission lines measured at 0.95sec and 1.65sec during and 3.00sec after the multiple dips is shown in Figure 5.2

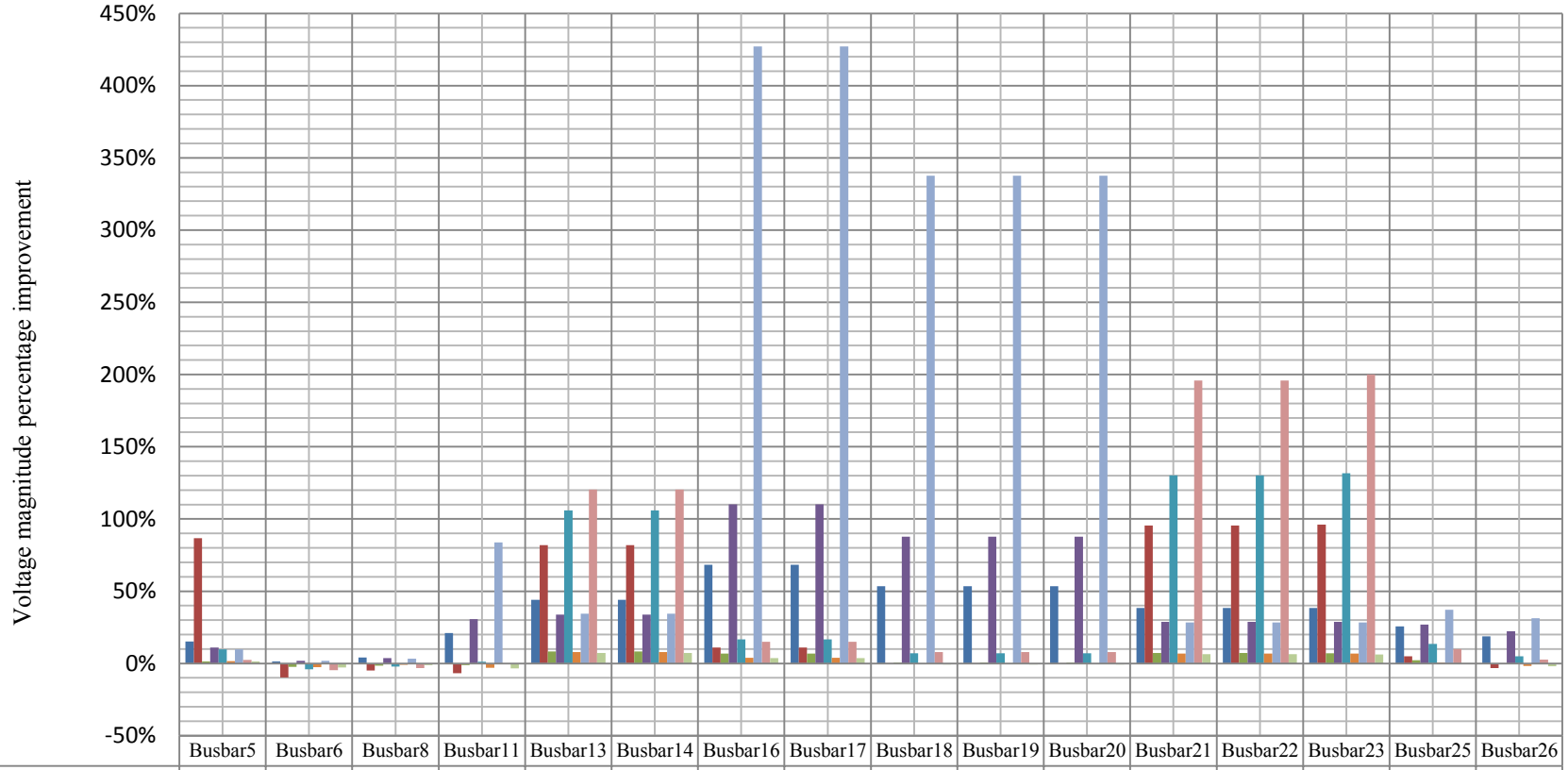

	Busbar5	Busbar6	Busbar8	Busbar11	Busbar13	Busbar14	Busbar16	Busbar17	Busbar18	Busbar19	Busbar20	Busbar21	Busbar22	Busbar23	Busbar25	Busbar26
%VD imp at 10% lines at 0.95s	15.2%	1.5%	4.2%	21.1%	44.1%	44.1%	68.4%	68.4%	53.5%	53.5%	53.5%	38.4%	38.4%	38.4%	25.6%	18.7%
%VD imp at 10% lines at 1.65s	86.7%	-9.7%	-4.8%	-6.7%	81.8%	81.8%	11.0%	11.0%	0.2%	0.2%	0.2%	95.4%	95.4%	96.2%	5.0%	-3.3%
%VD imp at 10% lines at 3.00s	1.5%	-2.4%	-1.6%	-1.1%	8.2%	8.2%	6.8%	6.8%	0.6%	0.6%	0.6%	7.2%	7.2%	7.1%	2.2%	0.0%
%VD imp at 50% lines at 0.95s	10.9%	1.9%	3.8%	30.6%	33.9%	33.9%	110.2%	110.2%	87.7%	87.7%	87.7%	28.8%	28.8%	28.8%	26.9%	22.3%
%VD imp at 50% lines at 1.65s	9.7%	-3.9%	-2.1%	1.1%	105.9%	105.9%	16.7%	16.7%	7.0%	7.0%	7.0%	130.2%	130.2%	131.6%	13.6%	4.9%
%VD imp at 50% lines at 3.00s	1.7%	-2.5%	-0.8%	-3.0%	7.8%	7.8%	4.0%	4.0%	-0.2%	-0.2%	-0.2%	6.9%	6.9%	6.9%	0.5%	-1.7%
%VD imp at 90% lines at 0.95s	9.8%	1.8%	3.4%	83.7%	34.4%	34.4%	427.1%	427.1%	337.6%	337.6%	337.6%	28.4%	28.4%	28.4%	37.1%	31.3%
%VD imp at 90% lines at 1.65s	2.4%	-4.7%	-3.2%	0.0%	120.4%	120.4%	15.0%	15.0%	7.9%	7.9%	7.9%	195.8%	195.8%	200.0%	10.0%	2.7%
%VD imp at 90% lines at 3.00s	1.3%	-2.8%	-1.2%	-3.4%	7.3%	7.3%	3.7%	3.7%	-0.7%	-0.7%	-0.7%	6.4%	6.4%	6.3%	0.2%	-2.0%

Figure 5.2: Percentage improvement of multiple dips with grid-connected wind power plants as a result of faults from the transmission lines (line8 and line15)

5.9.2 Scenario 4b: Grid-connected hydro-electric power plants

In this scenario, hydro-electric power plants are included in the test network as the only GRDGs in this study. These power plants include RDG01 which is connected to busbar26, RDG02 which is connected to busbar25, RDG08 and RDG09 which are connected to busbar20. RDG010 and RDG011 are connected to busbar21. All the grid-connected hydro-electric power plants remain connected to the network before, during and after the faults. The impact of grid-connected hydro-electric power plants is investigated using the multiple fault conditions in Table 5.3 which considers SLG and 2LG faults. Table 5.6 presents the result of voltage dip mitigation due to grid-connected hydro–electric power plants only integrated to the power network. It is observed that the hydro-electric power plants mitigate the multiple voltage dips more on the sub-transmission where they are connected as compare to the distribution network. This was observed on busbars25 (0.625p.u.) and busbar26 where the hydro plants were located.

The percentage improvement of voltage profile during and after the dip with the hydro plants connected was not as good as that of the wind plant. The grid-connected hydro generators in this study are made up of synchronous generators while the grid-connected wind generators include the DFIG, static generators with fully rated converter and synchronous generators. These types of generators have power electronics that is capable of reactive power control capability, which supported voltage profile and also have a favorable impact during voltage dip

Table 5.6: Mitigation of multiple dips with grid-connected renewable HP as a result of SLG and 2LG faults from the transmission lines (line8 and line15) measured at 0.95sec and 1.65sec during and 3.00sec after the multiple dips

Load busbar	Voltage magnitude with fault at 10% of the lines in (p.u.) at t=			Voltage magnitude with fault at 50% of the lines in (p.u.) at t=			Voltage magnitude with fault at 90% of the lines in (p.u.) at t=		
	0.95s	**1.65s**	**3.00s**	**0.95s**	**1.65s**	**3.00s**	**0.95s**	**1.65s**	**3.00s**
Busbar5	0.464	0.090	0.959	0.650	0.332	0.975	0.722	0.469	0.983
Busbar6	0.348	0.616	0.935	0.588	0.714	0.955	0.691	0.764	0.964
Busbar8	0.593	0.532	0.923	0.732	0.652	0.944	0.789	0.715	0.952
Busbar11	0.468	0.733	0.957	0.357	0.780	0.965	0.130	0.799	0.972
Busbar13	0.531	0.249	0.967	0.647	0.201	0.975	0.606	0.134	0.981
Busbar14	0.531	0.249	0.964	0.647	0.201	0.975	0.666	0.134	0.981
Busbar16	0.460	0.718	0.938	0.350	0.764	0.946	0.127	0.782	0.953
Busbar17	0.460	0.718	0.938	0.350	0.764	0.946	0.127	0.782	0.953
Busbar18	0.507	0.727	0.938	0.409	0.771	0.943	0.204	0.789	0.958
Busbar19	0.507	0.727	0.938	0.409	0.771	0.943	0.204	0.789	0.958
Busbar20	0.507	0.727	0.938	0.409	0.771	0.943	0.204	0.789	0.958
Busbar21	0.525	0.207	0.965	0.654	0.154	0.976	0.683	0.081	0.982
Busbar22	0.525	0.207	0.965	0.654	0.154	0.976	0.683	0.081	0.982
Busbar23	0.520	0.200	0.963	0.650	0.154	0.975	0.679	0.071	0.980
Busbar25	0.625	0.636	0.985	0.631	0.641	0.990	0.559	0.625	0.994
Busbar26	0.769	0.875	1.003	0.752	0.892	1.002	0.687	0.895	1.005

Figure 5.3 shows the percentage improvement as a result of grid-connected wind generators during and after multiple voltage dip mitigations.

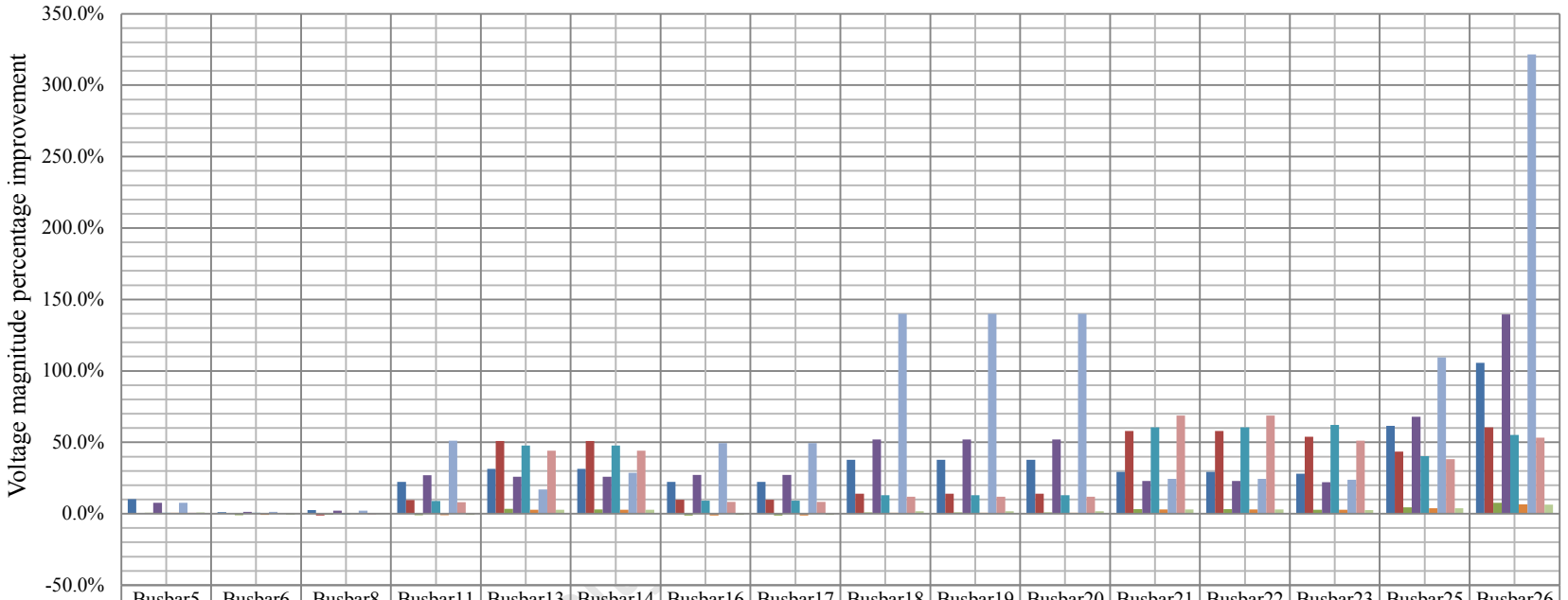

	Busbar5	Busbar6	Busbar8	Busbar11	Busbar13	Busbar14	Busbar16	Busbar17	Busbar18	Busbar19	Busbar20	Busbar21	Busbar22	Busbar23	Busbar25	Busbar26
%VD imp at 50% lines 0.95s	10.2%	1.2%	2.6%	22.2%	31.4%	31.4%	22.3%	22.3%	37.8%	37.8%	37.8%	29.3%	29.3%	28.1%	61.5%	105.6%
%VD imp at 50% lines 1.65s	0.0%	0.0%	-1.3%	9.6%	50.9%	50.9%	9.8%	9.8%	13.9%	13.9%	13.9%	58.0%	58.0%	53.8%	43.6%	60.6%
%VD imp at 50% lines 3.00s	0.6%	-1.1%	-0.6%	-1.1%	3.4%	3.1%	-1.2%	-1.2%	1.0%	1.0%	1.0%	3.2%	3.2%	2.9%	4.6%	7.7%
%VD imp at 50% lines 0.95s	7.6%	1.4%	2.2%	27.0%	25.9%	25.9%	27.3%	27.3%	52.0%	52.0%	52.0%	22.9%	22.9%	22.2%	67.8%	139.5%
%VD imp at 50% lines 1.65s	0.6%	0.6%	-0.5%	8.9%	47.8%	47.8%	9.1%	9.1%	12.9%	12.9%	12.9%	60.4%	60.4%	62.1%	40.3%	55.1%
%VD imp at 50% lines 3.00s	0.7%	-0.7%	-0.1%	-1.1%	2.8%	2.8%	-1.1%	-1.1%	0.6%	0.6%	0.6%	3.0%	3.0%	2.8%	3.9%	6.6%
%VD imp at 90% lines 0.95s	7.6%	1.3%	2.1%	51.2%	17.0%	28.6%	49.4%	49.4%	140.0%	140.0%	140.0%	24.4%	24.4%	23.7%	109.4%	321.5%
%VD imp at 90% lines 1.65s	0.6%	0.4%	-0.4%	8.1%	44.1%	44.1%	8.3%	8.3%	11.9%	11.9%	11.9%	68.8%	68.8%	51.1%	38.3%	53.3%
%VD imp at 90% lines 3.00s	0.8%	-0.5%	-0.1%	-0.9%	2.8%	2.8%	-0.8%	-0.8%	1.8%	1.8%	1.8%	2.9%	2.9%	2.6%	3.8%	6.5%

Figure 5.3: Percentage improvement of multiple dips with grid-connected renewable hydro generators as a result of faults from the transmission lines (line8 and line15)

5.9.3 Scenario 4c: Grid-connected solar PV power plants

The following grid-connected solar PV power plants are installed in the test network to supply power to critical loads. Solar PV plants RDG03 and RDG04 are connected at busbar16, RDG05 and RDG06 are connected at busbar22, and RDG07 is connected at busbar23. The PV generators lake reactive power and voltage support during and after the voltage dip. All the grid-connected solar PV power plants remain connected to the network before, during and after the study. The retained r.m.s voltage magnitude at the load busbars measured just like in other case studies. The result shows that the mitigation ability of solar PV plants is so low when compare with wind and hydro power plants. This is indicated in Table 5.7 and Figure 5.4. The Table and the Figure show the improved voltage magnitude and improved voltage percentage respectively. The highest percentage mitigation was experience at busbar16 and busbar17 from 0.085p.u. to 0.099 which are 16.47%. The voltage profile does not become worsened during and after mitigation with the grid-connected PV unlike the wind power plants, however, the voltage profile deteriorates at busbar18, busbar19 and busbar20 during and after the 2LG fault at 10% location of the two lines.

Table 5.7: Mitigation of multiple dips with grid-connected PV generator as a result of SLG and 2LG faults from the transmission lines (line8 and line15) measured at 0.95sec and 1.65sec during and 3.00sec after the multiple dips

Load busbar	Voltage magnitude with fault at 10% of the lines in (p.u.) at t=			Voltage magnitude with fault at 50% of the lines in (p.u.) at t=			Voltage magnitude with fault at 90% of the lines in (p.u.) at t=		
	0.95s	**1.65s**	**3.00s**	**0.95s**	**1.65s**	**3.00s**	**0.95s**	**1.65s**	**3.00s**
Busbar5	0.436	0.094	0.960	0.618	0.332	0.979	0.686	0.469	0.987
Busbar6	0.350	0.610	0.945	0.585	0.712	0.963	0.688	0.761	0.972
Busbar8	0.586	0.536	0.930	0.724	0.655	0.950	0.781	0.718	0.959
Busbar11	0.385	0.669	0.967	0.284	0.716	0.976	0.092	.739	0.981
Busbar13	0.425	0.170	0.950	0.537	0.141	0.967	0.544	0.096	0.975
Busbar14	0.425	0.170	0.950	0.537	0.141	0.967	0.544	0.096	0.975
Busbar16	0.376	0.664	0.953	0.286	0.710	0.965	0.099	0.732	0.969
Busbar17	0.376	0.664	0.953	0.286	0.710	0.965	0.099	0.732	0.969
Busbar18	0.370	0.631	0.923	0.272	0.688	0.938	0.090	0.705	0.941
Busbar19	0.370	0.631	0.923	0.272	0.688	0.938	0.090	0.705	0.941
Busbar20	0.370	0.631	0.923	0.272	0.688	0.938	0.090	0.705	.941
Busbar21	0.430	0.134	0.952	0.557	0.100	0.969	0.578	0.051	0.977
Busbar22	0.430	0.134	0.952	0.557	0.100	0.969	0.578	0.051	0.977
Busbar23	0.430	0.134	0.953	0.557	0.100	0.970	0.578	0.051	0.978
Busbar25	0.394	0.443	0.945	0.385	0.457	0.959	0.280	0.452	0.965
Busbar26	0.379	0.545	0.931	0.320	0.575	0.942	0.170	0.584	0.947

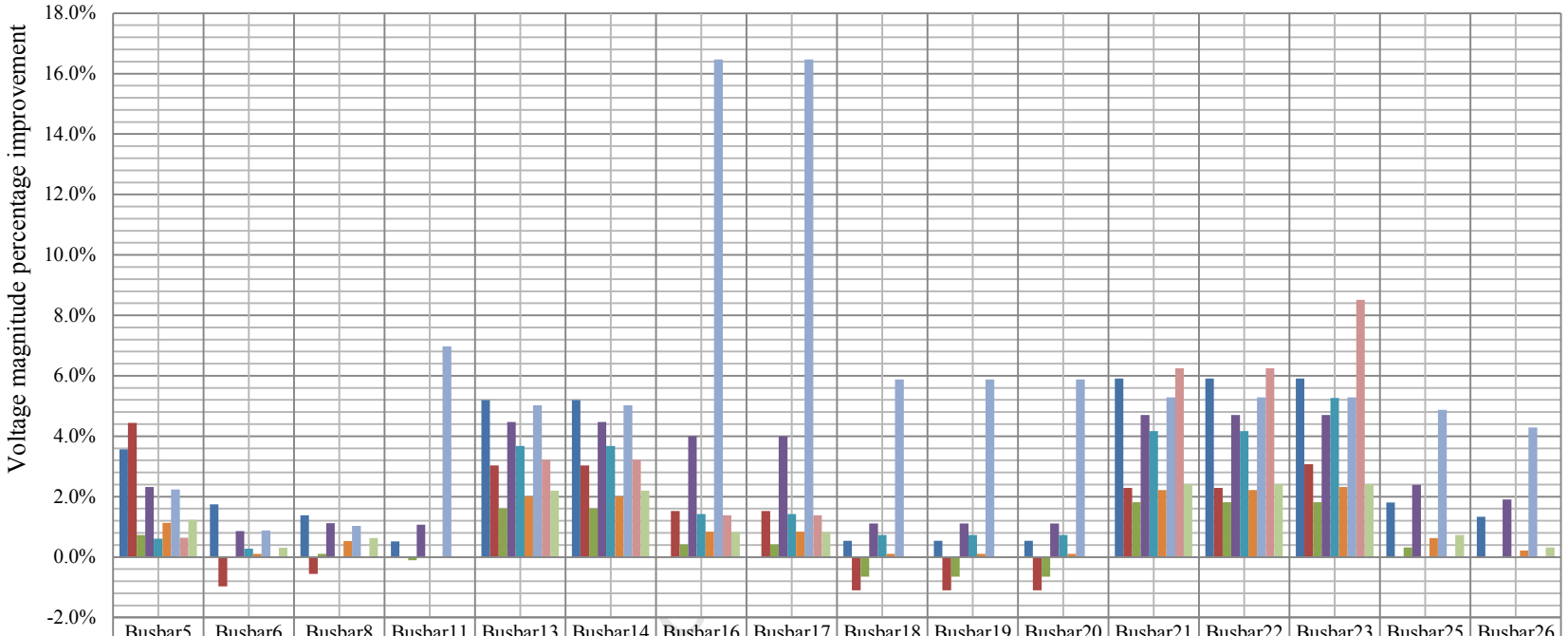

	Busbar5	Busbar6	Busbar8	Busbar11	Busbar13	Busbar14	Busbar16	Busbar17	Busbar18	Busbar19	Busbar20	Busbar21	Busbar22	Busbar23	Busbar25	Busbar26
%VD imp at 10% lines 0.95s	3.6%	1.7%	1.4%	0.5%	5.2%	5.2%	0.0%	0.0%	0.5%	0.5%	0.5%	5.9%	5.9%	5.9%	1.8%	1.3%
%VD imp at 10% lines 1.65s	4.4%	-1.0%	-0.6%	0.0%	3.0%	3.0%	1.5%	1.5%	-1.1%	-1.1%	-1.1%	2.3%	2.3%	3.1%	0.0%	0.0%
%VD imp at 10% lines 3.00s	0.7%	0.0%	0.1%	-0.1%	1.6%	1.6%	0.4%	0.4%	-0.6%	-0.6%	-0.6%	1.8%	1.8%	1.8%	0.3%	0.0%
%VD imp at 50% lines 0.95s	2.3%	0.9%	1.1%	1.1%	4.5%	4.5%	4.0%	4.0%	1.1%	1.1%	1.1%	4.7%	4.7%	4.7%	2.4%	1.9%
%VD imp at 50% lines 1.65s	0.6%	0.3%	0.0%	0.0%	3.7%	3.7%	1.4%	1.4%	0.7%	0.7%	0.7%	4.2%	4.2%	5.3%	0.0%	0.0%
%VD imp at 50% lines 3.00s	1.1%	0.1%	0.5%	0.0%	2.0%	2.0%	0.8%	0.8%	0.1%	0.1%	0.1%	2.2%	2.2%	2.3%	0.6%	0.2%
%VD imp at 90% lines 0.95s	2.2%	0.9%	1.0%	7.0%	5.0%	5.0%	16.5%	16.5%	5.9%	5.9%	5.9%	5.3%	5.3%	5.3%	4.9%	4.3%
%VD imp at 90% lines 1.65s	0.6%	0.0%	0.0%	0.0%	3.2%	3.2%	1.4%	1.4%	0.0%	0.0%	0.0%	6.2%	6.2%	8.5%	0.0%	0.0%
%VD imp at 90% lines 3.00s	1.2%	0.3%	0.6%	0.0%	2.2%	2.2%	0.8%	0.8%	0.0%	0.0%	0.0%	2.4%	2.4%	2.4%	0.7%	0.3%

Figure 5.4: Percentage improvement of multiple dips with grid-connected PV generators as a result of faults from the transmission lines (line8 and line15)

The PV plant does not support the voltage profile during the mitigation of voltage dip, and this is one of its weaknesses as it lacks reactive power and the ability to support the grid during the multiple dips.

5.9.4 Scenario 4d: Grid-connected wind and hydro-electric plants

This scenario investigates the integration of both the wind and hydro power. This combination shows a better improvement on voltage profile. The result is presented in Table 5.8. Figure 5.5 shows the percentage improvement as a result of mitigation with grid-connected wind and hydro generators. The highest improvement of voltage dip was recorded during the SLG fault at location 90%; this was at busbar16, busbar17, busbar18, busbar19 and busbar20. However, the voltage profile was further deteriorated during and after the 2LG fault at location 10%.

Table 5.8: Mitigation of multiple dips with Wind and Hydro grid-connected plants as a result of SLG and 2LG faults from the transmission lines (line8 and line15) measured at 0.95sec and 1.65sec during and 3.00sec after the multiple dips

Load busbar	Voltage magnitude with fault at 10% of the lines in (p.u.) at t=			Voltage magnitude with fault at 50% of the lines in (p.u.) at t=			Voltage magnitude with fault at 90% of the lines in (p.u.) at t=		
	0.95s	1.65s	3.00s	0.95s	1.65s	3.00s	0.95s	1.65s	3.00s
Busbar5	0.513	0.077	0.725	0.700	0.308	1.004	0.770	0.421	1.001
Busbar6	0.353	0.508	0.652	0.599	0.650	0.953	0.702	0.670	0.952
Busbar8	0.613	0.475	0.739	0.754	0.608	0.946	0.811	0.650	0.947
Busbar11	0.544	0.550	0.308	0.435	0.719	0.990	0.193	0.700	0.982
Busbar13	0.665	0.283	0.773	0.773	0.258	1.057	0.792	0.169	1.050
Busbar14	0.665	0.283	0.773	0.773	0.258	1.057	0.792	0.169	1.050
Busbar16	0.687	0.665	0.507	0.623	0.806	1.030	0.471	0.791	1.021
Busbar17	0.687	0.665	0.507	0.623	0.806	1.030	0.471	0.791	1.021
Busbar18	0.645	0.589	0.434	0.577	0.749	0.972	0.420	0.734	0.968
Busbar19	0.645	0.589	0.434	0.577	0.749	0.972	0.420	0.734	0.968
Busbar20	0.645	0.589	0.434	0.577	0.749	0.972	0.420	0.734	0.968
Busbar21	0.642	0.323	0.769	0.764	0.192	1.049	0.793	0.097	1.043
Busbar22	0.642	0.232	0.769	0.764	0.192	1.049	0.793	0.097	1.043
Busbar23	0.637	0.225	0.766	0.760	0.184	1.047	0.790	0.088	1.041
Busbar25	0.664	0.493	0.646	0.670	0.578	1.017	0.595	0.536	1.009
Busbar26	0.791	0.744	0.799	0.772	0.837	1.055	0.699	0.817	1.052

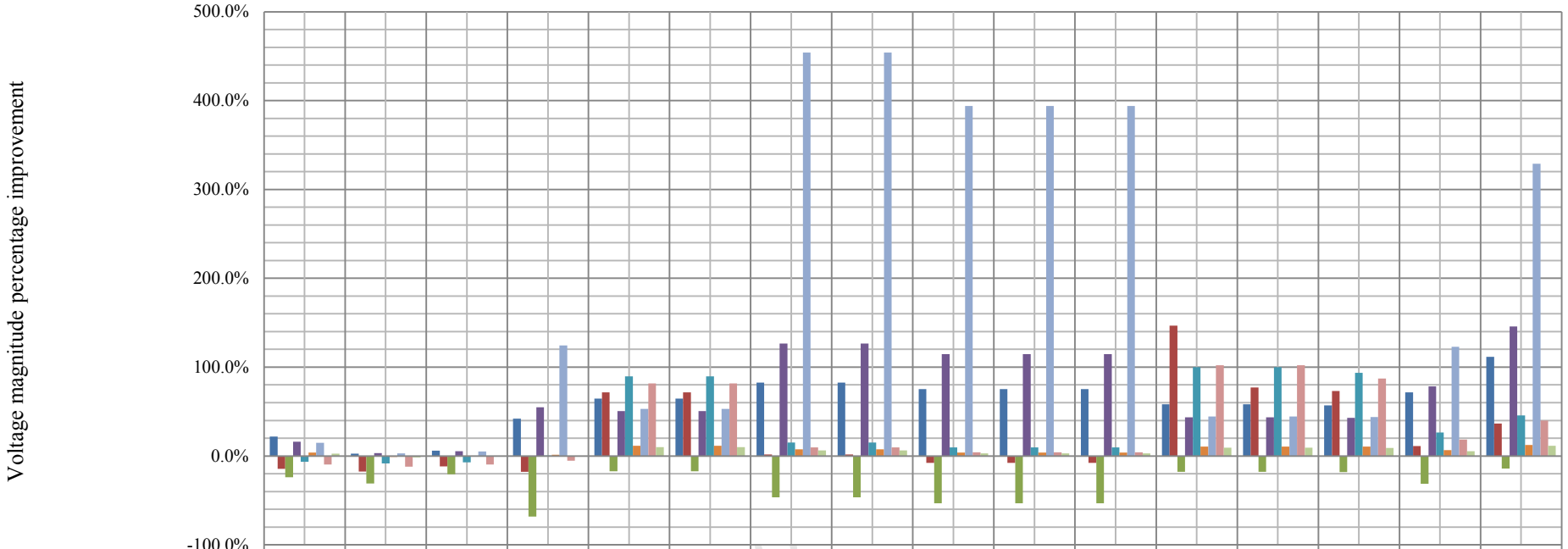

	Busbar5	Busbar6	Busbar8	Busbar11	Busbar13	Busbar14	Busbar16	Busbar17	Busbar18	Busbar19	Busbar20	Busbar21	Busbar22	Busbar23	Busbar25	Busbar26
%VD imp at 10% lines 0.95s	21.9%	2.6%	6.1%	42.0%	64.6%	64.6%	82.7%	82.7%	75.3%	75.3%	75.3%	58.1%	58.1%	56.9%	71.6%	111.5%
%VD imp at 10% lines 1.65s	-14.4%	-17.5%	-11.9%	-17.8%	71.5%	71.5%	1.7%	1.7%	-7.7%	-7.7%	-7.7%	146.6%	77.1%	73.1%	11.3%	36.5%
%VD imp at 10% lines 3.00s	-23.9%	-31.0%	-20.5%	-68.2%	-17.3%	-17.3%	-46.6%	-46.6%	-53.3%	-53.3%	-53.3%	-17.8%	-17.8%	-18.2%	-31.4%	-14.2%
%VD imp at 50% lines 0.95s	15.9%	3.3%	5.3%	54.8%	50.4%	50.4%	126.5%	126.5%	114.5%	114.5%	114.5%	43.6%	43.6%	42.9%	78.2%	145.9%
%VD imp at 50% lines 1.65s	-6.7%	-8.5%	-7.2%	0.4%	89.7%	89.7%	15.1%	15.1%	9.7%	9.7%	9.7%	100.0%	100.0%	93.7%	26.5%	45.6%
%VD imp at 50% lines 3.00s	3.7%	-0.9%	0.1%	1.4%	11.5%	11.5%	7.6%	7.6%	3.7%	3.7%	3.7%	10.7%	10.7%	10.4%	6.7%	12.2%
%VD imp at 90% lines 0.95s	14.8%	2.9%	4.9%	124.4%	52.9%	52.9%	454.1%	454.1%	394.1%	394.1%	394.1%	44.4%	44.4%	43.9%	122.8%	328.8%
%VD imp at 90% lines 1.65s	-9.7%	-12.0%	-9.5%	-5.3%	81.7%	81.7%	9.6%	9.6%	4.1%	4.1%	4.1%	102.1%	102.1%	87.2%	18.6%	39.9%
%VD imp at 90% lines 3.00s	2.7%	-1.8%	-0.6%	0.1%	10.1%	10.1%	6.2%	6.2%	2.9%	2.9%	2.9%	9.3%	9.3%	9.0%	5.3%	11.4%

Figure 5.5: Percentage improvement of multiple dips with grid-connected wind and hydro generators as a result of faults from the transmission lines (line8 and line15)

5.9.5 Scenario 4e: All the grid-connected renewable generators

The effect of all the generators is shown in Table 5.9 and Figure 5.6. Connecting all the generators simultaneously does not improve the voltage profile during and after the dip. The worst case was during and after the 2LG fault at location 90% of the lines, the voltage profile deteriorated as less as 51.38% of the voltage dip due to the fault. However, there was an improvement during SLG fault on any of the three locations (10%, 50% and 90%) studied.

Table 5.9: Mitigation of multiple dips with all the grid-connected renewable generators as a result of SLG and 2LG faults from the transmission lines (line8 and line15) measured at 0.95sec and 1.65sec during and 3.00sec after the multiple dips

Load busbar	Voltage magnitude with fault at 10% of the lines in (p.u.) at			Voltage magnitude with fault at 50% of the lines in (p.u.) at			Voltage magnitude with fault at 90% of the lines in (p.u.) at		
	0.95s	**1.65s**	**3.00s**	**0.95s**	**1.65s**	**3.00s**	**0.95s**	**1.65s**	**3.00s**
Busbar5	0.486	0.067	0.887	0.867	0.277	0.900	0.836	0.363	0.733
Busbar6	0.351	0.434	0.858	0.591	0.587	0.877	0.691	0.574	0.697
Busbar8	0.600	0.445	0.867	0.737	0.567	0.874	0.792	0.590	0.758
Busbar11	0.550	0.317	0.834	0.438	0.606	0.887	0.193	0.515	0.477
Busbar13	0.619	0.204	0.916	0.723	0.206	0.935	0.743	0.131	0.756
Busbar14	0.619	0.204	0.916	0.723	0.206	0.935	0.743	0.131	0.756
Busbar16	0.686	0.479	0.878	0.621	0.707	0.930	0.471	0.637	0.650
Busbar17	0.686	0.479	0.878	0.621	0.707	0.930	0.471	0.637	0.650
Busbar18	0.648	0.391	0.822	0.578	0.649	0.856	0.424	0.577	0.499
Busbar19	0.648	0.391	0.822	0.578	0.649	0.856	0.424	0.577	0.499
Busbar20	0.648	0.391	0.822	0.578	0.649	0.856	0.429	0.577	0.499
Busbar21	0.589	0.160	0.902	0.708	0.145	0.920	0.737	0.070	0.745
Busbar22	0.589	0.160	0.902	0.708	0.145	0.920	0.737	0.070	0.745
Busbar23	0.584	0.153	0.900	0.704	0.137	0.918	0.734	0.062	0.792
Busbar25	0.670	0.391	0.904	0.675	0.530	0.951	0.602	0.462	0.712
Busbar26	0.796	0.649	0.909	0.776	0.781	1.034	0.703	0.729	0.877

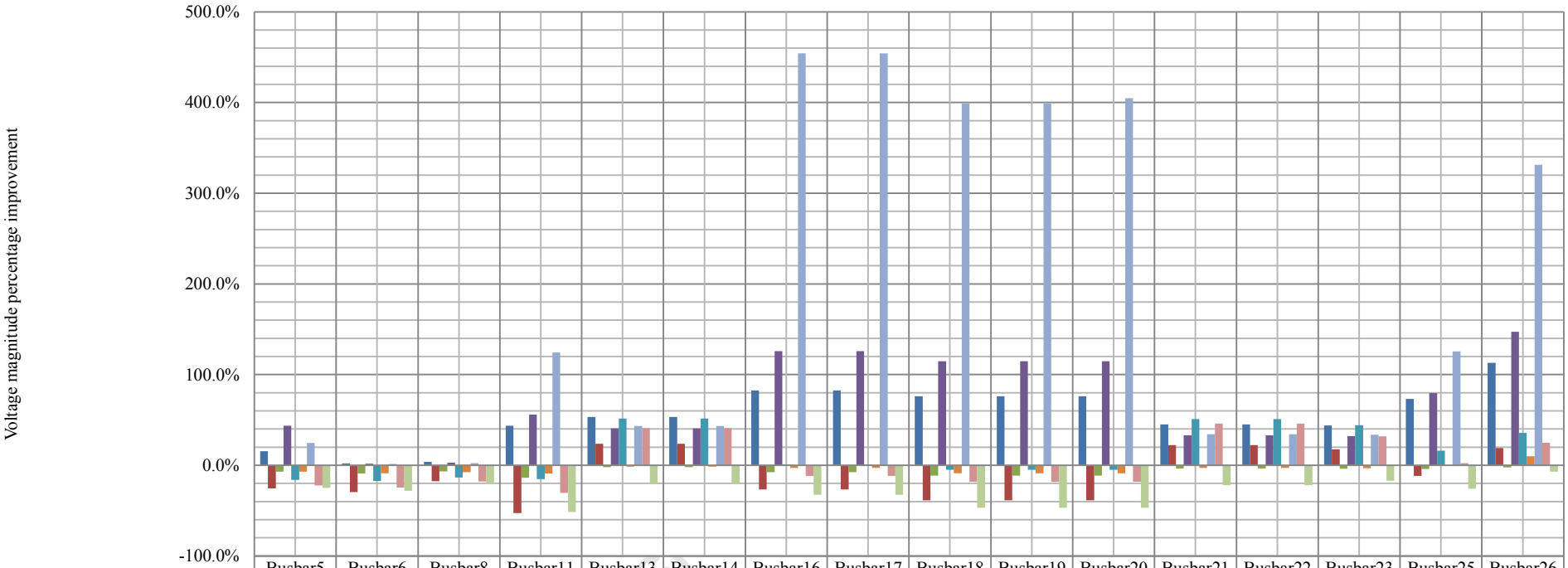

	Busbar5	Busbar6	Busbar8	Busbar11	Busbar13	Busbar14	Busbar16	Busbar17	Busbar18	Busbar19	Busbar20	Busbar21	Busbar22	Busbar23	Busbar25	Busbar26
%VD imp at 10% lines 0.95s	15.4%	2.0%	3.8%	43.6%	53.2%	53.2%	82.4%	82.4%	76.1%	76.1%	76.1%	45.1%	45.1%	43.8%	73.1%	112.8%
%VD imp at 10% lines 1.65s	-25.6%	-29.5%	-17.4%	-52.6%	23.6%	23.6%	-26.8%	-26.8%	-38.7%	-38.7%	-38.7%	22.1%	22.1%	17.7%	-11.7%	19.1%
%VD imp at 10% lines 3.00s	-6.9%	-9.2%	-6.7%	-13.8%	-2.0%	-2.0%	-7.5%	-7.5%	-11.5%	-11.5%	-11.5%	-3.5%	-3.5%	-3.8%	-4.0%	-2.4%
%VD imp at 50% lines 0.95	43.5%	1.9%	2.9%	55.9%	40.7%	40.7%	125.8%	125.8%	114.9%	114.9%	114.9%	33.1%	33.1%	32.3%	79.5%	147.1%
%VD imp at 50% lines 1.65s	-16.1%	-17.3%	-13.4%	-15.4%	51.5%	51.5%	1.0%	1.0%	-5.0%	-5.0%	-5.0%	51.0%	51.0%	44.2%	16.0%	35.8%
%VD imp at 50% lines 3.00s	-7.0%	-8.8%	-7.5%	-9.1%	-1.4%	-1.4%	-2.8%	-2.8%	-8.6%	-8.6%	-8.6%	-3.0%	-3.0%	-3.2%	-0.2%	10.0%
%VD imp at 90% lines 0.95s	24.6%	1.3%	2.5%	124.4%	43.4%	43.4%	454.1%	454.1%	398.8%	398.8%	404.7%	34.2%	34.2%	33.7%	125.5%	331.3%
%VD imp at 90% lines 1.65s	-22.1%	-24.6%	-17.8%	-30.3%	40.9%	40.9%	-11.8%	-11.8%	-18.2%	-18.2%	-18.2%	45.8%	45.8%	31.9%	2.2%	24.8%
%VD imp at 90% lines 3.00s	-24.8%	-28.1%	-20.5%	-51.4%	-20.8%	-20.8%	-32.4%	-32.4%	-47.0%	-47.0%	-47.0%	-21.9%	-21.9%	-17.1%	-25.7%	-7.1%

Figure 5.6: Percentage improvement of multiple dips with all the grid-connected generators as a result of faults from the transmission lines (line8 and line15)

5.10 Summary and discussion

The result of percentage improvement shown in Figures 5.2, 5.3 and 5.4 indicated that the grid-connected wind generators mitigate the multiple voltage dips far well than the hydro plant or the PV plant; this might be due to the type of wind energy conversion system technology used for the wind plant. The wind plants within the power network are made up of wind static generators with fully rated power electronics converter that enhance voltage support, variable-speed synchronous wind generators which are better than the fixed-speed wind generator during disturbances and also the DFIG systems which incorporate power electronic convertor that improved the DFIG reactive power regulation capability during the multiple voltage dips.

The PV plants do not have an impact on the voltage dip at all, since it lacks reactive power capability during a voltage dip event. Hydro plants do not provide adequate mitigation on the distribution busbars when compare to the wind generators. The connection of both wind and hydro plants improved the voltage profile during the dip as compare to wind plants only; however, the voltage profile deteriorated after the dip at location 10% of the two lines, and this was not so for the locations 50% and 90% as the voltage profile gets better.

When all the three plants (wind, hydro and PV plants) were connected, voltage dip for the first fault, SLG was improved for all the three locations (10%, 50% and 90%) has seen from Figure 5.4, however, the second dip cursed by 2LG was not mitigated rather it deteriorates the voltage profile along all the three locations. In addition, the post dip voltage profile becomes worse and a more severe voltage profile than the one caused as a result of the fault was experienced, which was due to integrating all the plants to the grid at the same time.

The measured voltage dip at the distribution network was not as severe as that of transmission network; this might be due to the fact that the faults emanated from the transmission grid. In addition, the present of GRDGs within the distribution grid has contributed to mitigation of voltage dip and providing ancillary services support to improve power quality of the system when compare to the transmission grid.

5.11 Scenario 5:

Impact of GRDGs on mitigation of multiple voltage dips due to faults in the distribution side of the test network

This scenario investigates the impact of various GRDGs on mitigation of multiple voltage dips due to faults in the distribution side of the test network.The study is based on the multiple voltage dip conditions in Table 5.4 where multiple faults are caused by different types of faults at location 50% on different distribution lines. The different cases of GRDGs considered are:

a. Grid-connected wind power plants (DFIG, PMSG and static generator)
   b. Grid-connected hydro-electric power plants
   c. Grid-connected solar PV power plants
   d. Grid-connected wind and hydro-electric generators
   e. All the GRDGs together

5.11.1 Scenario 5a: Grid-connected wind power plants

In this scenario, only the grid-connected wind power plants are connected. This study uses the multiple voltage dip conditions in Table 5.4 where multiple faults are caused by different types of faults at location 50% on different distribution lines.Table 5.10 shown the recorded voltage magnitudes during and after mitigation of voltage dips on different distribution lines and at various faults with grid-connected wind generators.

Table 5.10: Mitigation of multiple dips with grid-connected wind power plants as a result of multiple faults on various distribution lines at 50% of each line measured at 0.95sec and 1.65sec during and 3.00sec after the multiple dips

Load busbar	Voltage magnitude with 2P and SLG faults on line10 and line13 respectively in (p.u.) at t=			Voltage magnitude with 3P and 2LG faults on line12 and line14 respectively in (p.u.) at t=			Voltage magnitude with SLG and 2P faults on line9 and line11 respectively in (p.u.) at t=		
	0.95s	1.65s	3.00s	0.95s	1.65s	3.00s	0.95s	1.65s	3.00s
Busbar5	0.714	0.942	1.017	0.949	0.603	0.974	0.923	0.960	1.034
Busbar6	0.841	0.908	0.973	0.914	0.781	0.931	0.916	0.922	0.992
Busbar8	0.820	0.922	0.970	0.935	0.763	0.934	0.933	0.938	0.988
Busbar11	0.816	0.746	0.972	0.733	0.745	0.902	0.744	0.785	0.994
Busbar13	0.494	0.943	1.053	0.948	0.252	1.002	0.847	0.967	1.068
Busbar14	0.494	0.943	1.053	0.948	0.252	1.002	0.847	0.967	1.068
Busbar16	0.869	0.859	1.000	0.807	0.835	0.984	0.838	0.465	1.021
Busbar17	0.869	0.859	1.000	0.807	0.835	0.984	0.838	0.465	1.021

Busbar18	0.823	0.000	0.952	0.000	0.673	0.693	0.798	0.803	0.986
Busbar19	0.823	0.000	0.952	0.000	0.673	0.693	0.798	0.803	0.986
Busbar20	0.823	0.000	0.952	0.000	0.673	0.693	0.798	0.803	0.986
Busbar21	0.500	0.942	1.049	0.948	0.000	0.995	0.863	0.964	1.060
Busbar22	0.500	0.942	1.044	0.948	0.000	0.995	0.863	0.964	1.060
Busbar23	0.500	0.943	1.004	0.948	0.182	0.995	0.8/63	0.965	1.060
Busbar25	0.635	0.821	0.988	0.8250	0.513	0.927	0.512	0.851	1.007
Busbar26	0.781	0.781	0.963	0.777	0.614	0.892	0.000	0.812	0.971

From this result, it was observed that the wind generators mitigated the multiple voltage dips better around the distribution network, although the faults emanated from the distribution network. A voltage dip mitigation level of about 24.75% was seen at busbar13 and busbar14 within the distribution grid with 2LG fault on line14, while a further reduction of voltage magnitude was experienced on all the transmission busbars except busbar23, which might be due to presence of a grid-connected DFIG wind plant with power electronic interface (RDG 016) at busbar23.

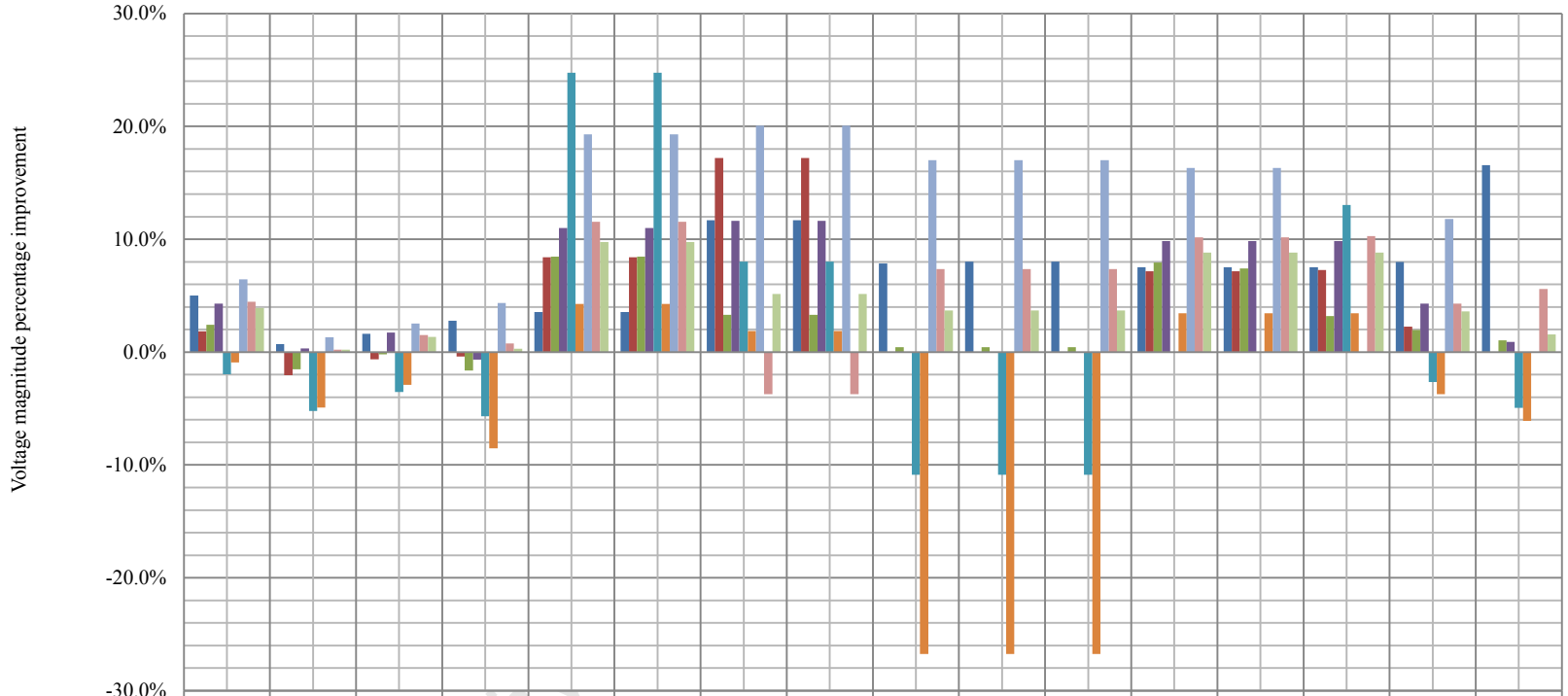

	Busbar5	Busbar6	Busbar8	Busbar11	Busbar13	Busbar14	Busbar16	Busbar17	Busbar18	Busbar19	Busbar20	Busbar21	Busbar22	Busbar23	Busbar25	Busbar26
2P and SLG faults on line10 and line13 at 0.95s	5.0%	0.7%	1.6%	2.8%	3.6%	3.6%	11.7%	11.7%	7.9%	8.0%	8.0%	7.5%	7.5%	7.5%	8.0%	16.6%
2P and SLG faults on line10 and line13 at 1.65s	1.8%	-2.0%	-0.6%	-0.4%	8.4%	8.4%	17.2%	17.2%	0.0%	0.0%	0.0%	7.2%	7.2%	7.3%	2.2%	0.0%
2P and SLG faults on line10 and line13 at 3.00s	2.4%	-1.5%	-0.2%	-1.6%	8.4%	8.4%	3.3%	3.3%	0.4%	0.4%	0.4%	7.9%	7.4%	3.2%	2.0%	1.0%
3P and 2LG faults on line12 and line14 at 0.95s	4.3%	0.3%	1.7%	-0.7%	11.0%	11.0%	11.6%	11.6%	0.0%	0.0%	0.0%	9.8%	9.8%	9.8%	4.3%	0.9%
3P and 2LG faults on line12 and line14 at 1.65s	-2.0%	-5.2%	-3.5%	-5.7%	24.8%	24.8%	8.0%	8.0%	-10.9%	-10.9%	-10.9%	0.0%	0.0%	13.0%	-2.7%	-5.0%
3P and 2LG faults on line12 and line14 at 3.00s	-0.9%	-4.9%	-2.9%	-8.5%	4.3%	4.3%	1.9%	1.9%	-26.7%	-26.7%	-26.7%	3.4%	3.4%	3.4%	-3.7%	-6.1%
SLG and 2P faults on line9 and line11 at 0.95s	6.5%	1.3%	2.5%	4.3%	19.3%	19.3%	20.1%	20.1%	17.0%	17.0%	17.0%	16.3%	16.3%	0.0%	11.8%	0.0%
SLG and 2P faults on line9 and line11 at 1.65s	4.5%	0.2%	1.5%	0.8%	11.5%	11.5%	-3.7%	-3.7%	7.4%	7.4%	7.4%	10.2%	10.2%	10.3%	4.3%	5.6%
SLG and 2P faults on line9 and line11 at 3.00s	3.9%	0.2%	1.3%	0.3%	9.8%	9.8%	5.1%	5.1%	3.7%	3.7%	3.7%	8.8%	8.8%	8.8%	3.6%	1.6%

Figure 5.7: Percentage improvement of multiple voltage dip mitigation with grid-connected wind generators as a result faults from the distribution network

5.11.2 Scenario 5b: Grid-connected hydro-electric power plants

This scenario investigates the impact of hydro-electric power on voltage dip mitigation. Table 5.11 and Figure 5.8 show mitigation of multiple voltage dip as a result of grid-connected hydro generators within the power network. The different lines within the distribution network were investigated as shown in Table 5.11at 50% of each line and with different fault types. The hydro- electric plants mitigate voltage dip better on the sub-transmission network where some of the plants are located such as busbar 25 and busbar 26. The percentage improvement is 28.27% and 41.95% on these busbars, however, all the distribution busbsrs such as 15, 16, 18, 19 and 20 have less than 15% percentage voltage profile improvement.

Table 5.11: Mitigation of multiple dips with grid-connected renewable hydro-electric power plants as a result of multiple faults on various distribution lines at 50% of each line measured at 0.95sec and 1.65sec during and 3.00sec after the multiple dips

Load busbar	Voltage magnitude with 2P and SLG faults on line10 and line13 respectively in (p.u.) at t=			Voltage magnitude with 3P and 2LG faults on line12 and line14 respectively in (p.u.) at t=			Voltage magnitude with SLG and 2P faults on line9 and line11 respectively in (p.u.) at t=		
	0.95s	1.65s	3.00s	0.95s	1.65s	3.00s	0.95s	1.65s	3.00s
Busbar5	0.695	0.946	0.992	0.929	0.624	0.988	0.858	0.931	0.995
Busbar6	0.846	0.929	0.976	0.914	0.288	0.971	0.880	0.913	0.979
Busbar8	0.815	0.933	0.964	0.926	0.792	0.760	0.894	0.920	0.968
Busbar11	0.839	0.768	0.975	0.742	0.836	0.770	0.687	0.794	0.977
Busbar13	0.475	0.929	0.985	0.899	0.231	0.982	0.725	0.914	0.987
Busbar14	0.475	0.929	0.985	0.899	0.231	0.982	0.725	0.914	0.987
Busbar16	0.823	0.752	0.956	0.727	0.819	0.952	0.673	0.473	0.958
Busbar17	0.823	0.752	0.956	0.727	0.819	0.952	0.673	0.473	0.958
Busbar18	0.847	0.000	0.962	0.000	0.821	0.950	0.709	0.786	0.963
Busbar19	0.847	0.000	0.962	0.000	0.821	0.950	0.709	0.786	0.963
Busbar20	0.847	0.000	0.962	0.000	0.821	0.950	0.709	0.786	0.963
Busbar21	0.469	0.934	0.987	0.906	0.000	0.983	0.758	0.918	0.989
Busbar22	0.469	0.934	0.987	0.906	0.000	0.983	0.758	0.918	0.989
Busbar23	0.470	0.932	0.986	0.905	0.175	0.982	0.758	0.918	0.989
Busbar25	0.672	0.913	0.991	0.864	0.676	0.993	0.498	0.905	0.993
Busbar26	0./865	0.977	0.992	0.904	0.917	1.000	0.200	0.959	1.001

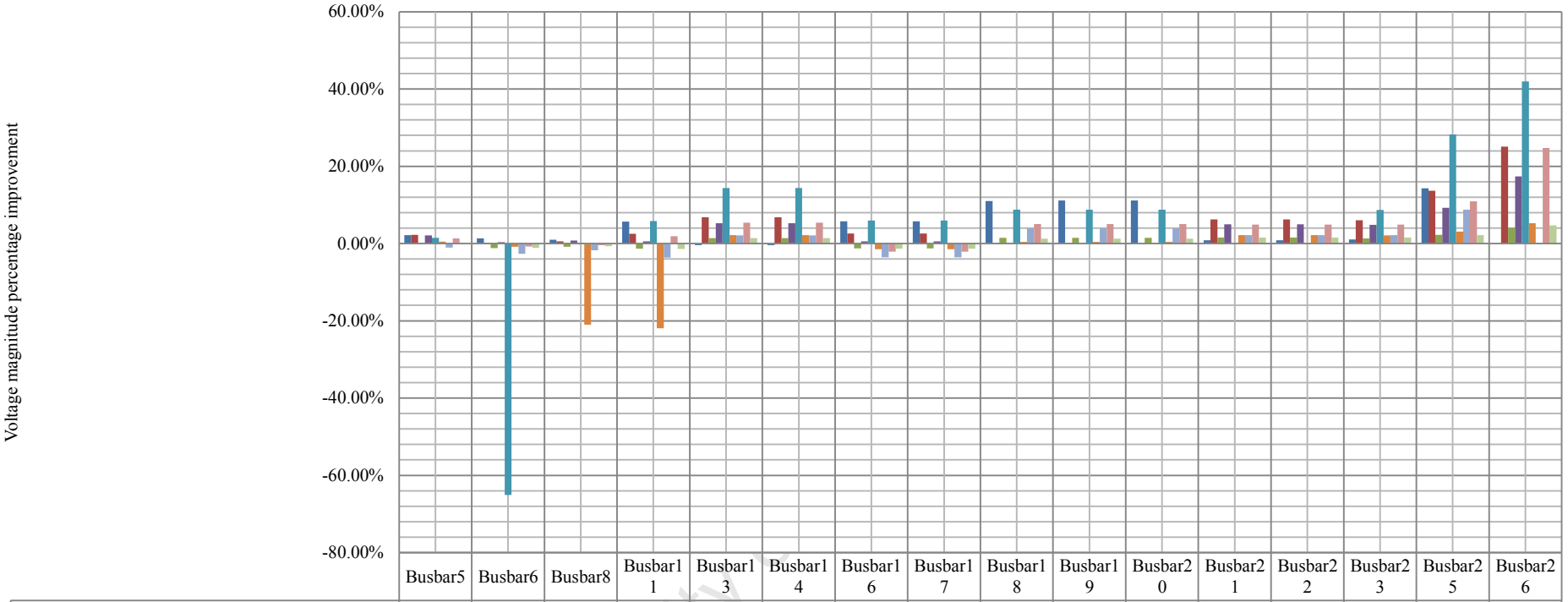

	Busbar5	Busbar6	Busbar8	Busbar11	Busbar13	Busbar14	Busbar16	Busbar17	Busbar18	Busbar19	Busbar20	Busbar21	Busbar22	Busbar23	Busbar25	Busbar26
2P and SLG faults on line10 and line13 at 0.95s	2.21%	1.32%	0.99%	5.67%	-0.42%	-0.42%	5.78%	5.78%	11.01%	11.15%	11.15%	0.86%	0.86%	1.08%	14.29%	0.00%
2P and SLG faults on line10 and line13 at 1.65s	2.27%	0.22%	0.54%	2.54%	6.78%	6.78%	2.59%	2.59%	0.00%	0.00%	0.00%	6.26%	6.26%	6.03%	13.70%	25.10%
3P and 2LG faults on line12 and line14 at 3.00s	-0.10%	-1.21%	-0.82%	-1.32%	1.44%	1.44%	-1.24%	-1.24%	1.48%	1.48%	1.48%	1.54%	1.54%	1.34%	2.27%	4.09%
3P and 2LG faults on line12 and line14 at 0.95s	2.09%	0.33%	0.76%	0.54%	5.27%	5.27%	0.55%	0.55%	0.00%	0.00%	0.00%	4.98%	4.98%	4.87%	9.23%	17.40%
3P and 2LG faults on line12 and line14 at 1.65s	1.46%	-65.05%	0.13%	5.82%	14.36%	14.36%	5.95%	5.95%	8.74%	8.74%	8.74%	0.00%	0.00%	8.70%	28.27%	41.95%
3P and 2LG faults on line12 and line14 at 3.00s	0.51%	-0.82%	-21.00%	-21.91%	2.19%	2.19%	-1.45%	-1.45%	0.42%	0.42%	0.42%	2.18%	2.18%	2.08%	3.12%	5.26%
SLG and 2P faults on line9 and line11 at 0.95s	-1.04%	-2.65%	-1.76%	-3.65%	2.11%	2.11%	-3.58%	-3.58%	3.96%	3.96%	3.96%	2.16%	2.16%	2.16%	8.73%	0.00%
SLG and 2P faults on line9 and line11 at 1.65s	1.31%	-0.76%	-0.43%	1.93%	5.42%	5.42%	-2.07%	-2.07%	5.08%	5.08%	5.08%	4.91%	4.91%	4.91%	10.91%	24.71%
SLG and 2P faults on line9 and line11 at 3.00s	0.00%	-1.11%	-0.72%	-1.41%	1.44%	1.44%	-1.34%	-1.34%	1.26%	1.26%	1.26%	1.54%	1.54%	1.54%	2.16%	4.71%

Figure 5.8: Percentage improvement of multiple voltage dip mitigation with grid-connected renewable hydro generators as a result faults from the distribution network

5.11.3 Scenario 5c: Grid-connected solar PV power plants

Scenario 5c investigates the impact of grid connected solar PV plants only on mitigation of voltage dip within the distribution network. The results are shown in table 5.12 and Figure 5.9.

Table 5.12: Mitigation of multiple dips with grid-connected solar PV power plants as result of multiple faults on various distribution lines at 50% of each line measured at 0.95sec and 1.65sec during and 3.00sec after the multiple dips

Load busbar	Voltage magnitude with 2P and SLG faults on line10 and line13 respectively in (p.u.) at			Voltage magnitude with 3P and 2LG faults on line12 and line14 respectively in (p.u.) at			Voltage magnitude with SLG and 2P faults on line9 and line11 respectively in (p.u.) at		
	0.95s	**1.65s**	**3.00s**	**0.95s**	**1.65s**	**3.00s**	**0.95s**	**1.65s**	**3.00s**
Busbar5	0.691	0.938	1.007	0.922	0.618	0.996	0.880	0.932	1.009
Busbar6	0.837	0.930	0.992	0.914	0.823	0.982	0.907	0.924	0.994
Busbar8	0.812	0.934	0.979	0.925	0.792	0.969	0.916	0.931	0.982
Busbar11	0.794	0.750	0.992	0.735	0.783	0.984	0.710	0.785	0.992
Busbar13	0.486	0.892	0.995	0.874	0.204	0.982	0.732	0.887	0.995
Busbar14	0.486	0.892	0.995	0.874	0.204	0.982	0.732	0.887	0.995
Busbar16	0.773	0.737	0.973	0.721	0.766	0.966	0.698	0.484	0.973
Busbar17	0.773	0.737	0.973	0.721	0.766	0.966	0.698	0.484	0.973
Busbar18	0.762	0.000	0.952	0.000	0.748	0.945	0.678	0.754	0.952
Busbar19	0.762	0.000	0.952	0.000	0.748	0.945	0.678	0.754	0.952
Busbar20	0.762	0.000	0.952	0.000	0.748	0.945	0.678	0.754	0.952
Busbar21	0.467	0.903	0.997	0.884	0.000	0.985	0.766	0.896	0.997
Busbar22	0.467	0.903	0.997	0.884	0.000	0.985	0.766	0.896	0.997
Busbar23	0.472	0.903	0.998	0.885	0.164	0.985	0.766	0.897	0.998
Busbar25	0.601	0.813	0.981	0.797	0.525	0.971	0.465	0.827	0.981
Busbar26	0.678	0.786	0.961	0.772	0.641	0.953	0.000	0.804	0.961

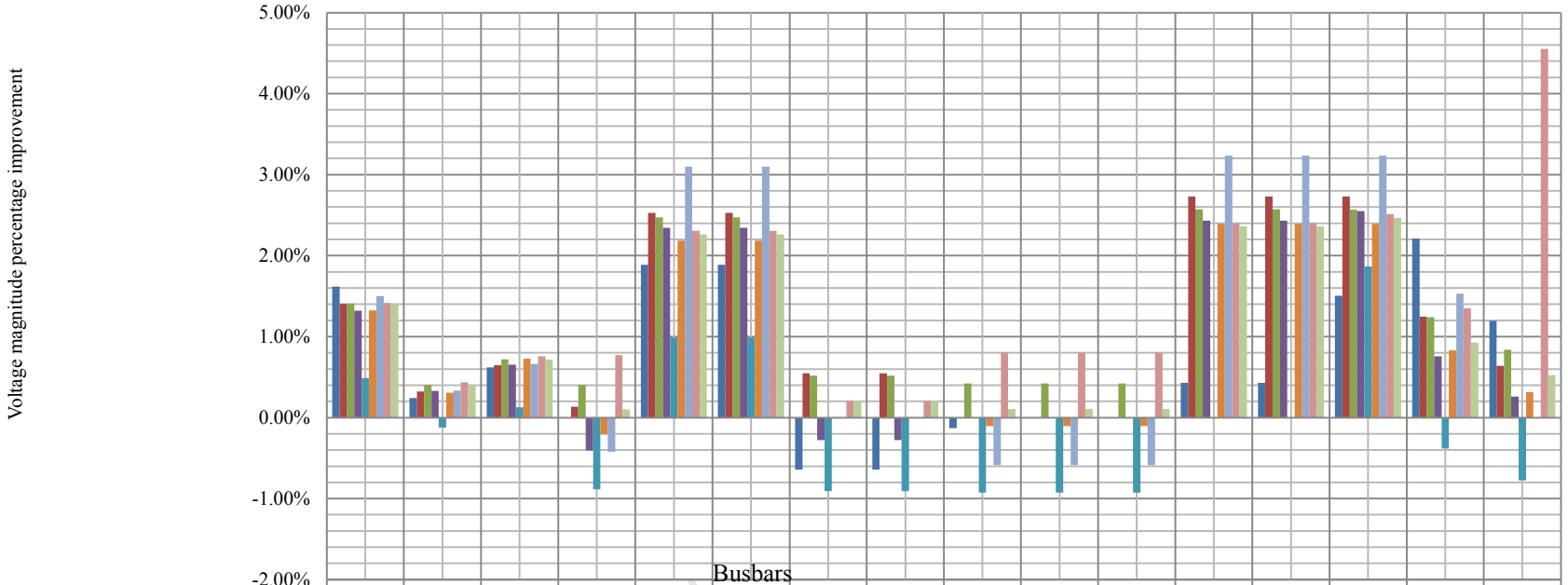

	Busbar5	Busbar6	Busbar8	Busbar11	Busbar13	Busbar14	Busbar16	Busbar17	Busbar18	Busbar19	Busbar20	Busbar21	Busbar22	Busbar23	Busbar25	Busbar26
2P and SLG faults on line10 and line13 at 0.95s	1.62%	0.24%	0.62%	0.00%	1.89%	1.89%	-0.64%	-0.64%	-0.13%	0.00%	0.00%	0.43%	0.43%	1.51%	2.21%	1.19%
2P and SLG faults on line10 and line13 at 1.65s	1.41%	0.32%	0.65%	0.13%	2.53%	2.53%	0.55%	0.55%	0.00%	0.00%	0.00%	2.73%	2.73%	2.73%	1.25%	0.64%
2P and SLG faults on line10 and line13 at 3.00s	1.41%	0.40%	0.72%	0.40%	2.47%	2.47%	0.52%	0.52%	0.42%	0.42%	0.42%	2.57%	2.57%	2.57%	1.24%	0.84%
3P and 2LG faults on line12 and line14 at 0.95s	1.32%	0.33%	0.65%	-0.41%	2.34%	2.34%	-0.28%	-0.28%	0.00%	0.00%	0.00%	2.43%	2.43%	2.55%	0.76%	0.26%
3P and 2LG faults on line12 and line14 at 1.65s	0.49%	-0.12%	0.13%	-0.89%	0.99%	0.99%	-0.91%	-0.91%	-0.93%	-0.93%	-0.93%	0.00%	0.00%	1.86%	-0.38%	-0.77%
3P and 2LG faults on line12 and line14 at 3.00s	1.32%	0.31%	0.73%	-0.20%	2.19%	2.19%	0.00%	0.00%	-0.11%	-0.11%	-0.11%	2.39%	2.39%	2.39%	0.83%	0.32%
SLG and 2P faults on line9 and line11 at 0.95s	1.50%	0.33%	0.66%	-0.42%	3.10%	3.10%	0.00%	0.00%	-0.59%	-0.59%	-0.59%	3.23%	3.23%	3.23%	1.53%	0.00%
SLG and 2P faults on line9 and line11 at 1.65s	1.41%	0.43%	0.76%	0.77%	2.31%	2.31%	0.21%	0.21%	0.80%	0.80%	0.80%	2.40%	2.40%	2.51%	1.35%	4.55%
SLG and 2P faults on line9 and line11 at 3.00s	1.41%	0.40%	0.72%	0.10%	2.26%	2.26%	0.21%	0.21%	0.11%	0.11%	0.11%	2.36%	2.36%	2.46%	0.93%	0.52%

Figure 5.9: Percentage improvement of multiple voltage dip mitigation with grid-connected PV generators as a result faults from the distribution network

5.11.4 Scenario 5d: Grid-connected wind and hydro power plants

Scenario 5d shows the impact of grid connected wind and hydro power plants only on mitigation of voltage dip within the distribution network. The results are shown in table 5.1 and Figure 5.10.

Table 5.13: Mitigation of multiple dips with grid-connected renewable Wind and HP generators as a result of multiple faults on various distribution lines at 50% of each line measured at 0.95sec and 1.65sec during and 3.00sec after the multiple dips

Load busbar	Voltage magnitude with 2P and SLG faults on line10 and line13 respectively in (p.u.) at			Voltage magnitude with 3P and 2LG faults on line12 and line14 respectively in (p.u.) at			Voltage magnitude with SLG and 2P faults on line9 and line11 respectively in (p.u.) at		
	0.95s	1.65s	3.00s	0.95s	1.65s	3.00s	0.95s	1.65s	3.00s
Busbar5	0.729	0.955	1.006	0.967	0.606	0.997	0.91	0.936	1.006
Busbar6	0.859	0.913	0.962	0.927	0.782	0.947	0.901	0.891	0.965
Busbar8	0.830	0.927	0.96	0.945	0.762	0.998	0.92	0.911	0.964
Busbar11	0.874	0.771	0.957	0.763	0.782	0.931	0.739	0.781	0.96
Busbar13	0.490	0.976	1.044	0.981	0.273	1.043	0.842	0.959	1.038
Busbar14	0.490	0.976	1.044	0.981	0.273	1.042	0.842	0.959	1.038
Busbar16	0.912	0.874	0.981	0.829	0.86	0.993	0.828	0.451	0.980
Busbar17	0.912	0.874	0.981	0.829	0.86	0.993	0.828	0.451	0.980
Busbar18	0.884	0.000	0.944	0.000	0.655	0.734	0.797	0.807	0.958
Busbar19	0.884	0.000	0.944	0.000	0.655	0.734	0.797	0.807	0.958
Busbar20	0.884	0.000	0.944	0.000	0.655	0.734	0.797	0.807	0.958
Busbar21	0.501	0.975	1.038	0.981	0.000	1.036	0.861	0.957	1.033
Busbar22	0.501	0.975	1.038	0.981	0.000	1.036	0.861	0.957	1.033
Busbar23	0.502	0.973	1.037	0.979	0.192	1.034	0.859	0.955	1.032
Busbar25	0.688	0.888	0.973	0.873	0.625	0.982	0.522	0.863	0.978
Busbar26	0.875	0.968	0.978	0.912	0.088	1.012	0.000	0.932	0.996

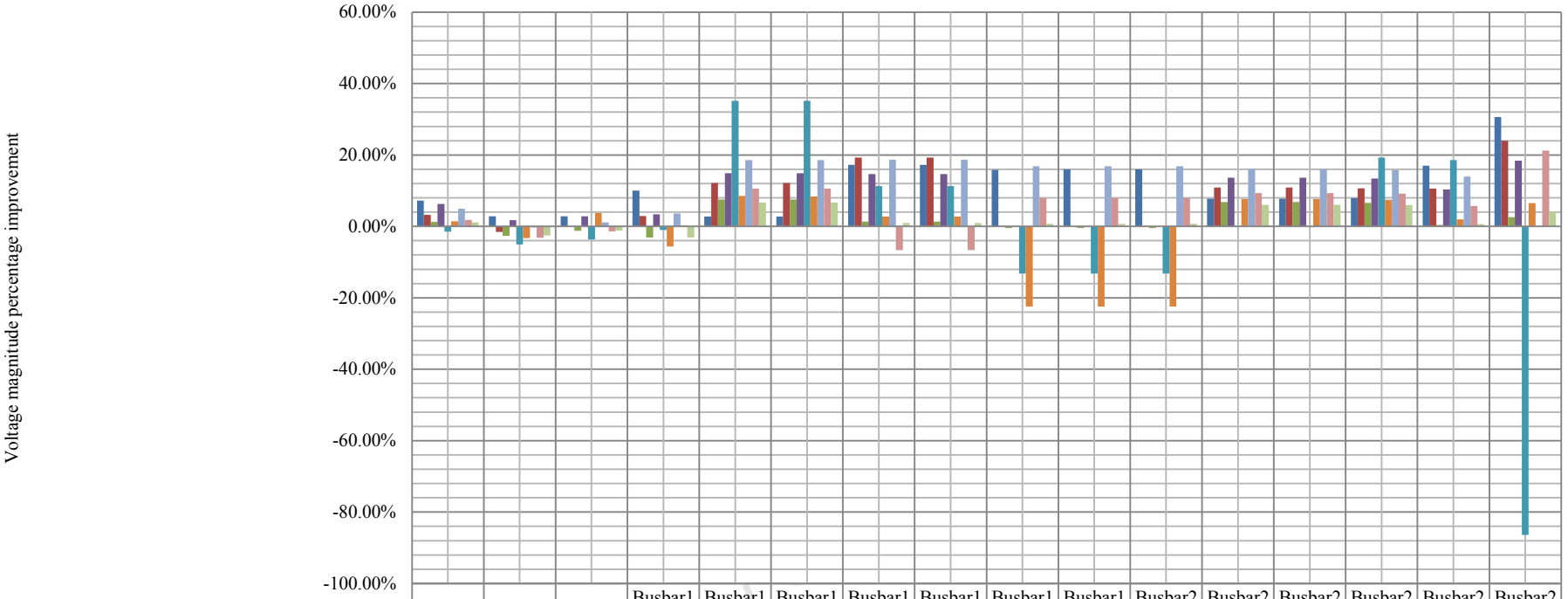

	Busbar5	Busbar6	Busbar8	Busbar11	Busbar13	Busbar14	Busbar16	Busbar17	Busbar18	Busbar19	Busbar20	Busbar21	Busbar22	Busbar23	Busbar25	Busbar26
2P and SLG faults on line10 and line13 at 0.95s	7.21%	2.87%	2.85%	10.08%	2.73%	2.73%	17.22%	17.22%	15.86%	16.01%	16.01%	7.74%	7.74%	7.96%	17.01%	30.60%
2P and SLG faults on line10 and line13 at 1.65s	3.24%	-1.51%	-0.11%	2.94%	12.18%	12.18%	19.24%	19.24%	0.00%	0.00%	0.00%	10.92%	10.92%	10.69%	10.59%	23.94%
2P and SLG faults on line10 and line13 at 3.00s	1.31%	-2.63%	-1.23%	-3.14%	7.52%	7.52%	1.34%	1.34%	-0.42%	-0.42%	-0.42%	6.79%	6.79%	6.58%	0.41%	2.62%
3P and 2LG faults on line12 and line14 at 0.95s	6.26%	1.76%	2.83%	3.39%	14.87%	14.87%	14.66%	14.66%	0.00%	0.00%	0.00%	13.67%	13.67%	13.44%	10.37%	18.44%
3P and 2LG faults on line12 and line14 at 1.65s	-1.46%	-5.10%	-3.67%	-1.01%	35.15%	35.15%	11.25%	11.25%	-13.25%	-13.25%	-13.25%	0.00%	0.00%	19.25%	18.60%	-86.38%
3P and 2LG faults on line12 and line14 at 3.00s	1.42%	-3.27%	3.74%	-5.58%	8.53%	8.43%	2.80%	2.80%	-22.41%	-22.41%	-22.41%	7.69%	7.69%	7.48%	1.97%	6.53%
SLG and 2P faults on line9 and line11 at 0.95s	4.96%	-0.33%	1.10%	3.65%	18.59%	18.59%	18.62%	18.62%	16.86%	16.86%	16.86%	16.04%	16.04%	15.77%	13.97%	0.00%
SLG and 2P faults on line9 and line11 at 1.65s	1.85%	-3.15%	-1.41%	0.26%	10.61%	10.61%	-6.63%	-6.63%	7.89%	7.89%	7.89%	9.37%	9.37%	9.14%	5.76%	21.20%
SLG and 2P faults on line9 and line11 at 3.00s	1.11%	-2.53%	-1.13%	-3.13%	6.68%	6.68%	0.93%	0.93%	0.74%	0.74%	0.74%	6.06%	6.06%	5.95%	0.62%	4.18%

Figure 5.10: Percentage improvement of multiple voltage dip mitigation with grid-connected wind and hydro generators as a result faults from the distribution network

5.11.5 Scenario 5e: All the grid-connected power plants

Scenario 5e investigates the impact of all the grid connected plants present within the test network on mitigation of voltage dip within the distribution network. The results are shown in table 5.14 and Figure 5.11.

Table 5.14: Mitigation of multiple dips with all the grid-connected renewable generators as a result of multiple faults on various distribution lines at 50% of each line measured at 0.95sec and 1.65sec during and 3.00sec after the multiple dips

Load busbar	Voltage magnitude with 2P and SLG faults on line10 and line13 respectively in (p.u.) at			Voltage magnitude with 3P and 2LG faults on line12 and line14 respectively in (p.u.) at			Voltage magnitude with SLG and 2P faults on line9 and line11 respectively in (p.u.) at		
	0.95s	1.65s	3.00s	0.95s	1.65s	3.00s	0.95s	1.65s	3.00s
Busbar5	0.714	0.915	0.916	0.928	0.576	0.955	0.871	0.879	0.954
Busbar6	0.857	0.827	0.942	0.913	0.757	0.931	0.887	0.858	0.938
Busbar8	0.821	0.904	0.934	0.923	0.737	0.924	0.899	0.874	0.932
Busbar11	0.886	0.765	0.946	0.761	0.761	0.92	0.736	0.759	0.938
Busbar13	0.464	0.921	0.978	0.926	0.255	0.984	0.788	0.883	0.964
Busbar14	0.464	0.921	0.978	0.926	0.255	0.984	0.788	0.883	0.964
Busbar16	0.916	0.867	0.972	0.825	0.837	0.987	0.823	0.437	0.962
Busbar17	0.916	0.867	0.972	0.825	0.837	0.987	0.823	0.437	0.962
Busbar18	0.891	0.000	0.943	0.000	0.642	0.618	0.794	0.787	0.931
Busbar19	0.891	0.000	0.943	0.000	0.642	0.618	0.794	0.787	0.931
Busbar20	0.891	0.000	0.943	0.000	0.642	0.618	0.797	0.787	0.931
Busbar21	0.461	0.912	0.966	0.917	0.000	0.969	0.8	0.874	0.952
Busbar22	0.461	0.912	0.966	0.917	0.000	0.969	0.8	0.874	0.952
Busbar23	0.467	0.91	0.964	0.716	0.174	0.698	0.797	0.873	0.951
Busbar25	0.719	0.895	0.963	0.876	0.640	0.986	0.525	0.851	0.959
Busbar26	0.889	0.967	0.972	0.914	0.884	1.027	0.000	0.921	0.987

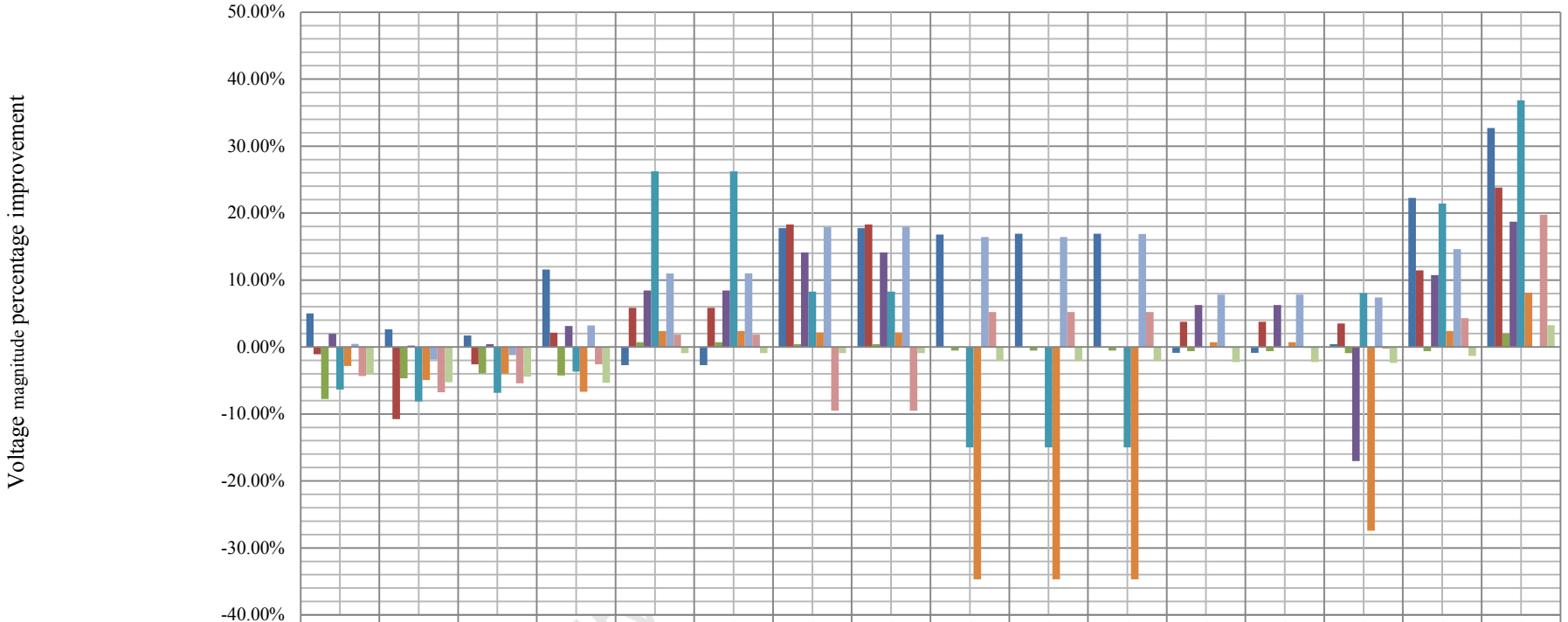

	Busbar5	Busbar6	Busbar8	Busbar11	Busbar13	Busbar14	Busbar16	Busbar17	Busbar18	Busbar19	Busbar20	Busbar21	Busbar22	Busbar23	Busbar25	Busbar26
2P and SLG faults on line10 and line13 at 0.95s	5.00%	2.63%	1.73%	11.59%	-2.73%	-2.73%	17.74%	17.74%	16.78%	16.93%	16.93%	-0.86%	-0.86%	0.43%	22.28%	32.69%
2P and SLG faults on line10 and line13 at 1.65s	-1.08%	-10.79%	-2.59%	2.14%	5.86%	5.86%	18.28%	18.28%	0.00%	0.00%	0.00%	3.75%	3.75%	3.53%	11.46%	23.82%
2P and SLG faults on line10 and line13 at 3.00s	-7.75%	-4.66%	-3.91%	-4.25%	0.72%	0.72%	0.41%	0.41%	-0.53%	-0.53%	-0.53%	-0.62%	-0.62%	-0.92%	-0.62%	1.99%
3P and 2LG faults on line12 and line14 at 0.95s	1.98%	0.22%	0.44%	3.12%	8.43%	8.43%	14.11%	14.11%	0.00%	0.00%	0.00%	6.26%	6.26%	-17.03%	10.75%	18.70%
3P and 2LG faults on line12 and line14 at 1.65s	-6.34%	-8.13%	-6.83%	-3.67%	26.24%	26.24%	8.28%	8.28%	-14.97%	-14.97%	-14.97%	0.00%	0.00%	8.07%	21.44%	36.84%
3P and 2LG faults on line12 and line14 at 3.00s	-2.85%	-4.90%	-3.95%	-6.69%	2.39%	2.39%	2.17%	2.17%	-34.67%	-34.67%	-34.67%	0.73%	0.73%	-27.44%	2.39%	8.11%
SLG and 2P faults on line9 and line11 at 0.95s	0.46%	-1.88%	-1.21%	3.23%	10.99%	10.99%	17.91%	17.91%	16.42%	16.42%	16.86%	7.82%	7.82%	7.41%	14.63%	0.00%
SLG and 2P faults on line9 and line11 at 1.65s	-4.35%	-6.74%	-5.41%	-2.57%	1.85%	1.85%	-9.52%	-9.52%	5.21%	5.21%	5.21%	-0.11%	-0.11%	-0.23%	4.29%	19.77%
SLG and 2P faults on line9 and line11 at 3.00s	-4.12%	-5.25%	-4.41%	-5.35%	-0.92%	-0.92%	-0.93%	-0.93%	-2.10%	-2.10%	-2.10%	-2.26%	-2.26%	-2.36%	-1.34%	3.24%

Figure 5.11: Percentage improvement of multiple voltage dip mitigation with all the grid-connected generators as a result faults from the distribution network

5.12 Scenario 6: The capabilities and effects of different types of grid-connected wind energy conversion systems on mitigation of multiple voltages dip in a power network with different fault resistance and fault reactance

Wind electric generation is on the increase around the globe, and it has been predicted that the installed capacity will be 300GW by 2030 [240]. This section studied the impacts of different grid-connected wind generators on multiple voltage dips within a short duration and from different fault locations on the two transmission lines. Various types of grid-connected wind distributed generations use different energy conversion systems such as generator, power converter control algorithms, etc. However, the same technology is used for prime mover control [251]. Grid connection requirements are important for suitable and smooth operation of grid-connected wind generators, especially with the increase in penetration of wind energy conversion systems. The power system utilities and regulatory bodies provide these requirements in other to maintain grid stability and good power quality, which include the grid code at both the normal and faults conditions [252]. The addition of wind plants to our existing power grids demands more flexible distribution and transmission grids that will be able to accommodation the adverse effects of wind power systems. Various types of grid-connected wind energy conversion systems have different effects on the grid. Ongoing research has shown that the wind-energy systems have been improved upon every day. In this investigation, three different grid integrated wind energy conversion systems were considered for mitigation of multiple voltage dips, and the applicability of these three wind energy technologies are evaluated and compared with different fault resistance and fault reactance. They were added to the power system one at a time in order to assess their impacts on multiple voltage dip mitigations, and this was done by monitoring the voltage magnitudes in p.u. along the load busbars.

5.13 Different grid integrated wind energy conversion systems

The grid-connected wind generators modeled and simulated in this investigation are the fixed-speed squirrel cage induction wind generators (SCIWG), variable-speed doubly-fed induction wind generators (DFIWG) and variable-speed synchronous wind generators (SWG). The impact of connecting each of the grid-connected wind generators is assessed to establish their effects regard mitigation of multiple voltage dips on the load busbars.

5.14 The test network description

The test network used in this investigation has been adapted from the power network described in Figure 4.1 and this is shown in Figure 5.12. The test network consists of a 66kV external grid with capacity of 60MW feeding the TX loads connected to TX busbar. The TX busbar feeds two 66kV transmission lines, line1 and line 2. Line1 supplies power to 66kVBusbar1 while line2 supplies 66kV DG busbar. Load2 on 22kVBus 2 is supplied from 66kV/22kV TR4. 66kV/22kV transformer TR1 supplies load1 connected to 22kVBus1. Line 3 and line 4 supply power to load 3 from 66kVBusbar1. The various grid-connected wind generators are connected at 11kV DG Busbar through the transformers TR2 and TR3. Two other renewable generators (DG1 and DG2) are connected within the network at 22kVBus1 and Busbar1b to supply load1 and load3 respectively. The three grid-connected wind energy conversion systems have relatively the same installed capacity of 15MVA. However, the three wind energy conversion systems have different generator parameters such as stator resistance and reactance, inertia, rotor resistance and reactance, R/X locked rotor as regards their configuration. The SCIWG is configured using asynchronous machine in DigSILENT while DFIWG and SWG are configured using the double-fed induction machine and synchronous machine respectively.

Modeling of DFIWG usually involves connection to a pulse-width modulated convertor through a three-winding transformer. It also has a capacitor bank that provides the reactive power compensation for the generator. The detailed parameters is shown in appendix 5

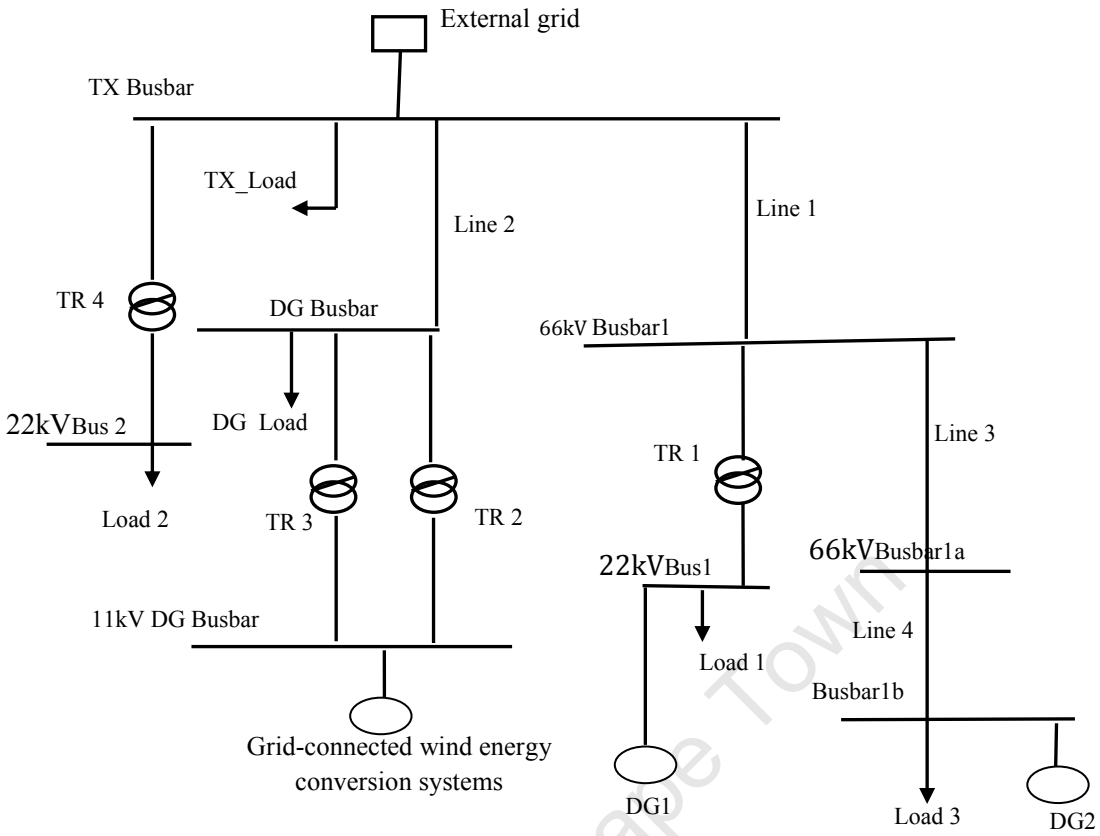

Figure 5.12: Adopted test network with grid-connected wind energy conversion

5.15 Fixed-speed squirrel cage induction wind generator (SCIWG)

Fixed-speed squirrel cage induction wind generators are the early technology of wind generators. They are simple and reliable, but are associated with low power quality [241]. The most common technology of SCIWG is the conventional induction generator due to the damping effect [208]. They also have a complex voltage control that involves the use of static-var compensators.

Most fixed speed wind turbine does not use any converters and are connected directly to the grid through a two winding step up transformer as the voltage of the DG is usually much lower than the grid voltages. SCIWGs are mostly induction generators; as a result, they absorb reactive power from the grid. Shunt capacitor can be provided to supply the reactive power since they do not have an internal excitation system [245]. Figure 5.13 shows the typical configuration of an SCIWG, in this type of generator the slip varies with the capacity of power generated.

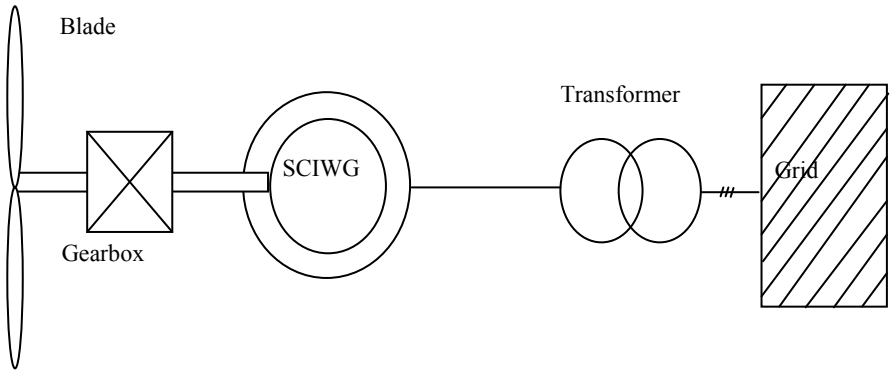

Figure 5.13: Fixed-speed squirrel cage induction wind generator [251]

5.16 Variable-speed doubly-fed induction wind generator (DFIWG)

DFIWG has a back-to-back converter which shared a common direct current link with one connected to the rotor while other is connected grid. The power electronics has the ability to control both the active and reactive power delivered to the grid [222]. The model of DFIWG is made up of the induction generator which is connected to DC link through the grid-side diode rectifier that converts the generator terminal voltage to a constant DC voltage. The self-commutated pulse-width modulated (PWM) inverter converts the DC voltage to an AC voltage at the frequency that is needed for the grid integration through a step-up transformer.

DFIG generators have excellent dynamic response and controllability as compare with traditional induction generators. Figure 5.14 show the variable-speed double-fed induction wind generator configuration.

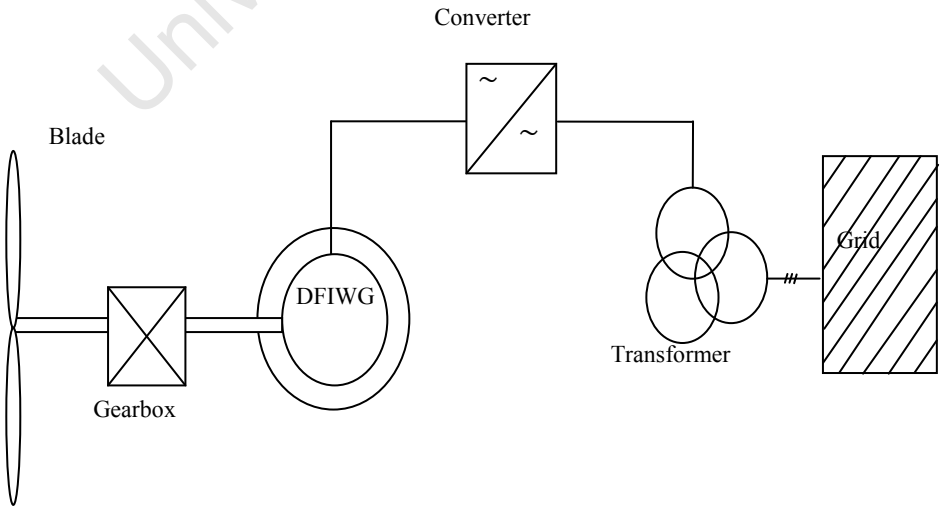

Figure 5.14: Variable-speed double-fed induction wind generator [251]

5.17 Variable-speed synchronous wind generator (SWG)

The variable-speed synchronous wind generator could be excited by an externally applied direct current or by permanent magnets [222]. An example of SWG such as fully rated converter wind turbine with permanent magnet synchronous generator allows gearless constructions and able to decouple the generator from the grid during fault. With this arrangement, the generator is able to withstand and ride through faults on a power network [246]. The variable-speed direct-driven synchronous wind generator is shown in Figure 5.15.

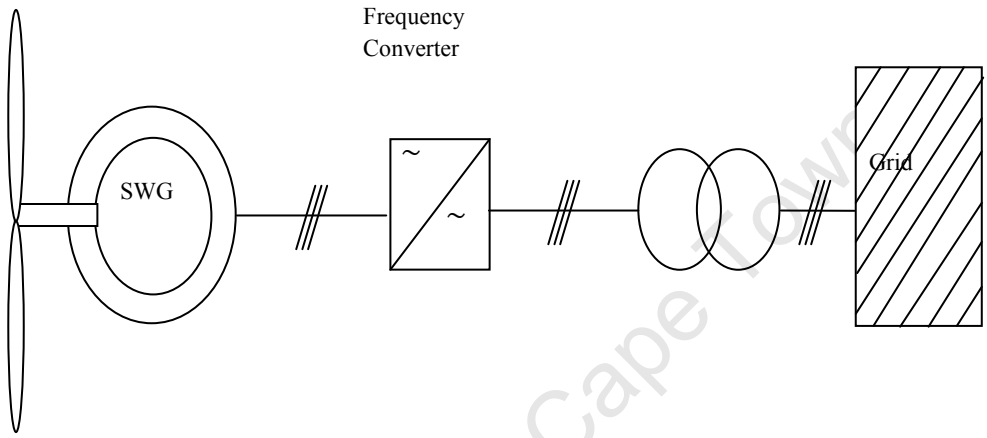

Figure 5.15: Variable-speed direct-driven synchronous wind generator [251]

5.18 Initial conditions

After modelling the test system, different types of multiple voltage dips were simulated with different fault resistance and fault reactance by applying faults on lines line4 and line2. The first fault (F1) was applied at 0.75sec and was cleared at 1.25sec while the second fault (F2) occurs at 1.85sec and was cleared at 2.45sec. Therefore, the Fault F1 duration is 0.50ses and fault F2 is 0.60ses. The simulation is run for 3.00sec. The voltage magnitude on the various load busbars was observed before the inception of the faults and was found to be 1p.u. along the load busbars when each of the grid-connected wind generators is connected to the grid at the points of integration one after the other for the study. The effect of each of the grid-connected wind generators on multiple voltage mitigation capabilities is investigated. The voltage dip magnitudes during the faults were recorded at 1.00sec for the first fault and at 2.15sec for the second fault and at 1.63sec after the first faults on all the load busbars.

5.19 Simulation and study case

Various types of the grid-connected wind generator respond differently to multiple voltage dips. In this investigation, both the balanced faults and unbalanced faults were considered. These faults were applied with different fault resistance and fault reactance. This is to investigate the impact of different fault resistance and fault reactance on different types of wind technology.

The multiple voltage dips was simulated by applying a two phase-to-ground (2LG) fault (phases a,b only) at 0.75sec on line4 followed by a three phases short-circuit (3P) fault (3P fault affects all the phases) at 1.85sec on line2. This was done for all cases of different fault resistance and fault reactance, and the simulations were repeated with each of the grid-connected wind generators.

5.20 Impact of different grid-connected wind generators on multiple voltage dips

The severity of multiple voltage dips as a result of 2LG fault and 3P fault with different fault resistance and fault reactance on the load measured from the load busbars are shown in Table 5.15. It is noticed from that the higher the fault resistance and fault reactance the lesser the severity of the multiple voltage dips.

Table 5.15: Multiple voltage dip magnitudes of 2LG and 3P faults in p.u.

Load busbar	fault resistance and fault reactance of F1 is 0Ω and 0Ω , F2 is 0Ω and 0Ω at			Fault resistance and fault reactance of F1 is 2.5Ω and 1.8 Ω, F2 is 1.77Ω and 0.45 Ω at			Fault resistance and fault reactance of F1 is 10Ω and 5 Ω, F2 is 8Ω and 3 Ω at		
	1.00s	1.63s	2.15s	1.00s	1.63s	2.15s	1.00s	1.63s	2.15s
BusbarTX	0.706	0.925	0.197	0.739	0.775	0.246	0.807	0.968	0.432
BusbarDG	0.691	0.889	0.000	0.722	0.746	0.074	0.786	0.931	0.291
Busbar1b	0.013	0.846	0.252	0.106	0.448	0.300	0.198	0.917	0.444
22kVBusbar1	0.714	0.880	0.192	0.755	0.703	0.263	0.828	0.947	0.514
22kVBusbar2	0.781	0.907	0.193	0.810	0.761	0.242	0.863	0.949	0.424

Table 5.15 shows multiple voltages dip magnitudes at the load busbar throughout the network and it indicates the depression as a result of faults F1 and F2 and the severities of which are dependent on the fault resistance and fault reactance. Before the inception of the faults the voltage magnitude was at 1p.u., however with the inception of the faults the voltage changed during and after the faults. Table 5.16, Table 5.17 and Table 5.18 show the multiple voltage magnitudes (p.u.) at time of measurement (1.00sec, 1.63sec and 2.15sec) with grid-connected SCIWG, DFIWG and SWG respectively. The graphs of the simulation are shown in Apendix 5.

The percentage voltage profile improvement when fixed-speed squirrel cage induction wind generator (SCIWG) is connected is shown in Figure 5.16. It was noticed to be unfavorable and the worst case at fault resistance and fault reactance of F1 is 0Ω and 0Ω, F2 is 0Ω and 0Ω than at F1 is 2.5Ω and 1.8 Ω, F2 is 1.77Ω and 0.45 Ω or F1 is 10Ω and 5 Ω, F2 is 8Ω and 3 Ω. This is because the SCIWG absorbs reactive power from the grid and adds more burden to on the multiple dip mitigation. However it was observed that the voltage level improved after the fault.

Table 5.16: Mitigation of multiple voltage dip of faults 2LG and 3P faults with SCIWG only connected

Load busbar	fault resistance and fault reactance of F1 is 0Ω and 0Ω, F2 is 0Ω and 0Ω at			fault resistance and fault reactance of F1 is 2.5Ω and 1.8 Ω, F2 is 1.77Ω and 0.45 Ω at			fault resistance and fault reactance of F1 is 10Ω and 5 Ω, F2 is 8Ω and 3 Ω at		
	1.00s	1.63s	2.15s	1.00s	1.63s	2.15s	1.00s	1.63s	2.15s
BusbarTX	0.722	0.913	0.191	0.754	0.786	0.243	0.820	0.965	0.457
BusbarDG	0.733	0.884	0.026	0.762	0.780	0.098	0.821	0.940	0.327
Busbar1b	0.013	0.837	0.225	0.108	0.472	0.318	0.308	0.926	0.539
22kVBusbar1	0.719	0.873	0.181	0.760	0.714	0.249	0.831	0.946	0.544
22kVBusbar2	0.785	0.895	0.187	0.813	0.771	0.239	0.865	0.945	0.449

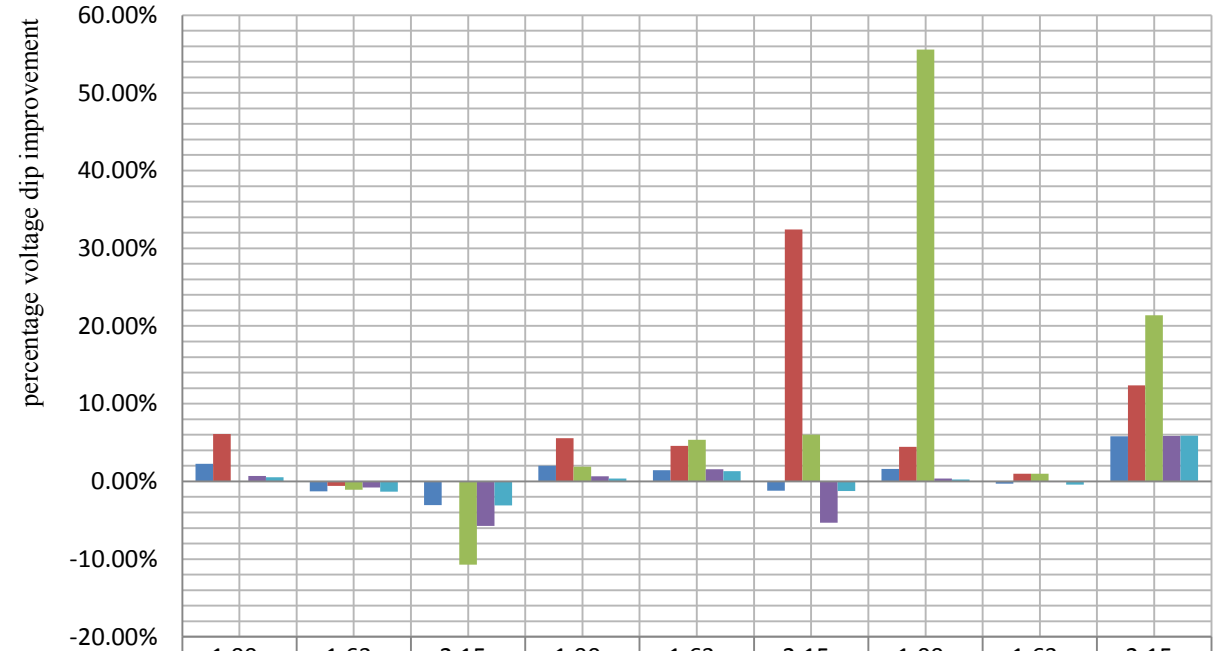

	1.00s	1.63s	2.15s	1.00s	1.63s	2.15s	1.00s	1.63s	2.15s
BusbarTX	2.27%	-1.30%	-3.05%	2.03%	1.42%	-1.22%	1.61%	-0.31%	5.79%
BusbarDG	6.08%	-0.56%	0.00%	5.54%	4.56%	32.43%	4.45%	0.97%	12.37%
Busbar1b	0.00%	-1.06%	-10.71%	1.89%	5.36%	6.00%	55.56%	0.98%	21.40%
22kVBusbar1	0.70%	-0.80%	-5.73%	0.66%	1.56%	-5.32%	0.36%	-0.11%	5.84%
22kVBusbar2	0.51%	-1.32%	-3.11%	0.37%	1.31%	-1.24%	0.23%	-0.42%	5.90%

Figure 5.16: Percentage voltage profile improvement with grid-connected SCIWG

Table 5.17: Mitigation of multiple voltage dip of faults 2LG and 3P faults with DFIG only connected

Load busbar	fault resistance and fault reactance of F1 is 0Ω and 0Ω , F2 is 0Ω and 0Ω at			fault resistance and fault reactance of F1 is 2.5Ω and 1.8 Ω, F2 is 1.77Ω and 0.45 Ω at			fault resistance and fault reactance of F1 is 10Ω and 5 Ω, F2 is 8Ω and 3 Ω at		
	1.00s	1.63s	2.15s	1.00s	1.63s	2.15s	1.00s	1.63s	2.15s
BusbarTX	0.815	0.982	0.257	0.833	0.986	0.306	0.870	0.994	0.563
BusbarDG	0.906	1.004	0.168	0.919	1.010	0.159	0.946	1.018	0.517
Busbar1b	0.065	0.908	0.278	0.126	0.913	0.322	0.251	0.918	0.542
22kVBusbar1	0.819	0.952	0.360	0.835	0.956	0.428	0.868	0.961	0.626
22kVBusbar2	0.903	0.962	0.252	0.912	0.966	0.300	0.930	0.974	0.551

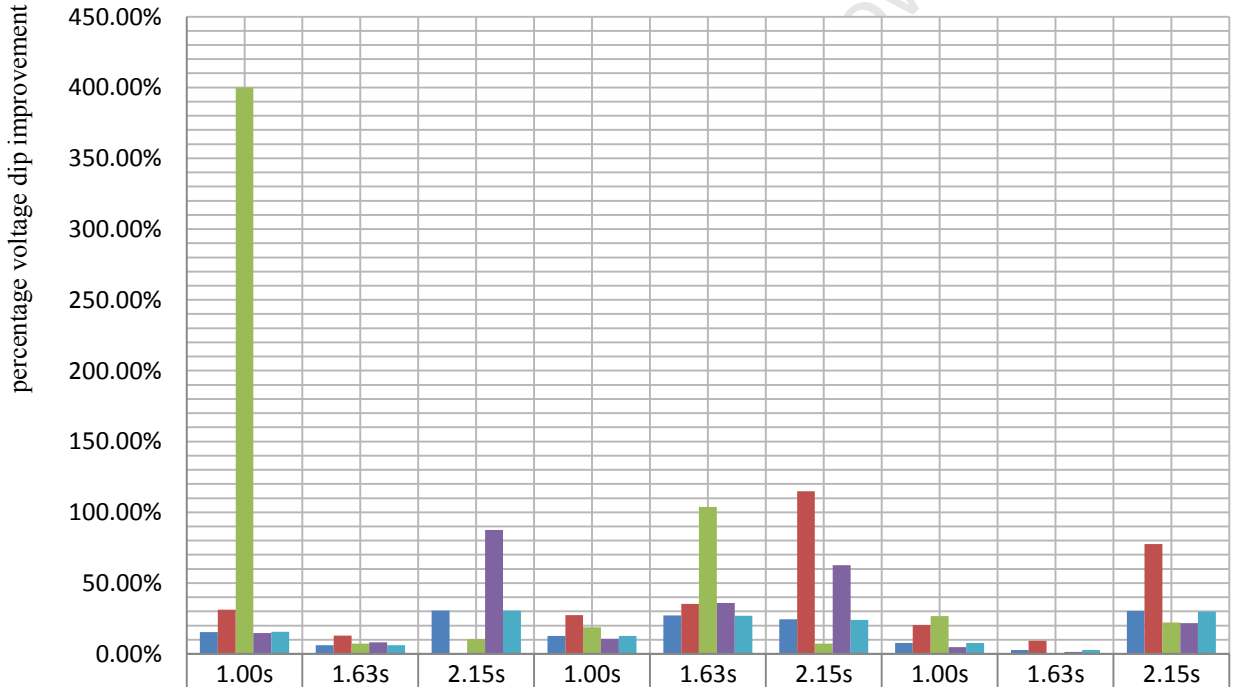

	1.00s	1.63s	2.15s	1.00s	1.63s	2.15s	1.00s	1.63s	2.15s
BusbarTX	15.44%	6.16%	30.46%	12.72%	27.23%	24.39%	7.81%	2.69%	30.32%
BusbarDG	31.11%	12.94%	0.00%	27.29%	35.39%	114.86%	20.36%	9.34%	77.66%
Busbar1b	400.00%	7.33%	10.32%	18.87%	103.79%	7.33%	26.77%	0.11%	22.07%
22kVBusbar1	14.71%	8.18%	87.50%	10.60%	35.99%	62.74%	4.83%	1.48%	21.79%
22kVBusbar2	15.62%	6.06%	30.57%	12.59%	26.94%	23.97%	7.76%	2.63%	29.95%

Figure 5.17: Percentage voltage profile improvement with grid-connected DFIG

Table 5.18: Mitigation of multiple voltage dip of faults 2LG and 3P faults in p.u. with SWG only connected

Load busbar	fault resistance and fault reactance of F1 is 0Ω and 0Ω , F2 is 0Ω and 0Ω at			fault resistance and fault reactance of F1 is 2.5Ω and 1.8 Ω, F2 is 1.77Ω and 0.45 Ω at			fault resistance and fault reactance of F1 is 10Ω and 5 Ω, F2 is 8Ω and 3 Ω at		
	1.00s	**1.63s**	**2.15s**	**1.00s**	**1.63s**	**2.15s**	**1.00s**	**1.63s**	**2.15s**
BusbarTX	0.837	0.988	0.375	0.851	0.990	0.466	0.881	0.994	0.628
BusbarDG	0.922	1.012	0.277	0.932	1.016	0.395	0.953	1.020	0.599
Busbar1b	0.146	0.914	0.384	0.196	0.917	0.459	0.299	0.920	0.599
22kVBusbar1	0.838	0.957	0.486	0.850	0.960	0.554	0.877	0.963	0.679
22kVBusbar2	0.913	0.967	0.368	0.920	0.970	0.546	0.934	0.974	0.615

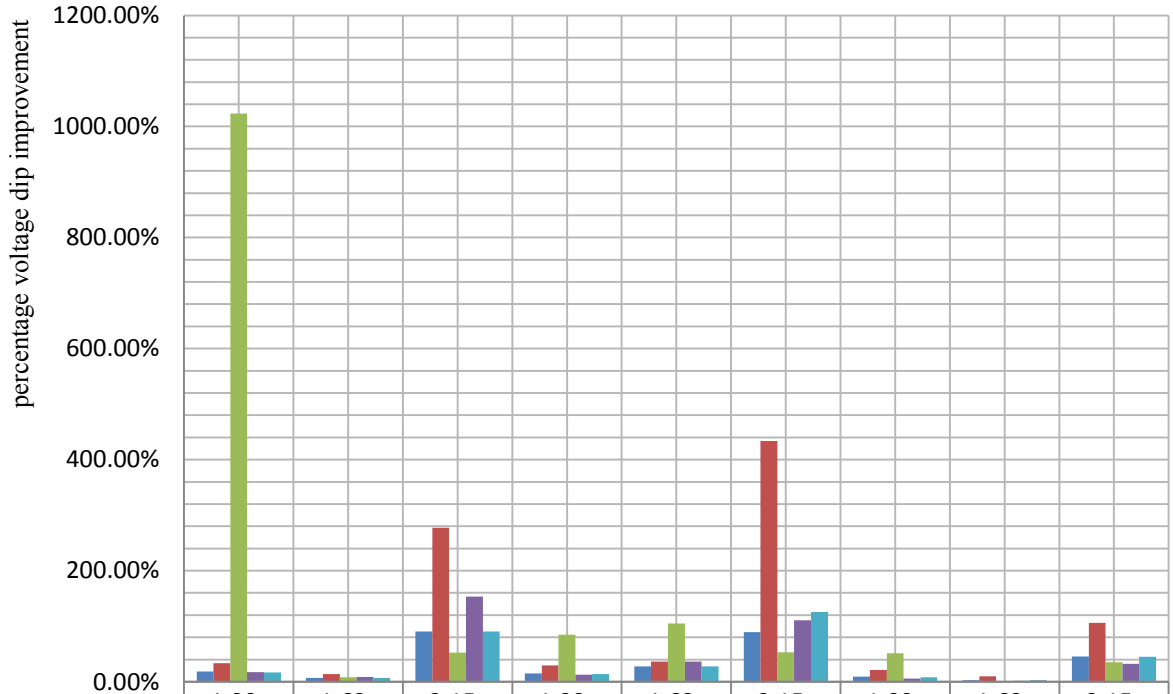

	1.00s	1.63s	2.15s	1.00s	1.63s	2.15s	1.00s	1.63s	2.15s
BusbarTX	18.56%	6.81%	90.36%	15.16%	27.74%	89.43%	9.17%	2.69%	45.37%
BusbarDG	33.43%	13.84%	277.00%	29.09%	36.19%	433.78%	21.25%	9.56%	105.84%
Busbar1b	1023.08%	8.04%	52.38%	84.91%	104.69%	53.00%	51.01%	0.33%	34.91%
22kVBusbar1	17.37%	8.75%	153.13%	12.58%	36.56%	110.65%	5.92%	1.69%	32.10%
22kVBusbar2	16.90%	6.62%	90.67%	13.58%	27.46%	125.62%	8.23%	2.63%	45.05%

Figure 5.18: The percentage voltage profile improvement with grid-connected SWG

Figure 5.18 presents the result of percentage voltage profile improvement with grid-connected SWG. SWG has the highest percentage voltage profile improvement during mitigation at time 1.00sec, 1.63sec and 2.15sec when compared to SCIWG and DFIWG along all the busbars. For example fault resistance and fault reactance of F1 is 0Ω and 0Ω, F2 is 0Ω and 0Ω at t =1.00sec,

gives 18.56%, 2.27% and 15.44% for SWG, SCIWG and DFIWG respectively. This result also indicated that SWG has reactive power regulation capability unlike SCIWG and DFIWG which create a reactive power burden for the power system rather than support it.

5.21 Scenario 7

This scenario investigates the effects of faults from different phases that cause voltage dips. First fault 2P (F1) is applied on line 3, at t=0.75sec and is cleared at t=1.25sec follow by the second fault 3P (F2) on line 1 at t=1.85sec and was cleared at t=2.45sec. F1 fault location is at 50% of line 3 follow by F2 fault location is at 10% of line 1 with and the fault impedance set to 0Ω in this study for both faults. However the WECS was not connected. The different phases are as follow:

a. F1 on 'phase a-b' follow by F2 on 'phase a', and repeated on 'phase b' and 'phase c'
b. F1 on 'phase b-c' follow by F2 on 'phase a', and repeated on 'phase b' and 'phase c'
c. F1 on 'phase c-a' follow by F2 on 'phase a', and repeated on 'phase b' and 'phase c'

The result of this study is shown in Tables 5.19, Table 5.20 and Table5. 21.

5.22 Simulation and study case

In this investigation, the effect of multiple voltage dips on different phases is investigated. The multiple dips are simulated by applying multiple faults of two phases short-circuit (2P) fault on line3 at 0,75sec, on each of the phases 'phase a-b', 'phase b-c' and 'phase c-a', and single phase-to-ground (SLG) on line1 at 1.85sec on each of the phases 'phase a', 'phase b' and 'phase c'. These two faults were cleared at 1.25sec and 2.45sec and the fault impedance was set to zero in this study for both faults. The simulation is run for 3.00sec.

The results show that the same fault resistance and reactance will produce different multiple voltage magnitudes as a result of phase change. This is can be seen from Table 5.19, 5.20 and 5.21.

In addition, the same simulation was repeated for 2P fault and SLG fault on lines line3 and line1 respectively. The faults were applied at different phases of the line. For 2P fault, it was applied on phase a-b, phase b-c and phase c-a, while SLG fault was applied on phase a, phase b and phase c and the results are shown below in Table 5.19, 5.20 and 5.21.

Table 5.19: Multiple voltage dip magnitudes of 2P and SLG faults in p.u. on 'phase a-b'

Load busbar	F1 on 'phase a-b' and F2 on 'phase a'			F1 on 'phase a-b' and F2 on 'phase b'			F1 on 'phase a-b' and F2 on 'phase c'		
	1.00s	1.63s	2.15s	1.00s	1.63s	2.15s	1.00s	1.63s	2.15s
BusbarTX	0.688	0.955	0.401	0.688	0.955	0.765	0.688	0.955	0.737
BusbarDG	0.662	0.918	0.420	0.662	0.918	0.739	0.662	0.918	0.681
Busbar1b	0.463	0.894	0.229	0.463	0.894	0.623	0.463	0.894	0.716
22kVBusbar1	0.797	0.921	0.397	0.797	0.921	0.726	0.797	0.921	0.516
22kVBusbar2	0.877	0.936	0.599	0.877	0.936	0.797	0.877	0.936	0.499

Table 5.20: Multiple voltage dip magnitudes of 2P and SLG faults in p.u. on 'phase b-c

Load busbar	F1 on 'phase b-c ' and F2 on 'phase a'			F1 on 'phase b-c ' and F2 on 'phase b'			F1 on 'phase b-c' and F2 on 'phase c'		
	1.00s	1.63s	2.15s	1.00s	1.63s	2.15s	1.00s	1.63s	2.15s
BusbarTX	0.926	0.950	0.401	0.926	0.950	0.766	0.926	0.950	0.738
BusbarDG	0.891	0.914	0.420	0.891	0.914	0.740	0.891	0.914	0.683
Busbar1b	0.902	0.889	0.228	0.902	0.889	0.623	0.902	0.889	0.716
22kVBusbar1	0.787	0.915	0.401	0.787	0.915	0.728	0.787	0.915	0.516
22kVBusbar2	0.756	0.931	0.599	0.756	0.931	0.798	0.756	0.931	0.501

Table 5.21: Multiple voltage dip magnitudes of 2P and SLG faults in p.u. on 'phase c-a'

Load busbar	F1 on 'phase c-a' and F2 on 'phase a'			F1 on 'phase c-a' and F2 on 'phase b'			F1 on 'phase c-a' and F2 on 'phase c'		
	1.00s	1.63s	2.15s	1.00s	1.63s	2.15s	1.00s	1.63s	2.15s
BusbarTX	0.534	0.956	0.401	0.534	0.956	0.764	0.534	0.956	0.736
BusbarDG	0.514	0.919	0.419	0.514	0.919	0.738	0.514	0.919	0.680
Busbar1b	0.479	0.894	0.229	0.479	0.894	0.622	0.479	0.894	0.716
22kVBusbar1	0.327	0.922	0.395	0.327	0.922	0.723	0.327	0.922	0.515
22kVBusbar2	0.462	0.937	0.598	0.462	0.937	0.796	0.462	0.937	0.499

5.23 Discussion

From this investigation, it is seen that the fault resistance and fault reactance can affect the impact and mitigation of multiple voltage dip. If the fault resistance and fault reactance is high the fault impact will be lessened, and the voltage dip will improve during mitigation with RDG, especially with SWG and DFIG. It was also noticed that the higher the fault resistance and fault reactance of the first fault the higher the pre-voltage magnitude for the second fault.

This type of wind generator is generally known as the fixed speed or constant speed generator. These types of plant are common technology of wind plant due to that fact that they are robust, inexpensive and have low maintenance requirement and cost. A fixed-speed WTG such as squirrel cage induction WTG without power electronic converters may lead to voltage collapse, especially after a fault since they consume a large amount of reactive power during fault.

The impacts of the single-cage induction wind generators (SCIWG) were found to be unfavorable as compared to other types of wind generators such as DFIWG and SWG. Fixed-speed wind turbines, such as squirrel cage induction wind generator impose special requirement on the grid because they have no automatic voltage regulator and no reactive power generation capability. They employ pure-without power electronic converters asynchronous generators, can lead to voltage collapse after a system fault or a trip of a nearby generator. They consume large amounts of reactive power during the fault, which impedes on the voltage restoration after the fault. Technical solutions to prevent voltage collapse after a fault include dynamic reactive power sources [75].

In DFIWG, the stator of the generator is directly connected to the grid, and it has the ability to supply constant voltage and frequency to the grid despite that it turbine is operated at a variable speed. DFIWG does not consume reactive power when equipped with power electronics, and they have better control over terminal voltage. However, their operation is not better than that of the SWG.

In SWG, the external excitation and conductor losses are avoided which results in high efficiency and reliability [234]. The synchronous generators can supply a sustainable voltage to the system during a dip due to it excitation systems and can control the reactive power by adjusting its excitation.

5.24 Scenario 8

The effects of high penetration level of different wind energy conversion systems (SCIWG, DFIWG and SWG) during voltage dip mitigation.

Initially, the present power network was not designed to accommodate renewable distributed generation units and high penetration of RDG has made the power network more complex and vulnerable. At present, the distribution networks where most of these RDG units are sited are not having enough controllers for effective operation and control of the RDG units. For example, in Cape Town, South Africa, there is no single control system in the active distribution network. It is necessary to install a system that will coordinate the operation of the RDG units when there is a voltage dip on the power network.

When distributed wind generators are connected properly in small capacity within the distribution network, they may not have negative effects on the power network. However, as the installed capacity increases the effect will be felt not only at the distribution network but also at the transmission network [248]

This section studies the penetration levels of the wind generators for multiple voltage dip mitigation. The wind generators are connected to assess how the increase penetration may affect voltage dip mitigation.

The penetration level of distributed generation in a power network is defined in equations 5.2 and 5.3 [13].

$$\%\text{DG penetration level} = \frac{P_{DG}}{P_{DG} + P_{CG}} x100\% \quad 5.2$$

$$= \frac{P_{DC}}{P_{LOAD}} x100\% \quad 5.3$$

Where $P_{CG} = (P_{load} - P_{DG})$ is total active power generated by centralized generator and P_{DG} equals the total active power generated by the DG

Chapter 6

6.1 Development and operating principle of the ANN module based on generated voltage dip data

The natures of data that need to be simulated in DIgSILENT PowerFactory 14.1 for voltage dip detection are either "dip" or "no dip conditions of the voltage magnitudes, in contrast to types of data generated for voltage dip classification, which are according to the seven classes of Eskom voltage dip windows. These voltage dip data are generated through application of different electrical power systems fault types, which include three phases short-circuit (3P) fault, two phases short-circuit (2P) fault, single phase-to-ground (SLG) fault and two phase-to-ground (2LG) fault with different fault impedances on the test network in Figure 4.1. This generates both balanced and unbalanced voltage dips for both the detector and classifier ANN models. The models are trained, tested and validated in Matlab environment, and the proposed method is implemented using Matlab codes in Appendix 3.

In addition, for classification of voltage dips, various kinds of fault resistance and fault reactance are assumed and different fault starting time, and duration is used for the simulated dip classes. This is based on the assumption and fact that no two dips can start simultaneously at the same location at the same time in the network, however, one after the other in the same location at the same time. The dip data is collected from both transmission and distribution networks through the load busbars to train the ANN models when the different fault with different impedances is applied. Each of these fault types had different impacts on the equipment and produces different types of voltage dip [42].

6.2 ANN- based detection and classification of different windows of voltage dips

One important factor for economic growth of a nation depends on reliable and quality power and energy infrastructures of the country. Usage of power quality sensitive loads makes power quality i.e. voltage and frequency quality at load terminals mandatory as a service provided by the energy utilities. For providing reliable and quality power to the customers, it is not only necessary and important to avoid power systems disturbances, but also detect and eliminate the disturbance in time and restore the system to its normal operating state [263].

Also, the detection and classification of voltage dips are very important and helpful to both the utility and the customers for it is possible for two different voltage dips to have the same characteristics such as voltage magnitude and duration but different impacts on the sensitive loads [36]. However, ancillary service provided by GRDG can be helpful in voltage dip mitigation. With this in view, this thesis aims to develop an intelligent voltage dip detection and classification module using synthesized data for voltage dip mitigation using grid-integrated distributed generation in a power network.

Today national electricity companies around the globe still use analytical techniques to detect and classify voltage dips on their power network. Utilities such as Power Holding Company of Nigeria (PHCN) Plc, Zambia Electricity Supply Corporation Limited (ZESCO), Eskom (South Africa), etc., use the 10-minute r.m.s. value(s) to determine the highest or the lowest voltage magnitude of all the samples taken during a 10-minute period [58], [139]. However, it is possible that the use of artificial intelligence (AI) such ANN can greatly improve the efficiency, reliability and robustness of power network through the timely detection and classification of voltage dip [62].

6.3 Simulation of voltage dip events and generating data

6.3.1 Simulation of voltage dip

The electrical power systems are dynamic and nonlinear [189] and according to IEEE definitions, each power quality disturbance has its own unique features and definition that distinguishes it from another type of disturbance [25]. Therefore, under normal condition, the voltage magnitude remains within the allowed upper and lower limits (1.05p.u. and 0.95p.u.) usually measured in per unit, and the phase angle remains constant. However, when disturbances occur within the power network that leads to voltage dips, the system's voltage magnitude, reactive power and phase angle change among other variables. The ANN can help to detect the incidence of change in any of these variables under these circumstances. The process involves acquiring the retained voltage magnitude in r.m.s. value, phase angle shift and the dip duration.

6.3.2 Simulation of 'dip' and 'no dip' data

Disturbances that lead to reduction of r.m.s. voltage value at the load busbars within 10ms and 60sec is simulated as different power system faults (3P, 2P, 2LG and SLG) as mentioned above and in previous chapters. The dip condition data are generated by the inception of different fault types in both transmission lines and distribution lines. The no dip condition data are generated when there is

no disturbance within the power network that is the network is in a normal state. Examples of no dip data from the simulation in DIgSILENT and listed as r.m.s. voltage magnitudes in Table 5.1 in chapter 5. This will be the reference data for the dip detection. Table 5.2, Table5.3 and Table 5.4 in chapter 5 show how different dip data are generated on different lines with various fault types. This is done so that the learning database have various fault scenarios of voltage dips in order to improve the detector ANN's generalization capability.

Features extracted from simulated data for detection of voltage dip are the remaining or retained r.m.s. voltage magnitude at the load busbars, dip duration and phase angle shift. These are used as input features to the ANN. These feature data are collected through export to windows clipboard in DIgSILENT and pasted on Microsoft excel and saved in CSV format in Microsoft excel (comma delimited). This CSV data format is fed into the Matlab neural network, and all the input files must be in CSV format with only numbers in the entries.

The data samples are divided into three samples of data sets, the training set, validation set and the test set. The training data set is used for training and also for computing the gradient and updating the network weights and biases. Network generalization is measured through the validation data sets and also to halt training when generalization stops improving. The test data samples provide an independent measure of network performance during and after training, and they have no effect on training.

6.4 Intelligent voltage dip detection with artificial neural network in power networks

Previously, power quality disturbances were monitored and detected through the use of oscilloscopes. This was later replaced by the digital signal processing methods. Lately researchers are developing and using pattern recognition and decision-making systems that are capable of giving much accurate results as compared to the older techniques of power quality detection [50].

This chapter presents the development of a novel technique for voltage dip detection in power networks with a feed-forward artificial neural network (ANN). The hyperbolic tangent sigmoid function is selected as the activation function for the hidden layers because of its good converging results and fast approximation capability when compared to other activation functions. The output layers have a sigmoid activation function since the output value is binary codification, which is either "dip" or "no dip.

6.5 Proposed intelligent approach for voltage dip detection

For any voltage dip mitigation system to mitigate voltage dip adequately, it must be able to detect the voltage dip first. Electrical variables such as r.m.s voltage magnitude, phase angle shift, reactive power, etc., change from the declared values whenever any of the factors that lead to voltage dip occur such as starting of big motor, power systems faults, etc. Based on this principle, ANN-based detector is applied to detect any change in the aforesaid variables using the IEEE Std 1159-2009 conditions for voltage dip as reference [5].

The architecture of the proposed intelligent voltage dip detection system is shown in Figure 6.1. To detect voltage dip at the beginning of an incident, it is necessary to acquire the r.m.s. voltage values, phase angle shift and dip duration from the power network. It is computed and compared with the required voltage magnitude, duration and the phase angle. If the magnitude of the r.m.s. value is between 10% and 90% of the nominal voltage and for the duration of 10ms to 60sec, then the voltage is computed to signify the occurrence of a voltage dip [263].

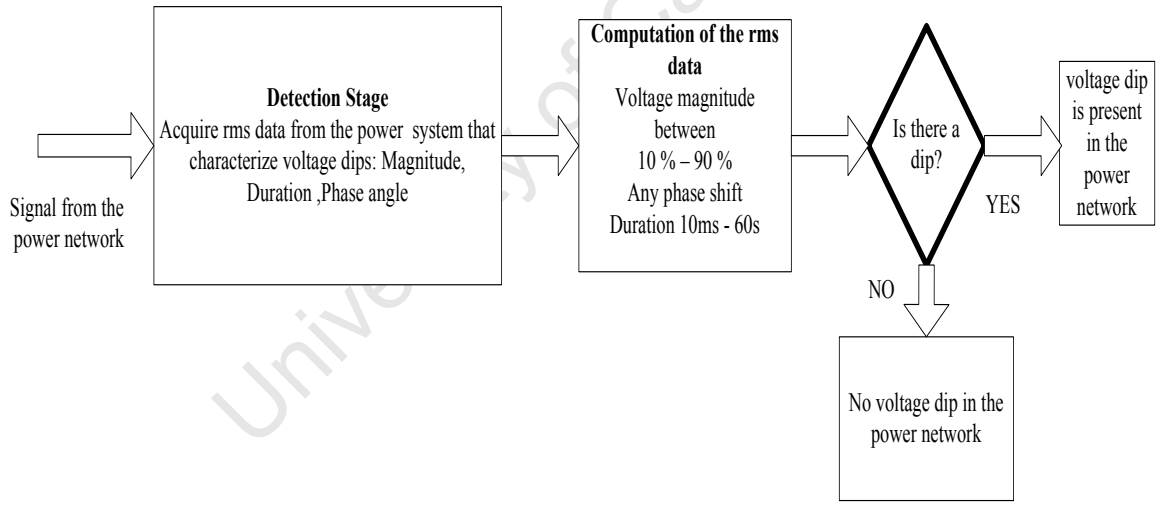

Figure 6.1: Architecture of the proposed intelligent voltage dip detection system

6.6 Creating the feed-forward ANN

Chapter 3 in section 3.17 shows how a feed-forward neural network (FFNN) can be created and implemented for voltage dip detection in an electrical power system. FFNN is usually made up of input layer, hidden layer and output layer. The numbers of input layer and output layer depend on the nature of the problem to be solved. For example, the input layer to the FFNN used for detecting

voltage dip in this work is based on the numbers of features used, and the output layer depends on the expected result from the detector ANN either the 'dip condition' or 'no dip condition'

The process of training a neural network to assign the correct target classes to a set of input patterns is called pattern recognition [263]. In this thesis, pattern recognition classification using FFNN is used to detect the incidence of voltage dips when the trained with the 'dip condition' and 'no dip condition' data. It detects and recognizes the voltage dip pattern feed into it by classifying them as a dip or no dip conditions.

The data generated from the simulation in DIgSILENT and listed as voltage magnitudes in Tables 5.2, 5.3 and 5.4 in Chapter 5 are organized into two matrices, such as, the input matrix which includes the three features of voltage dip (r.m.s. voltage magnitude, phase angle shift and dip duration) and the target matrix which defines the desired network output, and the target data is generated when there is a voltage dip in the system. This learning database is made up of variety of faulted scenarios to improve the ANN's generalization capability.

The input matrix is a 3 by M matrix defining the input features while the target matrix is 2 by M matrix defining the two classes ('dip' or 'no dip'). M represents the samples of three elements for the input matrix. M also represents the samples of 2 elements in the target matrix. Each column of the input matrix has 3 elements representing the features considered for detection of voltage dip. The corresponding column of the target matrix will have two elements, consisting of either a 0 or a 1 at any given time in a particular location indicating voltage dip and no voltage dip [263]. The output is of the form [dip, no dip], therefore the output of a dip is set as [1 0] and no dip is set as [0 1]. Table 6.1a shows "no dip" and "dip" data for detection and classification of voltage dip. The "no dip" data is represented with voltage dip magnitude as follows 0.961443, 0.961443, 0.961443 and 0.961443 and at phase angle of -1.7969, -1.7969, -1.7969, and -1.7969 and at the duration of 7.451761, 7.461761, 7.471761 and 7.481761 respectively. The "dip" data is represented with voltage dip magnitude as follows 0.76629, 0.766261, 0.766219, and 0.766177 and at phase angle of -13.9396, -13.9386, -13.9371, and -13.9357 and at the duration of 7.491761, 7.501761, 7.511761 and 7.521761 respectively. The voltage magnitude represents the remaining (retained) voltage magnitude.

Table 6.1a: Example of "no dip" and "dip" data for detection and classification of voltage dip

duration	7.451761	7.461761	7.471761	7.481761	7.491761	7.501761	7.511761	7.521761
Phase angle shift	-1.7969	-1.7969	-1.7969	-1.7969	-13.9396	-13.9386	-13.9371	-13.9357
Magnitude	0.961443	0.961443	0.961443	0.961443	0.76629	0.766261	0.766219	0.766177
	0	0	0	0	1	1	1	1
	1	1	1	1	0	0	0	0

Hyperbolic tangent sigmoid function is selected as the activation function for the hidden layers because of its good converging result and fast approximation as compared to other activation functions [152]. The output layer uses sigmoid as the activation function because it has the ability to assume values between 0 and 1 for either 'dip' or 'no dip' condition. The equations 3.6a and 3.6b in chapter 3 indicate the mathematically expressions for hyperbolic tangent sigmoid and sigmoid transfer function are renumber equations 6.1 and 6.2 in this chapter. Teaching algorithm is scaled conjugate gradient (SCG) propagation algorithm. The architecture of a two-layer feed-forward detector ANN is shown in Figure 6.2.

Hyperbolic tangent sigmoid transfer function

$$f(x) = \frac{2}{1+e^{-2x}} - 1 \qquad 6.1$$

Sigmoid transfer function

$$f(x) = \frac{1}{1+e^{-x}} \qquad 6.2$$

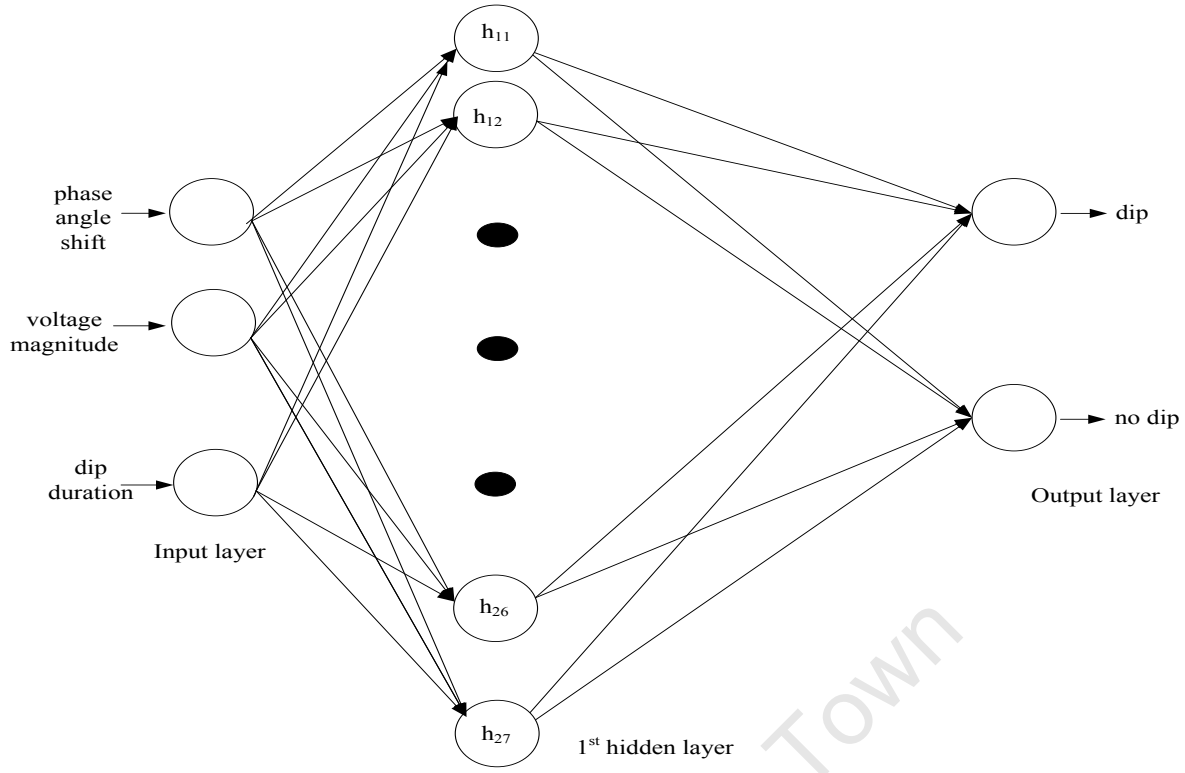

Figure 6.2: A two-layer feed-forward neural network for voltage dip detection with configuration 3-10-2

6.7 Training the detector neural network

The detector ANN is trained with data sample made up of both the 'dip' data and 'no dip' data samples. It contains 1,217 voltage 'dip' data samples and 295 of 'no dip' data samples, i.e., and 1,512 data samples in total. The 1,512 data samples are divided into three, 70% (1058), 15% (227) and 15% (227), which constitute are the training set, the validation set and the test sets respectively. The training data set is made available to the network during training, and is used for computing the gradient and updating the network weights and biases. The validation samples are used to measure the network generalization. Testing samples have no effect on training but provide an independent measure of network performance during and after training. The detector ANN is made up of 3 input neurons in the input layer, 27 neurons in the hidden layer, and 2 neurons output in the output layer. The hidden layer has no rule or formula for calculating the number of hidden neurons [152] as mentioned in chapter 3. The neuron number in the hidden layer is chosen by experimentation. To determine the best number of neurons in the hidden layer, different number of neurons is tested as shown in Table 6.1. The best number of hidden neurons with minimal error and highest accuracy is selected. The best number is determined to be 27 neurons for the detector ANN. 27 neurons give the minimum best validation performance (BVP) error of 2.5731e-008 occur at epoch 12. The

performance of ANN can be measured using either the mean squared error (mse) or mean absolute error (mae) . The mae measure network performance as the mean of absolute errors [146]. The mse is the average squared difference between the network outputs and the target outputs. The mse is implemented in this report and the lower the value of mse the better the accuracy and a value 'zero' mean no error.

Table 6.1: Different experimental process for determining detector ANN

ANN architecture	Number of neurons in hidden layer	Iterations epoch	Training time (ms)	Performance	NN Training error gradient	NN training performance BVP
3-5-2	5	19	10	1.12e-07	7.05e-07	1.8849e-007
3-10-2	10	22	10	7.82e-08	6.21e-07	1.0929e-007
3-16-2	16	15	10	9.21e-08	7.79e-07	1.007e-007
3-25-2	25	14	10	7.47e-08	7.85e-07	4.8668e-008
3-26-2	26	19	10	5.77e-08	9.54e-07	4.449e-008
3-27-2	27	12	10	3.07e-08	4.35e-07	2.5731e-008
3-28-2	28	24	10	5.65e-08	6.36e-07	3.7898e-008
3-30-2	30	33	20	5.33e-08	7.91e-07	2.6937e-008
3-45-2	45	33	20	3.61e-08	6.00e-07	3.8427e-008
3-100-2	100	24	20	0.0137	9.52e-07	0.017621

6.8 Results and evaluating the performance of the detector ANN

To analyse ANN performance after training two methods are used in this thesis these are the performance plot and confusion matrix. These methods are used to evaluate and judge the performance of the detector ANN. The confusion matrix is a form of table as shown in Figure 6.3 that shows the performances of the ANN.

There are four types of confusion matrix, these include training confusion matrix for training samples, testing confusion matrix for test samples, the validation confusion matrix for validation samples and the all confusion matrix which combines the three other matrixes. The percentage of the correctly detected voltage dip is the green squares on the matrices diagonal while the incorrectly

detected voltage dips is in red squares. The lower right blue squares indicate the overall detection accuracies. The confusion matrix is illustrated in Figure 6.3. This matrix structure holds for all of training, validation and test confusion matrices. Percentage of correctly detected voltage dips and percentage of incorrectly detected voltage dips are given by equations 6.3 and 6.4

$$\%\ \text{correctly detected dip} = \frac{\text{total correct detected dips}}{\text{total data}} \qquad 6.3$$

$$\%\ \text{incorrectly detected dip} = \frac{\text{total incorrect detected dips}}{\text{total data}} \qquad 6.4$$

Output Class				
Dip occurrence 1	No. of voltage dip detected correctly % of correctly detected voltage dip	No of voltage dip detected wrongly % of voltage dip that is wrongly detected as no-dip	% of row correctly detected % of row wrongly detected
No dip occurrence 2	No of no-dip detected wrongly % of no-dip that is wrongly detected as voltage dip	No. of correctly detected no-dip % of correctly detected no-dip	% of row correctly detected % of row wrongly detected
	% of column correctly detected % of column wrongly detected	% of column correctly detected % of column wrongly detected	% of overall correctly detected % of overall wrongly detected
	1	2	

Target Class

Figure 6.3: Detail of the Confusion matrix detail

The performance plot as shown in Figure 6.5 plot network performance and indicates the training, testing, and validation performances. The y-axis is the mean square error (mse) while the x-axis is the epoch. It also shows how the mse drops rapidly as the detector ANN learns. The blue line in the performance plot graph shows the decreasing error on training data, the green line shows the validation error and the red line shows the error on the test data indication how well the ANN has generalized on the data.

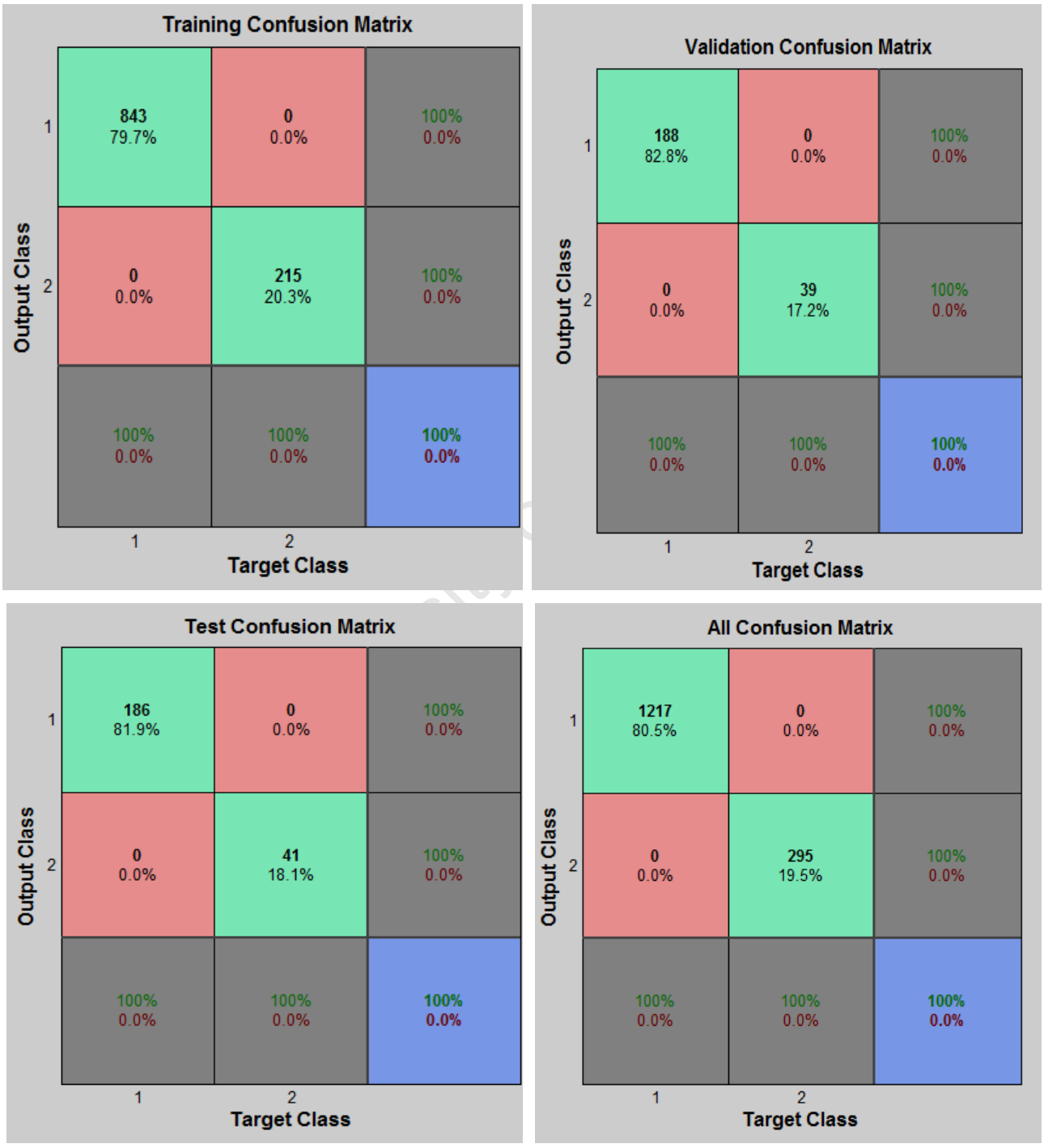

Figure 6.4: Training, test, validation and all confusion matrixes

The result of the performance of the detector ANN is judged by the confusion matrix in the Figure 6.4 and performance plot in Figure 6.5.

Figure 6.5 shows the training, validation, test performance plot for the detector ANN with architecture 3-27-2. This architecture has the best validation performance of 2.5731e-008 at epoch 12 when compare to others architecture as indicated in Table 6.1.

In addition, the confusion matrix in Figure 6.4 shows the result obtained from the training, validation, test and all confusion matrixes. These results show that both the dip, and the dip occurrences are correctly detected at 100%. There are no conditions of wrong detection.

The ANN is presented with a total number of 1058 data samples for training in which 843 (79.7%) is detected accurately as voltage dip and 215 (20.3%) is detected correctly as no dip occurrence. This is no wrong detection of either the dip or no dip occurrence; therefore, both are 0's (0.0%).

15% of the total data samples (227) are used to validate the ANN. Out of which 188 (82.8%) is detected accurately as voltage dip and 39 (17.2%) and is detected correctly as no dip occurrence. There is no wrong detection of either dip or no dip occurrence.

The test confusion matrix also shows that the detector ANN is well trained it recorded 81.9% (186) of the 227 data samples which are voltage dips and 18.1% (41) as no dip occurrence. The wrong detection percentages for both conditions are 0.0%.

All confusion matrixes combine the three matrixes and give the overall result. It has a total number of 1217 (80.5%) voltage dip samples are detected and 295 (19.5%) samples are also detected as no dip occurrence.

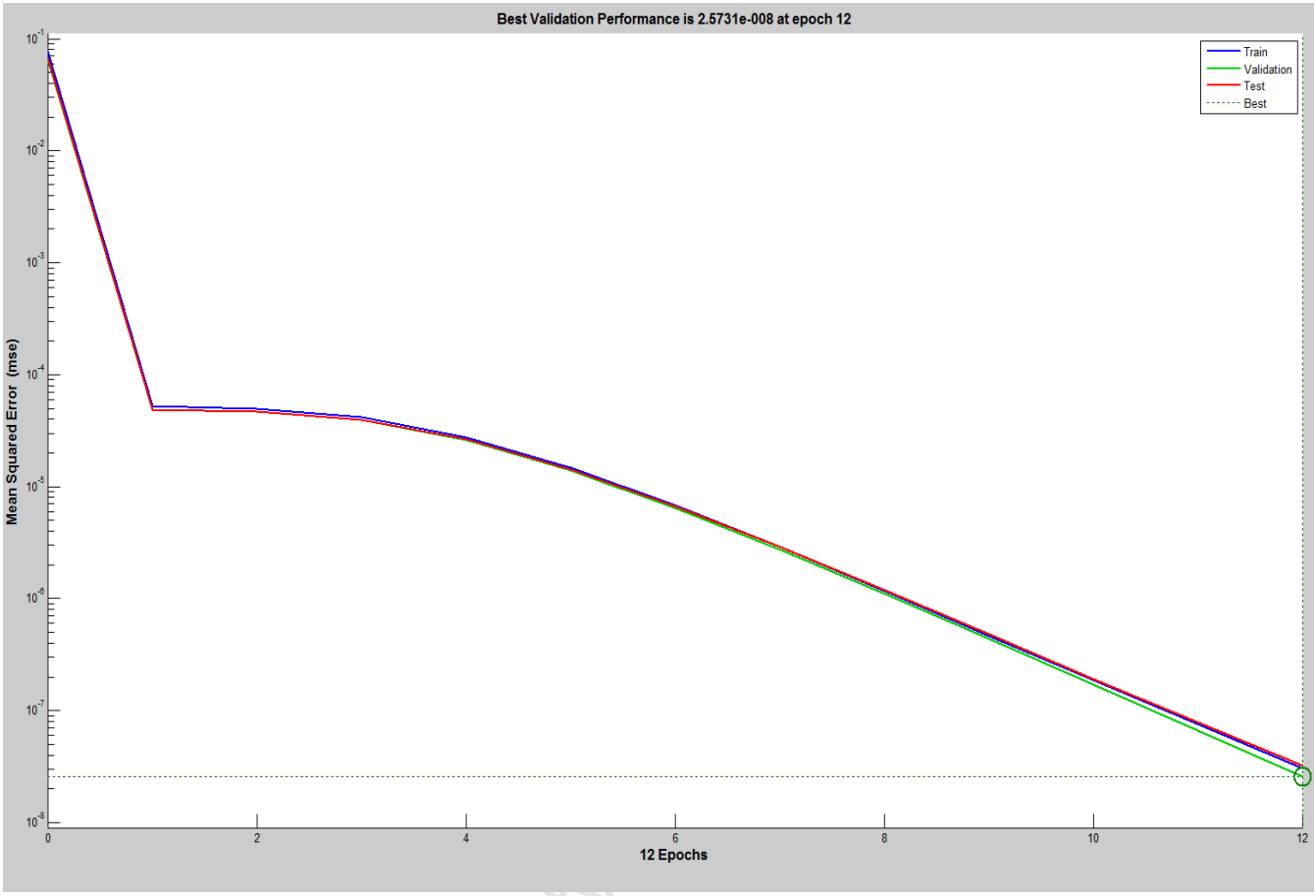

Figure 6.5: Performance plot of the detector ANN with BVP at 2.5731e-008 and epoch 12

6.9 Performance evaluation with 'dip' data only

This section evaluates the performance of the detector ANN when presented with voltage dip data samples only. This does not include the no-dip data and this is done to verify and validate the detector ANN and find out how well it will detect the dip.

The total data sample that is used is 1512 data samples, which are made up of voltage dip data samples only. The 1512 samples are divided into three, 70% (1058), 15% (227) and 15% (227), which constitute training set, validation set and test set respectively. The architecture of the detector ANN is shown in Table 6.2.

Table 6.2: Properties of the detector ANN

ANN architecture	Number of neurons in hidden layer	Iterations epoch	Training time (ms)	Performance	NN Training error gradient	NN training performance BVP
3-27-2	5	18	10	1.06e-07	7.95e-07	1.0374e-007

Figure 6.6 and Figure 6.7 show, the confusion matrix and the performance plot of the detector ANN using only voltage dip data samples. 1058 data samples were presented during the training. Training matrix shows that only 1051 (99.3%) is detected correctly as dip occurrences while 7 (0.7%) is wrongly detected as no dip occurrences. In addition, the validation confusion matrix shows 226 (99.6%) accurately detected voltage dip occurrence and 1 (0.4%) is incorrectly detected as no dip occurrence. The test matrix indicates that 225 (99.1%) is well detected as dip occurrence and 2 (0.9%) is wrongly detected as no dip occurrence. Furthermore, all confusion matrices show the total result of all the matrices in which 1502 (99.3%) is detected as dip occurrence while 10 (0.7%) is wrongly detected as no dip occurrence.

Figure 6.6: Training, test, validation and all confusion matrixes

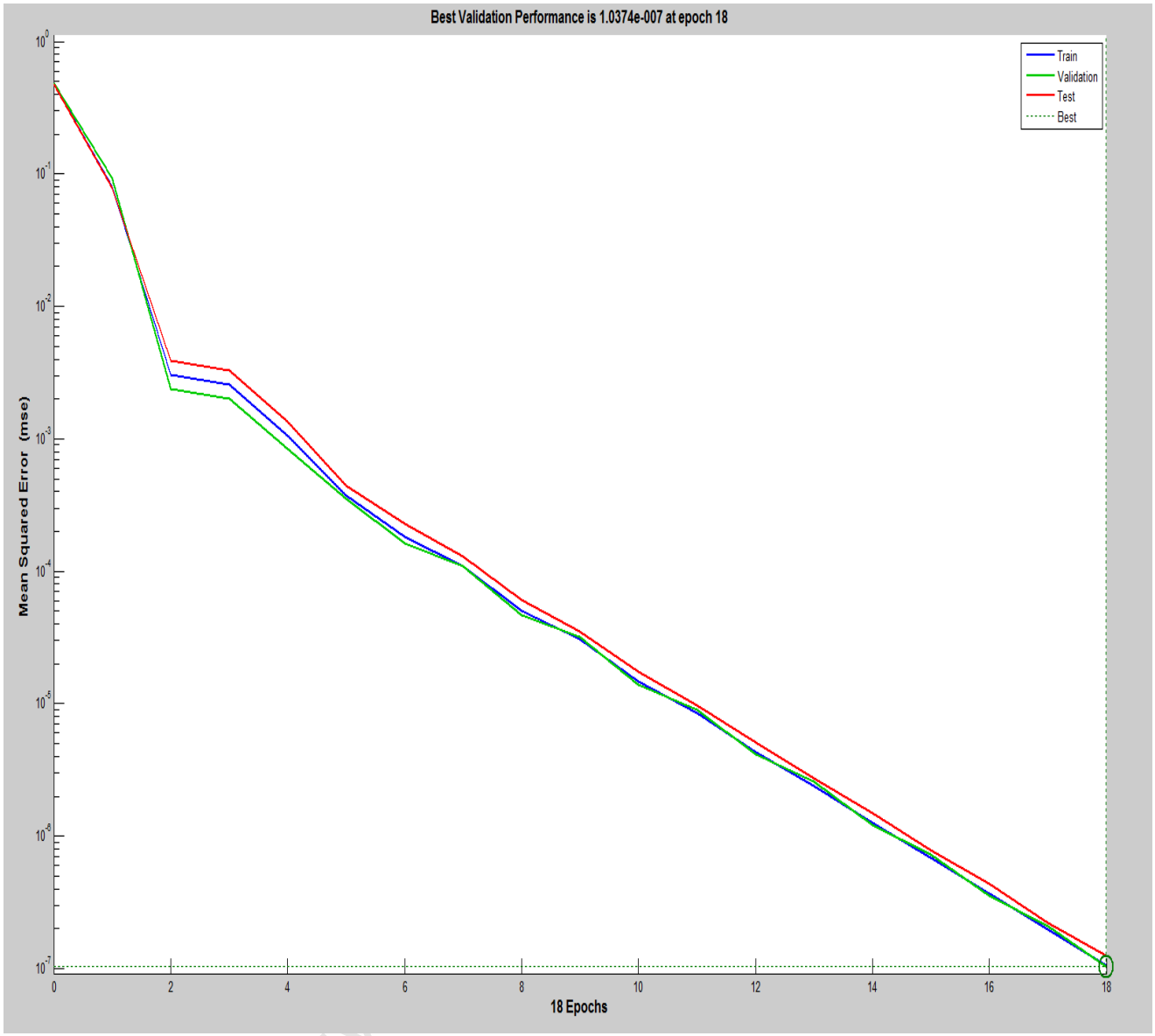

Figure 6.7: Performance plot showing the BVP at 1.0374e-007 of the detector ANN

The results shown in Figures 6.6 and 6.7 will help to interpret the accuracy of the detector ANN module when presented with dip data alone. This is different from the previous case where the ANN is presented with both dip and no dip data. There is a change in accuracy from 100% when both data was used to 99.3% when only dip data is used. This is due to incorrect detection of voltage dip as no dip. However, this thesis suggest the use of both data to train the ANN and also validate it accuracy with only dip data.

6.10 ANN- based classification system for different Eskom's voltage dip windows

The two main approaches used for classification of voltage dips are based on the definition and the description of different dip types as relate to three-phase nature, or the minimum magnitude and total duration approach. The first approach helps to classify dips into dip types according to the phase angles using their phasors instead of voltage magnitude values. The second method does not classify according to their three-phase nature instead they are represented by the minimum phase r.m.s voltage and the total duration of the dip in all the phases [51], [54]. This is the approach used by Eskom utility in classification, which was also adopted in this thesis. Figure 6.8 shows the architecture of the proposed intelligent voltage dip classification system according to Eskom voltage dip windows

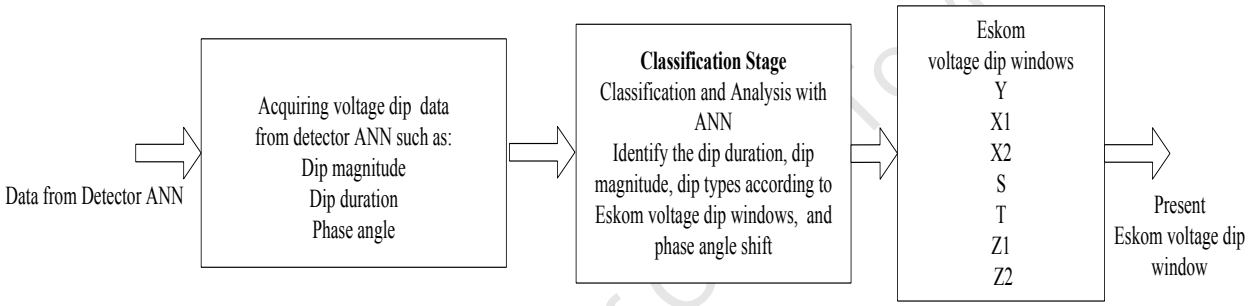

Figure 6.8: Architecture of the proposed intelligent voltage dip classification system

6.11 Classification of ESKOM voltage dip windows

This section presents voltage dip classification which is based on the voltage dip windows defined by the South African utility Eskom. It involves identifying which dip class is present as a result of voltage dip in a power network. The data used for this simulation and the modelling of the test network is officially provided by Eskom [201].

The Eskom YXSTZ classification is shown in chapter 1 in Table 1.8 renumbered as Table 6.3 in this chapter. It shows the voltage magnitudes both in terms of the missing (drop) voltage magnitude ΔU and retained voltage magnitude U_r and U_d is the nominal voltage [58]. However, in this thesis the retained voltage magnitude U_r is taken as the voltage dip magnitude as shown in Table 6.4.

Table 6.3: Characterization of depth and duration of voltage dips according to Eskom standard NRS 048-2 [58]

<table>
<tr><td>1</td><td>2</td><td>3</td><td>4</td><td>5</td></tr>
<tr><td rowspan="2">Range of dip
Depth
ΔU
(expressed as a % of U_d)</td><td rowspan="2">Range of residual
Depth
U_r
(expressed as
a % of U_r)</td><td colspan="3">Duration
t</td></tr>
<tr><td>20< t ≤ 150
ms</td><td>150 < t ≤ 600
ms</td><td>0.6 < t ≤ 3
s</td></tr>
<tr><td>$10 < \Delta U \leq 15$</td><td>$90 > U_r \geq 85$</td><td colspan="3">Y</td></tr>
<tr><td>$15 < \Delta U \leq 20$</td><td>$85 > U_r \geq 80$</td><td rowspan="3"></td><td rowspan="2"></td><td rowspan="2">Z1</td></tr>
<tr><td>$20 < \Delta U \leq 30$</td><td>$80 > U_r \geq 70$</td></tr>
<tr><td>$30 < \Delta U \leq 40$</td><td>$70 > U_r \geq 60$</td><td>X1</td><td rowspan="2">S</td><td rowspan="3">Z2</td></tr>
<tr><td>$40 < \Delta U \leq 60$</td><td>$60 > U_r \geq 40$</td><td>X2</td></tr>
<tr><td>$60 < \Delta U \leq 100$</td><td>$40 > U_r \geq 0$</td><td colspan="2">T</td></tr>
</table>

Table 6.4: Eskom voltage dip windows [58]

Dip class	R.M.S voltage magnitude (in %)	Dip duration	Dip duration (ms)
Y	$90 > u_r \geq 70$	> 20ms to 3sec	< 2980
X1	$70 > u_r \geq 60$	> 20ms to 150ms	< 130
X2	$60 > u_r \geq 40$	> 20ms to 150ms	< 130
S	$80 > u_r \geq 40$	> 150ms to 600ms	< 450
T	$40 > u_r \geq 0$	> 20ms to 600ms	< 580
Z1	$85 > u_r \geq 70$	> 600ms to 3sec	< 2400
Z2	$70 > u_r \geq 0$	> 600ms to 3sec	< 2400

6.12 Simulation of Eskom voltage dip windows and dip data generation training and testing the detector ANN

The different voltage dip class is simulated by applying different types of fault with different fault resistance and reactance on both the distribution lines and the transmission lines. This will create different classes of voltage dip. The features of these voltage dip classes are extracted, and seven different databases are created for the Eskom voltage dip windows. This enables the ANN classifier to learn different pattern and distinguish between Eskom voltage dip windows. Eskom dip data

Table 6.5: A sample of a typical fault resistance and reactance for generating different Eskom voltage dip windows on line 9

Dip class	Fault resistance(Ω)	Fault reactance (Ω)	Time in seconds			R.M.S voltage magnitude (p.u.)
			Fault time	Clearing time	Dip duration	
Y	80	40	0.5	3.42	2.92	$90 > u_r \geq 70$
X1	27	5.3	4.00	4.11	0.11	$70 > u_r \geq 60$
X2	14	8	4.22	4.34	0.12	$60 > u_r \geq 40$
S	30	10	5.00	5.42	0.42	$80 > u_r \geq 40$
T	10	3	5.80	6.33	0.53	$40 > u_r \geq 0$
Z1	60	20	7.50	9.80	2.30	$85 > u_r \geq 70$
Z2	25	5	11.55	13.91	2.36	$70 > u_r \geq 0$

generation process is explained more clearly in chapter 7. However, Table 6.5 shows a typical fault resistance and reactance for generating different Eskom voltage dip windows on line 9.

This features data samples are fed into the input of the classifier ANN for training. One of the assumptions is that no two dips can happen simultaneously on the same line at the same time. Therefore, all the classes of dip are simulated at different times. The voltage dip duration is the maximum length of time dip can be experience before the circuit breakers within the network act to isolate the faulty side of the network, and this is different for all the dip classes. The measurement and collection of dip data are done at the load busbars in DIgSILENT using the export to windows clipboard and imported to Microsoft Excel sheet and saved in CSV format.

The data samples are arranged in the form of input matrix and the target matrix. Each column of the input matrix has fifteen elements representing the features (r.m.s. voltage magnitude and phase angle shift for each of the classes and the dip duration) considered for classification of voltage dip. Each corresponding column of the target matrix will have seven elements, consisting of six 0s and a 1 in the location of the associated dip class. The classifier ANN is trained with 615 (70%) of the total data samples 879, 132 (15%) is used to validate the ANN and 132 (15%) is used to test and verify the performance of the classifier.

ANN classifier is a feed-forward neural network comprises of fifteen input layer, 20 neurons in the hidden layer and seven output layer. The radial basis transfer function is the activation function of the hidden layers, and sigmoid function is used as the activation function the output layer. Table 6.6 shows the different experimental process that is carried out to model the classifier ANN architecture. Experimental process involves training the ANN many times to obtain the best number of hidden neurons with minimal error and highest accuracy.

Table 6.6: Different experimental process for determining the classifier ANN

ANN architecture	No of neurons in hidden layer	Iterations epoch	Training time (ms)	Performance	NN Training error gradient	NN training performance BVP	Total % classified correctly	Total % classified wrongly
15-5-7	5	71	20	0.0105	9.49e-07	0.0097405	92.7	7.3
15-10-7	10	56	20	0.00604	7.38e-07	0.010823	95.1	4.1
15-15-2	15	37	20	4.17e-08	9.54e-07	2.6683e-007	100.0	0.0
15-20-7	20	59	20	1.68e-08	6.69e-07	1.7132e-008	100.0	0.0
15-25-7	25	71	20	0.00186	8.65e-07	0.0021646	98.9	1.1
15-26-2	26	61	20	0.00163	9.79e-07	0.0010825	99.0	1.0
15-27-7	27	60	20	0.00139	8.39e-07	0.0010824	99.0	1.0
3-30-2	30	54	20	0.00836	8.57e-07	0.0086582	93.9	6.1

Figure 6.9 shows a 15-20-7 fully connected FFNN is designed with resilient propagation algorithm for Eskom dip classification.

In Figure 6.9, the input layer has fifteen elements representing the features (r.m.s. voltage magnitude and phase angle shift for each of the classes and the dip duration) considered for classification of voltage dip.

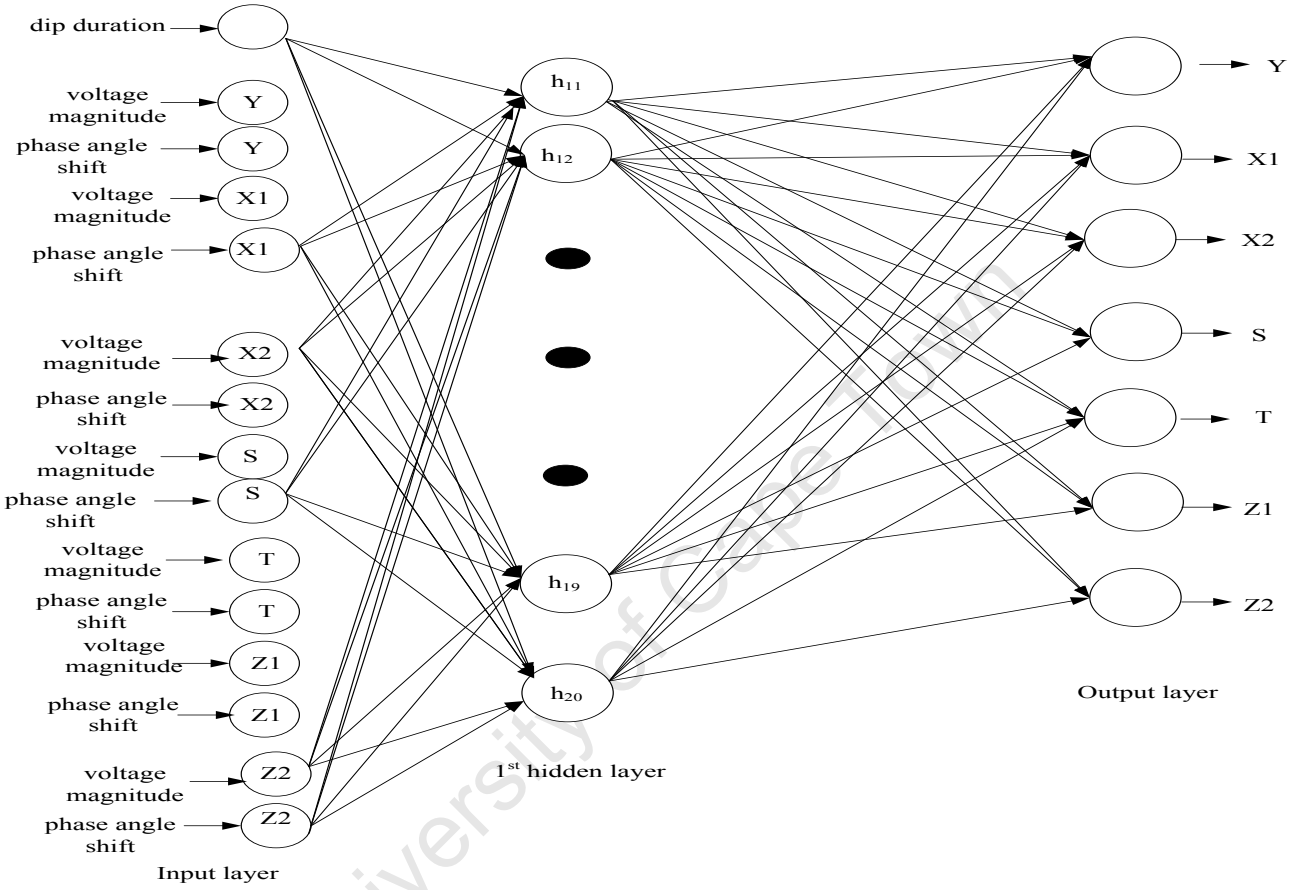

Figure 6.9: A two-layer feed-forward neural network for voltage dip classification 15-20-7

6.13 Evaluation of performance

To judge the performance of the ANN classifier, the performance plot and the confusion matrix are used. Figure 6.10 shows the confusion matrix while Figure 6.11 shows the performance plot.

Figure 6.10: Training, test, validation and all confusion matrixes

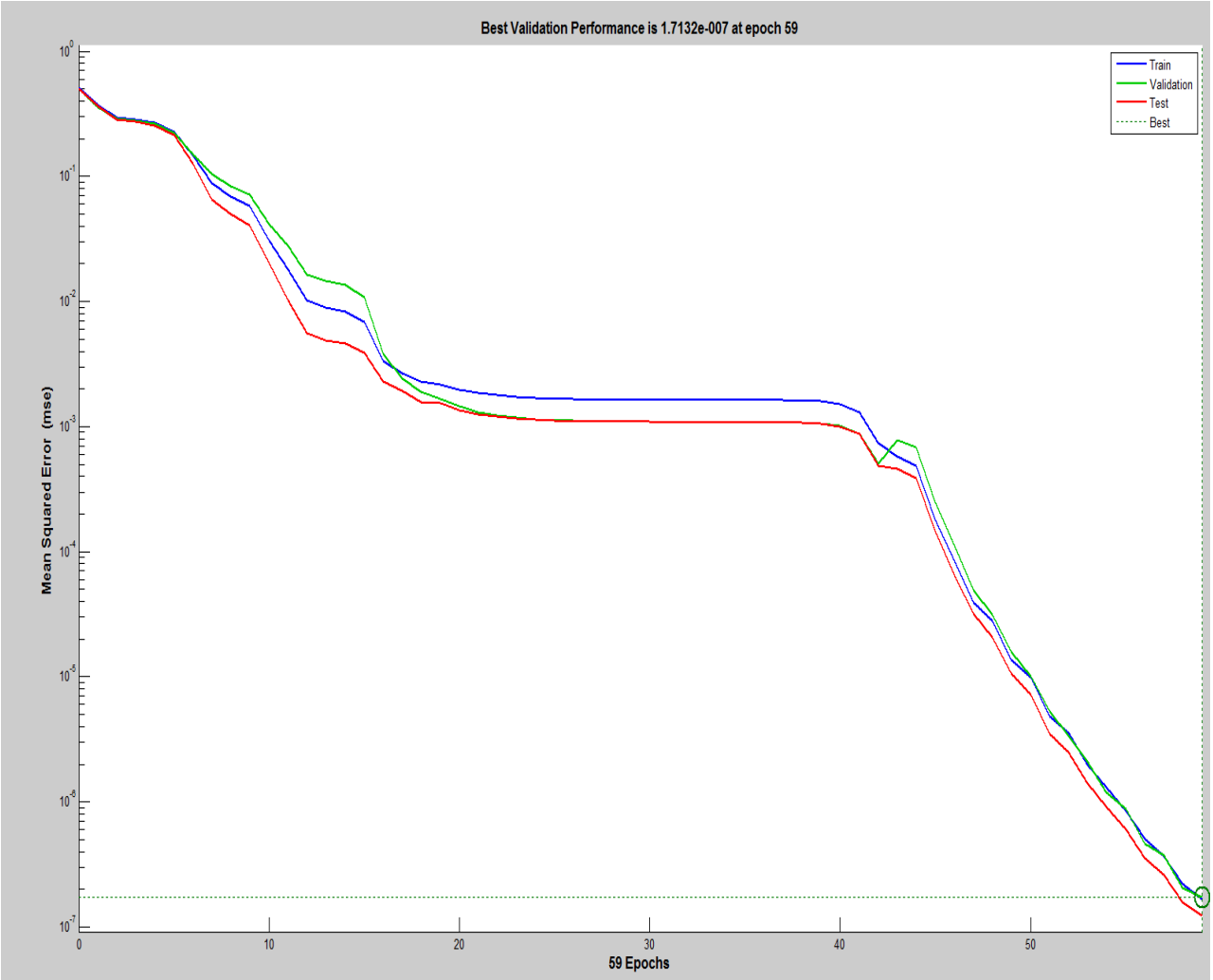

Figure 6.11: Performance plot of classifier ANN with BVP at 1.7132e-008 and epoch 59

The total training sample is 615 in which Y is 5 samples X1 is 4 samples, X2 is 31 samples, S is 35 samples, T is 158 samples, Z1 is 173 samples and Z2 is 209 samples. All these samples are correctly classified 100% as shown in the training confusion matrix. The validation confusion matrix is also having 100% correctly classified samples as shown by the blue box in Figure 6.10. It has 4, 1, 9, 10, 38, 31, and 39 for dip classes Y, X1, X2, S, T, Z1 and Z2 respectively. Also the test confusion matrix has 100% classification for Y, X1, X2, S, T, Z1 and Z2 with 1, 4, 3, 9, 35, 33, and 47 respectively. Furthermore, the all confusion matrix also has 100% correctly classification.

From the result obtained, it is shown that the classifier ANN have obtained 100% accuracy in the classification of Eskom voltage dip window. Samples of different classes of Eskom voltage dip windows are shown in Figure 6.12 below which are learned by the classifier ANN. It needs to learn the r.m.s. voltage magnitude change and the duration of the dip to classify them properly and accurately.

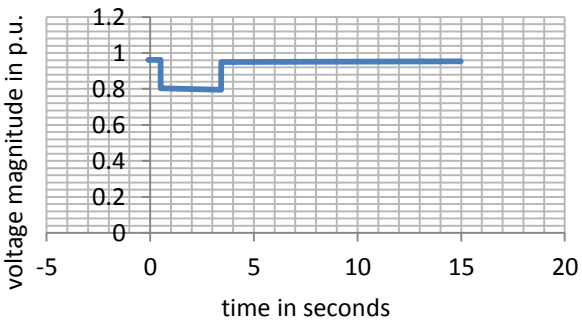

Figure: 6.12a. Voltage dip for Y class of ESKOM windows

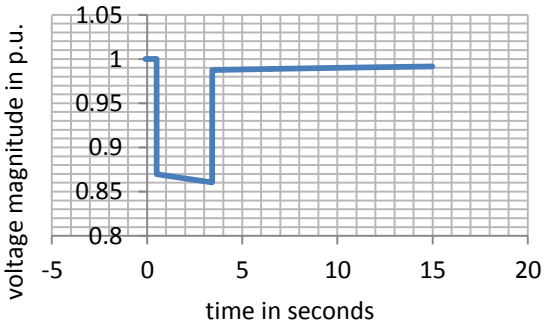

Figure: 6.12b. Voltage dip for Y class of ESKOM windows

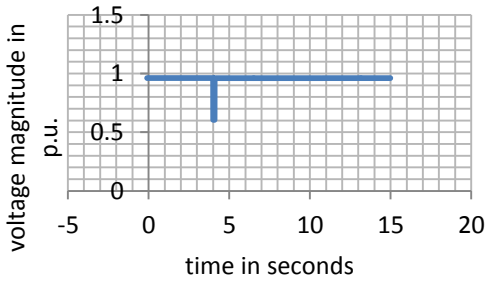

Figure: 6.12a. Voltage dip for X1 class of ESKOM windows

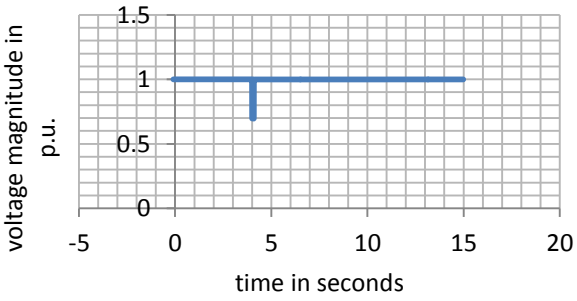

Figure: 6.12b. Voltage dip for X1 class of ESKOM windows

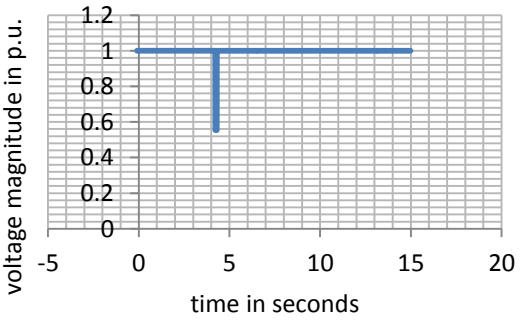

Figure: 6.12a. Voltage dip for X2 class of ESKOM windows

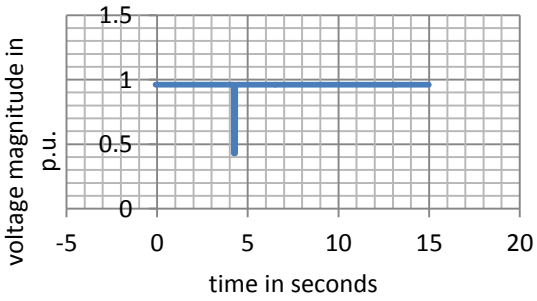

Figure: 6.12b. Voltage dip for X2 class of ESKOM windows

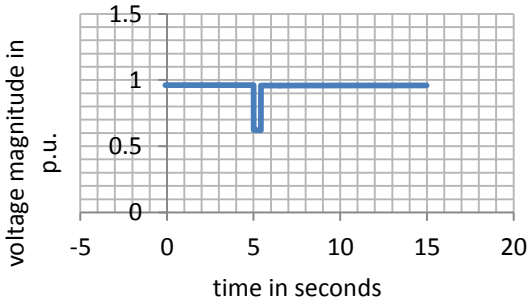

Figure: 6.12a. Voltage dip for S class of ESKOM windows

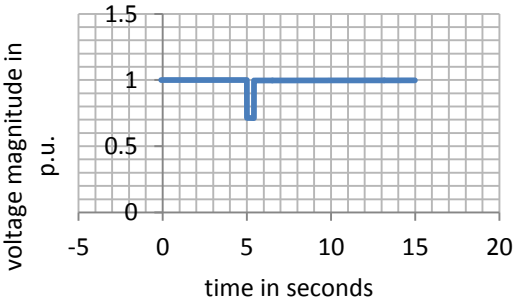

Figure: 6.12b. Voltage dip for S class of ESKOM windows

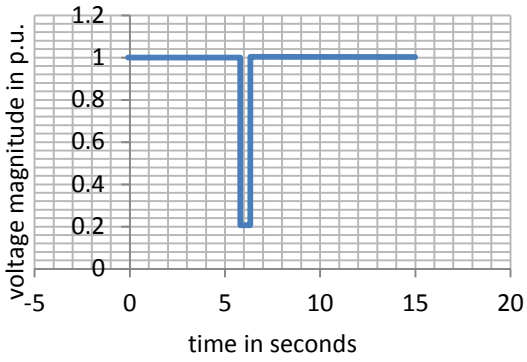

Figure: 6.12a. Voltage dip for T class of ESKOM windows

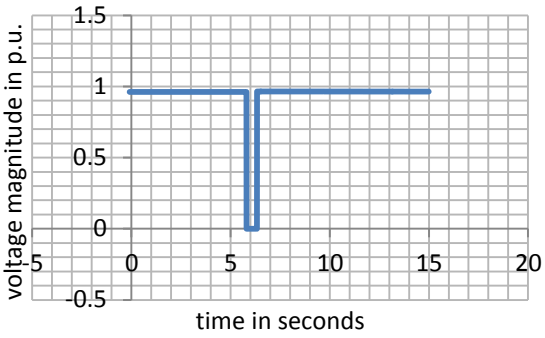

Figure: 6.12b. Voltage dip for T class of ESKOM windows

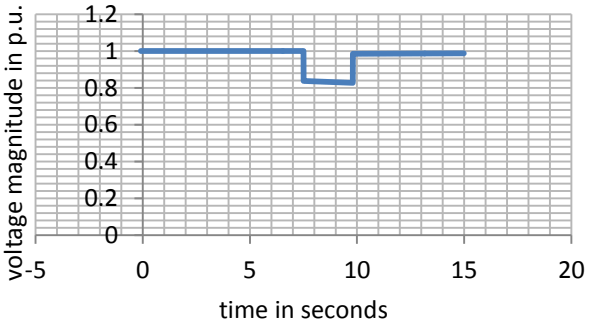

Figure: 6.12a. Voltage dip for Z1 class of ESKOM windows

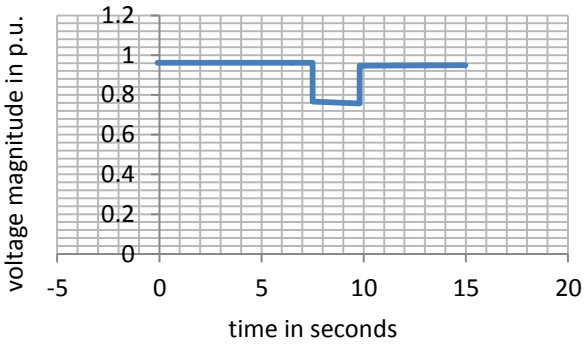

Figure: 6.12b. Voltage dip for Z1 class of ESKOM windows

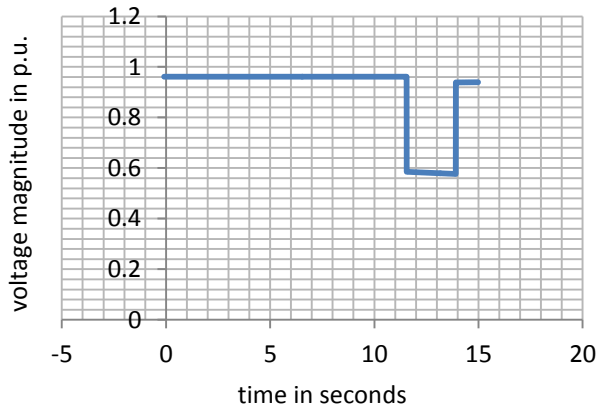

Figure: 6.12a. Voltage dip for Z2 class of ESKOM windows

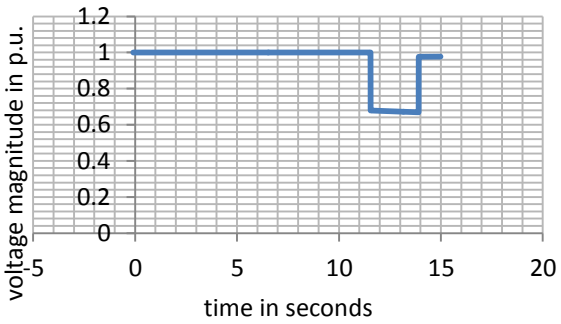

Figure: 6.12b. Voltage dip for Z2 class of ESKOM windows

The confusion matrices and performance plot for other architectures of classifier ANNs from the experimental process are shown in the appendix 6. This is necessary in other to model and obtain the best number of hidden neurons with minimal error and highest accuracy for the classifier ANN architecture.

6.14 Advantage of detection and classification of voltage dip in this thesis

The main advantage of voltage dip detection and classification is to improve voltage quality. The next chapter shows how classification of voltage dip helps to decide if a voltage dip is severe or not (through classification into magnitude and duration) so that both the power customers and utilities can protect their equipment and plants. In addition, chapter 7 shows the effect and participation of different types of GRGDs during mitigation of voltage dip.

Chapter 7

7.1 Discussion of results of the ANN module and its application in voltage dip mitigation

To improve voltage quality, the concept of voltage standards under engineering practices and electromagnetic compatibility is introduced by different standard organizations such as, IEEE, IEC, CBEMA and SEMI. These organizations have various voltage-tolerance curves and indices (e.g CBEMA curve, ITIC curve and system average rms variation frequency index (SARFI)) for voltage acceptability, however power utilities like Eskom also have chart to compare the voltage quality of the power system [34].

The Eskom voltage dip window chart in Figure 7.1. This chart can also help to decide if a voltage dip is severe or not so that both the power customers and utilities can protect their equipment and plants. This work presents the development and testing of use of an ANN-based system for voltage dip detection and classification based on Eskom voltage dip windows aimed to aid the chart which will help experts engineers and researchers to evaluate voltage dip severity and to gives suggest them an idea on how it is possible to mitigate with grid-integrated renewable distributed generation (GRDGs) in the utility system based on GRDG systems.

It is difficult at present to eradicate voltage dip from our power network. This is as a result of unpredictable nature of factors that influence and contribute to the causes of voltage dips. Therefore, intelligent system such as ANN has been selected as a tool for in order to mitigate voltage dip effectively using the GRDG systems. After detection and classification of these dips by plotting them with ANN the dip can be plotted on the Eskom voltage dip windows chart. This is followed by the assessment of different types of GRDGs as to how effectively they can mitigate these dips. The Eskom voltage dip window chart can be used to describe the performance and analyze the impacts of GRDG systems. The Eskom chart is shown in Figure 1.17 in chapter 1; however, it is renumbered as Figure 7.1 in this chapter, and this is described in chapter 1 section 1.16.3.

The following actions are performed by the ANN module.

- Detection of voltage dip,
- Classification of voltage dips into different Eskom classes
- The assessments of GRDGs for voltage dip mitigation which will improve dip mitigation.

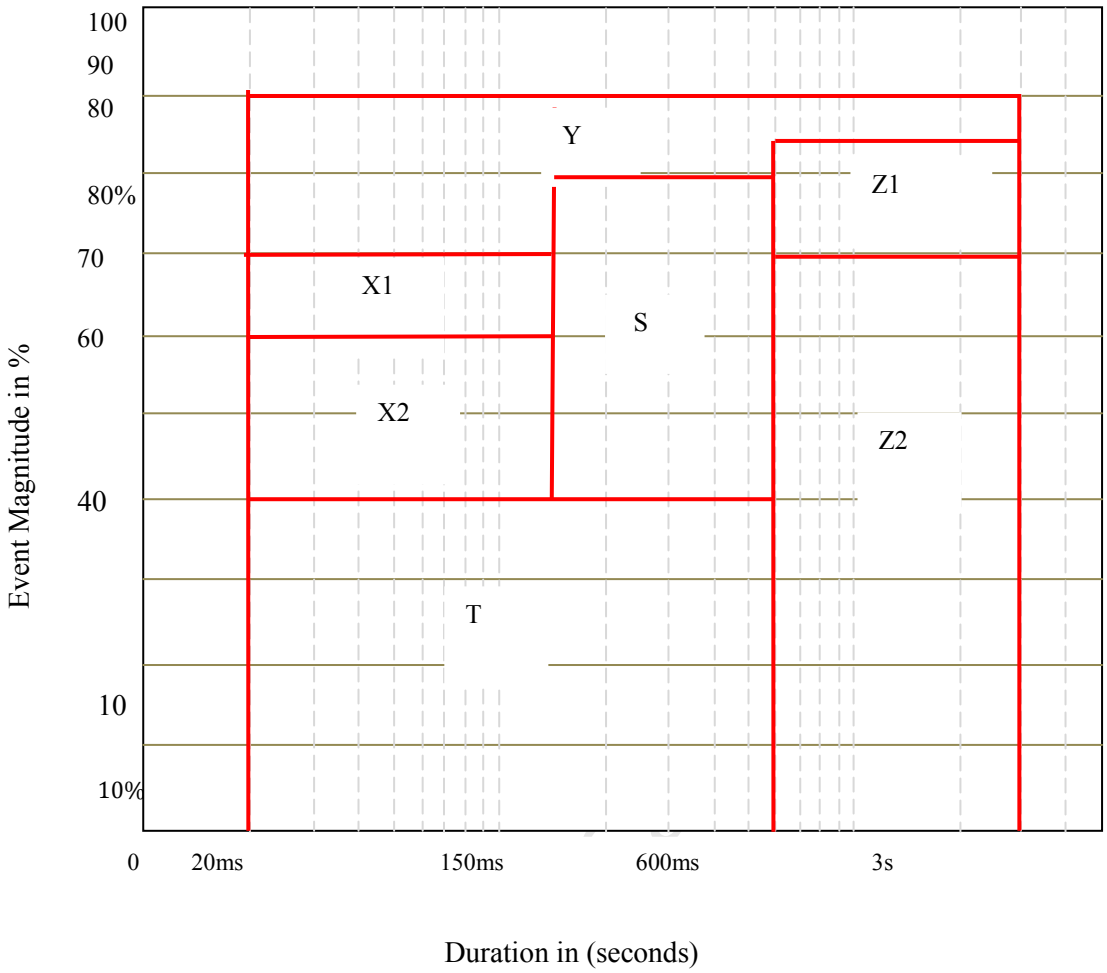

Figure 7.1: Eskom voltage dip window chart according to remaining (retained) voltage magnitude [34].

7.2 Simulation of various dip class

To simulate samples of various Eskom voltage dip windows using the test network in Figure 4.1., a three-phase short circuit fault is applied at time t_1 sec and cleared at t_2 sec, at 50% of line9 to generate different dip classes this by varying the fault resistance and reactance. The dip measurement is taken at $(t_2 + t_1)/2$ sec from in the form of retained p.u. voltage magnitude at busbar18 and busbar21 at various dip classes. This is shown in Table 7.1 and Table 7.2. This is due to the fact that all the dip classes have different duration and a 3P fault is assumed to produce a type A dip which is the most severe dip since it affects all the three phases. The two tables also show the impact of GRDG on various dip classes; however it was recorded at different times. This is based on the assumption from chapter 6 in section 6.1 that no two dips can start simultaneously in the same location at the same time in a power network, however, one after the other in the same location at the same time.

Table 7.1: Voltage magnitude recorded on busbar18 due to 3P fault on line 9 at 50% of the line with different fault resistance and reactance

Dip class	Fault resistance(Ω)	Fault reactance (Ω)	Time in seconds		Retained Voltage magnitude in p.u.					
			Fault time (t_1)	Clearing time (t_2)	Due to 3P fault	With wind	With hydro	With PV	With Hydo +Wind	All GRDG
Y	80	40	0.5	3.42	0.875	0.909	0.922	0.902	0.922	0.923
X1	27	5.3	4.00	4.11	0.696	0.860	0.882	0.829	0.891	0.898
X2	14	8	4.22	4.34	0.554	0.711	0.730	0.684	0.738	0.745
S	30	10	5.00	5.42	0.713	0.847	0.887	0.814	0.907	0.927
T	10	3	5.80	6.33	0.387	0.579	0.617	0.555	0.640	0.664
Z1	60	20	7.50	9.80	0.832	0.898	0.920	0.886	0.933	0.943
Z2	25	5	11.55	13.91	0.674	0.784	0.818	0.753	0.829	0.838

Dip class	Dip duration (t_2 -t_1) (sec)	Mid-dip duration (t_2 -t_1)/2 (sec)	Time on Eskom chart (ms)	Recoding time (t_r) = (t_2 +t_1)/2 (sec)
Y	2.92	1.460	1460	1.96
X1	0.11	0.055	55	4.06
X2	0.12	0.060	60	4.28
S	0.42	0.210	210	5.21
T	0.53	0.265	265	6.07
Z1	2.30	1.150	1150	8.65
Z2	2.36	1.180	1180	12.73

Table 7.2: Voltage magnitude recorded on busbar21 due to 3P fault on line9 at 50% of the line with different fault resistance and reactance

Dip class	Fault resistance(Ω)	Fault reactance (Ω)	Time in seconds		Voltage magnitude in p.u.					
			Fault time (t_1)	Clearing time (t_2)	Due to 3P fault	With wind	With hydro	With PV	With Hydo +Wind	All GRDG
Y	80	40	0.5	3.42	0.856	0.973	1.003	0.938	1.012	1.019
X1	27	5.3	4.00	4.11	0.606	0.919	0.955	0.869	0.968	0.980
X2	14	8	4.22	4.34	0.429	0.773	0.810	0.721	0.824	0.835
S	30	10	5.00	5.42	0.621	0.906	0.957	0.851	0.980	1.001
T	10	3	5.80	6.33	0.338	0.635	0.690	0.575	0.715	0.738
Z1	60	20	7.50	9.80	0.762	0.955	0.996	0.917	1.014	1.050
Z2	25	5	11.55	13.91	0.581	0.816	0.863	0.759	0.879	0.890

Dip class	Dip duration (t_2 -t_1) (sec)	Mid-dip duration (t_2 -t_1)/2 (sec)	Time on Eskom chart (ms)	Recoding time (t_r) = (t_2 +t_1)/2 (sec)
Y	2.92	1.460	1460	1.96
X1	0.11	0.055	55	4.06
X2	0.12	0.060	60	4.28
S	0.42	0.210	210	5.21
T	0.53	0.265	265	6.07
Z1	2.30	1.150	1150	8.65
Z2	2.36	1.180	1180	12.73

Voltage dip events in the Tables 7.1 and 7.2 are mapped on the Eskom window in Figure 7.2. The voltage dip events are located in the area Y, X1, X2, S, T, Z1 and Z2 at the different voltage levels as measured at time t_r when the GRDG units are disconnected from the power network. Voltage dip magnitudes on basbar18 are represented with * on the chart while that of busbar22 is represented with +

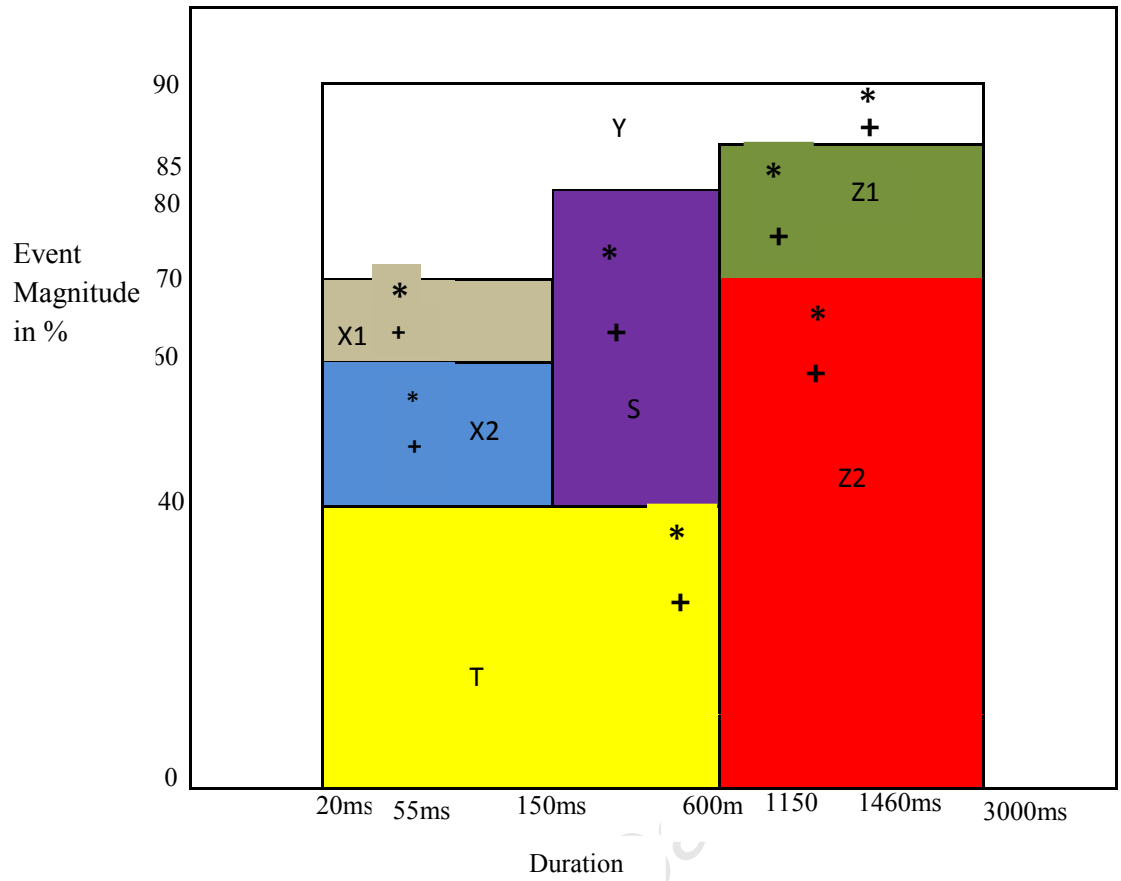

Figure 7.2: Scatter diagram of voltage dip magnitude recorded at the load busbars18 and basbar22 due to 3P fault

The scatter diagram in Figure 7.2 show how the detected voltage dip is classified according to Eskom voltage dip window. This is done by plotting the voltage dip magnitude and duration on the chart.

7.3 Monitoring the effect and participation of each GRGD

The impact and participation of each GRGD can be monitored using the Eskom chart and also it can be determined if customer's sensitive load can ride-through the voltage dip. These are shown in the scatter diagrams of Figures 7.3 through 7.7 below.

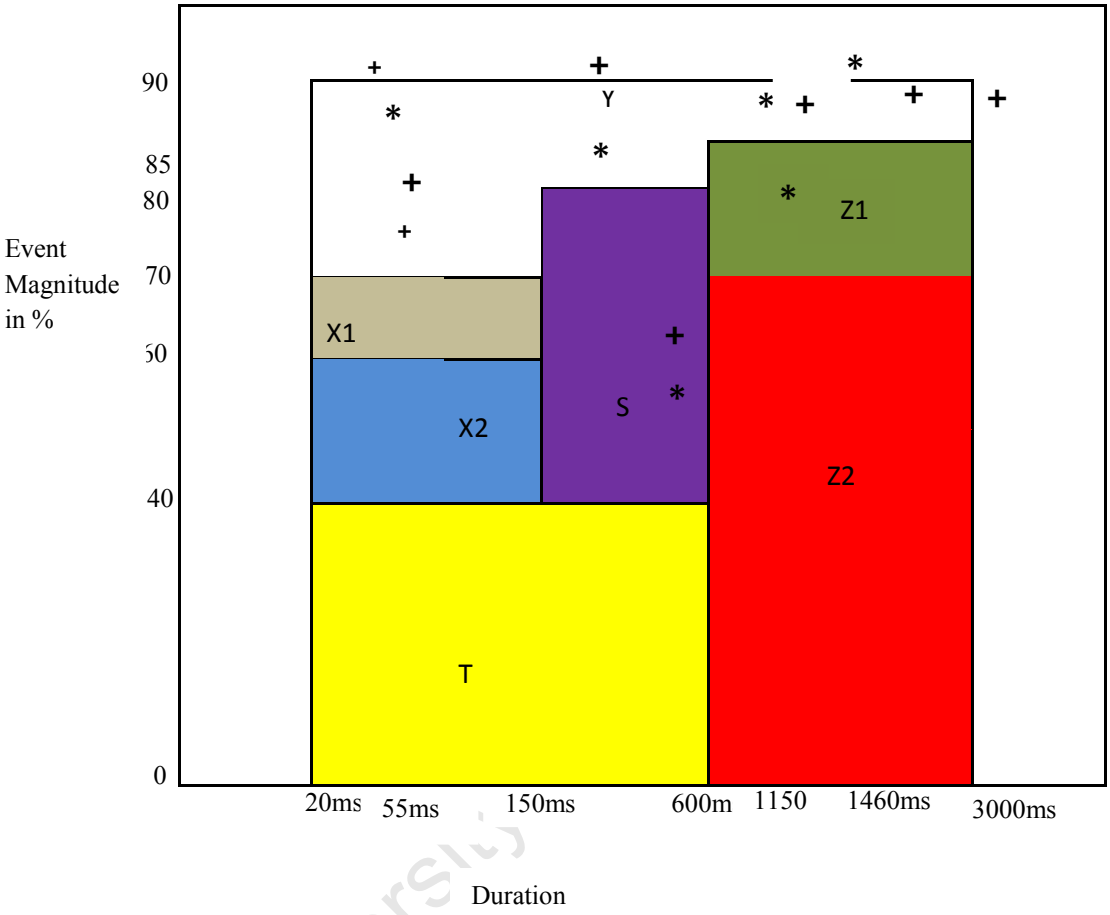

Figure 7.3: Scatter diagram of voltage dip mitigation with wind generators at busbars18 and basbar22 due to 3P fault

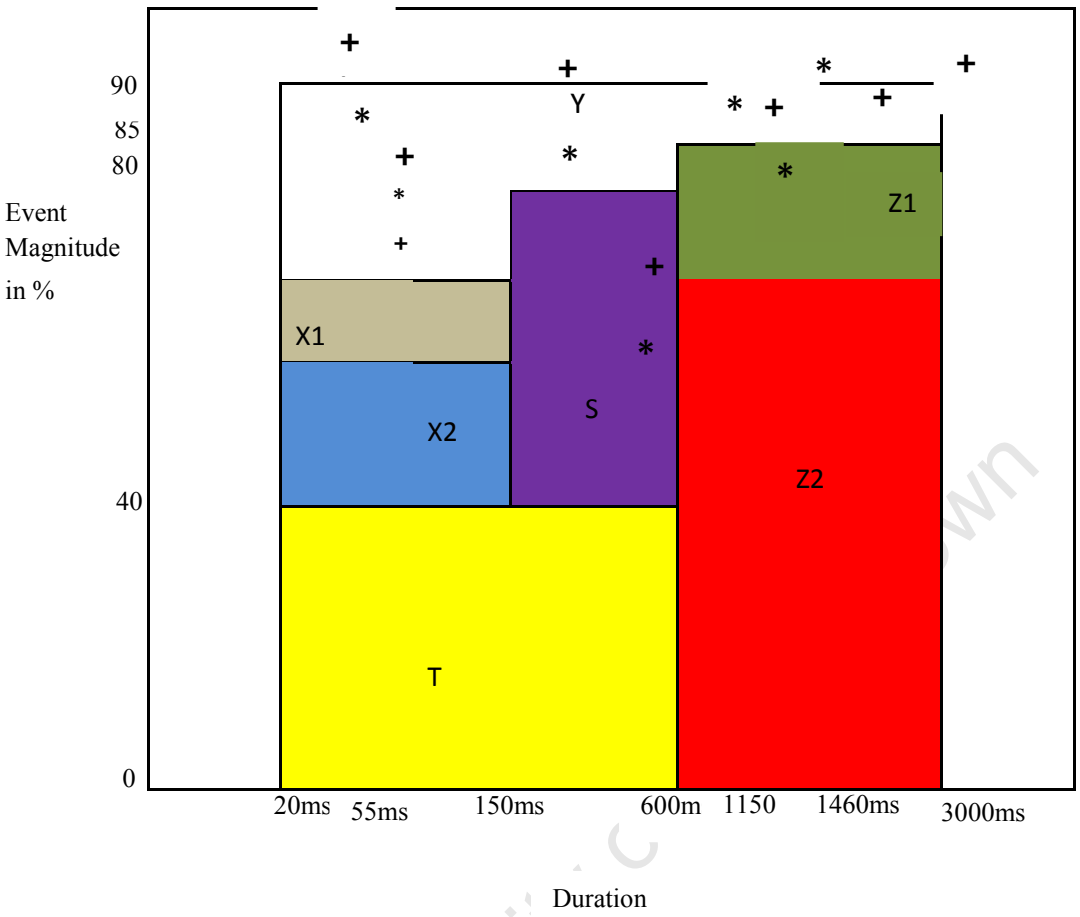

Figure 7.4: Scatter diagram of voltage dip mitigation with hydro generators at busbars18 and basbar22 due to 3P fault

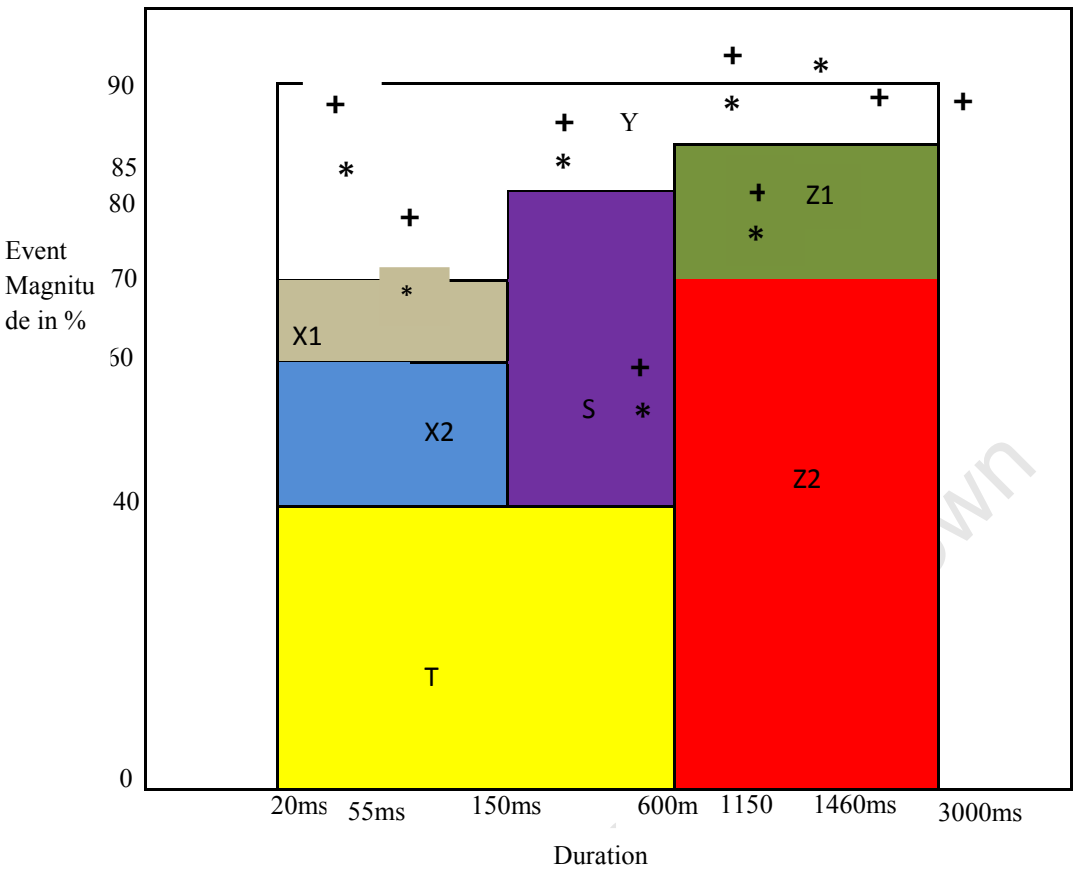

Figure 7.5: Scatter diagram of voltage dip mitigation with PV generators at busbars18 and basbar22 due to 3P fault

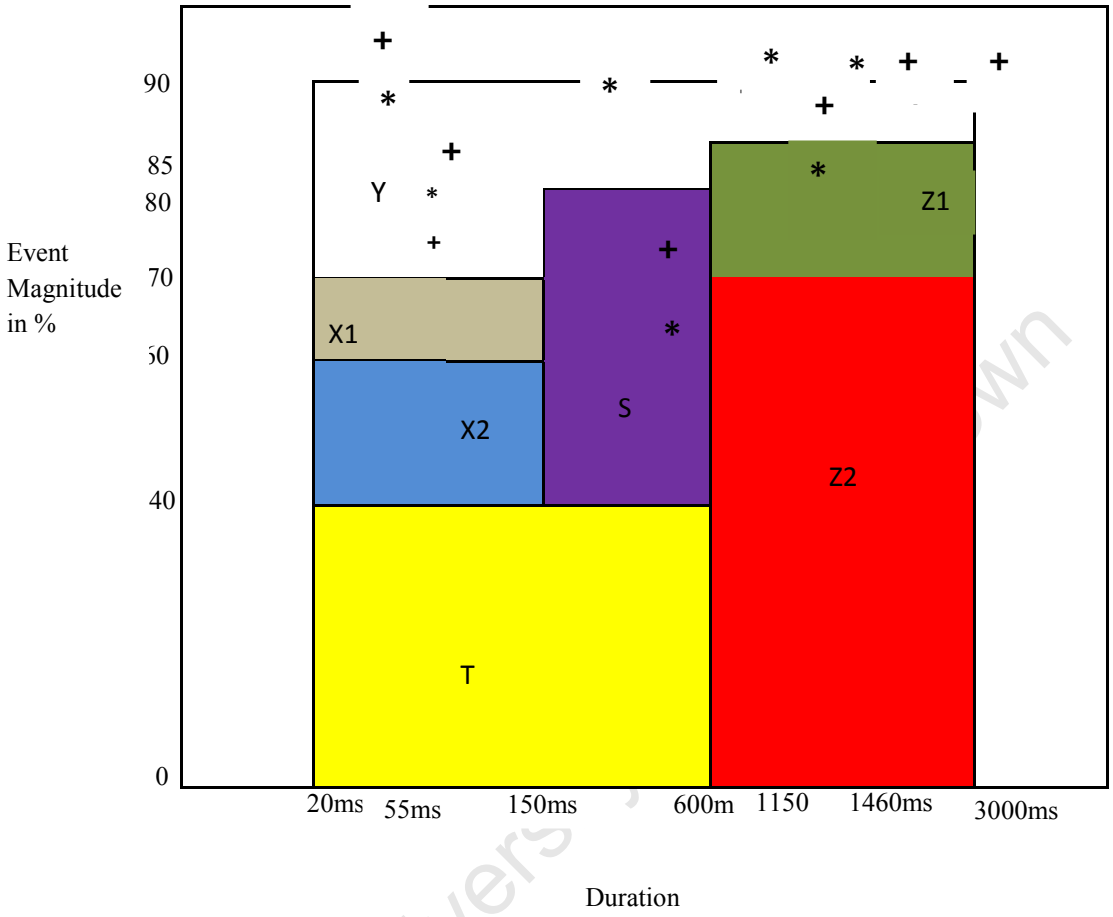

Figure 7.6: Scatter diagram of voltage dip mitigation with wind and hydro generators at busbars18 and basbar22 due to 3P fault

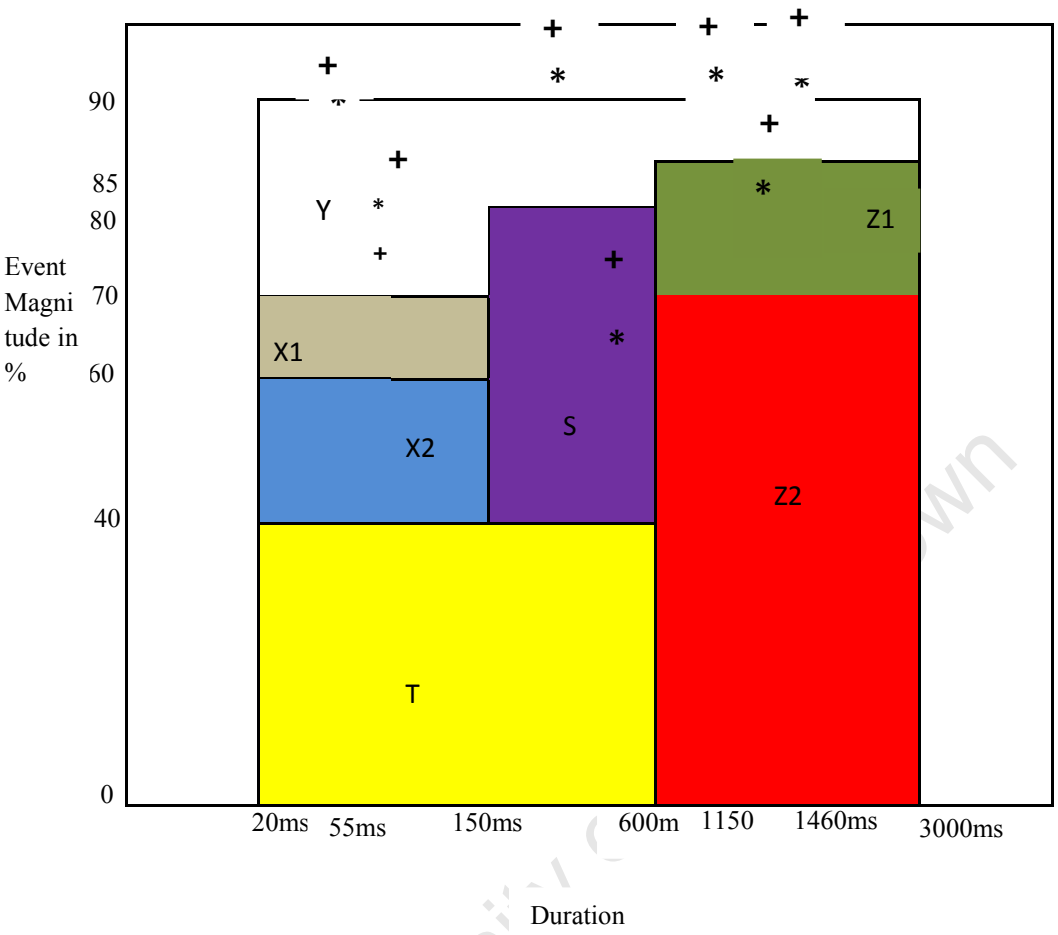

Figure 7.7: Scatter diagram of voltage dip mitigation with all GRDG generators at busbars18 and basbar22 due to 3P fault

Chapter 8

8.1 Conclusion, recommendation and future work

Power quality (PQ) is a major concern for electric utilities, end users of electric power and power systems researchers. The power network is becoming more vulnerable as a result of an increase in power demand due to population growth, rapid growth in the industrial equipment with microprocessor-based controls and power electronic devices [11]. In consequence, electrical components, equipment and sensitive loads are sensitive to variations in voltage and frequency quality, which might lead to time wastage, technical and financial losses. Within PQ issues, voltage quality problem such as voltage dip has been a serious concern and big challenge to power system experts due to their stochastic nature, its severity and number of occurrences per annum. The stochastic nature of voltage dip has made it practically difficult to eliminate it from the regular power systems [62].

However, its impacts on power systems can be monitored with good voltage quality monitoring (PQM) systems such as detector and classifier ANN. This might be helpful for early detection and classification of voltage dip in other to provide appropriate and adequate mitigation through GRDG. This will in turn reduce the risks of shutdown of sensitive equipment leading to loss of production or services with direct financial impact for the affected customers and the power utility.

8.2 Motivation for the Work

With the increasing usage of sophisticated sensitive electronic equipments in various industries, offices and household appliances, it is important to protect them from any power quality disturbances in other to avoid unnecessary losses of any kind. Most consumers think that the best solution to the voltage dip problem is to purchase equipment that has the necessary ride through capability. Even with the ride through capability, a level of voltage still needs to be maintained so that the ride through capability system can work. Since the severity of the voltage dip is defined by the voltage level during the dip and the duration of the dip. The voltage has to be mitigated to the level useful for equipment with ride through capability to work has designed.

Process industry equipment and industrial plant with induction motors, especially the textile industry or refineries can be particularly susceptible to problems with voltage dip because the equipment is interconnected and a trip of any component in the process can cause the whole plant to shut down. This results in financial damages to the organization which include lost productivity,

labour costs for clean-up and restart, damaged product, reduced product quality, delays in delivery, and reduced customer satisfaction. It has been reported that the voltage dips of 85% to 90% of nominal voltage lasting as short as 16 ms will cause immediate outages in critical industrial processes [253]. Hence the problem of voltage dip needs to be mitigated. This will reduce the possibilities of shutdown of sensitive equipment leading to shutting down a production line that requires time to restart due to power disturbance would have a direct cost impact.

Voltage dip mitigation helps to avoid a blackout by preventing trip of the protective device like reclosers and circuit breakers. If for any reason, a sub-station circuit breaker or a recloser is tripped, then some part of the network will be temporarily disconnected. Voltage dip mitigation reduces fault impact on the power network which can have effect even on more customers. Customers hundreds of miles from the fault location can still experience a voltage dip resulting in equipment mal-operation when the fault is on the transmission system.

Technology change and specific application of an electrical device like the new generation of the nanotechnology and programmable logic controllers (PLC's) require high-voltage quality and power quality. The need to meet the voltage standards is proposed by electrical engineering practise and regulatory bodies. While at the same time permitting the maximum amount of distributed generation to be installed and operated [254]. The domestic consumer demand high voltage quality because of the increase usage of ICT and semiconductor devices. This has increased the challenges for utility and industry to focus on power quality.

Privatization and deregulation of electric utility have led to open competition, which has resulted in a demand for higher reliability and quality than ever before. This has resulted in faster and prompt fault detection and fault clearance technique and the use of Modern Energy Management Systems (EMS) which must be capable of dealing with the numerous alarms received during fault and emergency conditions as a result of discrete and analogue data received by the SCADA (Supervisory Control and Data Acquisition) computers. These alarms are generated for a variety of system conditions such as voltage deviation [255].

8.3 Summary of Research

This thesis presents a corrective scheme through early detection and classification using ANN-based intelligent system and the GRDGs to mitigate its impact on the power network. The methods of voltage dip detection and classification presented in this thesis is characterized by the r.m.s. remaining (retained) voltage magnitude, the phase-angle shift and the dip duration. It is advisable to detect it early in an electrical network, so that a proper and adequate mitigation measure (such as using renewable DG) can be taken to avoid further power quality problems that might arise from inappropriate mitigation approach.

The proposed method is based on retained rms voltage, phase angle shift and dip duration. It provides fast simple and straightforward techniques in detecting, classifying, analyzing and mitigating voltage dips through the deployment of GRDG. The advantages of the proposed corrective scheme include a rapid response time when compare to 10-minute rms value presently used by Eskom and some other African utilities [58], [139]. The method has a remarkable accuracy with less computational complexity and burden as compared to other methods.

The software developed in this thesis can be used by utility and power consumers on their computer to detect and classify voltage dip as to improve voltage dip mitigation capability through the presence of GRDG that provides voltage support for the power network. The amount of newly installed RDGs have increased rapidly and growing further because of several reasons such as the need to reduce environmental pollution and global warming caused by greenhouse gases, the need for generation augmentation, power restoration, alleviating transmission congestion, loss reduction, etc., [66].

This model can be used and even further extended in order to study different aspects related to the connection of other conventional DGs and non-conventional DGs to the grid for voltage dip mitigation. The outcome of simulation results indicates the positive aspects and the technical benefits of the proposed ANN method of detecting and classifying voltage dip regards mitigation with GRDG over the conventional method.

This thesis is able to present the consequences of various GRDG in a power network and also discusses how GRDG impact on voltage dips mitigation both on the transmission and the distribution networks.

It also investigates the impact of different wind energy conversion systems on voltage dip and high penetration of DG in a power system and simulation of high penetration of grid-connected wind distributed generators using DIgSILENT.

8.4 Key Results

Based on the results obtained from this work, it has been observed and established that use of artificial neural network approach can enhance voltage support and mitigation of voltage dip through the ancillary services support of renewable distributed generation.

The scheme is able to provide guidelines for the automatic processing of different voltage dip types in terms of voltage level, dip duration time, and effectiveness of GRDGs during and after the voltage dip mitigation. This thesis also suggest the use of both the dip and no dip data to train the ANN and also validate it accuracy with only dip data.

In addition, the thesis shows the impacts and effects of various types GRDGs such as wind, hydro and solar power plants on a power network during multiple voltage dips as a result of different faults from either transmission or distribution network.

Modelling of different types of GRDGs and their impact on voltage dip mitigation. The maximum levels of different types of wind GRDG penetration that will be good for voltage dip mitigation with different types of faults. Modelling of the best architecture of FFNN with the best network topology, activation function and the learning rule that provides minimal error and highest accuracy for both the detector and classifier ANNs.

Another advantage of this project is to improve detection and classification of voltage dip through the use of an intelligent system. The detection and classification algorithm in this work is developed based on voltage dip disturbance events from seven categories of Eskom voltage dip windows. However it can be modified and utilised by any other utility and industrial power consumers to mitigate the effects of voltage dip.

The early detection of voltage dip is important for proper mitigation of voltage dip as most utilities depends on the use the 10-minute rms value to analysis or mitigates voltage dip. Presently, utilities are using dip recorder's data for detection, analyzing and mitigation of voltage dip. This is a long duration of time, which does not encourage early mitigation of the dip.

8.5 Main Contributions and Advantage of this Research

The main contributions of the work can be summarized as follows:

1. The thesis introduces a method of intelligent voltage dip detection and classification based on utility perspective.

2. It overcomes the drawbacks of analytical methods of voltage dip detection and classification use by utilities and it proposes an intelligent approach to these methods.

3. It also investigates the use of GRDG with an intelligent system to solve the problems of voltage dip.

4. It investigates the contribution of different types of dips such as symmetrical and unsymmetrical dips.

5. It derives the equations to classify different Eskom windows of voltage dip during the occurrence of faults in a power system.

6. The thesis also presents clear algorithms to perform voltage dip detection and classification that can be used by both the utility and the consumer with sensitive loads.

7. The investigation results have shown that the proposed voltage dip corrective scheme provides a convenient way for comparing different GRDG systems with various voltage dip windows.

8. The obtained results show that trained FFNN can be used as a proper tool to detect as well as classify voltage dip into classes with a reasonable accuracy.

9. It makes identification of any particular type of voltage dip class easy, for now it is difficult to pinpoint the exact type of voltage dip class without analysis.

10. Another important contribution of this work is the fact that it can be used by power utilities, independent power producers and power customers. The software can be installed within their facilities to monitor, detect analysis and classify voltage dip. Furthermore, the algorithm developed can be adopted and modified by any utility apart from Eskom and use to enhance voltage dip mitigation.

8.6 Benefits and Application Areas of Research

Voltage dips are one of the most important disturbances in power networks. Economic losses caused by this type of disturbances can be greater than those due to long and short interruptions, as a result of daily improvement on a power network in order to reduce the number and duration of interruptions [278]. Nevertheless, voltage dips have a negative economic impact on an electricity network. Each year in United States voltage dips and interruptions cause major economic damage and are estimated to cost between U.S. $ 104 billion and U.S. $ 164 billion [60]. Table 1.10 and Table 1.11 show the summary of financial losses as a result of voltage dip [61].

In order to secure the provision of good voltage quality and mitigate the negative impacts of voltage dip. This thesis proposes a corrective scheme through the application of ANNs and the ancillary services support of GRDG. This research work is useful in the area of voltage quality in power systems. It will help the utility to plan and eliminate the power quality problems arising out of voltage dips in a power network, thereby affecting power quality sensitive loads. In addition, it will guide the utility in selecting judiciously a RDG-based voltage dip mitigation scheme which might lead to a robust and reliable power network and also reduce the financial losses of many industrial and commercial electrical power users.

Recommendations

Recommendations and future research directions

According to the findings from the thesis, the following recommendations and future research work are proposed:

Future work should research into how to predict voltage dips before they occur. For it is difficult at present to predict it occurrence (due to its stochastic nature) since no method or tool at present can pinpoint or predict how and when a particular fault happens, predict, of what fault type, impedance and location. This might eradicate voltage dip completely from the regular power network.

Controlling and more coordination of DGs during voltage dip mitigation using intelligent systems so that the presence of DGs will not lead to more power quality problems. These DGs can be equipped with a set of devices that will enable them to seamlessly interconnect to the grid and capacity to dispatched electrical power if needed during voltage dip.

List of publications

List of publications towards the PhD

Conference papers

[1] O. Ipinnimo, S. Chowdhury, S.P. Chowdhury, "Voltage dip mitigation with DG integration: A comprehensive review," Power Electronics, Drives and Energy Systems (PEDES) & 2010 Power India, 2010 Joint International Conference on , vol., no., pp.1,10, 20-23 Dec. 2010.

[2] O. Ipinnimo, S. Chowdhury, S.P. Chowdhury, "ANN-based voltage dip mitigation in power networks with distributed generation," Power Systems Conference and Exposition (PSCE), 2011 IEEE/PES , vol., no., pp.1,8, 20-23 March 2011.

[3] O. Ipinnimo, S. Chowdhury, S.P. Chowdhury, "Effects of Distributed Generation (DG) on Voltage Dips in Electricity Networks", pg. 82-87, *SAUPEC 13-15 July 2011.*

[4] O. Ipinnimo, S. Chowdhury, S.P. Chowdhury, "Application of Grid Integrated Wind Energy Conversion Systems for Mitigation of Multiple Voltage Dips in a Power Network," Universities' Power Engineering Conference (UPEC), Proceedings of 2011 46th International , vol., no., pp.1,6, 5-8 Sept. 2011.

[5] O. Ipinnimo, S. Chowdhury, S.P. Chowdhury, "Effects of renewable distributed generation (RDG) on voltage dip mitigation in microgrids," Developments in Power Systems Protection, 2012. DPSP 2012. 11th International Conference on , vol., no., pp.1,6, 23-26 April 2012.

[6]O. Ipinnimo, S. Chowdhury, S.P. Chowdhury, "Mitigation of multiple voltage dips in a weak grid using wind and hydro-based distributed generation," Transmission and Distribution Conference and Exposition (T&D), 2012 IEEE PES , vol., no., pp.1,9, 7-10 May 2012.

[7]O. Ipinnimo, S. Chowdhury, S.P. Chowdhury, J. Mitra, "Intelligent voltage dip detection in power networks with distributed generation (DG)," North American Power Symposium (NAPS), 2012 , vol., no., pp.1,6, 9-11 Sept. 2012.

[8]O. Ipinnimo, S. Chowdhury, "ANN-based classification system for different windows of voltage dips in a power network," Power Engineering Conference (UPEC), 2013 48th International Universities', vol., no., pp.1,6, 2-5 Sept. 2013.

Journal papers

[9] O. Ipinnimo, S. Chowdhury, S.P. Chowdhury, J. Mitra, "A Review of Voltage Dip Mitigation Techniques with Distributed Generation in Electricity Networks" ELSEVIER, Electric Power Systems Research, Volume 103, October 2013, Pages 28-36.

The author has also contributed to the following publications

Joint Conference papers

[1] C. Buque, O. Ipinnimo, S. Chowdhury, S.P. Chowdhury, "Modeling and simulation of an Adaptive Relaying Scheme for a Microgrid," Power and Energy Society General Meeting, 2012 IEEE , vol., no., pp.1,8, 22-26 July 2012.

[2]M. Chidi, O. Ipinnimo, S. Chowdhury, S.P. Chowdhury, "Investigation of impact of integrating on-grid home based solar power systems on voltage rise in the utility network," Power and Energy Society General Meeting, 2012 IEEE , vol., no., pp.1,7, 22-26 July 2012.

[3]P. Sekhoto, O. Ipinnimo, S. Chowdhury, "Voltage dip analysis of electricity networks on wind energy integration," Power Engineering Conference (UPEC), 2013 48th International Universities' , vol., no., pp.1,6, 2-5 Sept. 2013.

List of References

[1] C.J. Mozina, "Impact of Smart Grids and Green Power Generation on Distribution Systems," Industry Applications, IEEE Transactions on, vol.49, no.3, pp.1079, 1090, May-June 2013.

[2] J.T.S. Rajan, S. Surya, M. Viknesh, G. Sivakumar, "Silhouette analysis—"The waste of Koyambedu to electricity of Chennai" the future power generation: An outlook," Intelligent Systems and Control (ISCO), 2013 7th International Conference on , vol., no., pp.84,89, 4-5 Jan. 2013.

[3] J. Wentzel, T.S. Ustun, C. Ozansoy,A. Zayegh, "Investigation of micro-grid behavior while operating under various network conditions," Smart Grid Engineering (SGE), 2012 IEEE International Conference on , vol., no., pp.1,5, 27-29 Aug. 2012.

[4] B. Renders, K. De Gussemé, W.R.Ryckaert, K.Stockman, L. Vandevelde and M.H.J.Bollen, "Distributed Generation for Mitigating Voltage Dips in Low-Voltage Distribution Grids," Power Delivery, IEEE Transactions on , vol.23, no.3, pp.1581,1588, July 2008.

[5] IEEE Recommended Practice for Monitoring Electric Power Quality," IEEE Std 1159-2009 (Revision of IEEE Std 1159-1995), vol., no., pp.c1, 81, June 26, 2009.

[6] V. Ignatova, P. Granjon and S. Bacha, "Space Vector Method for Voltage Dips and Swells Analysis", IEEE Transactions on Power Delivery, Vol.24, No.4, pp.2054-2061, Oct.2009.

[7] M.H.J. Bollen, Review what is power quality, Electric Power Systems Research, 66 (1) (2003), pp. 5–14.

[8] I. Monedero, C. Leon,J. Ropero, A. Garcia,J.M. Elena, J.C. Montano, "Classification of Electrical Disturbances in Real Time Using Neural Networks," *Power Delivery, IEEE Transactions on* , vol.22, no.3, pp.1288,1296, July 2007.

[9] K.S Manish, K. Rajiv, Classification of power quality events – A review, International Journal of Electrical Power & Energy Systems, Volume 43, Issue 1, December 2012, Pages 11-19.

[10] Mohibullah, S.H. Laskar, "Power quality issues and need of intelligent PQ monitoring in the smart grid environment," Universities Power Engineering Conference (UPEC), 2012 47th international, vol., no., pp.1,6, 4-7 Sept. 2012.

[11] H. Shareef, A. Mohamed,"An alternative voltage sag source identification method utilizing radial basis function network," Electricity Distribution (CIRED 2013), 22nd International Conference and Exhibition on , vol., no., pp.1,4, 10-13 June 2013.

[12] T. Ise, Y. Hayashi, K. Tsuji, "Definitions of power quality levels and the simplest approach for unbundled power quality services," Harmonics and Quality of Power, 2000. Proceedings. Ninth International Conference on, vol.2, no., pp.385- 390 vol.2, 2000.

[13] M. Reza, W. L. Kling, and L. van der Sluis, "Stability analysis of transmission system with high penetration of distributed generation." 21-Dec-2006.

[14] F.A. Viawan, 'Steady State Operation and Control of Power Distribution Systems in the Presence of Distributed Generation,' Thesis for the degree of licentiate engineering, 2006.

[15] D. P. Kaundinya, P. Balachandra, and N. H. Ravindranath, "Grid-connected versus stand-alone energy systems for decentralized power—A review of literature," Elsevier, Renewable and Sustainable Energy Reviews, vol. 13, no. 8, pp. 2041–2050, Oct. 2009.

[16] M. Joorabian, D. Mirabbasi, A. Sina,"Voltage flicker compensation using STATCOM," Industrial Electronics and Applications, 2009. ICIEA 2009. 4th IEEE Conference on, vol., no., pp.2273, 2278, 25-27 May 2009.

[17] K. Chmielowiec, "Flicker effect of different types of light sources," Electrical Power Quality and Utilisation (EPQU), 2011 11th International Conference on , vol., no., pp.1,6, 17-19 Oct. 2011.

[18] H. Awad, F. Blaabjerg, "Mitigation of voltage swells by static series compensator," Power Electronics Specialists Conference, 2004. PESC 04. 2004 IEEE 35th Annual, vol.5, no., pp.3505, 3511 Vol.5, 20-25 June 2004.

[19] K.J.P. Macken, H.J.Bollen and R.J.M. Belmans, "Mitigation of voltage dips through distributed generation systems," Industry Applications, IEEE Transactions on, vol.40, no.6, pp.1686,1693, Nov.-Dec. 2004.

[20] Electrical Generation and Distribution Systems and Power Quality Disturbances, Edited by Gregorio Romero Rey and Luisa Martinez Muneta, ISBN 978-953-307-329-3, Hard cover, 304 pages, Publisher: InTech, Chapters published November 21, 2011 under CC BY 3.0 license DOI: 10.5772/1426.

[21] N. Keo-Yamg, C. Sang-bong, R. Hee-suk, J. Seong-hwan, L. Jae-Duck, K. Dae-Kyeong, "A Survey on Interruption Costs of Korean Industrial Customers," Transmission and Distribution Conference and Exhibition, 2005/2006 IEEE PES , vol., no., pp.781,787, 21-24 May 2006.

[22] EPRI Technical Report, Effects of Temporary Overvoltage on Residential Products, System Compatibility Research Project, 1008540 Final Report, March 2005.

[23] N. Kumar, V. PrakashVerma, V.K. Singh, S. Nandi, V. Ventru, "Double relay based sag, swell, over and under voltage protection and detection scheme," Communications and Signal Processing (ICCSP), 2013 International Conference on , vol., no., pp.1008,1012, 3-5 April 2013.

[24] Minea Skok "The 1st Workshop on the QoSR Session 2 - Voltage Quality" ECS/ECRB Study.

[25] S. Manish Kumar, R. Kapoor, S. Bharat Bhushan, "PQ events classification and detection - A survey," Sustainable Energy and Intelligent Systems (SEISCON 2011), International Conference on, vol., no., pp.490, 495, 20-22 July 2011

[26] L.C. Saikia, S.M. Borah, S. Pait,"Detection and classification of power quality disturbances using wavelet transform, fuzzy logic and neural network," India Conference (INDICON), 2010 Annual IEEE , vol., no., pp.1,5, 17-19 Dec. 2010.

[27] S. Mishra, C. N. Bhende, K.B. Panigrahi,"Detection and Classification of Power Quality Disturbances Using S-Transform and Probabilistic Neural Network," Power Delivery, IEEE Transactions on , vol.23, no.1, pp.280,287, Jan. 2008.

[28] Jack V. Tu, Advantages and disadvantages of using artificial neural networks versus logistic regression for predicting medical outcomes, Journal of Clinical Epidemiology, Volume 49, Issue 11, November 1996, Pages 1225-1231, ISSN 0895-4356.

[29] N. Jiteurtragool, C. Wannaboon, W. San-Um, W., "A power control system in DC-DC boost converter integrated with photovoltaic arrays using optimized back propagation Artificial Neural Network," Knowledge and Smart Technology (KST), 2013 5th International Conference on , vol., no., pp.107,112, Jan. 31 2013-Feb. 1 2013.

[30] A.K. Jain, M. Jianchang, K. M. Mohiuddin, "Artificial neural networks: a tutorial," Computer, vol.29, no.3, pp.31, 44, Mar 1996.

[31] R. Aggarwal, S. Yonghua, "Artificial neural networks in power systems. III. Examples of applications in power systems," Power Engineering Journal, vol.12, no.6, pp.279, 287, Dec. 1998.

[32] E. Espinosa-Juarez, J. R. Espinoza-Tinoco, A. Hernandez, "Neural Networks Applied to Solve the Voltage Sag State Estimation Problem: An Approach Based on the Fault Positions Concept," Electronics, Robotics and Automotive Mechanics Conference, 2009. CERMA '09, vol., no., pp.88-93, 22-25 Sept. 2009.

[33] O. Ipinnimo, S. Chowdhury, S.P. Chowdhury, "ANN-based voltage dip mitigation in power networks with distributed generation," Power Systems Conference and Exposition (PSCE), 2011 IEEE/PES, vol., no., pp.1-8, 20-23 March 2011.

[34] C.C .Shen, A.C .Wang, R.F. Chang, C.N. Lu, "Quantifying disturbance level of voltage sag events," Power Engineering Society General Meeting, 2005. IEEE, vol., no., pp. 2314- 2318 Vol. 3, 12-16 June 2005.

[35] European Standard EN-50160, Voltage Characteristics of Electricity Supplied by Public Distribution Systems, CENELEC, Brussels, 1994.

[36] M.H.J Bollen., 'Understanding Power Quality Problems': Voltage sags and interruptions, Wiley-IEEE Press New York 2000.

[37] IEC 61000-2-1:1990, Electromagnetic Compatibility. Part 2: Environment. Section 1: Description of the environment – Electromagnetic environment for low frequency conducted disturbances and signaling in public power supply system.

[38] IEC60050-604, International Electrotechnical Vocabulary. Chapter 604: Generation, transmission and distribution of electricity - Operation, IEC, 1998.

[39] M.H.J. Bollen, K. Stockman, R. Neumann, G. Ethier, J.R. Gordon, K van Reussel, S.Z Djokic, FS. Cundeva, Voltage dip immunity of equipment and installations - messages to takeholders, Harmonics and Quality of Power (ICHQP), 2012 IEEE 15th International Conference, (June) (2012) 915-919.

[40] M. A. El-Gammal, A. Y. Abou-Ghazala, and T. I. El-Shennawy, Voltage sag effects on the process continuity of a refinery with induction motors loads, Iranian Journal of Electrical And Computer Engineering, 9 (1) (2010) 67-72.

[41] S.Z. Djokic, M.H.J. Bollen, "Dip segmentation method," *Harmonics and Quality of Power, 2008. ICHQP 2008. 13th International Conference on*, vol., no., pp.1,8, Sept. 28 2008-Oct. 1 2008.

[42] M.H.J Bollen, Mark Stephens, et al., "Voltage Dip Immunity of Equipment and Installations" CIGRE/CIRED/UIE Joint Working Group C4.110, April 2010.

[43] O. Ipinnimo, S. Chowdhury, S.P. Chowdhury, "Effects of Distributed Generation (DG) on Voltage Dips in Electricity Networks", Southern African Universities Power Engineering Conference, pg. 82-87, SAUPEC 13-15 July 2011.

[44] F.R. Zaro,M.A. Abido, S. Ameenuddin, I.M. Elamin,"Characterization of short-duration voltage events," Power and Energy (PECon), 2012 IEEE International Conference on , vol., no., pp.650,654, 2-5 Dec. 2012.

[45] S.Z. Djokic, J.V. Milanovic, S. M. Rowland, "Advanced voltage sag characterisation ii: point on wave," Generation, Transmission & Distribution, IET, vol.1, no.1, pp.146, 154, January 2007.

[46] P. Saninta, P. Premrudeepreechacharn, "Assessment and prediction of voltage sag in transmission system in northern area of Thailand," *Harmonics and Quality of Power, 2008. ICHQP 2008. 13th International Conference on*, vol., no., pp.1,6, Sept. 28 2008-Oct. 1 2008.

[47] E. Gómez-Lá aro, J.A. Fuentes, A. Molina-Garciá, Canas-Carreton, M., "Characterization and Visualization of Voltage Dips in Wind Power Installations," Power Delivery, IEEE Transactions on , vol.24, no.4, pp.2071,2078, Oct. 2009.

[48] M. Venmathi, J. Vargese, L. Ramesh, E.S. Percis, "Impact of grid connected distributed generation on voltage sag," Sustainable Energy and Intelligent Systems (SEISCON 2011), International Conference on , vol., no., pp.91,96, 20-22 July 2011.

[49] Djokic SZ, Milanovic JV, Kirschen DS, "Sensitivity of AC Coil Contactors to Voltage Sags, Short Interruptions and Undervoltage Transients", IEEE Transactions on Power Delivery,Volume 19, No. 3, July 2004.

[50] R.A. Flores,"State of the art in the classification of power quality events, an overview," Harmonics and Quality of Power, 2002. 10th International Conference on, vol.1, no., pp.17,20 vol.1, 6-9 Oct. 2002.

[51] J. Melendez, X. Berjaga, S. Herraiz, V. Barrera, J. Sanchez, M. Castro,"Classification of sags according to their origin based on the waveform similarity," Transmission and Distribution

Conference and Exposition: Latin America, 2008 IEEE/PES , vol., no., pp.1,6, 13-15 Aug. 2008.

[52] E .Styvaktakis, M.H.J .Bollen, I.Y.H. Gu,"Classification of power system events: voltage dips," Harmonics and Quality of Power, 2000. Proceedings. Ninth International Conference on , vol.2, no., pp.745-750 vol.2, 2000.

[53] O. Ipinnimo, S. Chowdhury, "ANN- Based Classification System for Different Windows of Voltage Dips in a Power Network" Universities' Power Engineering Conference (UPEC), 2013 48th International 2-5 Sept. 2013.

[54] S.Z. Djokic, J.V. Milanovic, D.J. Chapman, M.F. McGranaghan, "Shortfalls of existing methods for classification and presentation of voltage reduction events," Power Delivery, IEEE Transactions on , vol.20, no.2, pp.1640,1649, April 2005.

[55] M.H.J. Bollen, L.D. Zhang, Different methods for classification of three-phase unbalanced voltage dips due to faults, Electric Power Systems Research, Volume 66, Issue 1, July 2003, Pages 59-69.

[56] L. Guasch, F. Corcoles and J. Pedra, "Effects of Symmetrical and Unsymmetrical Voltage Sags on Induction Machines," IEEE, Trans. Power Delivery, vol. 19, No.2, April 2004.

[57] D. Aguilar, A. Luna, A. Rolan, G. Vazquez, and G. Acevedo, "Modeling and simulation of synchronous machine and its behavior against voltage sags," Industrial Electronics, 2009. ISIE 2009. IEEE International Symposium on, vol., no., pp.729-733, 5-8 July 2009.

[58] NRS 048-2, "Electricity Supply – Quality of Supply Standards – Part 2: Voltage characteristics, compatibility levels, limits and assessment methods, Edition 3.0, December 2007.

[59] O. Ipinnimo, S. Chowdhury, S.P. Chowdhury, J. Mitra, "Intelligent Detection and classification System for Different Windows of Voltage Dips" Submitted to IEEE Transactions on Power Systems 2013.

[60] V.H Dirk, D. Marcel, D. Johan, and B. Ronnie, "Choosing the correct mitigation method against voltage dips and interruptions: A Customer-Based Approach," Power Delivery, IEEE Transactions on, vol.22, no.1, pp.331-339, Jan.2007.

[61] Endeavour Energy Power Quality & Reliability Centre, "Voltage Sag Mitigation" Technical Note 11 August 2012.

[62] O. Ipinnimo, S. Chowdhury, S.P. Chowdhury, J. Mitra, "A Review of Voltage Dip Mitigation Techniques with Distributed Generation in Electricity Networks" ELSEVIER, *Electric Power Systems Research,* Volume 103, October 2013, Pages 28-36.

[63] T. Ackermann, G. Andersson and L. Soder, "Distributed generation: a definition" ELSEVIER, Electric Power System Research 57 pp 195-204, 2001.

[64] G. N Koutroumpezis, A.S Safigianni, G.S Demetzos and J.G Kendristakis "Investigation of the distributed generation penetration in a medium voltage power distribution network", International Journal of Energy Research, 34: pp583-593, 2010.

[65] M. Fahrioglu, R.H. Lasseter, F.L. Alvarado, Y. Taiyou, "Integrating distributed generation technology into demand management schemes," Sustainable Alternative Energy (SAE), 2009 IEEE PES/IAS Conference on, vol., no., pp.1,5, 28-30 Sept. 2009.

[66] G. Pepermans, J. Driesen, D. Haeseldonckx, R. Belmans, W. D'haeseleer, Distributed generation: definition, benefits and issues, Energy Policy, Volume 33, Issue 6, April 2005, pp 787-798, ISSN 0301-4215.

[67] A. Saidian, D. Mirabbasi, M. Heidari, "The effect of size of DG on voltage flicker and voltage sag in closed-loop distribution system," Industrial Electronics and Applications (ICIEA), 2010 the 5th IEEE Conference on, vol., no., pp.68-72, 15-17 June 2010.

[68] K. Honghai, L. Shengqing, W. Zhengqiu, "Discussion on advantages and disadvantages of distributed generation connected to the grid," *Electrical and Control Engineering (ICECE), 2011 International Conference on*, vol., no., pp.170, 173, 16-18 Sept. 2011.

[69] O. Ipinnimo, S. Chowdhury, S.P. Chowdhury, "Voltage dip mitigation with DG integration: A comprehensive review," Power Electronics, Drives and Energy Systems (PEDES) IEEE/PES & 2010 Power India, 2010 Joint International Conference on , vol., no., pp.1-10, 20-23 Dec. 2010.

[70] W El-Khattam, M.M.A Salama, Distributed generation technologies, definitions and benefits, Electric Power Systems Research, Volume 71, Issue 2, October 2004, Pages 119-128, ISSN 0378-7796.

[71] F. Rosillo-Calle, Peter de Groot and Sarah L. Hemstock, The biomass Assessment Handbook, 2007.

[72] R. Baldick, U. Helman, B.F Hobbs, and R.P O'Neil, "Design of Efficient Generation Markets," Proceedings of the IEEE , vol.93, no.11, pp.1998,2012, Nov. 2005.

[73] K. Narinder, P. E Trehan, "Ancillary Services-Reactive and Voltage Control", Power Engineering Society Winter Meeting, 2001.

[74] G. Strbac, N. Jenkins, M. Hird, P. Djapic, G. Nicholson, "Integration of operation of embedded generation and distribution networks", Report University of Manchester, 2002.

[75] M. Triggianese, F. Liccardo, P. Marino, "Ancillary Services performed by Distributed Generation in grid integration," Clean Electrical Power, 2007. ICCEP '07. International Conference on, vol., no., pp.164, 170, 21-23 May 2007.

[76] I. Perez-Arriaga: Managing Large Scale Penetration of Intermittent Renewables, MITEI Symposium on Managing Large-Scale Penetration of Intermittent Renewables, Cambridge, U.S.A, 20 April 2011.

[77] International Electrotechnical Commission Market Strategy Board: Grid Integration of Large-capacity Renewable Energy Sources and Use of Large-Capacity Electrical Energy Storage: The IEC's role from 2010 to 2030, White Paper, October 2012.

[78] D. Altinbilek, R. Abdel-Malek, R. Devernay, J. M. et al.: Hydropower's Contribution to Energy Security. World Energy Congress, Rome 2007.

[79] M. Braun, provision of ancillary services by distributed generators technological and economic perspective, Kassel University press GmbH, Kassel, 2009.

[80] IEEE Application Guide for IEEE Std 1547, IEEE Standard for Interconnecting Distributed Resources with Electric Power Systems," IEEE Std 1547.2-2008 , vol., no., pp.1,207, April 15 2009.

[81] R. Caldon, F. Rossetto, R. Turro, "Analysis of dynamic performance of dispersed generation connected through inverter to distribution system", CIRED 17th International conference on electricity distribution, Barcelona 12-15 May 2003.

[82] S. Jain, J. Jin, H. Xinhong, S. Stevandic, "Modeling of Fuel-Cell-Based Power Supply System for Grid Interface," Industry Applications, IEEE Transactions on, vol.48, no.4, pp.1142, 1153, July-Aug. 2012.

[83] ECW de Jong, K Consulting, "Low Carbon Electricity Systems" Report of the seminar Electricity in the next decade Arnhem, 1 September 2009.

[84] WindTurbines.net, [Online Available]: http://www.slideshare.net/windturbinesnet/how-wind-turbines-generate-electricity-6995868

[85] The institution of engineering and technology, IET– factfiles, [Online]: Available online: http://www.theiet.org/factfiles/energy/renewable-power.cfm

[86] IEEE Recommended Practise for Utility Interface of Photovoltaic (PV) Systems, IEEE standard 929, 2000.

[87] Energy Efficiency and Renewable Energy (EERE), [Online Available]: http://www.eere.energy.gov/basics/renewable_energy/geothermal_electricity.html

[88] L. Varnado, N.C. Solar Center, N.C. State University, Interstate Renewable Energy Council (IREC), Connecting to the Grid, A Guide to Distributed Generation Interconnection Issues, Sixth Edition 2009.

[89] B. Magoro and T. Mchunu, Overview of SA Renewable Energy Grid Code, Eskom Transmission Division, System Operator Grid Code Management, 2013. [Online Available]: http://www.kznenergy.org.za/download/forum_meetings/ksef_meeting:_electricity_grid/Overview%20of%20the%20SA%20RE%20Code%20(KSEF).pdf

[90] Eskom Distribution Guide, network planning guideline for wind turbine generation (steady state studies) Distribution Guide – Part 2

[91] J.A. Martinez-Velasco, J. Martin-Arnedo,"Distributed generation impact on voltage sags in distribution networks," Electrical Power Quality and Utilisation, 2007. EPQU 2007. 9th International Conference on, vol., no., pp.1, 6, 9-11 Oct. 2007.

[92] O. Ipinnimo, S. Chowdhury, S.P. Chowdhury, "Mitigation of multiple voltage dips in a weak grid using wind and hydro-based distributed generation," Transmission and Distribution Conference and Exposition (T&D), 2012 IEEE PES , vol., no., pp.1,9, 7-10 May 2012.

[93] F. Pilo, G. Pisano and G. G. Soma, "Considering Voltage Dips Mitigation in Distribution Network Planning," Power Tech, 2007 IEEE Lausanne , vol., no., pp.1528,1533, 1-5 July 2007.

[94] N. Chiangkakun, S. Premrudeepreechacharn, C. Pongsriwat, Y. Baghzouz,"Analysis of voltage sag in an industrial distribution system of the provincial electricity authority of Thailand," Harmonics and Quality of Power (ICHQP), 2012 IEEE 15th International Conference on , vol., no., pp.197,202, 17-20 June 2012.

[95] J.A. Martinez, J. Martin-Arnedo, "Impact of distributed generation on distribution protection and power quality," Power & Energy Society General Meeting, 2009. PES '09. IEEE, vol., no., pp.1, 6, 26-30 July 2009.

[96] O. Amanifar and M. E H. Golshan,"Optimal DG allocation and sizing for mitigating voltage sag in distribution systems with respect to economic consideration using Particle Swarm Optimization," Electrical Power Distribution Networks (EPDC), 2012 Proceedings of 17th Conference on , vol., no., pp.1,8, 2-3 May 2012.

[97] P. Phonrattanasak,"Optimal placement of DG using multiobjective particle swarm optimization," Mechanical and Electrical Technology (ICMET), 2010 2nd International Conference on, vol., no., pp.342, 346, 10-12 Sept. 2010.

[98] A.C.L Ramos, A.J. Batista, R.C. Leborgne, P. Emiliano, "Distributed generation impact on voltage sags," Power Electronics Conference, 2009. COBEP '09. Brazilian, vol., no., pp.446-450, Sept. 27 2009-Oct. 1 2009.

[99] A. Cziker, M. Chindris, A. Miron, "Voltage unbalance mitigation using a distributed generator," Optimization of Electrical and Electronic Equipment, 2008. OPTIM 2008. 11th International Conference on , vol., no., pp.221,226, 22-24 May 2008.

[100] S. Surisunthon, T. Tayjasanant, "Impacts of distributed generation on voltage sag assessment in distribution systems," Electrical Engineering/Electronics, Computer, Telecommunications and Information Technology (ECTI-CON), 2011 8th International Conference on, vol., no., pp.889, 892, 17-19 May 2011.

[101] Siemens Energy USA, (2013)[Online Available]: http://www.energy.siemens.com/us/en/power-transmission/facts/series-compensation/

[102] H. Awad, J. Svensson, M.H.J. Bollen,, "Static series compensator for voltage dips mitigation," Power Tech Conference Proceedings, 2003 IEEE Bologna , vol.3, no., pp.8 pp. Vol.3,, 23-26 June 2003.

[103] S. Wang, Y. Kun-shan, T. Guang-fu, "Mitigation of Voltage Sags by Grid-Connected Distributed Generation System in Series and Shunt Configurations," Power System Technology and IEEE Power India Conference, 2008. POWERCON 2008. Joint International Conference on, vol., no., pp.1,6, 12-15 Oct. 2008.

[104] X. Liu and P. Li,"The effect of DVR on distribution system with distributed generation," Electrical Machines and Systems, 2007. ICEMS. International Conference on, vol., no., pp.277,281, 8-11 Oct. 2007.

[105] R.S. Bajpai, R. Gupta, "Series compensation to mitigate harmonics and voltage sags/swells in distributed generation based on symmetrical components estimation," Industrial Electronics (ISIE), 2011 IEEE International Symposium on , vol., no., pp.1639,1644, 27-30 June 2011.

[106] M. Bongiorno, J. Svensson, "Voltage Dip Mitigation Using Shunt-Connected Voltage Source Converter," Power Electronics, IEEE Transactions on , vol.22, no.5, pp.1867,1874, Sept. 2007.

[107] I. Wasiak, R. Mienski, R. Pawelek, and P. Gburczyk,"Application of DSTATCOM compensators for mitigation of power quality disturbances in low voltage grid with distributed generation," Electrical Power Quality and Utilisation, 2007. EPQU 2007. 9th International Conference on , vol., no., pp.1,6, 9-11 Oct. 2007.

[108] F. Magueed and H. Awad, "Voltage Compensation in Weak Grids Using Distributed Generation with Voltage Source Converter as a Front End," Power Electronics and Drives Systems, 2005. PEDS 2005. International Conference on, vol.1, no., pp.234, 239, 0-0 0.

[109] A. Xin, L. Zhili, C. Mingyong,"Combined compensation strategy of voltage sags for distribution network with distributed generation", 21st International Conference on Electricity Distribution, CIRED,Paper No 0288, Frankfurt, 6-9 June 2011.

[110] M. H. Haque,"Compensation of distribution system voltage sag by DVR and D-STATCOM," Power Tech Proceedings, 2001 IEEE Porto, vol.1, no., pp.5 pp. vol.1,, 2001.

[111] F. Carastro, M. Sumner, P. Zanchetta,"Mitigation of Voltage Dips and Voltage Harmonics within a Micro-grid, using a Single Shunt Active Filter with Energy Storage," IEEE Industrial Electronics, IECON 2006 - 32nd Annual Conference on , vol., no., pp.2546,2551, 6-10 Nov. 2006.

[112] T. Vandoorn, J. De Kooning, B. Meersman,J. Guerrero,L. Vandevelde, "Voltage-Based Control of a Smart Transformer in a Microgrid," Industrial Electronics, IEEE Transactions on , vol.60, no.4, pp.1291,1305, April 2013.

[113] A. Cataliotti, G. Cocchiara, M.G. Ippolito and G. Morana, "Applications of the Fault Decoupling Device to Improve the Operation of LV Distribution Networks", IEEE Transactions on Power Delivery, Vol. 23, No.1, pp.328-337, Jan 2008.

[114] S.M. Farashbashi-Astaneh, A. Dastfan, Optimal placement and sizing of DG for loss reduction, voltage profile improvement and voltage sag mitigation, International Conference on Renewable Energies and Power Quality (ICREPQ) (March) (2010).

[115] M. J. Jahromi, E. Farjah, M. Zolghadri,"Mitigating voltage sag by optimal allocation of Distributed Generation using Genetic Algorithm," Electrical Power Quality and Utilisation, 2007. EPQU 2007. 9th International Conference on , vol., no., pp.1,6, 9-11 Oct. 2007.

[116] `, W. Xiaodong,"Voltage Sags Detection and Identification Based on Phase-Shift and RBF Neural Network," Fuzzy Systems and Knowledge Discovery, 2007. FSKD 2007. Fourth International Conference on, vol.1, no., pp.684, 688, 24-27 Aug. 2007.

[117] I. Y. H. Gu, N. Ernberg, E. Styvaktakis, and M. H. J. Bollen, "A statistical-based sequential method for fast online detection of fault-induced voltage dips," IEEE Trans. Power Del., vol. 19, no. 2, pp. 497–504, Apr. 2004.

[118] F. Ortiz and A. Ortiz and M. Manana and C. J. Renedo and F. Delgado and L. I. Egu´Õluz, "Articial Neural Networks approach to the voltage sag classication",International Conference on Renewable Energies and Power Quality'07, Sevilla, 2007.

[119] E.M. Siavashi, A. Rouhani, R. Moslemi,"Detection of voltage sag using unscented Kalman smoother," Environment and Electrical Engineering (EEEIC), 2010 9th International Conference on , vol., no., pp.128,131, 16-19 May 2010.

[120] A. Deihimi, A. Momeni,"Expert system for classification of measured three-phase unbalanced voltage dips," Mechanical and Electrical Technology (ICMET), 2010 2nd International Conference on , vol., no., pp.213-216, 10-12 Sept. 2010.

[121] B. Soma, K.G. Swapan, C. Amitava, "Optimum distributed generation placement with voltage sag effect minimization", ELSEVIER, Energy Conversion and Management, 53 (2012) 163–174.

[122] M.T. Arab YarMohammadi, M. Faramarzi, "PSO algorithm for sitting and sizing of distributed generation to improve voltage profile and decreasing power losses," Electrical Power Distribution Networks (EPDC), 2012 Proceedings of 17th Conference on , vol., no., pp.1,5, 2-3 May 2012.

[123] M.R. Banaei, S.H Hosseini, M.D. Khajee, "Mitigation of Voltage Sag Using Adaptive Neural Network with Dynamic Voltage Restorer," Power Electronics and Motion Control Conference, 2006. IPEMC 2006. CES/IEEE 5th International, vol.2, no., pp.1,5, 14-16 Aug. 2006.

[124] D. Rajasekaran, S.S Dash, D. T. Rufus Arun, "Dynamic voltage restorer based on fuzzy logic control for voltage sag restoration," Sustainable Energy and Intelligent Systems (SEISCON 2011), International Conference on , vol., no., pp.26,30, 20-22 July 2011.

[125] A. Riyasat, H. Ashraful, A fuzzy logic based dynamic voltage restorer for voltage sag and swell mitigation for industrial induction motor load, International Journal of Computer Applications 30 (8) September (2011) 0975 – 8887.

[126] B. Ferdi, C. Benachaiba, S. Dib, R. Dehini, Adaptive PI Control of Dynamic Voltage Restorer Using Fuzzy Logic, Journal of Electrical Engineering, Theory & Application,1 (3) (June) (2010), 165-173.

[127] J. Dixon, L. Moran, J. Rodriguez, R. Domke, "Reactive Power Compensation Technologies: State-of-the-Art Review," Proceedings of the IEEE, vol.93, no.12, pp.2144-2164, Dec. 2005.

[128] S. Haddad, A. Haddouche, and H. Bouyeda "The use of Facts devices in disturbed Power Systems-Modeling, Interface, and Case Study" International Journal of Computer and Electrical Engineering, Vol. 1, No. 1,pg 1793-8198 April 2009.

[129] K.E. Stahlkopf and M R. Wilhelm, "Tighter Controls for Busier Systems", IEEE Spectrum, Vol. 34, N° 4, April 1997, pp. 48-52.

[130] R. Grünbaum, Å. Petersson and B. Thorvaldsson, "FACTS, Improving the performance of electrical grids", ABB Review, March 2003, pp. 11-18.

[131] T. J. Miller, "Reactive power Control in Electric Systems," John Willey & Sons, 1982.

[132] Canadian Electrical Association, "Static Compensators for Reactive Power Control," Cantext Publications, 1984.

[133] C. Miguel, M. Jaume, C. Antonio, M. Jose, A. Eduardo, Coordinated reactive power control for static synchronous compensators under unbalanced voltage sags, Industrial Electronics (ISIE), IEEE International Symposium, (May) (2012) 987-992.

[134] A. Edris, "Facts Technology Development: An Update, IEEE Power Engineering Review, March 2000, pp. 4-9.

[135] K.M. Silva, B.A. Souza, N S.D. Brito,"Fault detection and classification in transmission lines based on wavelet transform and ANN," Power Delivery, IEEE Transactions on , vol.21, no.4, pp.2058,2063, Oct. 2006.

[136] A. D. Hansen, S. Poul, F. Blaabjerg and J. Becho, Dynamic modelling of wind farm grid interaction, Wind Engineeing Volume 26, NO. 4 [Online Available]:http://digsilent.de/tl_files/digsilent/files/powerfactory/application- examples/p191s.pdf, 2002, PP 191–208.

[137] H. Zang, Y. Zhao, "Intelligent Identification System of Power Quality Disturbance," Intelligent Systems, 2009. GCIS '09. WRI Global Congress on, vol.1, no., pp.258-261, 19-21 May 2009.

[138] S. Kaewarsa, K. Attakitmongcol, T. Kulworawanichpong, "Recognition of power quality events by using multiwavelet-based neural networks, " International Journal of Electrical Power & Energy Systems, Volume 30, Issue 4, May 2008, Pages 254-260, ISSN 0142-0615.

[139] Zambia Bureau of Standard, Electricity Supply – Power Quality and Reliability, Part 1: Overview of Implementation and Minimum Standards, ICS: 29.240:03.120, DZS 387-1: 2009.

[140] S. Bhattacharyya, S. Cobben, W. Kling,"Proposal for defining voltage dip-related responsibility sharing at a point of connection," Generation, Transmission & Distribution, IET , vol.6, no.7, pp.619,626, July 2012.

[141] M.A Laughton, "Artificial intelligence techniques in power systems," Artificial Intelligence Techniques in Power Systems (Digest No: 1997/354), IEE Colloquium on , vol., no., pp.1/1,119, 3 Nov 1997.

[142] O. Genevieve, S. Nici and C. Fred, Neural Networks Lecture Notes, [Online Available]: http://www.willamette.edu/~gorr/classes/cs449/ann-overview.html

[143] A.A. Zhdanov, "The mathematical models of neuron and neural network in autonomous adaptive control methodology," Neural Networks Proceedings, 1998. IEEE World Congress on Computational Intelligence. The 1998 IEEE International Joint Conference on, vol.2, no., pp.1042, 1046 vol.2, 4-9 May 1998.

[144] M. Hudson Beale, M. T. Hagan and H. B. Demuth, Neural Network Toolbox™ 7 R2013a [Online]. Available: http://www.mathworks.com/help/pdf_doc/nnet/nnet_ug.pdf

[145] G.M. Nicoletti, "Artificial neural networks (ANN) as simulators and emulators-an analytical overview," Intelligent Processing and Manufacturing of Materials, 1999. IPMM '99. Proceedings of the Second International Conference on, vol.2, no., pp.713, 721 vol.2, 1999.

[146] Matlab Neural Network Toolbox7.0, R2011a Reference.

[147] R.M. Yoo, L.Han K. Chow, H.-H.S.Lee, "Constructing a Non-Linear Model with Neural Networks for Workload Characterization," Workload Characterization, 2006 IEEE International Symposium on , vol., no., pp.150,159, 25-27 Oct. 2006.

[148] K.C. Luk, J.E. Ball, and A. Sharma, "A study of optimal model lag and spatial inputs to artificial neural network for rainfall forecasting," J. Hydrol., 227, 56–65, 2000.

[149] N.Q. Hung, M.S. Babel, S. Weesakul, and N.K. Tripathi, An artificial neural network model for rainfall forecasting in Bangkok, Thailand.[Online Available]: http://www.hydrol-earth-syst-sci.net/13/1413/2009/hess-13-1413-2009.pdf

[150] M.Valtierra-Rodriguez, R. de Jesus Romero-Troncoso,R.A. Osornio-Rios, A. Garcia-Perez,"Detection and Classification of Single and Combined Power Quality Disturbances Using Neural Networks," Industrial Electronics, IEEE Transactions on , vol.61, no.5, pp.2473,2482, May 2014.

[151] W.Liao, H. Wang, P. Han, "Neural network-based detection and recognition method for power quality disturbances signal," Control and Decision Conference (CCDC), 2010 Chinese , vol., no., pp.1023,1026, 26-28 May 2010.

[152] J. Ahmed, M. N. Jafri, J. Ahmad, and I.M. Khan, "Design and Implementation of a Neural Network for Real-Time Object Tracking," World Academy of Science, Engineering and Technology 6 2007.

[153] H.B. Mark, T.H. Martin B.D.Demuth, Matlab Neural Network ToolboxTM Getting Started Guide R2013a.

[154] H.Yonaba, F. Anctil, and V. Fortin. "Comparing sigmoid transfer functions for neural network multistep ahead streamflow forecasting." Journal of Hydrologic Engineering 15, no. 4 (2010): 275-283.

[155] D. Hunter, H. Yu, M. S. Pukish III, J. Kolbusz, and B. M. Wilamowski, "Selection of proper neural network sizes and architectures: a comparative study," IEEE Transactions on Industrial Informatics, vol. 8, no. 2, pp. 228–240, 2012.

[156] C.A. Doukim, J.A. Dargham, A.Chekima, "Finding the number of hidden neurons for an MLP neural network using coarse to fine search technique," Information Sciences Signal Processing and their Applications (ISSPA), 2010 10th International Conference on , vol., no., pp.606,609, 10-13 May 2010.

[157] K. Gnana Sheela and S. N. Deepa, "Review on Methods to Fix Number of Hidden Neurons in Neural Networks," Mathematical Problems in Engineering, vol. 2013, Article ID 425740, 11 pages, 2013.

[158] C. Donalek, Supervised and Unsupervised Learning, April 2011, [Online Available]: http://www.astro.caltech.edu/~george/aybi199/Donalek_Classif.pdf

[159] Neuro AI, [Online Available]: http://www.learnartificialneuralnetworks.com/introduction-to-neural-networks.html#Intro

[160] Y.H. Hu and J.Hwang, Handbook of Neural Network Signal Processing, CRC Press, 12 Dec 2010 - Technology & Engineering.

[161] C. Stergiou and D. Siganos, neural networks, [Online Available]: http://www.doc.ic.ac.uk/~nd/surprise_96/journal/vol4/cs11/report.html#A simple neuron.

[162] R. Sathya, A. Abraham, "Comparison of Supervised and Unsupervised Learning Algorithms for Pattern Classification", (IJARAI) International Journal of Advanced Research in Artificial Intelligence, Vol. 2, No. 2, 2013.

[163] Learning Rule, [Online Available]: http://penta.ufrgs.br/edu/telelab/3/learning.htm
[164] B.M. Wilamowski, N.J. Cotton, O. Kaynak, G. Dundar, "Computing Gradient Vector and Jacobian Matrix in Arbitrarily Connected Neural Networks," Industrial Electronics, IEEE Transactions on , vol.55, no.10, pp.3784,3790, Oct. 2008.
[165] B.M. Wilamowski,"How to not get frustrated with neural networks," Industrial Technology (ICIT), 2011 IEEE International Conference on, vol., no., pp.5,11, 14-16 March 2011.
[166] B. M. Wilamowski, Hao Yu, "Improved Computation for Levenberg–Marquardt Training," Neural Networks, IEEE Transactions on , vol.21, no.6, pp.930,937, June 2010.
[167] R. M. Ahmed, M. A. El Sayed, S. A. Gadsden, S. R. Habibi,"Fault detection of an engine using a neural network trained by the smooth variable structure filter," Control Applications (CCA), 2011 IEEE International Conference on , vol., no., pp.1190,1196, 28-30 Sept. 2011.
[168] B. M. Wilamowski, "Neural Network Architectures and Learning Algorithms: How Not to Be Frustrated with Neural Networks," IEEE Ind. Electron. Mag., vol. 3, no. 4, pp. 56-63, 2009.
[169] H. Yu, M. Bogdan and Wilamowski, Levenberg–Marquardt Training, [Online Available]: http://www.eng.auburn.edu/~wilambm/pap/2011/K10149_C012.pdf
[170] A.S.Benemar,N.S.D. Brito, W. L. A. Neves, Silva, M. Kleber, R.B.V. Lima, S.S.B. da Silva, "Comparison between backpropagation and RPROP algorithms applied to fault classification in transmission lines," Neural Networks, 2004. Proceedings. 2004 IEEE International Joint Conference on, vol.4, no., pp.2913, 2918 vol.4, 25-29 July 2004.
[171] T. Falas, A. Stafylopatis,"Temporal differences learning with the scaled conjugate gradient algorithm," Neural Information Processing, 2002. ICONIP '02. Proceedings of the 9th International Conference on, vol.5, no., pp.2625,2629 vol.5, 18-22 Nov. 2002.
[172] C. Xia, Z. Yang, B. Lei, Q. Zhou, "SCG and LM Improved BP Neural Network Load Forecasting and Programming Network Parameter Settings and Data Preprocessing," Computer Science & Service System (CSSS), 2012 International Conference on , vol., no., pp.38,42, 11-13 Aug. 2012.
[173] P. Navneel, S. Rajeshni, L. Sunil Pranit, "Comparison of Back Propagation and Resilient Propagation Algorithm for Spam Classification," Computational Intelligence, Modelling and Simulation (CIMSim), 2013 Fifth International Conference on , vol., no., pp.29,34, 24-25 Sept. 2013.
[174] T. Falas, A. Stafylopatis, "Symbolic rule extraction with a scaled conjugate gradient version of CLARION," Neural Networks, 2005. IJCNN '05. Proceedings. 2005 IEEE International Joint Conference on, vol.2, no., pp.845, 848 vol. 2, 31 July-4 Aug. 2005.
[175] N. Mohamad, F. Zaini, A. Johari, I. Yassin, A. Zabidi, "Comparison between Levenberg-Marquardt and Scaled Conjugate Gradient training algorithms for Breast Cancer Diagnosis using MLP," Signal Processing and Its Applications (CSPA), 2010 6th International Colloquium on , vol., no., pp.1,7, 21-23 May 2010.
[176] M. Fawzi Al-Naima and Ali H. Al-Timemy, Resilient Back Propagation Algorithm for Breast Biopsy Classification Based on Artificial Neural Networks, Computational Intelligence and Modern Heuristics, Al-Dahoud Ali (Ed.), Published: February 1, 2010 under CC BY-NC-SA 3.0 license.
[177] M. Riedmiller, H. Braun, "A direct adaptive method for faster backpropagation learning: the RPROP algorithm," Neural Networks, 1993. IEEE International Conference on, vol., no., pp.586, 591 vol.1, 1993.
[178] J. He, T. Jiang, Z. Xing,"A method of target detection and identification based on RPROP and UWB channel characteristic parameters," Globecom Workshops (GC Wkshps), 2012 IEEE , vol., no., pp.1460,1463, 3-7 Dec. 2012.
[179] F. Choong, M.B.I. Reaz, F. Mohd-Yasin,"Power Quality Disturbance Detection Using Artificial Intelligence: A Hardware Approach," Parallel and Distributed Processing Symposium, 2005. Proceedings. 19th IEEE International, vol., no., pp.146a, 146a, 04-08 April 2005.
[180] J.C. Morton, "Boosting a fast neural network for supervised land cover classification," Computers & Geosciences, Volume 35, Issue 6, June 2009, Pages 1280-1295.

[181] M. Wang, A.V. Mamishev,"Classification of power quality events using optimal time-frequency representations-Part 1: theory," Power Delivery, IEEE Transactions on, vol.19, no.3, pp.1488, 1495, July 2004.

[182] M. A. El-Gammal, A. Y. Abou-Ghazala, and T. I. El-Shennawy, "Dynamic Voltage Restorer (DVR) for Voltage Sag Mitigation," International Journal on Electrical Engineering and Informatics - Volume 3, Number 1, 2011.

[183] P. Barendse, R. Naidoo, H. Douglas, P. Pillay, "A New Algorithm for Improved Dip/Sag Detection with Application to Improved Performance of Wind Turbine Generators," Industry Applications Conference, 2006. 41st IAS Annual Meeting. Conference Record of the 2006 IEEE, vol.1, no., pp.118, 123, 8-12 Oct. 2006.

[184] M.E.Baran, K. Jinsang,"A classifier for distribution feeder overcurrent analysis," Power Delivery, IEEE Transactions on, vol.21, no.1, pp.456, 462, Jan. 2006.

[185] P.K. Ray, S.R. Mohanty, N. Kishor,"Classification of Power Quality Disturbances Due to Environmental Characteristics in Distributed Generation System," Sustainable Energy, IEEE Transactions on , vol.4, no.2, pp.302,313, April 2013.

[186] E. Styvaktakis, I.Y.-H.Gu, M.H.J.Bollen,"Voltage dip detection and power system transients," Power Engineering Society Summer Meeting, 2001, vol.1, no., pp.683, 688 vol.1, 2001.

[187] A. Moschitta, P. Carbone, C. Muscas, "Performance Comparison of Advanced Techniques for Voltage Dip Detection," Instrumentation and Measurement, IEEE Transactions on, vol.61, no.5, pp.1494, 1502, May 2012.

[188] R. Naidoo and P. Pillay, "A new method of voltage sag and swell detection," IEEE Trans. Power Del., vol. 22, no. 2, pp. 1056–1063, Apr. 2007.

[189] M. V. Rajesh, R. Archana, A. Unnikrishnan, R. Gopikakumari, J. Jacob, Evaluation of the ANN Based Nonlinear System Models in the MSE and CRLB Senses, World Academy of Science, Engineering and Technology 24 2008.

[190] H. Ismail, N. Hamzah, Z. Zakaria, S. Shahbudin,"Investigation on the effectiveness of classifying the voltage sag using support vector machine," Power Engineering and Optimization Conference (PEOCO), 2010 4th International , vol., no., pp.402,405, 23-24 June 2010.

[191] F. Martin and J. A. Aguado, "Wavelet based ANN approach for transmission line protection," IEEE Trans on Power Delivery, vol. 18, no. 4, pp. 1572–4, 2003.

[192] D. Saxena, K.S. Verma and S.N. Singh, Power quality event classification: an overview and key issues, International Journal of Engineering, Science and technology, Vol. 2, No. 3, pp. 186-199, 2010.

[193] S. Chauhan, and K.V. Prema, "Car Classification Using Artificial Neural Network," International Journal of Scientific and Research Publications, Volume 2, Issue 12, December 2012, ISSN 2250-3153.

[194] Herself's Artificial Intelligence, [Online Available]: http://herselfsai.com/2007/03/probabilistic-neural-networks.html

[195] Herself's Artificial Intelligence, [Online Available]: http://herselfsai.com/2007/03/probabilistic-neural-networks.html

[196] P. K. Dash, B. K. Panigrahi, and G. Panda, "Power quality analysis using S-transform," Power Delivery, IEEE Transactions on, vol. 18, no. 2, pp.406–411, Apr. 2003.

[197] DTREG, [Online Available]: http://www.dtreg.com/pnn.htm

[198] J. Smrekar, M. Assadi, Comparison Study of an In-house Developed Tool and Commercial Software for ANN Modeling, IEEE The 17th International Conference on Industrial Engineering and Engineering Management, October 2010, Xiamen, China.

[199] C. K. Goh, E. J. Teoh and K. C. Tan, "Hybrid Multiobjective Evolutionary Design for Artificial Neural Networks," IEEE Trans. on Neural Networks, vol. 19, no. 9, pp. 1531-1548, Sept 2008.

[200] V. Arulmozhi, "Classification task by using Matlab Neural Network Tool Box – A Beginner's View," International Journal of Wisdom Based Computing, Vol. 1 (2), August 2011.

[201] Eskom generic data officially through Eskom

[202] DIgSILENT PowerFactory, Technical Documentation, [Online Available]: http://siphiwebillysigudla.yolasite.com/resources/digsilent-general.pdf
[203] T. Gözel, M. Hakan Hocaoglu, An analytical method for the sizing and siting of distributed generators in radial systems, Electric Power Systems Research, Volume 79, Issue 6, June 2009, Pages 912-918, ISSN 0378-7796.
[204] A.M. El-Zonkoly, Optimal placement of multi-distributed generation units including different load models using particle swarm optimization, Swarm and Evolutionary Computation, Volume 1, Issue 1, March 2011, Pages 50-59, ISSN 2210-6502
[205] R.K. Singh, S.K. Goswami, Optimum allocation of distributed generations based on nodal pricing for profit, loss reduction, and voltage improvement including voltage rise issue, International Journal of Electrical Power & Energy Systems, Volume 32, Issue 6, July 2010, Pages 637-644, ISSN 0142-0615.
[206] J.A. Martinez, G. Guerra, "Optimum placement of distributed generation in three-phase distribution systems with time varying load using a Monte Carlo approach," Power and Energy Society General Meeting, 2012 IEEE , vol., no., pp.1,7, 22-26 July 2012.
[207] G. Sudipta, S.P. Ghoshal, G. Saradindu, Optimal sizing and placement of distributed generation in a network system, International Journal of Electrical Power & Energy Systems, Volume 32, Issue 8, October 2010, Pages 849-856, ISSN 0142-0615.
[208] Data from Eskom website, [Online Available]: https://lft.eskom.co.za/cgi-bin/pnp/files.cgi?dir=HQNflTgTL
[209] Data from DIgSILENT- Power Factory Version 14.1.6(Electrical Simulation Software), Licensed to UCT, 1986-2012.
[210] S. Achilles, and M. Poeller, 'Direct drive synchronous machine models for stability assessment of wind farms', Fourth Int. Workshop on Large Scale Integration of Wind Power and Transmission Networks for Offshore Windfarms, Billund, Denmark, October 2003.
[211] A. Griffo, J. Wang, "State-space average modelling of synchronous generator fed 18-pulse diode rectifier," Power Electronics and Applications, 2009. EPE '09. 13th European Conference on, vol., no., pp.1, 10, 8-10 Sept. 2009.
[212] P. Kudur, "Power System Stability and Control", New York: McGraw-Hill, Inc. 1994.
[213] N.S. Jayalakshmi, D.N. Gaonkar, K.S.K. Kumar,"Dynamic modeling and performance analysis of grid connected PMSG based variable speed wind turbines with simple power conditioning system," Power Electronics, Drives and Energy Systems (PEDES), 2012 IEEE International Conference on , vol., no., pp.1,5, 16-19 Dec. 2012.
[214] N.K. Roy, M. J. Hossain, H.R. Pota,"Effects of load modeling in power distribution system with distributed wind generation," Universities Power Engineering Conference (AUPEC), 2011 21st Australasian , vol., no., pp.1,6, 25-28 Sept. 2011.
[215] F. D. Kanellos, A. I. Tsouchnikas, N. D. Hatziargyriou, "Micro-Grid Simulation during Grid-Connected and Islanded Modes of Operation," Presented at the International Conference on Power Systems, Transients (IPST'05) in Montreal, Paper No. IPST05 - 113, Canada on June 19-23, 2005.
[216] A. D. Hansen, F.Iov, P. Sørensen, N. Cutululis. J. Clemens, F. Blaabjerg, 'Dynamic wind turbine models in power system simulation tool DIgSILENT', August 2007.
[217] Z. Wang, Y. Sun, G. Li, B. Ooi, "Magnitude and frequency control of grid-connected doubly fed induction generator based on synchronised model for wind power generation," Renewable Power Generation, IET , vol.4, no.3, pp.232,241, May 2010.
[218] N. Mohan, Advanced electric drives. MNPERE, 2001. ISBN -9715-2920-5.
[219] K. Fernando, A. Kalam,"Voltage instability in power systems and the use of artificial intelligence methods for its prediction," Power Engineering Conference, 2008. AUPEC '08. Australasian Universities, vol., no., pp.1,4, 14-17 Dec. 2008.
[220] K.W.E. Cheng, J.K. Lin, Y.J. Bao, X.D. Xue, "Review of the wind energy generating system," Advances in Power System Control, Operation and Management (APSCOM 2009), 8th International Conference on , vol., no., pp.1,7, 8-11 Nov. 2009.

[221] S. Lindenberg, B. Smith, K. O'Dell, and E. DeMeo, "20 Percent Wind Energy by 2030: Increasing Wind Energy's Contribution to U.S. Electricity Supply," tech. rep., U.S. Department of Energy, July 2008. [Online Available]: http://www.nrel.gov/docs/fy08osti/41869.pdf.

[222] C. Zhe, J.M. Guerrero and F. Blaabjerg, "A Review of the State of the Art of Power Electronics for Wind Turbines," IEEE Trans. Power Electronics, vol. 24, pp. 1859-1875, Aug. 2009.

[223] F. Iov, B.Frede, Power electronics control of wind energy in distributed power systems, Department of energy technology, Aalborg University Denmark. [Online]: Available online: http://cdn.intechopen.com/pdfs-wm/9336.pdf

[224] M. Singh, S. Santoso, "Dynamic Models for Wind Turbines and Wind Power Plants," national renewable energy laboratory, January 11, 2008 – May 31, 2011.

[225] M. Behnke, A. Ellis, Y. Kazachkov, T. McCoy, E. Muljadi, W. Price, and J. Sanchez-Gasca, "Development and validation ofWECC variable speed wind turbine dynamic models for grid integration studies," in AWEA Wind Power Conference, 2007.

[226] E. Muljadi and A. Ellis, "Validation of wind power plant models," in 2008 IEEE Power and Energy Society General Meeting-Conversion and Delivery of Electrical Energy in the 21st Century, pp. 1–7, 2008.

[227] F.M Gonzalez-Longatt, et al., "Dynamic Behavior of Constant Speed WT based on Induction Generator Directly connected to Grid," presented at the Proceeding of 6th World Wind Energy Conference and Exhibition (WWEC 2007), Mar del Plata, Argentina, 2007.

[228] F.M.Gonzalez-Longatt, P. Wall,V. Terzija,"A simplified model for dynamic behavior of permanent magnet synchronous generator for direct drive wind turbines," PowerTech, 2011 IEEE Trondheim , vol., no., pp.1,7, 19-23 June 2011.

[229] L. Peng, Y. Li, B. Francois, "Dynamic behavior of doubly fed induction generator wind turbines under three-phase voltage dips," Power Electronics and Motion Control Conference, 2009. IPEMC '09. IEEE 6th International, vol., no., pp.620,626, 17-20 May 2009.

[230] M. Huynh Quang, F. Nollet, N. Essounbouli, A Hamzaoui, "Control of permanent magnet synchronous generator wind turbine for stand-alone system using fuzzy logic," EUSFLAT-LFA 2011. Aix-les-Bains, France, July 2011.

[231] L. Wang, L. Yu-Hung,C. Yi-Ting, "Load-Flow Analysis of a Wind Farm Containing Multiple Wind-Driven Wound-Rotor Induction Generators With Dynamic Slip Control Using RX Models," Sustainable Energy, IEEE Transactions on , vol.2, no.3, pp.256,264, July 2011.

[232] A.G. Abo-Khalil, L. Dong-Choon, "Dynamic Modeling and Control of Wind Turbines for Grid-Connected Wind Generation System," Power Electronics Specialists Conference, 2006. PESC '06. 37th IEEE , vol., no., pp.1,6, 18-22 June 2006.

[233] O. Ipinnimo, S. Chowdhury, S.P. Chowdhury, "Application of Grid Integrated Wind Energy Conversion Systems for Mitigation of Multiple Voltage Dips in a Power Network," Universities' Power Engineering Conference (UPEC), Proceedings of 2011 46th International, vol., no., pp.1-6, 5-8 Sept. 2011.

[234] F. Mei, B. Pal,"Modal Analysis of Grid-Connected Doubly Fed Induction Generators," Energy Conversion, IEEE Transactions on , vol.22, no.3, pp.728,736, Sept. 2007.

[235] L. Nguyen Tung, "Power quality investigation of grid connected wind turbines," Industrial Electronics and Applications, 2009. ICIEA 2009. 4th IEEE Conference on , vol., no., pp.2218,2222, 25-27 May 2009.

[236] N.G. Voros, C.T. Kiranoudis, and Z.B. Maroulis, Short-cut design of small hydroelectric plants. Renewable Energy, 2000. 19(4): p. 545-563.

[237] H. Li, Z. Chen, L. Han, "Comparison and Evaluation of Induction Generator Models in Wind Turbine Systems for Transient Stability of Power System," Power System Technology, 2006. PowerCon 2006. International Conference on , vol., no., pp.1,6, 22-26 Oct. 2006.

[238] S. Shao, E. Abdi, R. McMahon, "Dynamic analysis of the Brushless Doubly-Fed Induction Generator during symmetrical three-phase voltage dips," Power Electronics and Drive Systems, 2009. PEDS 2009. International Conference on , vol., no., pp.464,469, 2-5 Nov. 2009.

[239] M. Edouard and N. Donatien, mathematical modeling and digital simulation of PV solar panel using MATLAB software, International Journal of Emerging Technology and Advanced Engineering, Volume 3, Issue 9, September 2013.

[240] H. Q. Zhou, Z.P. Song, J.P. Wang, Y. Xue,"A Review on Dynamic Equivalent Methods for Large Scale Wind Farms," Power and Energy Engineering Conference (APPEEC), 2011 Asia-Pacific , vol., no., pp.1,7, 25-28 March 2011.

[241] O. Anaya-Lara, N. Jenkins, J. Ekanayake, P. Cartwright, M. Hughes, Wind Energy Generation: Modelling and Control, John Wiley & Sons, UK, 2009, ISBN 978-0-470-71433-

[242] A.H.M. Nordin, A.M. Omar, "Modeling and simulation of Photovoltaic (PV) array and maximum power point tracker (MPPT) for grid-connected PV system," Sustainable Energy & Environment (ISESEE), 2011 3rd International Symposium & Exhibition in , vol., no., pp.114,119, 1-3 June 2011.

[243] R. J.A Hernanz., et al "Dynamic Simulation of Photovoltaic Installation", International Conference on Renewable Energies and Power Quality (ICREPQ'09), April 2009.

[244] K.C. Kong, M. Mustafa bin , M.Z. Ibrahim, A.M. Muzathik, New Approach on Mathematical Modeling of Photovoltaic Solar Panel, Applied Mathematical Sciences, Vol. 6, 2012, no. 8, 381 – 401.

[245] S. Chowdhury, S.P. Chowdhury, G.A. Taylor, Y. Song, "Mathematical modelling and performance evaluation of a stand-alone polycrystalline PV plant with MPPT facility," Power and Energy Society General Meeting - Conversion and Delivery of Electrical Energy in the 21st Century, 2008 IEEE , vol., no., pp.1,7, 20-24 July 2008.

[246] M.G. Villalva, J.R Gazoli, E.R. Filho, "Modeling and circuit-based simulation of photovoltaic arrays," Power Electronics Conference, 2009. COBEP '09. Brazilian, vol., no., pp.1244,1254, Sept. 27 2009-Oct. 1 2009.

[247] Power Quality In Electrical Systems, [Online Available]: http://www.powerqualityworld.com/2011/04/voltage-sag-types-abc-classification.html

[248] J. Caicedo, F. Navarro,E. Rivas, F. Santamaria,"Voltage sag characterization with Matlab/Simulink," Engineering Applications (WEA), 2012 Workshop on , vol., no., pp.1,6, 2-4 May 2012

[249] R.Angelino, G. Carpinelli, D. Proto, A. Bracale, Dispersed generation and storage systems for providing ancillary services in distribution systems, Power Electronics Electrical Drives Automation and Motion, SPEEDAM, pp 343-351, 2010.

[250] S. Shen-Xing and X. Dong,"A Self-healing Scheme of Single-phase-to-ground Fault in Smart Power Distribution System, "Journal of International Council on Electrical Engineering Vol. 2, No. 1, pp. 14-19, 2012.

[251] E. Muljadi, M. Singh, V. Gevorgian,"Fixed-speed and variable-slip wind turbines providing spinning reserves to the grid," Power and Energy Society General Meeting (PES), 2013 IEEE, vol., no., pp.1, 5, 21-25 July 2013.

[252] S. F. Patrick, Doubly Fed Induction Generator Wind Turbines with Series Grid Side Converter for Robust Voltage Sag Ride-through, ProQuest LLC, 2008 - 177 pages, UMI Number 3327913.

[253] T. Thasananutariya, S. Chatratana, "Stochastic prediction of voltage sags in an industrial estate," Industry Applications Conference, 2005. Fourtieth IAS Annual Meeting. Conference Record of the 2005, vol.2, no., pp. 1489- 1496 Vol. 2, 2-6 Oct. 2005.

[254] J. Hiscock,N. Hiscock and A. Kennedy "Advanced Voltage Control For Networks With Distributed Generation"19th International Conference on Electricity Distribution, paper no 148, CIRED Vienna, 21-24 May 2007.

[255] D.G. Esp, "Real-time fault diagnosis for transmission systems," Artificial Intelligence Techniques in Power Systems (Digest No: 1997/354), IEE Colloquium on, vol., no., pp.5/1-5/4, 3 Nov 1997.

[256] F. Ye, X. Huang, C. Wang, G. Zhou, P. Luo, "The impact and simulation on large wind farm connected to power system," Electric Utility Deregulation and Restructuring and Power

Technologies, 2008. DRPT 2008. Third International Conference on , vol., no., pp.2608,2614, 6-9 April 2008.

[257] Tobias, R. D.. 2003. An Introduction to partial least squares regression, [Online Available] : <http://www.ats.ucla.edu/stat/sas/library/pls.pdf>.

[258] K. Kazys, P. Rimantas,"Missing Data Restoration Algorithm" Institute of Mathematics and Informatics, Vilnius University, Akademijos 4, LT-08663 Vilnius, Lithuania , [online Available]:http://www.mii.lt/informatica/pdf/INFO1011.pdf

Appendices

Appendix 3

Appendix 3A

The proposed FFNN algorithm implementation of voltage dip detection and classification in Matlab code

The following Matlab codes can be used to detect and classify any Eskom voltage dip window. Classification of voltage dips is a process of identifying voltage dip classes based on their magnitude and time. It involves training a neural network to assign the correct dip class to a set of input patterns. After the ANN is trained, it can be used to classify the voltage dip classes it has not been trained with.

The detection and classification algorithm in this work was developed based on voltage dip disturbance events from seven categories of Eskom voltage dip windows. However it can be modify and utilise by any other utility and industrial power consumers


```
clc;
close all;
clear all;
%% Reading in files  from data.
disp('**********************************************************************')
disp('All input files must be in CSV format with only numbers in the entries')
disp('**********************************************************************')
disp('')
disp('')
disp('.....Reading in primary data from input files.....')
Yin=csvread('Yinput.csv');X1in=csvread('X1input.csv');
X2in=csvread('X2input.csv');Sin=csvread('Sinput.csv');
Tin=csvread('Tinput.csv');Z1in=csvread('Z1input.csv');
Z2in=csvread('Z2input.csv');

Load=[Yin(:,1),X1in(:,2:3),X2in(:,2:3),Sin(:,2:3),Tin(:,2:3),Z1in(:,2:3),Z2in(:,2:3),Yin(:,2:3)];
Y=Yin';X1=X1in';X2=X2in';S=Sin';T=Tin';Z2=Z2in';Z1=Z1in';%Load=Load';
Utrain=Load(:,3:2:end)';
r=length(Utrain(1,:));
neurons=6;
Training_Algorithm ='trainscg';
```

```
%% Initializing Target matrix
B=sparse(7,r);
n=1:r;
%% Dip Detection
a=0;
b=0;
while a<r

   New_input = menu('Do you want to test a new sample Data for Dip or No Dip?','Yes','No');
    if b<a && Test < 9
       close(mess)
    end
   if New_input == 1
      [Filename,Path,Filter]= uigetfile('*.csv', 'Select your File ');
      filename = Filename;
      sample=csvread(filename);
      Uin=sample';
      r2=length(Uin(:,1));
   else

      disp('-----------------------------------')
      disp('Continue program with default data')
      disp('-----------------------------------')
   end



   Test = menu('Test for Dip/No Dip','Y Data','X1 Data','X2 Data','S Data','T Data','Z1 Data','Z2 Data','Other','None');

   if Test == 1 && New_input ~= 1
      Input_Matrix = Y;
      break
   elseif Test == 2 && New_input ~= 1
      Input_Matrix = X1;
      break
   elseif Test == 3 && New_input ~= 1
      Input_Matrix = X2;
      break
   elseif Test == 4 && New_input ~= 1
      Input_Matrix = S;
      break
   elseif Test == 5 && New_input ~= 1
      Input_Matrix = T;
      break
   elseif Test == 6 && New_input ~= 1
      Input_Matrix = Z1;
      break
   elseif Test == 7 && New_input ~= 1
      Input_Matrix = Z2;
      break
```

```
  elseif Test == 9 && New_input ~= 1
      break
   elseif Test == 8

      if New_input == 1
         input_ = Uin; %input('Enter the data to be checked for Voltage Dip or No dip: ');
         Input_Matrix= input_;
         e=length(Input_Matrix(:,1));
         if e~=3

            mess=msgbox('Enter a 3 input sample data for Dip detection, with colunms in the order: Dip Duration, Phase Angle and Voltage Magnitude','Error','error');
            delete(findobj(mess,'string','OK'));
            delete(findobj(mess,'style','frame'));
            b=a;
            a=a+1;



         else
            if e~=3
            close(mess)
            end
            break
         end
      else

         mess=msgbox('Enter a sample data with colunms in the order: Dip Duration, Phase Angle and Voltage Magnitude','Error','error');
         delete(findobj(mess,'string','OK'));
         delete(findobj(mess,'style','frame'));
         a=a+1;

      end


   end




end

if Test < 9


ml=length(Input_Matrix(:,1));
fprintf('This system has %d inputs (Dip Duration,Phase Angle and Voltage) \n',ml)
disp('------------------------------------------------------------------------')
C=sparse(ml,r);
```

```
Check=find(0<=Input_Matrix(3,:)& Input_Matrix(3,:)<0.9);
if Check == 0
   C(3,:)=0;
   C(2,:)=1;
else
   C(3,Check)=1;
   Time_ms=length(Check);
   no_dip =setdiff(n,Check);
   C(2,no_dip) = 1;
end

LL=C(2:3,:);
input= Input_Matrix;
output=full(LL);

% Dip detection process with neural network
net.divideFcn = '';
net = newpr(input,output,neurons,{},Training_Algorithm);
[net,tr]=train(net,input,output);
outInput = sim(net,input);

if Time_ms  >= 10


   mess = msgbox(' Voltage dip has occured on this input');
   delete(findobj(mess,'string','OK'));
   delete(findobj(mess,'style','frame'));


else


   mess=msgbox('No Voltage Dip has occured on this input');
   delete(findobj(mess,'string','OK'));
   delete(findobj(mess,'style','frame'));

end
end
%% Dip Classification process

   %******************************
   % Checking Dip Conditions
   %******************************
   y=find(0.7<=Utrain(7,:) & Utrain(7,:)<0.9);
   x1=find(0.6<=Utrain(1,:) & Utrain(1,:)<0.7);
   x2=find(0.4<=Utrain(2,:) & Utrain(2,:)<0.6);
   s=find(0.4<=Utrain(3,:) & Utrain(3,:)<0.8);
   t=find(0<=Utrain(4,:) & Utrain(4,:)<0.4);
```

```
z1=find(0.7<=Utrain(5,:) & Utrain(5,:)<0.85);
z2=find(0.0<=Utrain(6,:) & Utrain(6,:)<0.7);

%---------------------------------
%    Assembling Target matrix
%---------------------------------
B(1,x1(1,:))=1;
B(2,x2(1,:))=1;
B(3,s(1,:))=1;
B(4,t(1,:))=1;
B(5,z1(1,:))=1;
B(6,z2(1,:))=1;
B(7,y(1,:))=1;

%-------------------------------------------------------------
% Sorting Dip Conditions for the Target and Input matrices
%-------------------------------------------------------------
m=union(union(union(y,x1),union(x2,s)),union(union(t,z1),z2));
Utrain=Utrain(1:7,m);% Voltage magnitudes for training
B=B(1:7,m); % B matrix for traininig or classification

input=Load(m,:)'; %input matrix for default classification
output=full(B); % Outputs target matrix for classification

%---------------------------------
% Classify sample data
%---------------------------------
Sample=menu('Do you want to classify a sample data','Yes','No');
if Sample == 1
   if Test< 9
   close(mess)
   end
   close all
   % Read in data from file
   [F,PathName,FilterIndex]= uigetfile('*.csv', 'Select your File ');
   filename=F; % Sample file for classification
   in=csvread(filename);
   Uin=in';
   [rs y2]=find(0<=Uin(3:2:end,:) & Uin(3:2:end,:)<0.9); % Dip Detectection
   Time_y2=length(y2);Time_m=length(m);
   if Time_y2 == Time_m
      Dip_Time=m;
   elseif Time_y2==0
      Dip_Time=m;

   else
      y3=setdiff(m,y2);
      Time_y3=Time_m-Time_y2;
      ny3=y3(1,1:Time_y3);
```

```
        y4=union(y2,ny3);
        Dip_Time=y4;
    end
    input=Uin(2:end,Dip_Time);

   %  Classification process
    Train=menu('Classify Sampledata','Yes','No');
    if Train == 1

        k=0;
        while k<10000*n
            net.divideFcn = '';
            net = newpr(input,output,neurons,{},Training_Algorithm);
            [net,tr]=train(net,input,output);
            outInput = sim(net,input);

            retrain=menu('Reclassify sample data','Yes','No');

            if retrain == 1
                close all
                k=k+1;
            else
                break
            end
        end
    end
else

end

%% Classify default data

Train=menu('Do you want to classify the default data','Yes','No');

if Train == 1
    close all
    if Sample~=1
        if Test< 9
        close(mess)
        end
    end
 %--------------------------------------------------
 % Classification process via Neural Network
 %--------------------------------------------------
    k=0;
    while k<10000*n % infinite loop in case of reclassification
        net.divideFcn = ''; % Use all input for classification
        net = newpr(input,output,neurons,{},Training_Algorithm);
        [net,tr]=train(net,input,output);
```

```
        outInput = sim(net,input);
        retrain=menu('Reclassify Default Data','Yes','No');

        if retrain == 1 %Condition for re-training
            close all
            k=k+1;
        else
            break
        end
    end
end

%% Program completed
Close_=menu('Do you wish to exit matlab','OK','Continue with matlab');
if Train ~= 1 && Sample ~= 1
        if Test< 9
        close(mess)
        end
end
if Close_==1

    exit

end
```

Appendix 4

Appendix 4A: Test network model parameters

Table 4A.1 gives the parameters for static PV generator

Table 4A.1: PV generator data as static generator [201]

Generator Name	Generator description	Link to Busbar	Nominal apparent power MVA	No of Parallel machines	Local voltage controller	MW	p.f	kV	Time constants	
									Td''	Td'
RDG 06	0.4kV 1 MW PV Plant	22	0.5	2	Power factor	0.5	0.95	0.415	0.03	1.2
RDG 05	22kV 20MW PV Plant	22	0.5	8	Power factor	0.25	0.95	22	0.03	1.2
RDG 07	22kV 20MW PV Plant	23	0.5	4	voltage	0.448	1	22	0.03	1.2
RDG 04	0.4kV 20MW PV Plant	16	0.6	4	Power factor	0.5	0.95	0.415	0.03	1.2
RDG 03	0.4kV0.5MVA Plant	16	0.5	1	Power factor	0.448	0.95	0.415	0.03	1.2

The parameters for hydro synchronous generators is given in Table 4A.2,

where:

Xd: Direct Axis Synchronous Reactance

X'd: Direct Axis Transient Reactance in p.u.

T'd: Direct Axis Open Circuit Transient Time Constant

T"d: Direct Axis Open Circuit Sub-Transient Time Constant

Xq: Quadrature Axis Synchronous Reactance

X'q: Quadrature Axis Transient Reactance in p.u.

T'q: Quadrature Axis Open Circuit Transient Time Constant

T"q: Quadrature Axis Open Circuit Sub-Transient Time Constant

Table 4A.2: Hydro generator parameter [201]

Generator Name	Generator description	Link to Bus	kV	No of Parallel machines	MVA	pf		xd (p.u.)	xq (p.u.)	Xd' (p.u.)	Xq' (p.u.)	Td' (s)	Tq' (s)	Td" (s)	Tq" (s)
RDG 01	20MVA Turbo Machine Type	26	66	1	20	0.8	YN	2.2	2.1	0.31	0.465	0.84545	0.442850	0.01845161	0.0193978 5
RDG 02	10MVA Hydro (Sym-1) SG Type	25	22	2	10	0.8	YN	2	2	0.30		1.00000		0.05	0.05
RDG 08	5 MVA (DG) Hydro SG Type	20	0.415	1	5	0.8	YN	1.5	0.75	0.26		0.53000	0.03000	0.03	0.03
RDG 09	50MVA Hydro SG Type	20	0.415	1	50	0.8	YN	1.75	0.9	0.26		0.40000			
RDG 010	1.5 MVA Hydro SG Type	21	0.415	1	1.5	0.8	YN	1.4	0.8	0.24		0.29142		0.02	0.0225
RDG 011	5MVA Turbo SGType	21	0.415	1	5	0.8	YN	2.1	2	0.3	0.45	0.75000	0.405000	0.022	0.02

Table 4A.3 shows the parameter of the doubly-fed induction wind generator

R_S= stator resistance, X_M = Mag. Reactance

Table 4A.3: DFIG generator parameter [201]

Generator Name	Generator description	MW	Mvar	kV	Link to Bus	Resistance (p.u.)	No of parallel machines	R_S	X_M	Local voltage controller
RDG 012	11kV 15MW DFIG Wind Farm wind	15	7.5	11	11	0.01	1	0.01	3.5	Power factor
RDG 013	DFIG_5MW wind	5	1.78	11	11	0.01	2	0.01	3.5	Power factor
RDG 014	DFIG_3.4MW wind	3.4	1.02	0.145	15	0.01	6	0.01	3.5	Power factor
RDG 015	DFIG_2.3MW wind	2.3	0.66	0.145	15	0.01	1	0.01	3.5	Power factor
RDG 016	DFIG_6.5MW wind	6.5	2.66	11	16	0.01	1	0.01	3.5	Power factor

Table 4A.4 shows the parameters of the wind static generator

Table 4A.4: Wind generator data as static generator [201]

name	terminal	no of parallel	MVA	pf
RDG 017	Busbar14	2	6	0.9
RDG 018	Busbar14	1	2.778	0.9
RDG 019	Busbar18	6	24	0.9
RDG 020	Busbar18	6	4	0.9

Table 4A.5 shows the parameters of the load model

Table 4A.5: Load parameter [208]

Name	Terminal Busbar	Active power MW	Reactive power Mvar	power factor	MVA		Balanced/ Unbalanced	Input mode
Load A	Busbar5	125	50	0.9284767	134.6291	ind.	balanced	DEF
Load B	Busbar6	90	30	0.9486833	94.86833	ind.	balanced	DEF
Load C	Busbar8	100	35	0.9438584	105.9481	ind.	balanced	DEF
Load 20	Busbar23	10	3	0.9578263	10.44031	ind.	balanced	PQ
Load 21	Busbar23	12.55	3.45	0.9642299	13.01557	ind.	balanced	PQ
Load 1	Busbar11	8.4	2.77	0.9496959	8.844936	ind.	balanced	PQ
Load 10	Busbar17	5	1.77	0.9426767	5.304046	ind.	unbalanced	PQ
Load 11	Busbar18	4.55	2.77	0.8541623	5.326857	ind.	balanced	PQ
Load 12	Busbar18	8.2	3.64	0.9139953	8.9716	ind.	balanced	PQ
Load 13	Busbar19	1	0.4	0.9284768	1.077033	ind.	balanced	PQ
Load 14	Busbar19	2	0.6	0.9578263	2.088061	ind.	balanced	PQ
Load 15	Busbar20	16	4	0.9701425	16.49242	ind.	Balanced	PQ
Load 16	Busbar20	10	3	0.9578263	10.44031	ind.	Balanced	PQ
Load 17	Busbar21	3.33	1.2	0.9407793	3.539618	ind.	Balanced	PQ
Load 18	Busbar21	5.59	2.5	0.9128664	6.12356	ind.	Balanced	DEF
Load 19	Busbar22	1.9	0.6	0.9535826	1.992486	ind.	Balanced	PQ
Load 2	Busbar11	9.55	3.45	0.9405102	10.15406	ind.	Balanced	PQ
Load 3	Busbar13	2	0.312659	0.9880000	2.024292	ind.	Balanced	PC
Load 4	Busbar13	-11	3.5	-0.9529250	11.5434	cap.	Balanced	QC
Load 5	Busbar14	1.5	0.42	0.9629640	1.557691	ind.	Balanced	DEF
Load 6	Busbar14	1.5	0.42	0.9629640	1.557691	ind.	balanced	DEF
Load 7	Busbar16	0.82	0.22	0.9658428	0.848999	ind.	unbalanced	DEF
Load 8	Busbar16	2	0.6	0.9578263	2.088061	ind.	balanced	PQ
Load 9	Busbar17	10	5	0.8944272	11.18034	ind.	unbalanced	PQ
Load D	Busbar26	19.6	8.0688	0.9247078	21.19588	ind.	Balanced	PQ
Load E	Busbar26	30	13.5	0.9119215	32.89757	ind.	Balanced	PQ
Load F	Busbar25	6	-1.01467	0.9860000	6.085193	cap.	Balanced	PC
Load G	Busbar25	5.5247	0.863677	0.9879999	5.591802	ind.	balanced	PC

Table 4A.6 shows the busbars parameters

Table 4A.6: Busbar parameter [201]

7ame	System Type	Usage	Phase Technology	Nom.L-L Volt. (kV)	Nom.L-G Volt. (kV)
Busbar1	AC	Busbar	ABC	16.5	9.526279
Busbar10	AC	Busbar	ABC	230	132.7906
Busbar11	AC	Busbar	ABC	11	6.350853
Busbar12	AC	Busbar	ABC	11	6.350853
Busbar13	AC	Busbar	ABC	0.415	0.2396
Busbar14	AC	Busbar	ABC	0.415	0.2396
Busbar15	AC	Busbar	ABC	0.415	0.2396
Busbar16	AC	Busbar	ABC	0.415	0.2396
Busbar17	AC	Busbar	ABC	0.415	0.2396
Busbar18	AC	Busbar	ABC	0.415	0.2396
Busbar19	AC	Busbar	ABC	0.415	0.2396
Busbar2	AC	Busbar	ABC	18	10.3923
Busbar20	AC	Busbar	ABC	0.415	0.2396
Busbar21	AC	Busbar	ABC	0.415	0.2396
Busbar22	AC	Busbar	ABC	0.415	0.2396
Busbar23	AC	Busbar	ABC	11	6.350853
Busbar24	AC	Busbar	ABC	230	132.7906
Busbar3	AC	Busbar	ABC	13.8	7.967434
Busbar4	AC	Busbar	ABC	230	132.7906
Busbar5	AC	Busbar	ABC	230	132.7906
Busbar6	AC	Busbar	ABC	230	132.7906
Busbar7	AC	Busbar	ABC	230	132.7906
Busbar8	AC	Busbar	ABC	230	132.7906
Busbar9	AC	Busbar	ABC	230	132.7906

Table 4A.8 shows the parameters of the transformers

Table 4A.8: Transformer parameter [201]

Name	rtd pow MVA	HV-rtd. Volt.(kV)	LV-rtd. Volt.(kV)	Freq	HV-Vec.Grp	LV-Vec.Grp	HV-side	LV-side
TF1	250	230	16.5	50	YN	D	Busbar4	Busbar1
TF2	200	230	18	50	YN	D	Busbar7	Busbar2
TF3	150	230	13.8	50	YN	D	Busbar9	Busbar3
TF4	150	230	11	50	YN	YN	Busbar10	Busbar11
TF5	12.5	230	66	50	YN	YN	Busbar10	Busbar27
TF6	10	22	11	50	YN	YN	Busbar25	Busbar11
TF7	12.5	66	22	50	YN	YN	Busbar26	Busbar25
TF8	100	11	0.415	50	YN	YN	Busbar23	Busbar14
TF9	150	230	11	50	YN	YN	Busbar24	Busbar23
TF10	100	11	0.415	50	YN	YN	Busbar23	Busbar21
TF11	12.5	22	0.415	50	YN	YN	Busbar25	Busbar14
TF12	12.5	11	0.415	50	YN	YN	Busbar11	Busbar17
TF13	12.5	11	0.415	50	YN	YN	Busbar11	Busbar18

Table 4A.9: External Grid Parameters [201]

Bus Type = SL
Active power = 370 MW
Reactive power = 80 Mvar
X/R Ratio = 10
Short-Circuit Power Sk" max = 740.9713 MVA
Short-Circuit Current Ik" max = 1.86 kA

Table 4A10: Busbar voltage levels [201],[209]

Name	Target Voltage
	kV
Busbar1	16.5
Busbar10	230
Busbar11	11
Busbar12	11
Busbar13	0.415
Busbar14	0.415
Busbar15	0.415
Busbar16	0.415
Busbar17	0.415
Busbar18	0.415
Busbar19	0.415

Busbar2	18
Busbar20	0.415
Busbar21	0.415

Busbar22	0.415
Busbar23	11
Busbar24	230
Busbar25	22
Busbar26	66
Busbar3	13.8
Busbar4	230
Busbar5	230
Busbar6	230
Busbar7	230
Busbar8	230
Busbar9	230

The IEEE 9-bus system parameters are taken from DIgSILENT- Power Factory Version 14.1.6, Licensed to UCT, 1986-2012. [209]

Table 4A.11 shows the parameters of the lines

Table 4A.11: The line parameter for the 9 bus system [209]

	$l[km]$	$I_{max}[kA]]$	$Z[\Omega]$	$R[\Omega]$	$X[\Omega]$
Line 1	1.00	1.00	45.275	5.290	44.965
Line 2	1.00	1.00	45.275	5.290	44.965
Line 3	1.00	1.00	38.353	4.497	38.088
Line 4	1.00	1.00	53.694	6.295	53.323
Line 5	1.00	1.00	92.292	20.631	89.930
Line 6	1.00	1.00	49.492	8.993	48.668

Table 4A.12. Synchronous generators [209]

Generator	Active power (MW)	Nominal apparent power (MVA)	Power factor	Nominal voltage (KV)	Reactive power (Mvar)	Connection
SG1	100	247.5	0.85	18.0	80	NY
SG2	100	192.0	1.00	13.8	80	NY
SG3	100	128.0	0.85	16.5	80	NY

Table 4A.13: Load parameter [209]

Load	Active power (MW)	Reactive power (MVar)	Voltage (p.u.)	Power factor	Load Type
A	125	50	1	0.894427	inductive
B	90	30	1	0.894427	inductive
C	100	35	1	0.894427	inductive

Appendix 4B

The second test network in Figure 5.12 has the following network parameters.

Laod parameter [201]

Load name	Terminal busbar	MW	Mvar
DG Load	Busbar DG	20	10
Load1	22kV Bus1	10	5
Load2	22 kVBus2	10	5
Load3	Busbar1b	10	5
TX Load	Busbar TX	10	5

External Grid Parameters [201]

Bus Type = PQ
Active power = 60 MW
Reactive power = 42 Mvar
X/R Ratio = 10
Short-Circuit Power Sk" max = 212.6266 MVA
Short-Circuit Current Ik" max = 1.86 kA

Transformer parameter [201]

Name	Primary	Secondary	Impedance	Vector Group	MVA	TAP No	Max Prim kV	Min Prim kV	V_{max}	V_{min}
TR 1	66	22	9	YNd11	15	17	69.3	56	1.05	1.02
TR 2	66	11	7.36	YNd11	18	17	69.3	56.1	1.05	1.02
TR 3	66	11	7.39	YNd11	18	17	69.3	56.1	1.05	1.02
TR 4	66	22	9	YNd11	15	17	69.3	56	1.05	1.02

Line parameter [201]

Line Name	V_R (kV)	Length (km)	Temp(^oC)	I_R(kA)	Z1	R1	X1	R0	X0
Line 1	66	20.2	60	0.357	10.1426	5.532765	8.500642	11.42014	27.11137
Line 2	66	20.2	50	0.378	9.258302	3.7976	8.443601	9.5546	29.7546
Line 3	66	20	60	0.357	10.04218	5.477985	8.416477	11.30707	26.84294
Line 4	66	15	60	0.357	7.531636	4.108489	6.312358	8.4803	20.1322

V_R = Line Voltage Rating
I_R = Rated Current
Z1 = Pos. Seq. Impedance,
R1 = Pos. Seq. Resistance,
X1 = Pos. Seq. Reactance,
R0 = Zero Seq. Resistance,
X0 = Zero Seq. Reactance

DFIG induction generator values [201]

Parameter	Value
Nominal Apparent Power	15 MVA
Nominal Voltage	11 kV
Power Factor	0.8
Power Output	10 MW
Frequency	50 Hz
Connection	YN

DFIG three-winding transformer Values [201]

Parameter	Value
Rated Power	15 MVA
Rated Voltage (HV)	230 kV
Rated Voltage (LV)	11 kV
Rated Voltage (LV)	0.69 kV
Nominal Frequency	50 Hz
Connection	YN
X/R	5

Renewable DG parameter [201]

Xd: Direct Axis Synchronous Reactance

X'd: Direct Axis Transient Reactance in p.u.

T'd: Direct Axis Open Circuit Transient Time Constant

T"d: Direct Axis Open Circuit Sub-Transient Time Constant

Xq: Quadrature Axis Synchronous Reactance

X'q: Quadrature Axis Transient Reactance in p.u.

T'q: Quadrature Axis Open Circuit Transient Time Constant

T"q: Quadrature Axis Open Circuit Sub-Transient Time Constant

Appendix 5

Samples of graphs of voltage dip simulation and its mitigation with and without GRDG systems are shown in Appendix 5.

Appendix 5A- Graphs of multiple voltage dips without the grid-connected RDG systems as a result of 2P and 3P faults on the transmission lines 'line8' and 'line15' respectively.

Appendix 5:A1: Faults at 10% of the two lines

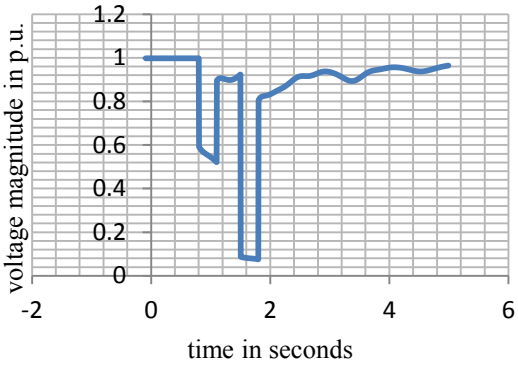

Figure: A1:a. Multiple voltage dip magnitude measured on Busbar5

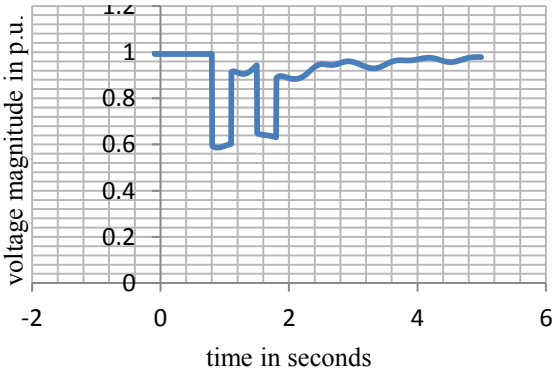

Figure: A1: b. Multiple voltage dip magnitude measured on Busbar11

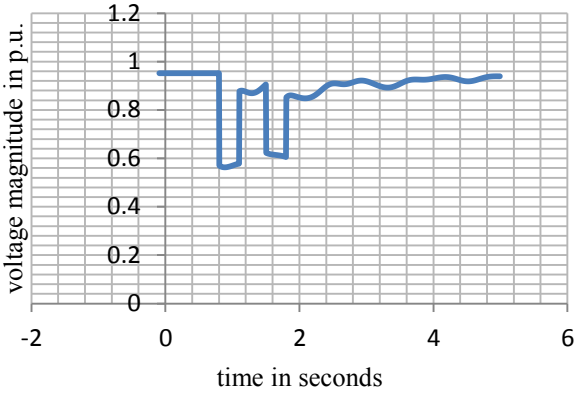

Figure: A1: c. Multiple voltage dip magnitude measured on Busbar18

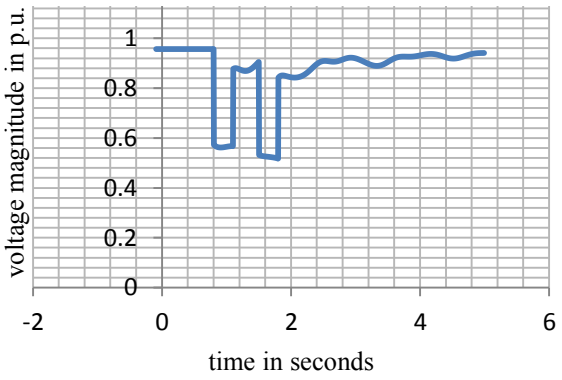

Figure: A1: d. Multiple voltage dip magnitude measured on Busbar26

Appendix 5: A2: Faults at 50% of the two lines

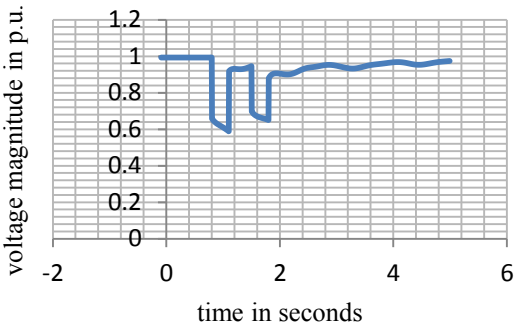

Figure: A2:a. Multiple voltage dip magnitude measured on Busbar6

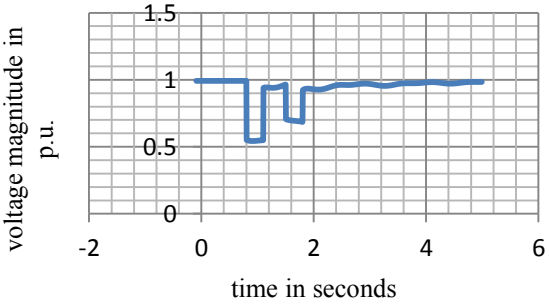

Figure: A2:c. Multiple voltage dip magnitude measured on Busbar 11

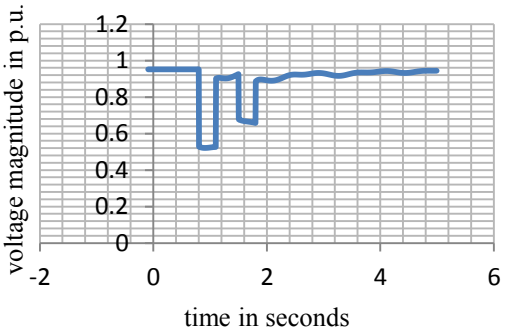

Figure: A2:b. Multiple voltage dip magnitude measured on Busbar 18

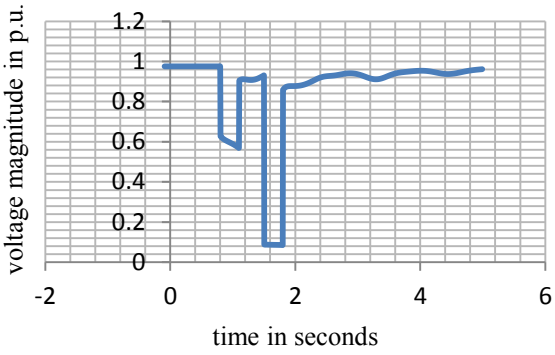

Figure: A2:d. Multiple voltage dip magnitude measured on Busbar 21

Appendix 5: A3: Faults at 90% of the two lines

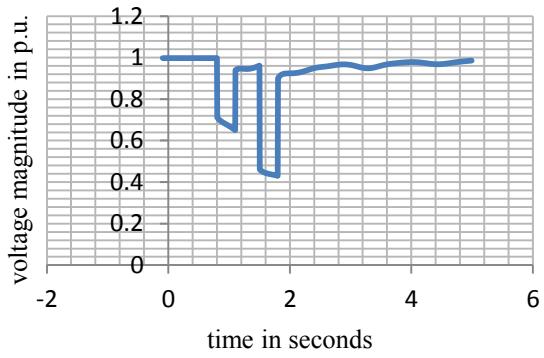

Figure: A3:a. Multiple voltage dip magnitude measured on Busbar5

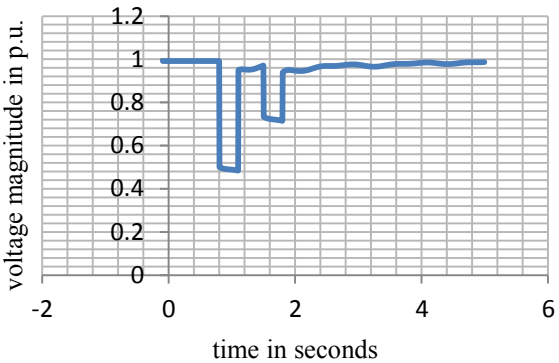

Figure: A3:c. Multiple voltage dip magnitude measured on Busbar 11

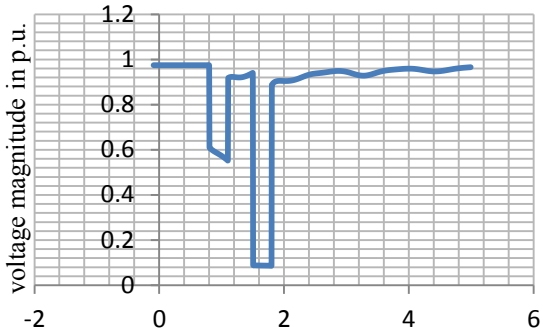

Figure: A3:b. Multiple voltage dip magnitude measured on Busbar 14

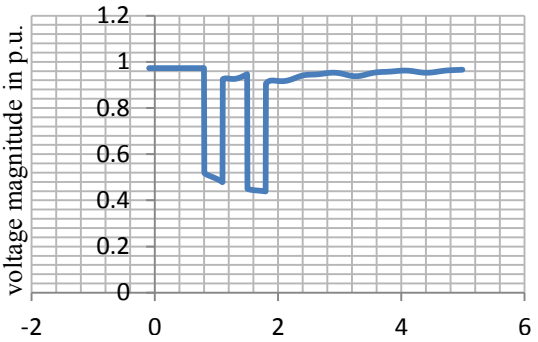

Figure: A3:d. Multiple voltage dip magnitude measured on Busbar 25

Appendix 5B- Graphs of multiple voltage dips without the grid-connected RDG systems as a result of SLG and 2LG faults on the transmission lines 'line8' and 'line15' respectively.

Appendix 5: B1: Faults at 10% of the two lines

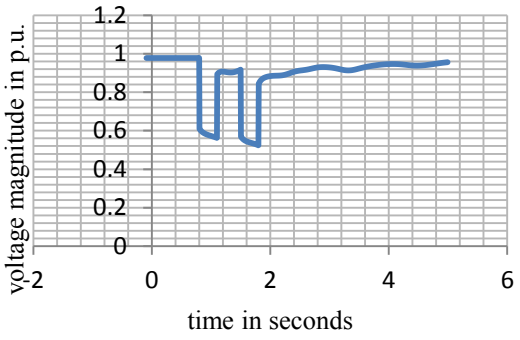

Figure: B1:a. Multiple voltage dip magnitude measured on Busbar 8

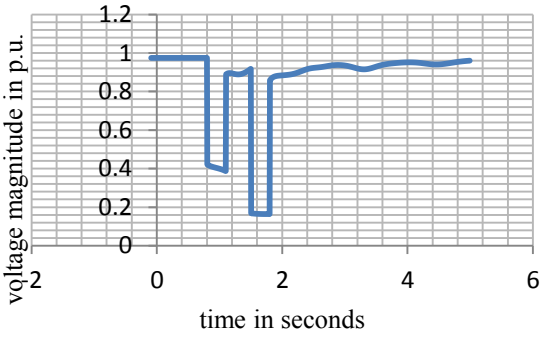

Figure: B1:c. Multiple voltage dip magnitude measured on Busbar 13

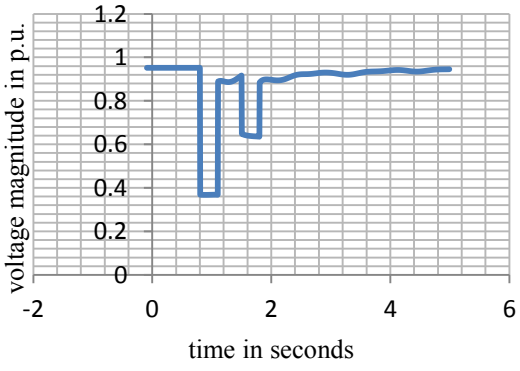

Figure: B1:b. Multiple voltage dip magnitude measured on Busbar 18

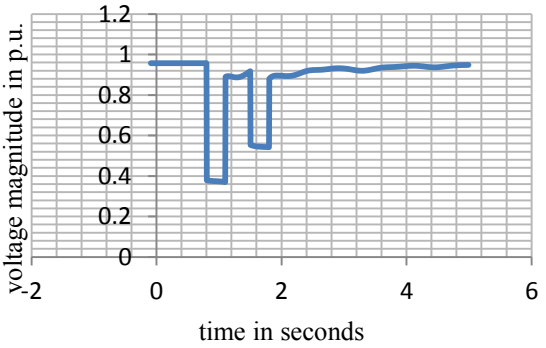

Figure: B1:d. Multiple voltage dip magnitude measured on Busbar 26

Appendix 5: B2: Faults at 50% of the two lines

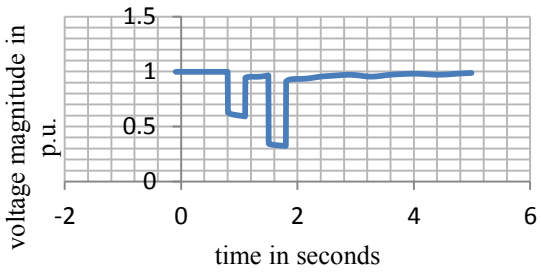

Figure: B2:a. Multiple voltage dip magnitude measured on Busbar5

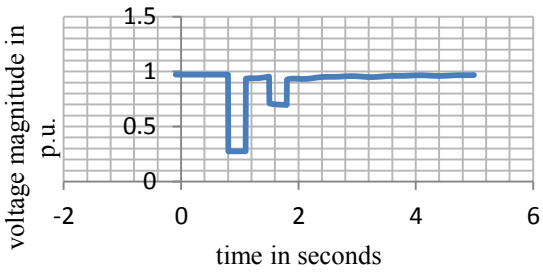

Figure: B1:c. Multiple voltage dip magnitude measured on Busbar 16

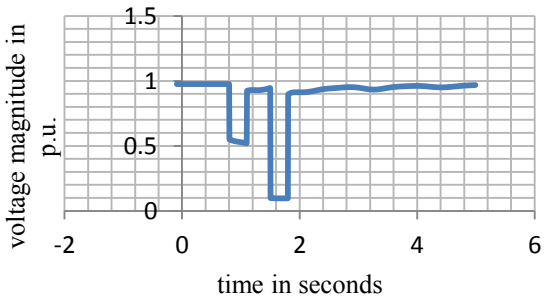

Figure: B1:b. Multiple voltage dip magnitude measured on Busbar 22

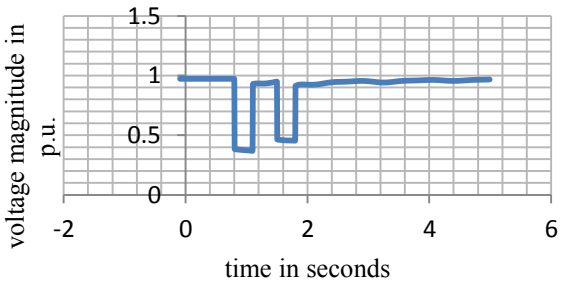

Figure: B1:d. Multiple voltage dip magnitude measured on Busbar 25

Appendix 5: B3: Faults at 90% of the two lines

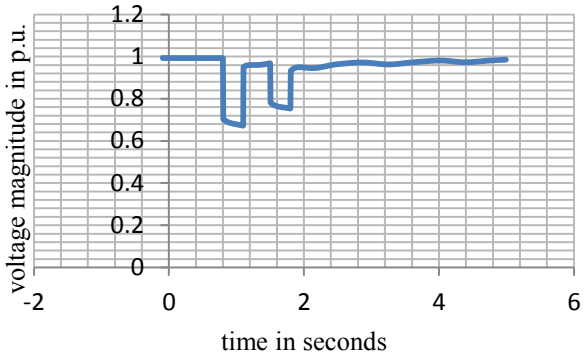

Figure: B3:a. Multiple voltage dip magnitude measured on Busbar 6

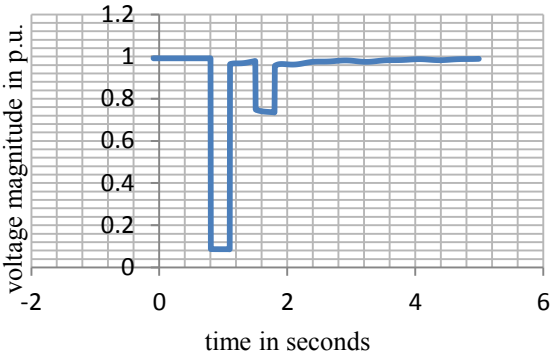

Figure: B3:c. Multiple voltage dip magnitude measured on Busbar 11

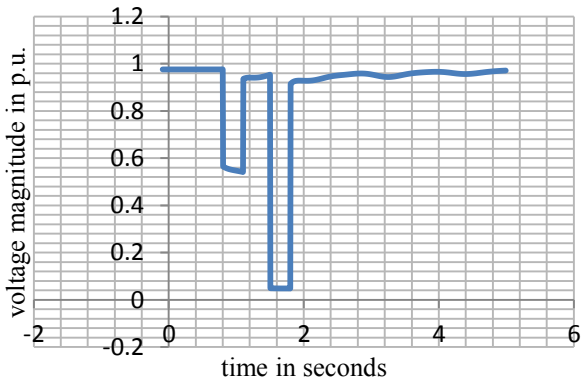

Figure: B3:b. Multiple voltage dip magnitude measured on Busbar 21

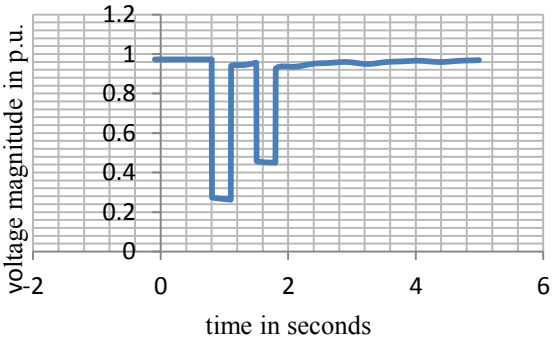

Figure: B3:d. Multiple voltage dip magnitude measured on Busbar 25

Appendix 5C- Graphs of mitigation of multiple voltage dips with the grid-connected wind generators as a result of SLG and 2LG faults on the transmission lines 'line8' and 'line15' respectively.

Appendix 5: C1: Faults at 10% of the two lines

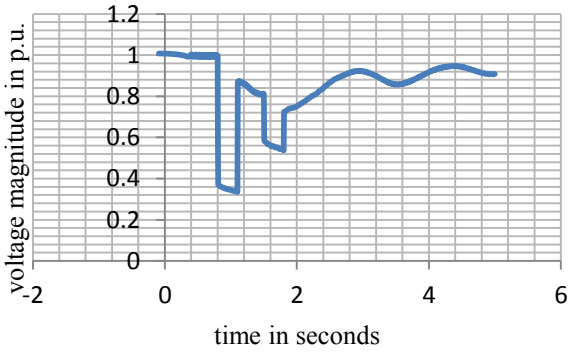

Figure: C1: a. Mitigation of multiple voltage dips magnitude measured on Busbar6

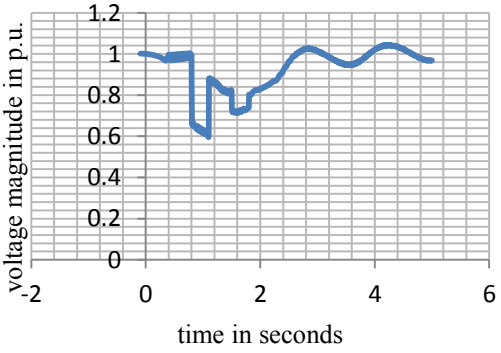

Figure: C1: c. Mitigation of multiple voltage dips magnitude measured on Busbar17

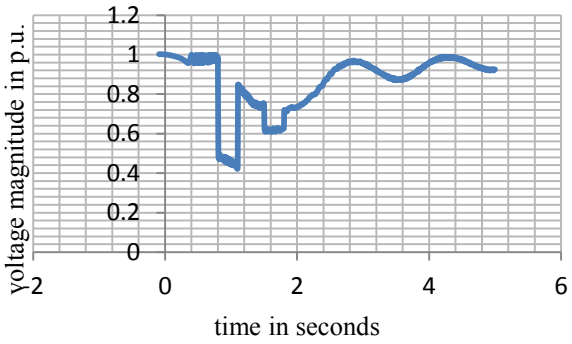

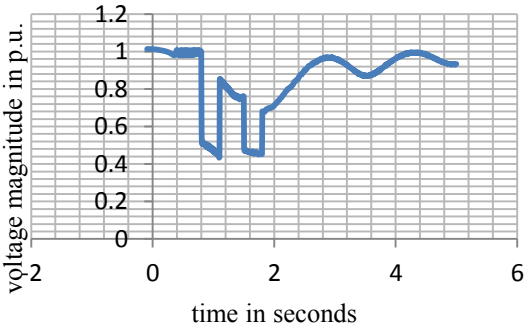

Appendix 5: C2: Faults at 50% of the two lines

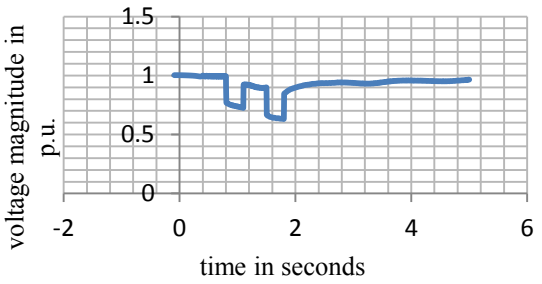

Figure: C2: a. Mitigation of multiple voltage dips magnitude measured on Busbar8

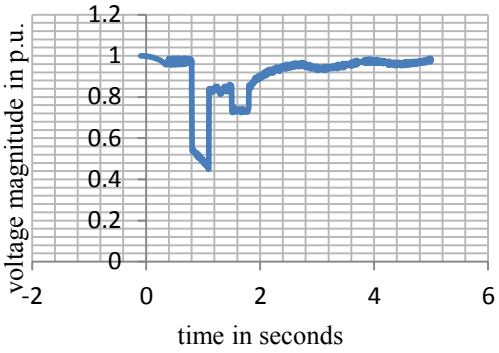

Figure: C2: c. Mitigation of multiple voltage dips magnitude measured on Busbar19

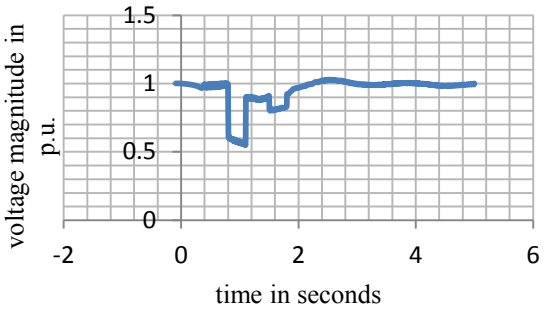

Figure: C2: b. Mitigation of multiple voltage dips magnitude measured on Busbar16

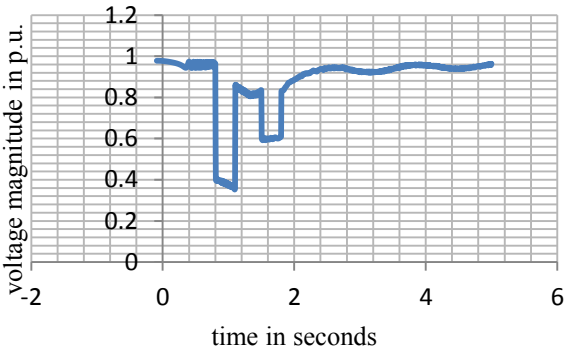

Figure: C2: d. Mitigation of multiple voltage dips magnitude measured on Busbar26

Appendix 5: C3: Faults at 90% of the two lines

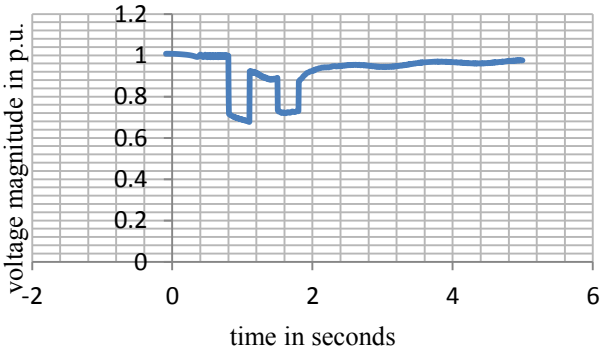

Figure: C3: a. Mitigation of multiple voltage dips magnitude measured on Busbar6

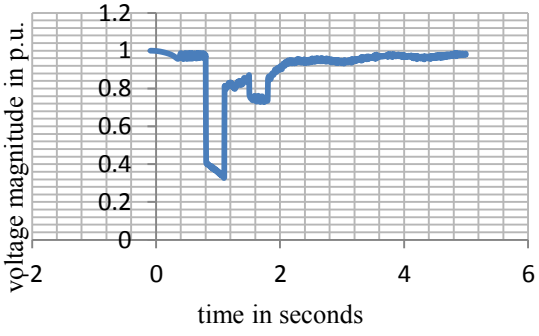

Figure: C3: c. Mitigation of multiple voltage dips magnitude measured on Busbar 18

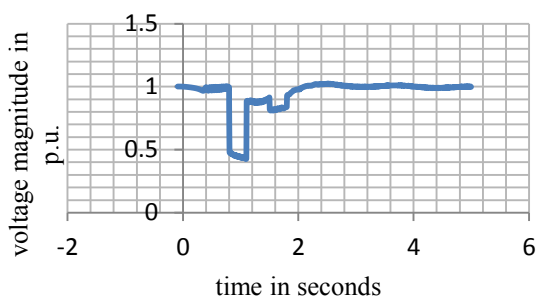

Figure: C3: b. Mitigation of multiple voltage dips magnitude measured on Busbar 17

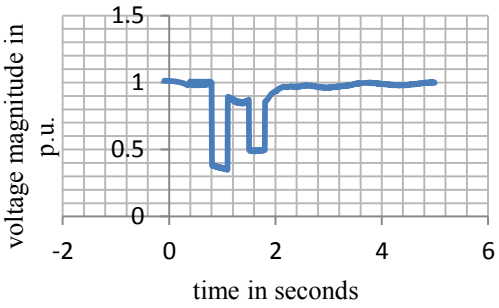

Figure: C3: d. Mitigation of multiple voltage dips magnitude measured on Busbar 25

Appendix 5D- Graphs of mitigation of multiple voltage dips with the grid-connected hydro generators as a result of SLG and 2LG faults on the transmission lines 'line8' and 'line15' respectively.

Appendix 5:D1: Faults at 10% of the two lines

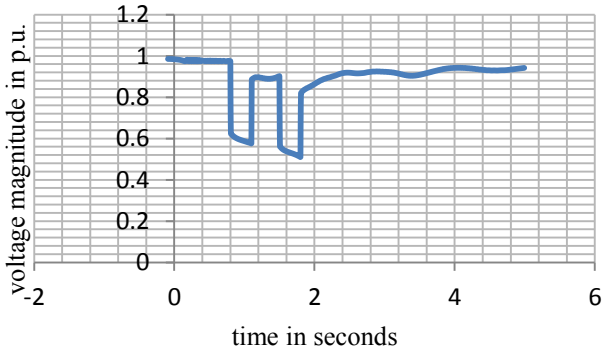

Figure: D1: a. Mitigation of multiple voltage dips magnitude measured on Busbar 8

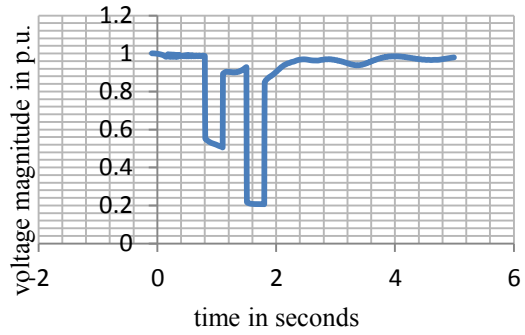

Figure: D1: c. Mitigation of multiple voltage dips magnitude measured on Busbar 22

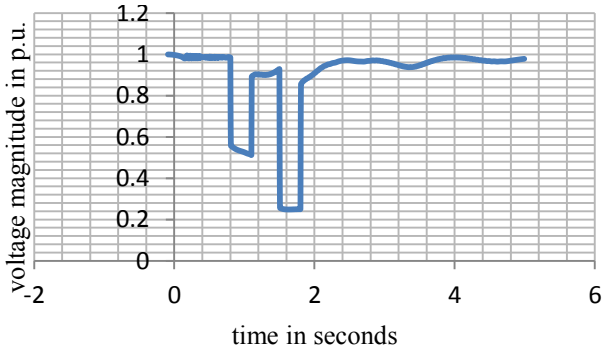

Figure: D1: a. Mitigation of multiple voltage dips magnitude measured on Busbar 13

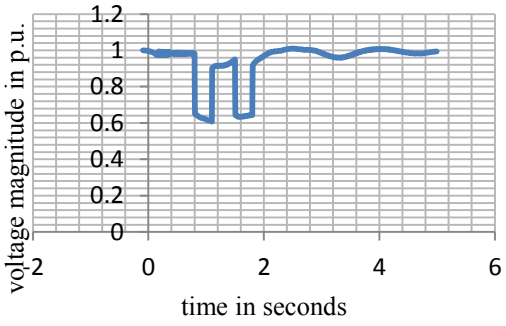

Figure: D1: d. Mitigation of multiple voltage dips magnitude measured on Busbar 25

Appendix 5:D2: Faults at 50% of the two lines

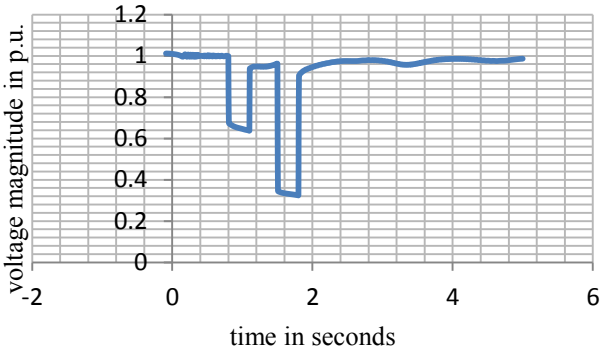

Figure: D2: a. Mitigation of multiple voltage dips magnitude measured on Busbar 5

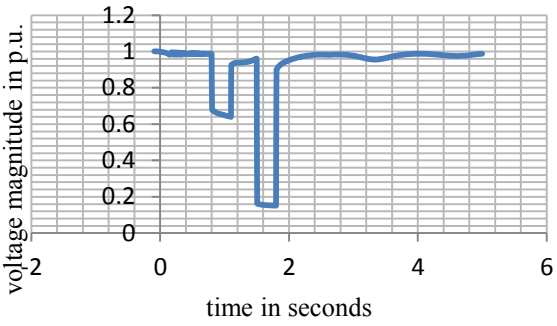

Figure: D2: c. Mitigation of multiple voltage dips magnitude measured on Busbar 22

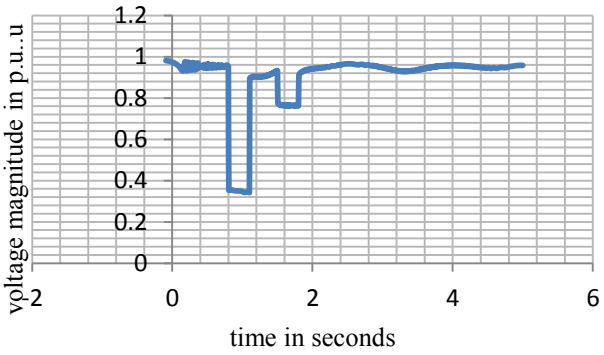

Figure: D2: b. Mitigation of multiple voltage dips magnitude measured on Busbar 17

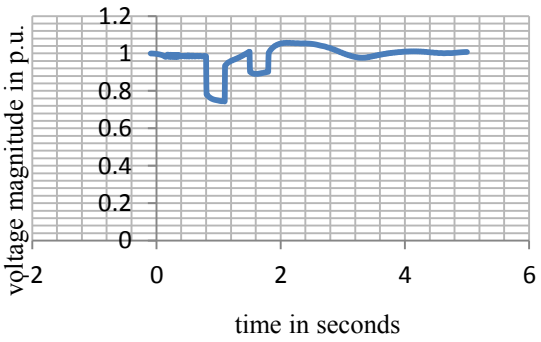

Figure: D2: d. Mitigation of multiple voltage dips magnitude measured on Busbar 26

Appendix 5: D3: Faults at 90% of the two lines

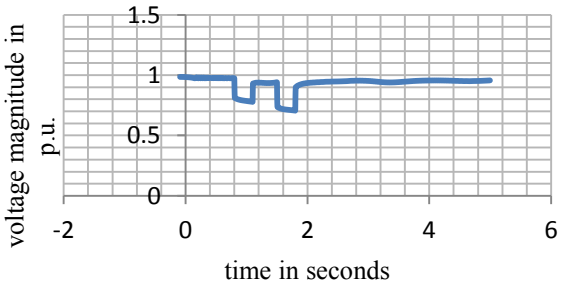

Figure: D3: a. Mitigation of multiple voltage dips magnitude measured on Busbar8

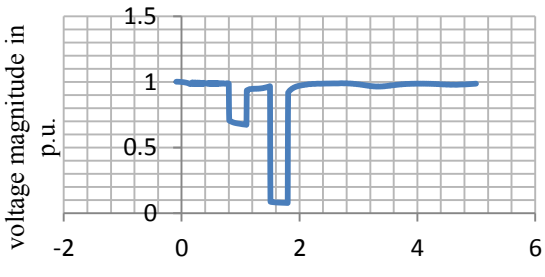

Figure: D3: c. Mitigation of multiple voltage dips magnitude measured on Busbar 22

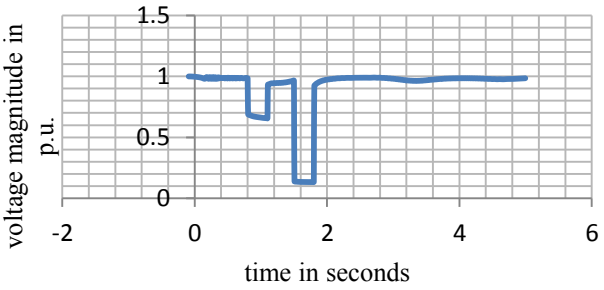

Figure: D3: b. Mitigation of multiple voltage dips magnitude measured on Busbar 13

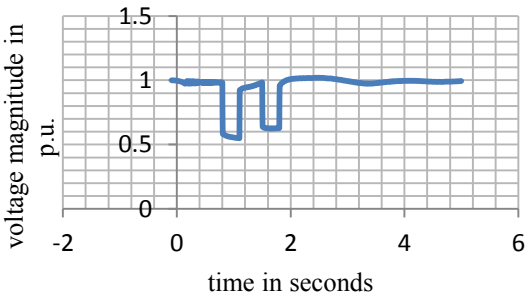

Figure: D3: d. Mitigation of multiple voltage dips magnitude measured on Busbar 25

Appendix E- Graphs of mitigation of multiple voltage dips with the grid-connected PV generators as a result of SLG and 2LG faults on the transmission lines 'line8' and 'line15' respectively.

Appendix 5: E1: Faults at 10% of the two lines

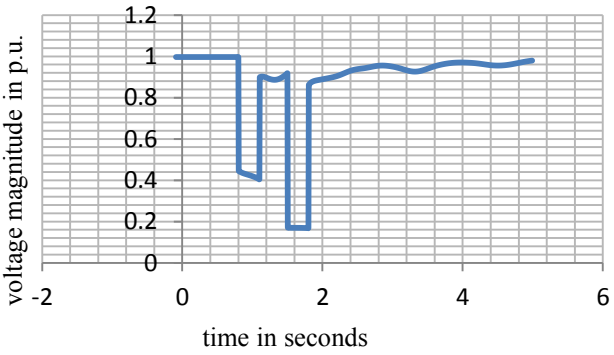

Figure: E1: a. Mitigation of multiple voltage dips magnitude measured on Busbar13

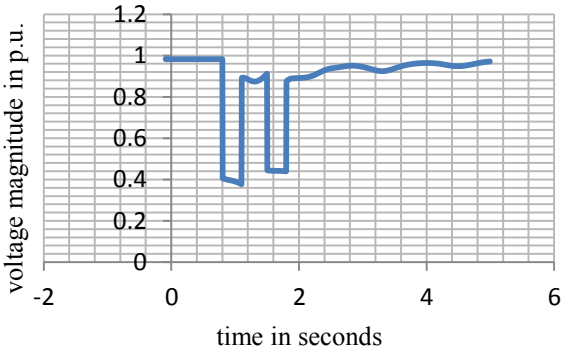

Figure: E1: c. Mitigation of multiple voltage dips magnitude measured on Busbar 25

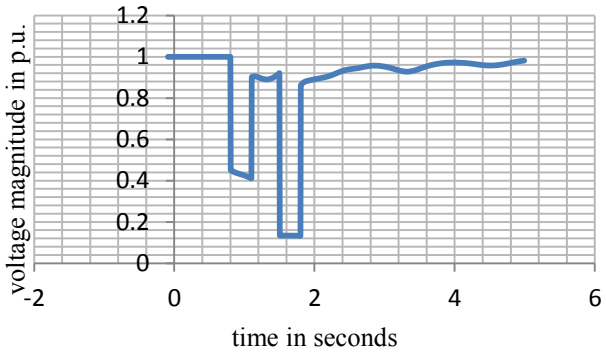

Figure: E1: b. Mitigation of multiple voltage dips magnitude measured on Busbar 21

Appendix 5: E2: Faults at 50% of the two lines

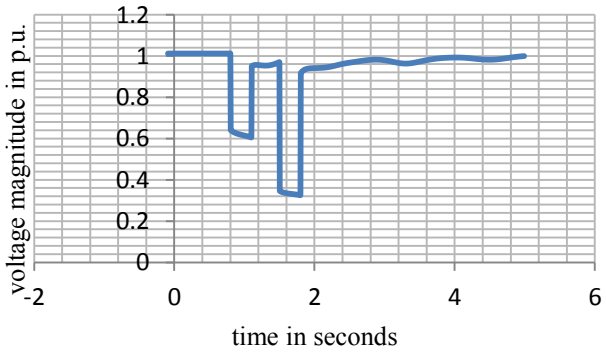

Figure: E2: a. Mitigation of multiple voltage dips magnitude measured on Busbar5

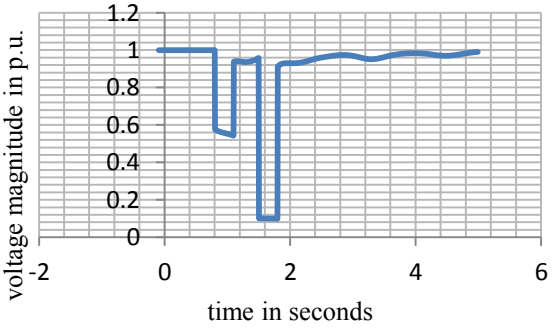

Figure: E2: c. Mitigation of multiple voltage dips magnitude measured on Busbar 22

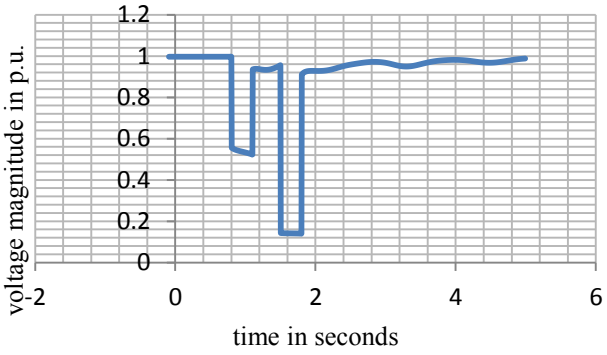

Figure: E2: b. Mitigation of multiple voltage dips magnitude measured on Busbar 13

Appendix 5: E3: Faults at 90% of the two lines

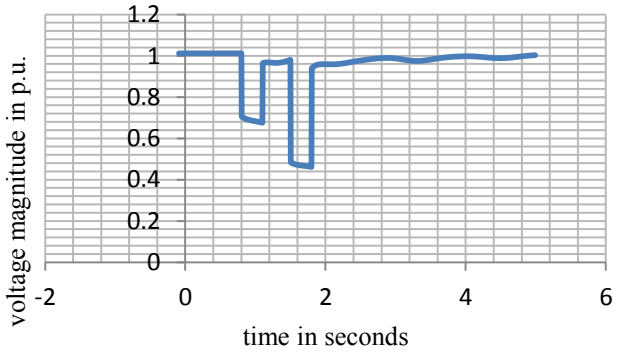

Figure: E3: a. Mitigation of multiple voltage dips magnitude measured on Busbar5

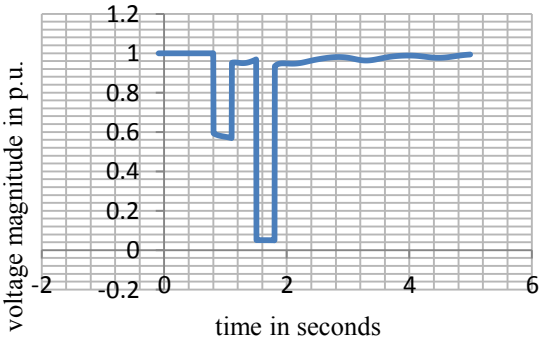

Figure: E3: c. Mitigation of multiple voltage dips magnitude measured on Busbar 22

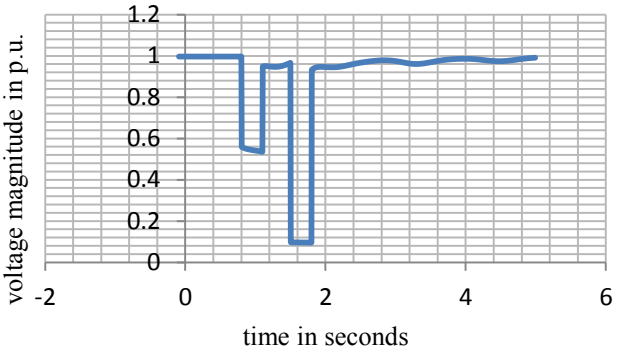

Figure: E3: b. Mitigation of multiple voltage dips magnitude measured on Busbar 13

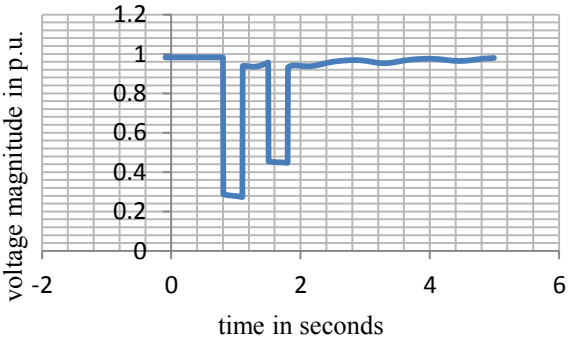

Figure: E3: d. Mitigation of multiple voltage dips magnitude measured on Busbar 25

Appendix F- Graphs of mitigation of multiple voltage dips with the grid-connected wind and hydro generators as a result of SLG and 2LG faults on the transmission lines 'line8' and 'line15' respectively.

Appendix 5F: 3 Faults at 90% of the two lines

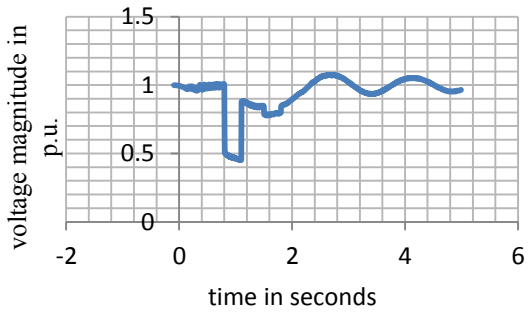

Figure: F3: a. Mitigation of multiple voltage dips magnitude measured on Busbar 16

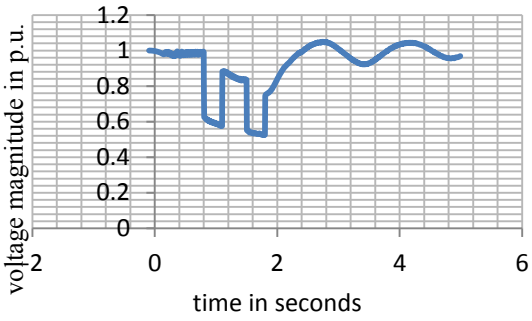

Figure: F3: c. Mitigation of multiple voltage dips magnitude measured on Busbar 25

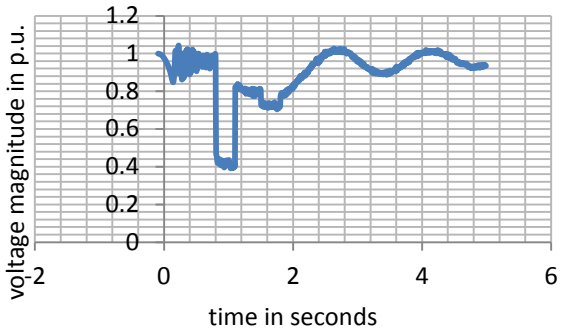

Figure: F3: b. Mitigation of multiple voltage dips magnitude measured on Busbar 18

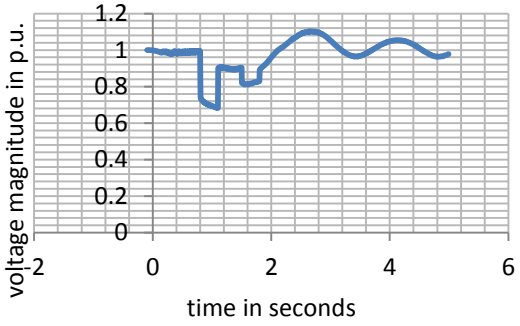

Figure: F3: d. Mitigation of multiple voltage dips magnitude measured on Busbar 26

Appendix G- Graphs of mitigation of multiple voltage dips with all the grid-connected generators as a result of SLG and 2LG faults on the transmission lines 'line8' and 'line15' respectively.

Appendix 5G: 1 Faults at 10% of the two lines

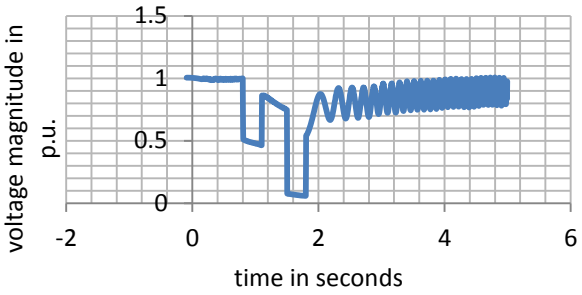

Figure: G1: a. Mitigation of multiple voltage dips magnitude measured on Busbar 5

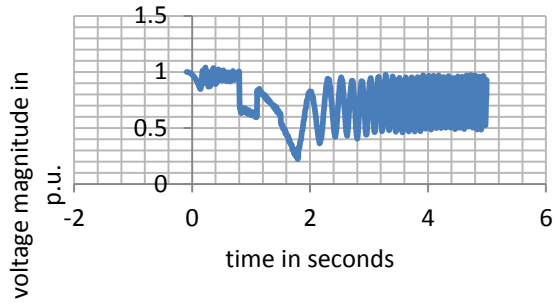

Figure: G1: d. Mitigation of multiple voltage dips magnitude measured on Busbar 18

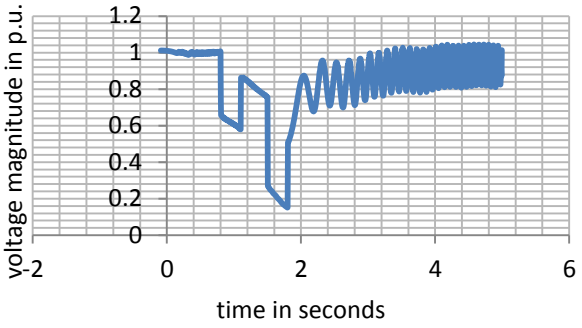

Figure: G1: b. Mitigation of multiple voltage dips magnitude measured on Busbar 13

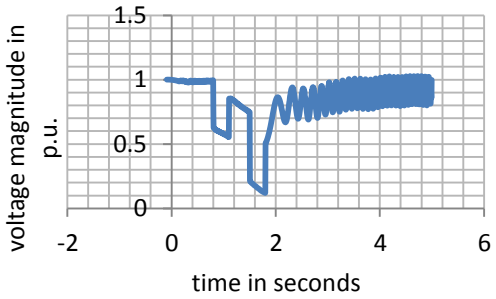

Figure: G1: e. Mitigation of multiple voltage dips magnitude measured on Busbar 21

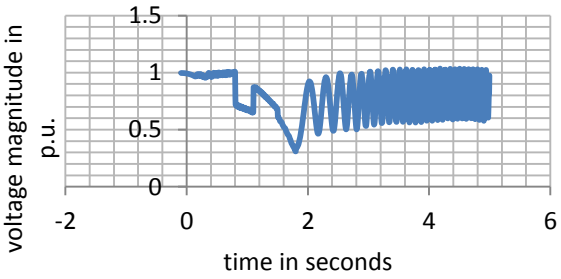

Figure: G1: c. Mitigation of multiple voltage dips magnitude measured on Busbar 16

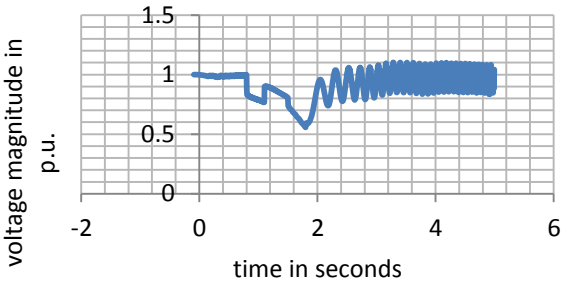

Figure: G1: f. Mitigation of multiple voltage dips magnitude measured on Busbar 26

Appendix 5H- Graphs of multiple voltage dips without the grid-connected RDG systems as a result of multiple faults from the distribution lines.

Appendix 5H: 1 Multiple faults 2P and SLG on line10 and line13 respectively

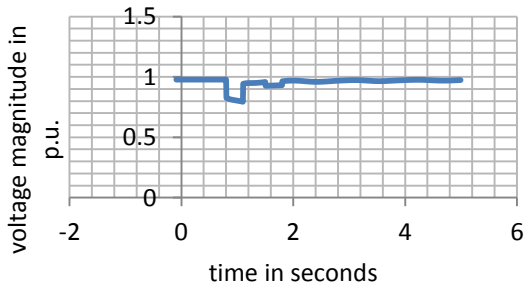

Figure: H1: a. Mitigation of multiple voltage dips magnitude measured on Busbar 8

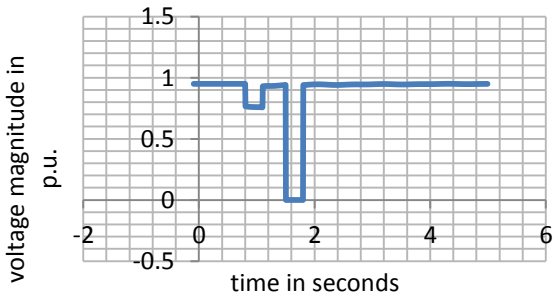

Figure: H1: c. Mitigation of multiple voltage dips magnitude measured on Busbar 20

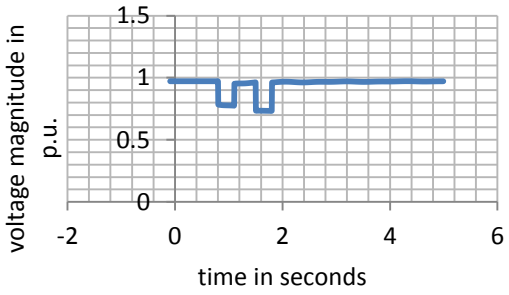

Figure: H1: b. Mitigation of multiple voltage dips magnitude measured on Busbar 17

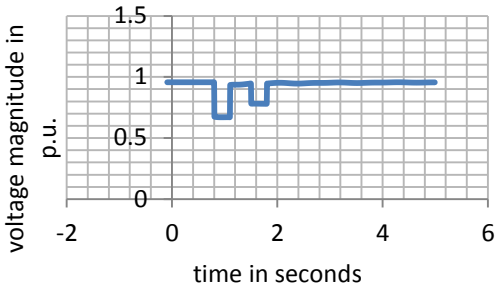

Figure: H1: d. Mitigation of multiple voltage dips magnitude measured on Busbar 26

Appendix 5: H2: Multiple faults 3P and 2LG on line12 and line14 respectively

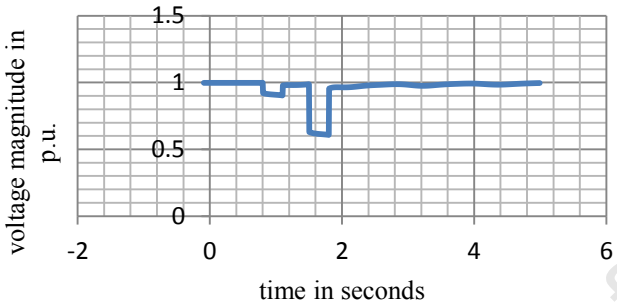

Figure: H2: a. Multiple voltage dips magnitude measured on Busbar5

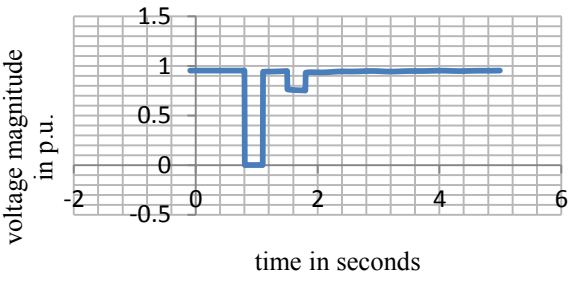

Figure: H2: c. Multiple voltage dips magnitude measured on Busbar 19

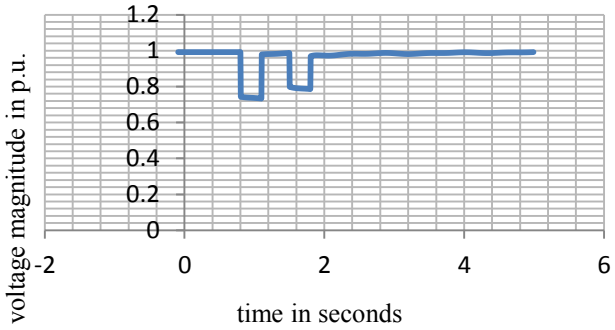

Figure: H2: b. Multiple voltage dips magnitude measured on Busbar 11

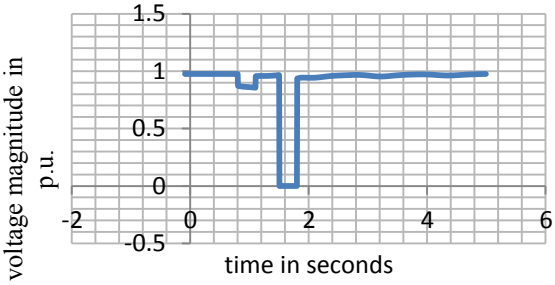

Figure: H2: d. Multiple voltage dips magnitude measured on Busbar 22

Appendix 5H: 3 Multiple faults SLG and 2P on line9 and line11 respectively

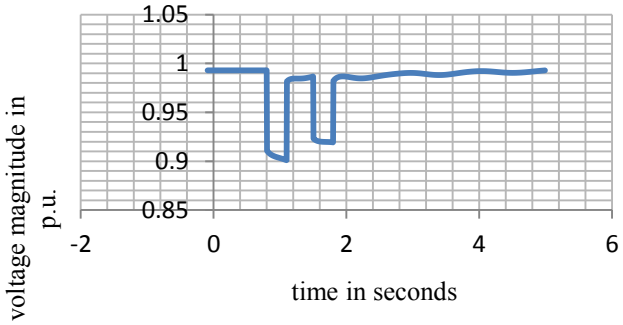

Figure: H3: a. Multiple voltage dips magnitude measured on Busbar6

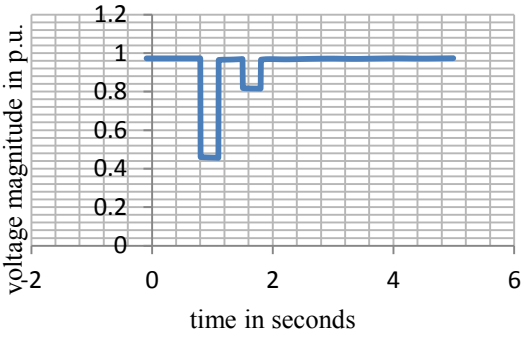

Figure: H3: c. Multiple voltage dips magnitude measured on Busbar 25

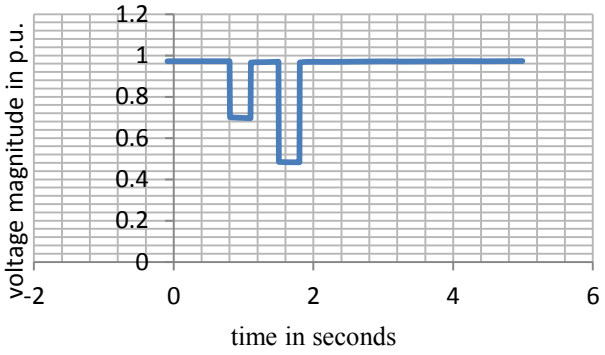

Figure: H3: b. Multiple voltage dips magnitude measured on Busbar 17

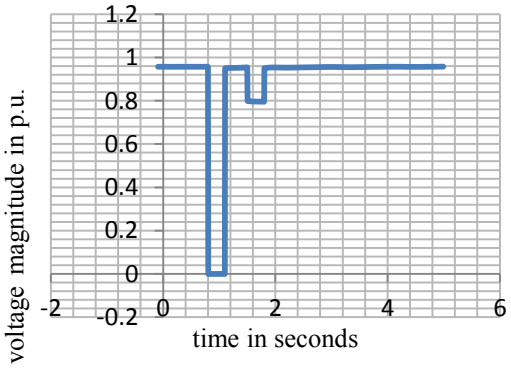

Figure: H3: d. Multiple voltage dips magnitude measured on Busbar 26

Appendix 5I- Graphs of mitigation of multiple voltage dips with the grid-connected wind generators as a result of multiple faults from the distribution lines.

Appendix 5I: 3 Mitigation of multiple faults SLG and 2P on line9 and line11 respectively

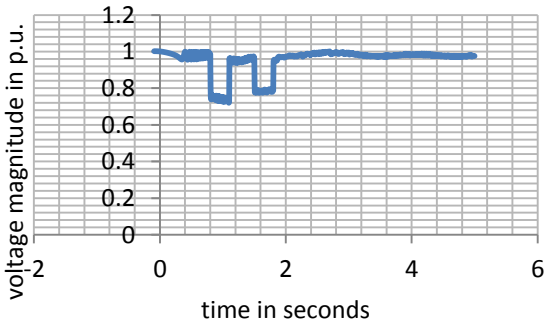

Figure: I1: a. Mitigation of multiple voltage dips magnitude measured on Busbar 11

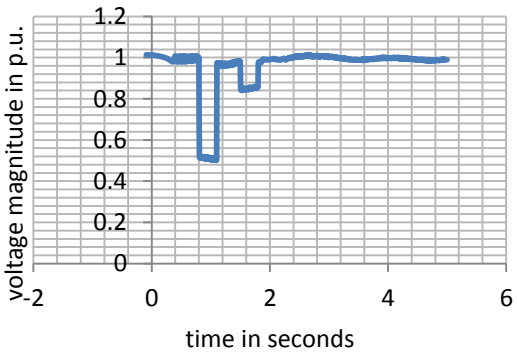

Figure: I1: d. Mitigation of multiple voltage dips magnitude measured on Busbar 25

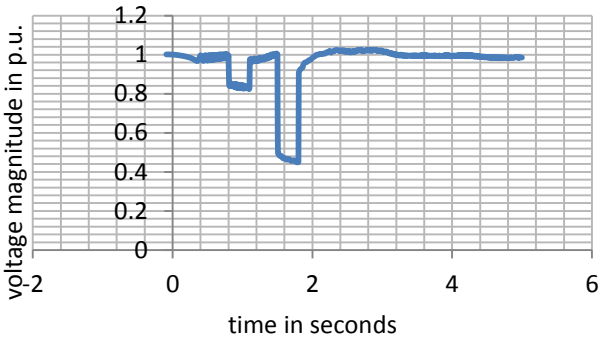

Figure: I1: b. Mitigation of multiple voltage dips magnitude measured on Busbar 17

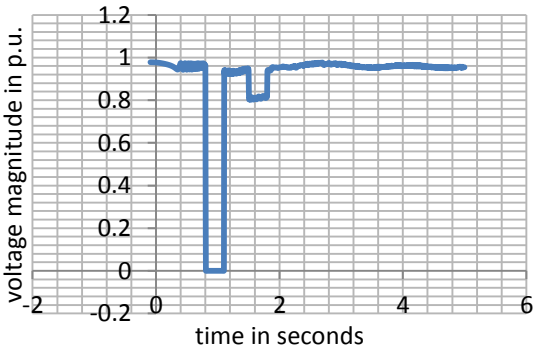

Figure: I1: e. Mitigation of multiple voltage dips magnitude measured on Busbar 26

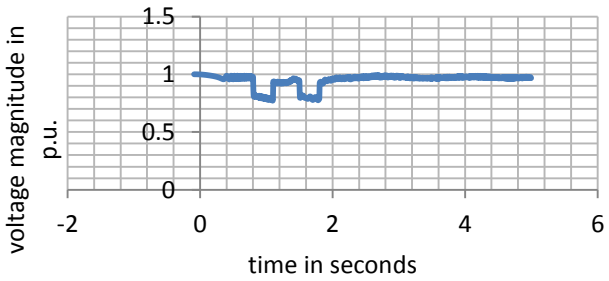

Figure: I1: c. Mitigation of multiple voltage dips magnitude measured on Busbar 19

Appendix 5J- Graphs of mitigation of multiple voltage dips with the grid-connected hydro generators as a result of multiple faults from the distribution lines.

Appendix 5J: 2 Mitigation of multiple faults 3P and 2LG on line12 and line14 respectively

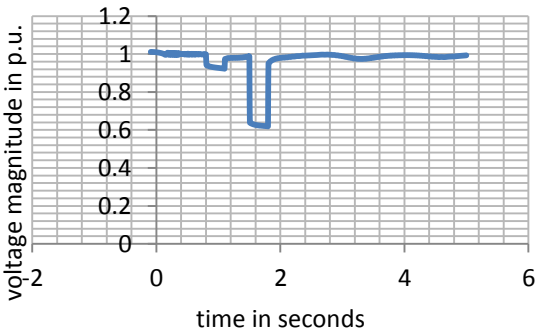

Figure: J2: a. Mitigation of multiple voltage dips magnitude measured on Busbar 5

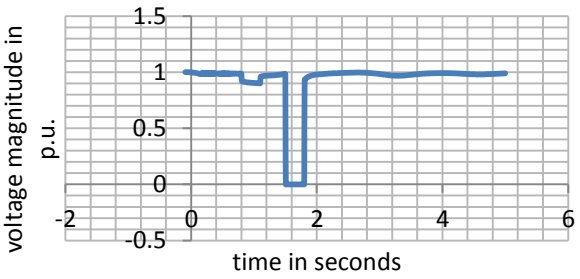

Figure: J2: c. Mitigation of multiple voltage dips magnitude measured on Busbar 21

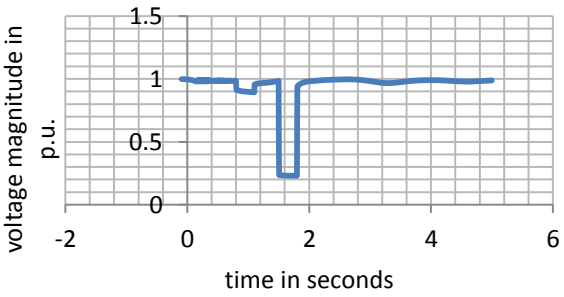

Figure: J2: b. Mitigation of multiple voltage dips magnitude measured on Busbar 13

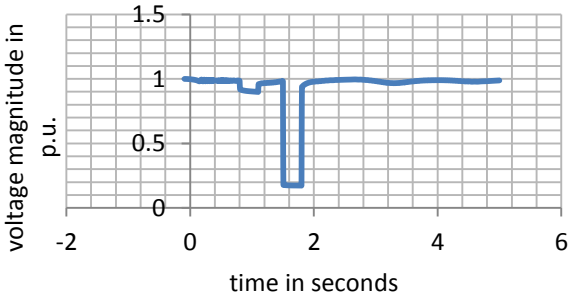

Figure: J2: d. Mitigation of multiple voltage dips magnitude measured on Busbar 23

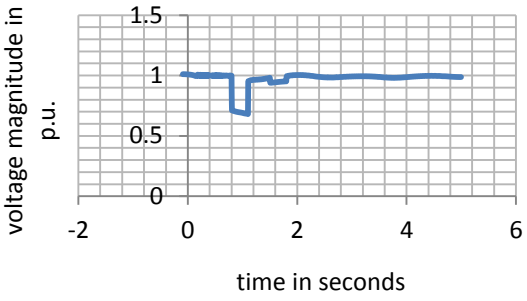

Figure: J3: a. Mitigation of multiple voltage dips magnitude measured on Busbar 5

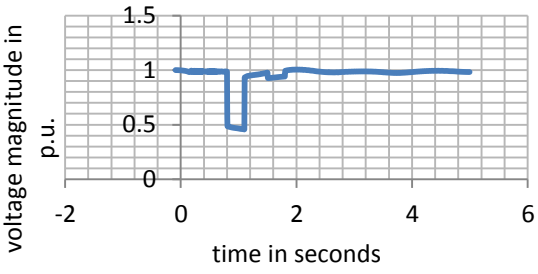

Figure: J3: c. Mitigation of multiple voltage dips magnitude measured on Busbar 21

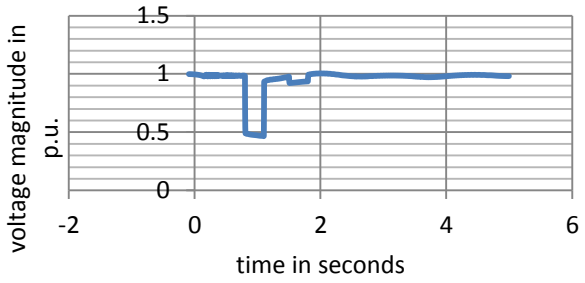

Figure: J3: b. Mitigation of multiple voltage dips magnitude measured on Busbar 13

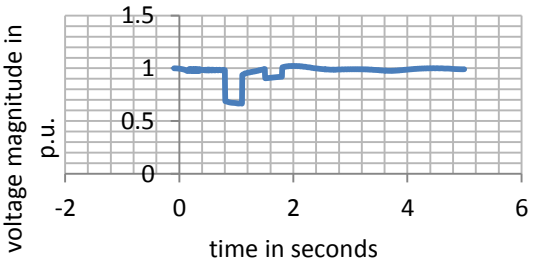

Figure: J3: d. Mitigation of multiple voltage dips magnitude measured on Busbar 25

Appendix 5K- Graphs of mitigation of multiple voltage dips with the grid-connected PV generators as a result of multiple faults from the distribution lines.

Appendix 5K: 1 Mitigation of multiple faults 2P and SLG on line10 and line13 respectively

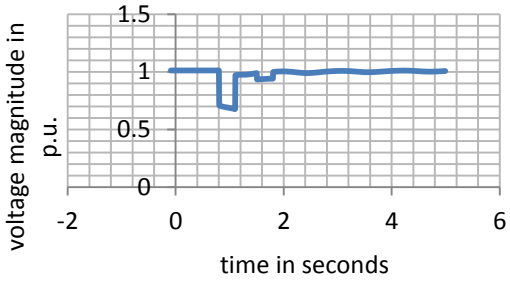

Figure: K1: a. Mitigation of multiple voltage dips magnitude measured on Busbar 5

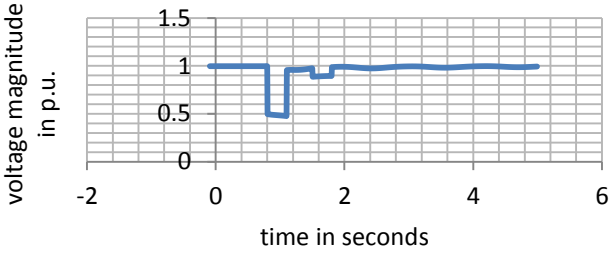

Figure: K1: c. Mitigation of multiple voltage dips magnitude measured on Busbar 13

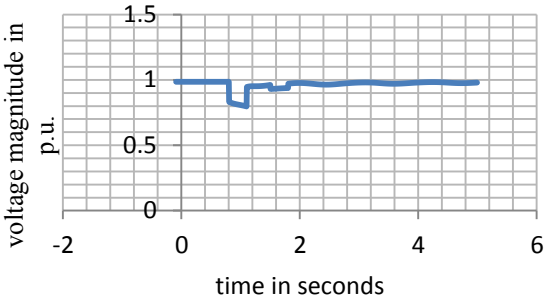

Figure: K1: b. Mitigation of multiple voltage dips magnitude measured on Busbar 8

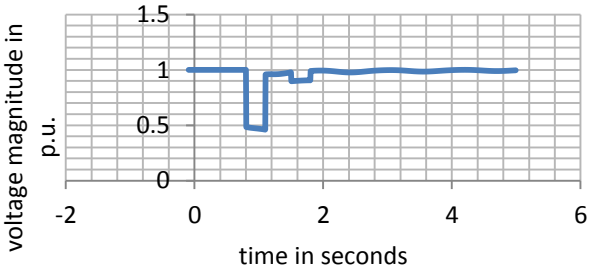

Figure: K1: d. Mitigation of multiple voltage dips magnitude measured on Busbar 23

Appendix 5K: 2 Mitigation of multiple faults 3P and 2LG on line12 and line14 respectively

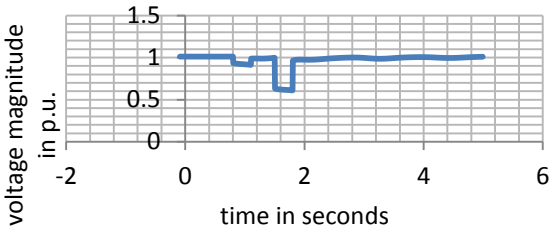

Figure: K2: a. Mitigation of multiple voltage dips magnitude measured on Busbar 5

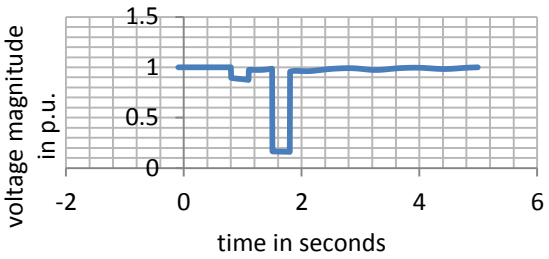

Figure: K2: c. Mitigation of multiple voltage dips magnitude measured on Busbar 23

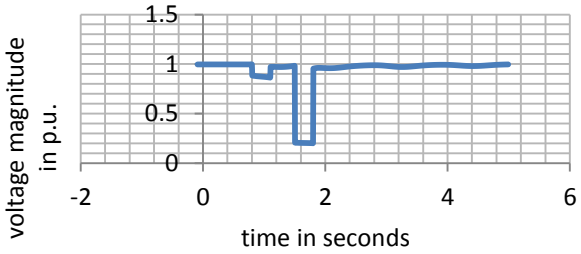

Figure: K2: b. Mitigation of multiple voltage dips magnitude measured on Busbar 13

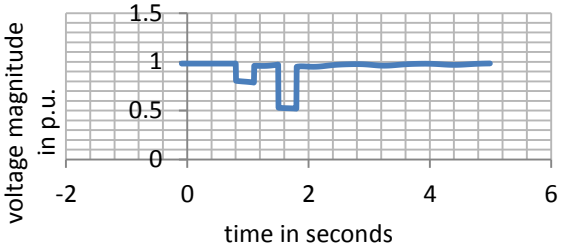

Figure: K2: d. Mitigation of multiple voltage dips magnitude measured on Busbar 25

Appendix 5L- Graphs of mitigation of multiple voltage dips with the grid-connected wind and hydro generators as a result of multiple faults from the distribution lines.

Appendix 5L: 2 Mitigation of multiple faults 3P and 2LG on line12 and line14 respectively

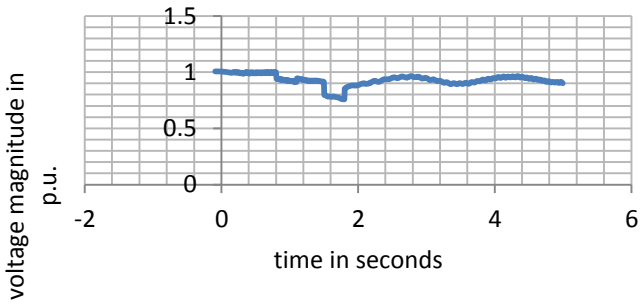

Figure: L2: a. Mitigation of multiple voltage dips magnitude measured on Busbar 6

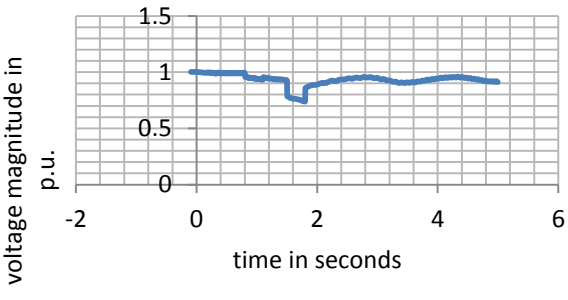

Figure: L2: b. Mitigation of multiple voltage dips magnitude measured on Busbar 8

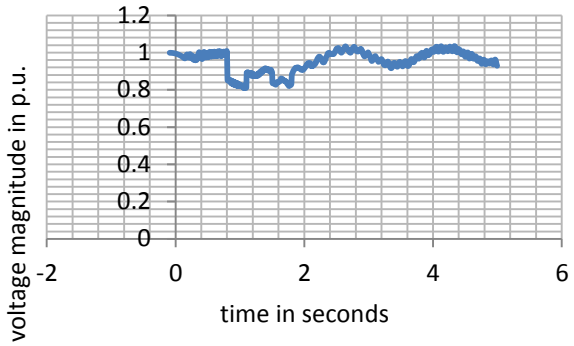

Figure: L2: c. Mitigation of multiple voltage dips magnitude measured on Busbar 16

Appendix 5M- Graphs of mitigation of multiple voltage dips with all the grid-connected generators as a result of multiple faults from the distribution lines.

Appendix 5M: 3 Mitigation of multiple faults SLG and 2P on line9 and line11 respectively

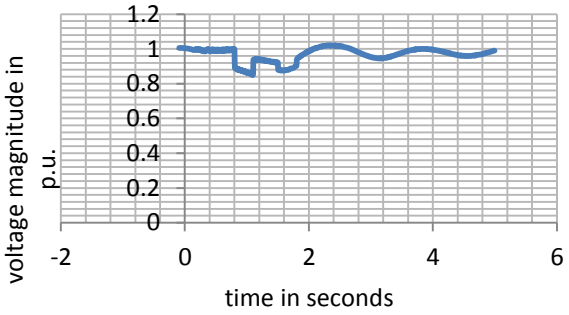

Figure: M3: b. Mitigation of multiple voltage dips magnitude measured on Busbar 5

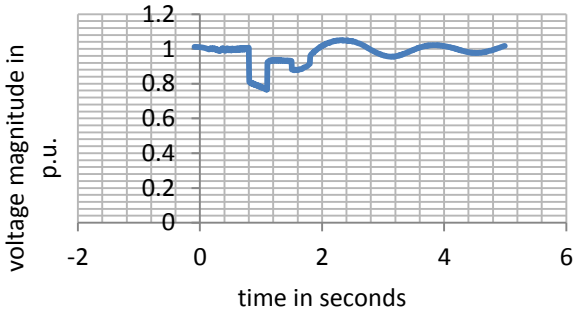

Figure: M3: b. Mitigation of multiple voltage dips magnitude measured on Busbar 13

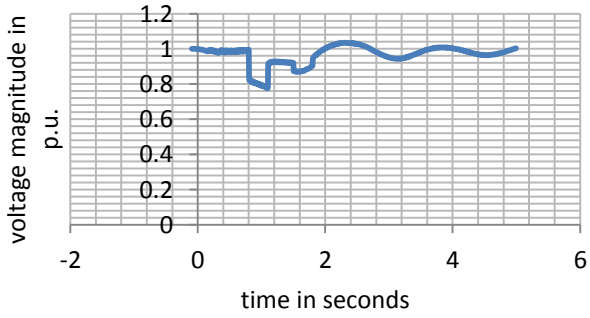

Figure: M3: b. Mitigation of multiple voltage dips magnitude measured on Busbar 21

Appendix 5N

Missing Data Restoration Algorithm [258]

Consider a signal x(n) = {$x_1(n)$, $x_2(n)$, x3(n)}, n = 0, 1, . . . , n − 1 where $x_1(n)$, n = 0, 1, . . . , N_1 − 1 is the first given segment of the signal x(n); $x_2(n)$, n = N_1, N_1 + 1, . . . , N_1 + N_2 – 1 is the missing segment of the signal x(n), and x3(n), n = M,M + 1, . . . , n − 1, where M = N_1 + N_2, is the second given segment of the signal x(n).

For the first given segment $x_1(n)$, using forward–backward approach, estimating c_k , k = 1, 2, . . . , p_1 (c0 = 1) of the first AR model.

The model order p_1 = floor $(\frac{2}{3}N_1 - 1)$,

where the function floor(x) maps a real number x to the largest previous integer, floor(x) = max{m ∈ Z!, m < x}.

the first given segment $x_1(n)$, n = 0, 1, . . . ,N_1 − 1 is forward extrapolated to get the forward estimates of missing samples. The forward extrapolated estimates $x_2^f(N_1),\ldots,x_2^f(N_1+N_1-1)$ of missing samples, we have obtained as follows

$$x_2^f(N_1+j) = -\sum_{k=1}^{p1(j)} c_k x_1(N_1+j-k), \quad j=0,1,\ldots,N_2-1$$

Appendix 6

Confusion matrices and performance plot for different architecture of detector ANNs during experimental process for determining the best detector ANN.

The result of 3-5-2 architecture

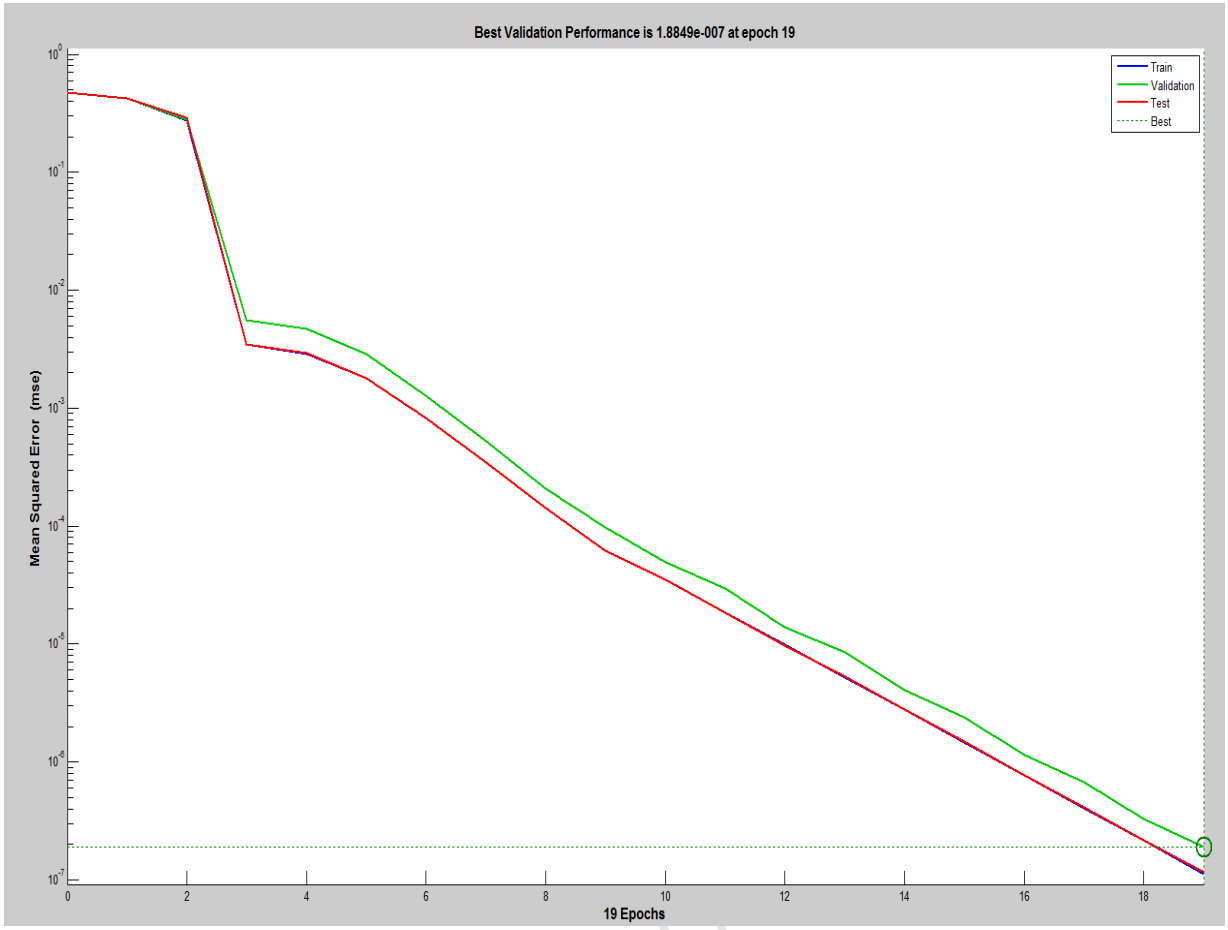

The result of 3-25-2 architecture

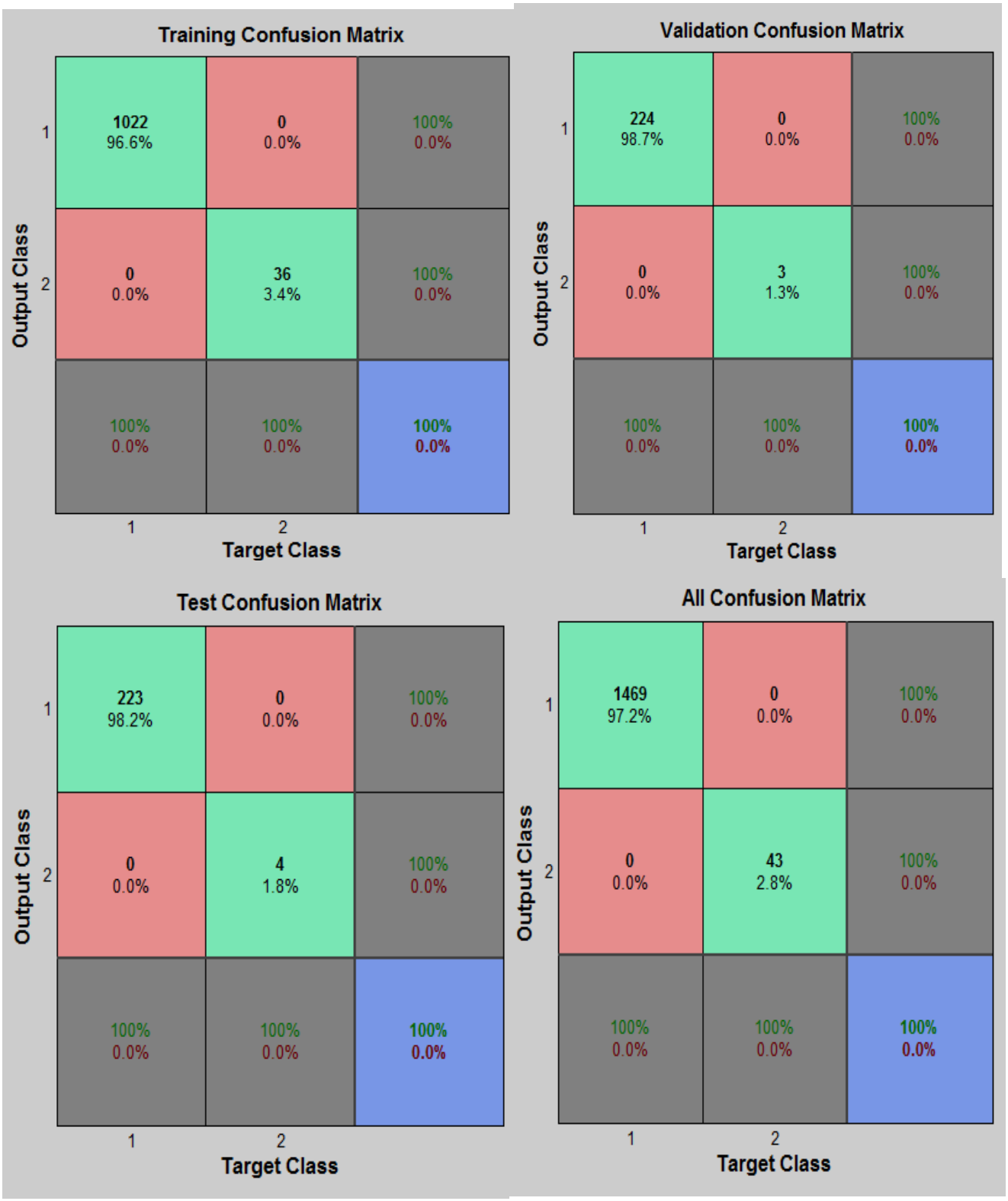

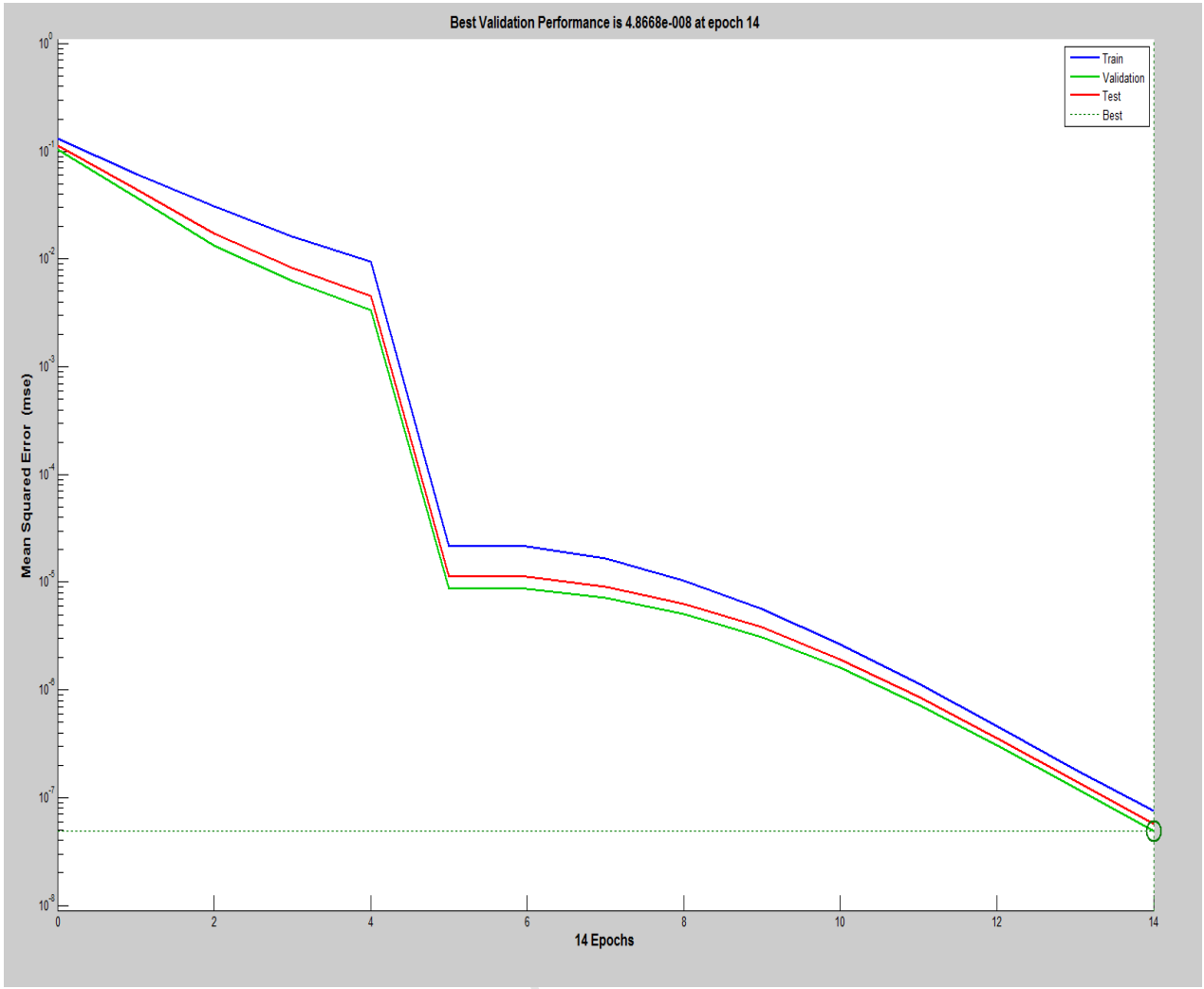
Best Validation Performance is 4.8668e-008 at epoch 14
Train
Validation
Test
Best
Mean Squared Error (mse)
14 Epochs

The result of 3-27-2 architecture

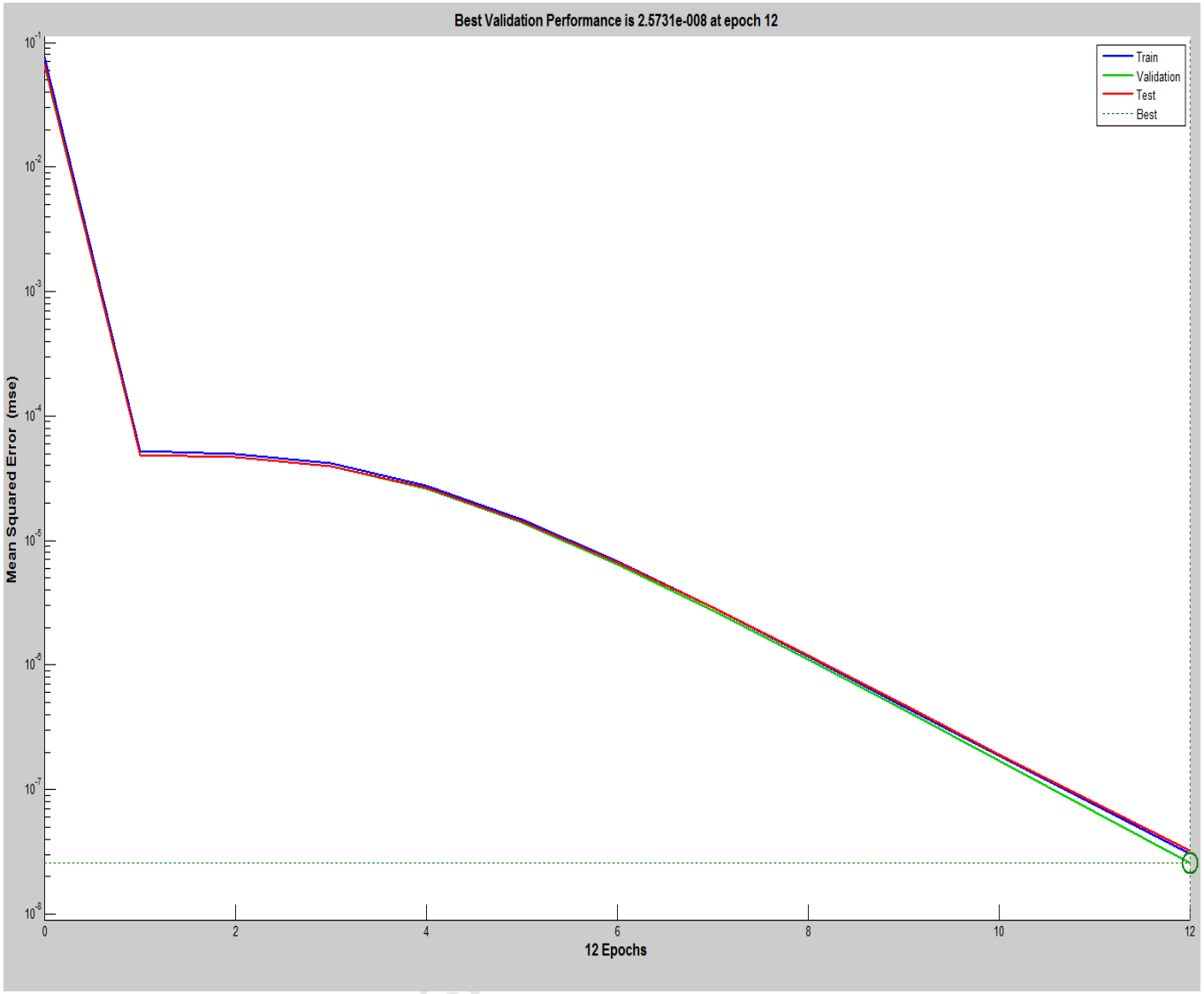
Best Validation Performance is 2.5731e-008 at epoch 12
Train
Validation
Test
Best
Mean Squared Error (mse)
12 Epochs

Confusion matrices and performance plot for different architecture of classifier ANNs during experimental process for determining the best classifier ANN.

Architecture of classifier ANN 15-5-7

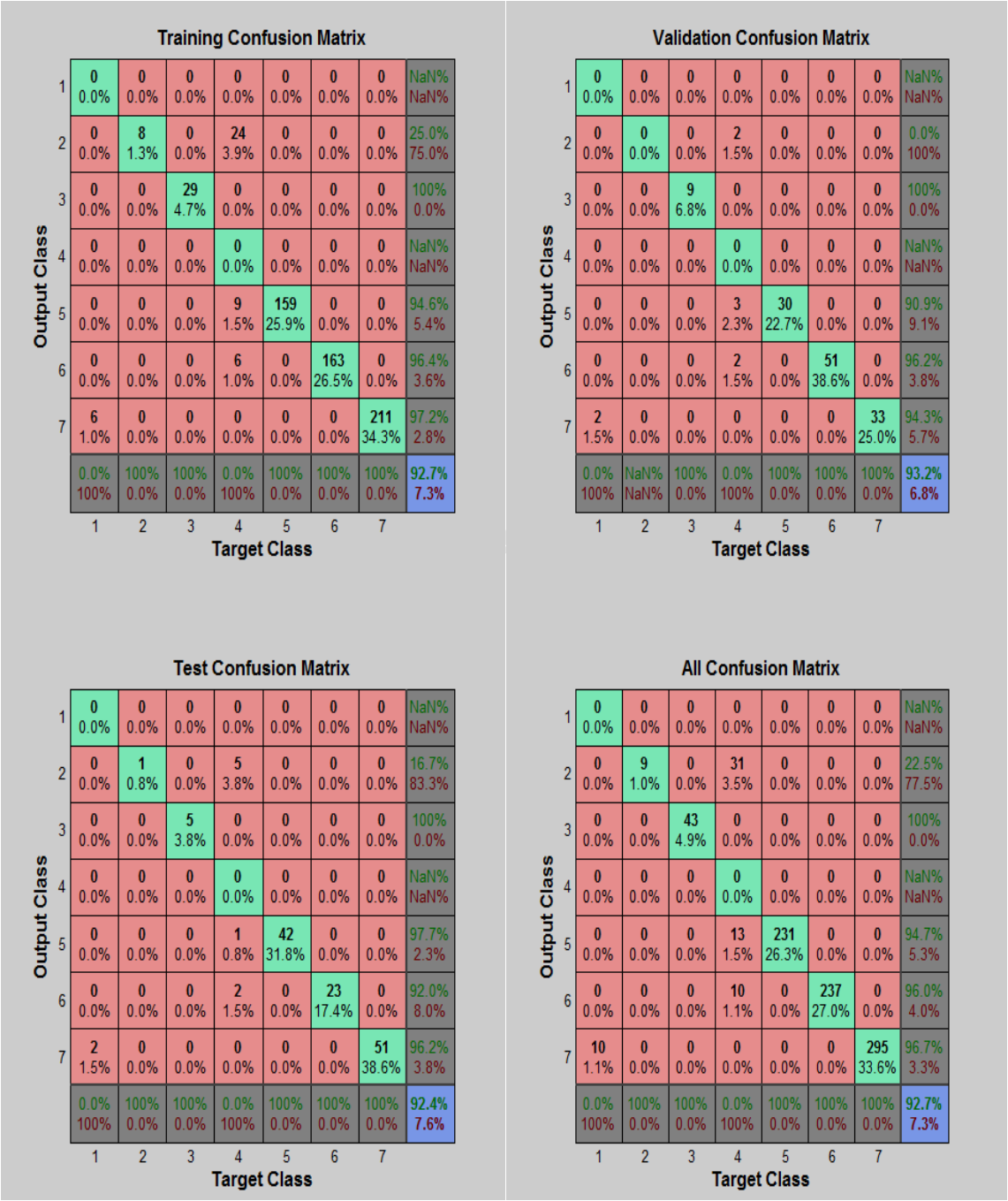

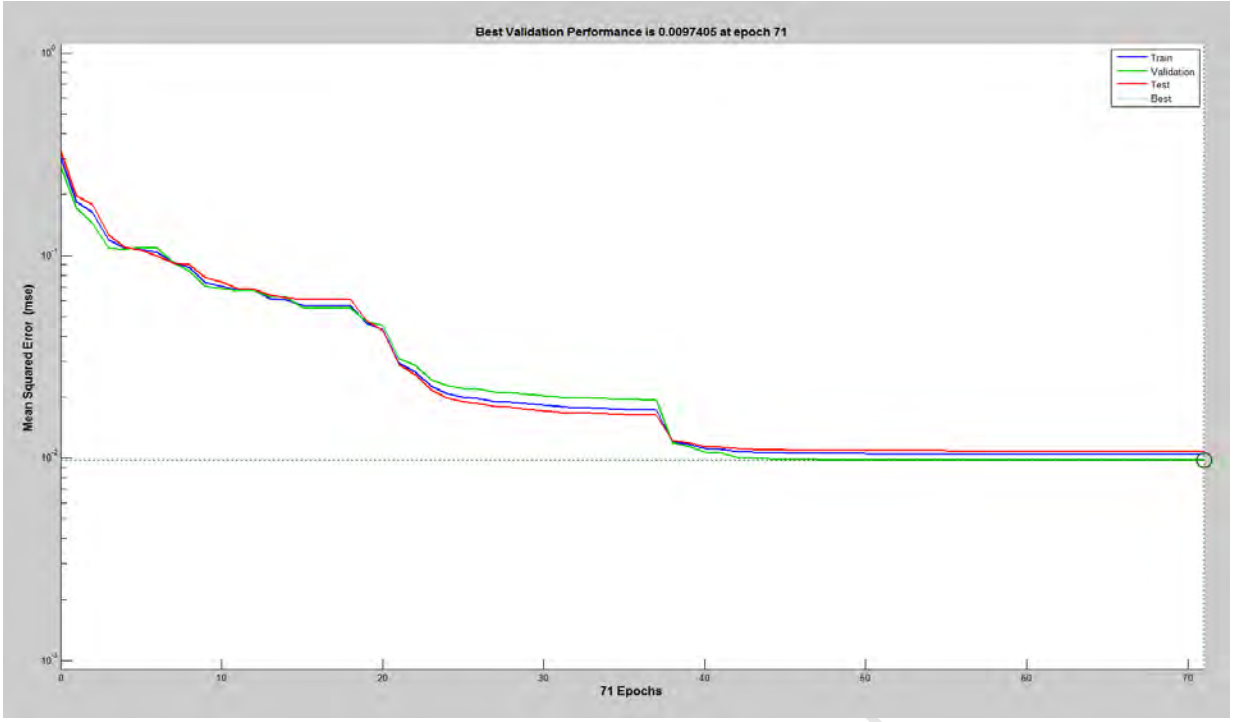

Architecture of classifier ANN 15-10-7

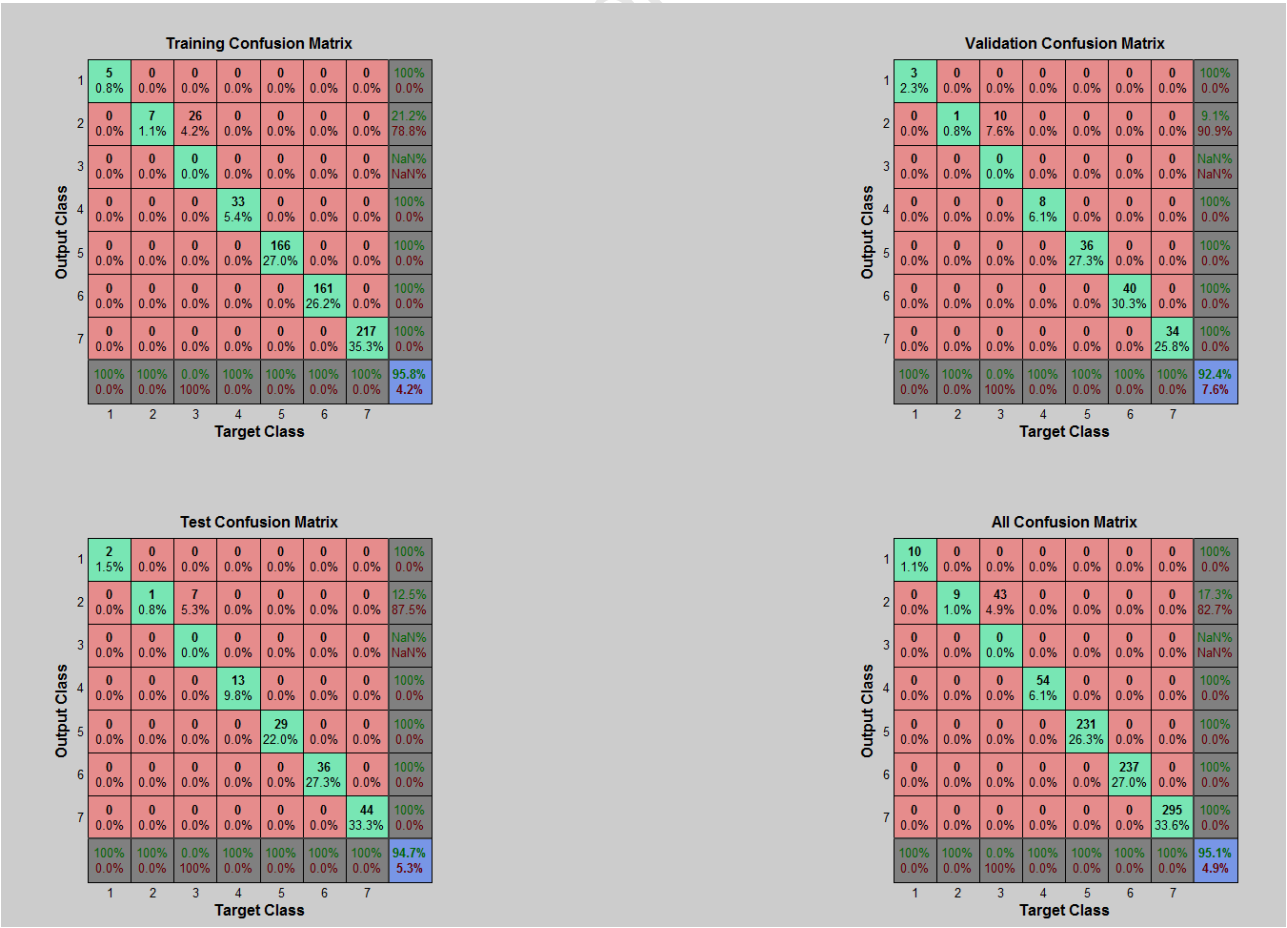

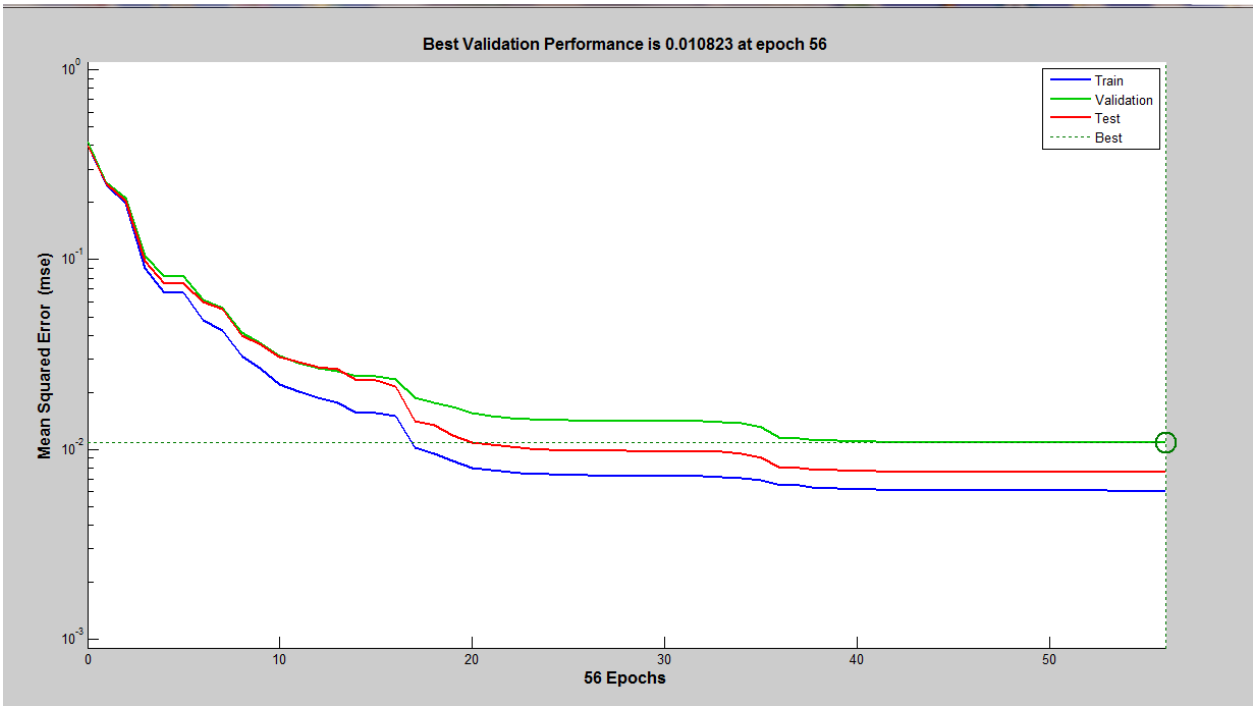

Architecture of classifier ANN 15-26-7